UNIVERSIDADE FEDERAL DO RIO GRANDE DO SUL
INSTITUTO DE BIOCIÊNCIAS
PROGRAMA DE PÓS-GRADUAÇÃO EM GENÉTICA E BIOLOGIA MOLECULAR

Padrões de variação genética e morfológica em *Oxymycterus* (Rodentia: Sigmodontinae) no Sul da Mata Atlântica e nos Pampas

Willian Thomaz Peçanha

Tese submetida ao Programa de Pós-Graduação em Genética e Biologia Molecular da UFRGS como requisito parcial para a obtenção do grau de Doutor em Ciências (Genética e Biologia Molecular)

Orientador: Prof. Dr. Thales Renato Ochotorena de Freitas

Co-orientadora: Dra. Gislene Lopes Gonçalves

Porto Alegre

Abril de 2019

Este trabalho foi desenvolvido no laboratório de Citogenética e Evolução do Departamento de Genética do instituto de Biociências da Universidade Federal do Rio Grande do Sul, subvencionado pelo: Conselho Nacional de Desenvolvimento Científico e Tecnológico (CNPq), Coordenação de Aperfeiçoamento de Pessoal de Nível Superior (CAPES) e Fundação de Amparo à Pesquisa do Estado do Rio Grande do Sul (FAPERGS).

AGRADECIMENTOS

Agradeço ao Prof. Thales R. O. Freitas (UFRGS) pela oportunidade, orientação, suporte, confiança e liberdade de desenvolvimento ao longo de 6 anos de trabalho. Também, a supervisão da Dra. Gislene Lopes Gonçalves (UFRGS), pela coorientação, motivação e auxilio técnico durante todo período de doutorado e suas contribuições relevantes às questões dos artigos/capítulos da tese.

Agradeço também aos pesquisadores Renan Maestri (UFRGS) e Sergio Luiz Althoff (FURB) que colaboraram de forma efetiva ao desenvolvimento da minha tese, e meu profundo reconhecimento ao pesquisador Fernando Marques Quintela (FURG) pela amizade e comprometimento no desenvolvimento dos estudo com os Rato-do-brejo, valeu camarada!

Aos diversos curadores e pesquisadores que gentilmente permitiram o acesso e cederam materiais de coleções para empréstimo que foram fundamentais para este estudo: Enrique M. González (MNHN), Enrique P. Lessa (FCIEN/UDELAR), Letícia Lima e Antenor Silva Junior (MHNCI), Alexandre Uarth Christoff (MCNU/ULBRA), Sérgio Luiz Althoff (CZFURB/FURB), Juliana Gualda (MZUSP), Márcia Maria de Assis Jardim (FZB-MCN), Ives José Sbalqueiro (UFPR/GEN), Fernando de Camargo Passos (UFPR/ZOO), Acir Franco (PUC-PR), Pablo Rodrigues Gonçalves (UFRJ), João Alves de Oliveira (MN/UFRJ), Robert Owen (Paraguai/TTU), Joseph A. Cook (MSB), Chris Conroy e Michael Nachman (MVZ-UC Berkeley), meu agradecimento.

Agradeço todo conhecimento teórico e prático ofertado pelo departamento de genética da UFRGS, através do PPGBM, onde o elevado nível dos professores foram essenciais para a construção deste trabalho. Agradeço os funcionários Luciano Silva, Clenio Machado, Lúcia Oliveira, Rodrigo Fritz e

Elmo Cardoso, que sempre foram atenciosos nas questões burocráticas e técnicas relacionadas a este trabalho. Também gostaria de agradecer aos seguranças Leopoldo Dorneles e Fernando Santos pelas conversas e convívio durante todos estes anos.

Queria agradecer a todos meus colegas da sala 103, do Laboratório de Citogenética e Evolução (LACE): Leonardo Leipnitz, Rafael Carvalho, Sandra Eloisa, Bruna Valenzuela, Bruna Szynwelski, Cristina Matzenbacher, Mayara Medeiros, Luiz Ribas, Lucas, Leandro Borges, Thamara, Rafael Kretschmer, Thaís Duarte, Marcelo Cruz, Luiza Gasparetto entre outros tantos! Também, aos colegas do Laboratório de Evolução Humana e Molecular (Lucas, Bibiana, Guillermo, Pedro) que compartilharam as alegrias e dificuldades que a vida acadêmica proporciona.

Por fim, serei eternamente grato aqueles familiares (mãe Cynthia Mary, avós Eurema Araci e Edison Pitanga, meus irmãos Vine e Rafa, tios avós Vital Carlos e Antônia, e minha companheira Lucieli) e amigos (TV, Thauy, Dudu, Rick, Possiede, Jule, Juco, Thargus, Giovane, Digão, Vico, Benn Ale, Lupe Furtado, Zaca, Marlonei, Elainy, Itacir, Léo, Pavel, Alessandra, Giovani Paoli e outros tantos) que me deram atenção, me incentivaram e deram suporte, em Paranaguá, Curitiba e Porto Alegre, durante toda a minha vida acadêmica, no bacharelado, mestrado e durante o doutorado.

SUMÁRIO

RESUMO

Oxymycterus é um dos principais gêneros com taxonomia controversa dentro da subfamília Sigmodontinae, em especial pela dificuldade em detectar variações morfológicas e citogenéticas discretas. De origem recente (~ 2 milhões de anos atrás), 15 espécies nominais atualmente são reconhecidas, porém, a delimitação genética entre essas formas, distribuição geográfica e história natural, é ainda desconhecida para diversos táxons. Esse gênero tem sido alvo de diversos estudos de sistemática, os quais proporcionaram avanços na taxonomia alfa; entretanto, as espécies ocorrentes extremo no sul da Floresta Atlântica e nos Pampas (i.e., *O. nasutus, O. quaestor, O. delator e O. dasytrichus*) foram em grande parte negligenciadas, permanecendo abertos aspectos fundamentais da taxonomia, história evolutiva e biogeografia dos táxons endêmicos a esses biomas. Assim, essa tese tem como objetivo central caracterizar padrões de variação genética e morfológica em formas de *Oxymycterus*, em especial *Oxymycterus nasutus* e *Oxymycterus quaestor* ocorrentes no extremo sul da Floresta Atlântica e Pampas. Utilizou-se uma abordagem integrativa com marcadores moleculares, morfometria do crânio, modelos de nicho ecológico e reconstrução de áreas ancestrais de forma a inferir (1) padrões de diferenciação populacional e de linhagens filogenéticas, (2) influência de fatores ambientais na variação observada, e (3) padrões biogeográficos relacionados a história evolutiva. Para *O. nasutus*, os resultados indicaram marcada variação genética e morfológica intraspecífica. Seis clados de mtDNA foram encontrados, estruturando populações ocorrentes no Pampa e Mata Atlântica em grupos distintos; diferenças na forma do crânios entre as linhagens nas duas ecorregiões foram detectadas. Considerando que os seis clados se estruturaram concomitante ao último período interglacial, a redução em condições adequadas durante esse período pode ter resultado em um possível processo de vicariância associado ao isolamento em refúgio. Também se verificou que *O. nasutus* possui um gradiente

latitudinal de variação da forma e tamanho do crânio, sendo os maiores tamanhos encontrados mais ao norte da distribuição (nos domínios da Mata Atlântica) e os menores mais ao sul (nos Pampas). Além disso, apesar da influência genética e ambiental atuar em conjunto para a forma, os atributos ambientais influenciram significativamente o tamanho do crânio. Durante as revisão de *Oxymycterus* nas coleções científicas se identificou um material associado a *O. delator* como algo distinto, o que resultou na descrição de uma nova espécie, *Oxymycterus itapeby*, que habita uma área de transição entre o Cerrado Meridional e a Mata Atlântica no Sul e Sudeste do Brasil. *Oxymycterus itapeby* é diferenciada das demais espécies pelo tamanho e forma do crânio, em particular por uma combinação de características cranianas. Uma análise filogenética bayesiana mostrou que *Oxymycterus itapeby*. representa um grupo monofilético, relacionado a *O. delator e O. amazonicus*. Por fim, uma abordagem taxonômica e filogeográfica do 'grupo *judex*' revelou o status de espécie para *Oxymycterus quaestor* com limites conspícuos em relação a *O. judex* e *O. misionalis*. Ainda, os dados evidenciaram três linhagens associadas, sendo duas com potencial status de espécie distintas, sendo a mais divergente ocorrente no domínios dos campos de altitude no estado do Rio Grande do Sul, e outra restrita a Serra dos Órgãos no estado do Rio de Janeiro.

ABSTRACT

Oxymycterus is one of the main genera with controversial taxonomy within the subfamily Sigmodontinae, in particular for the difficulty to detect discrete morphological and cytogenetic variations. From recent origin (~ 2 millions years ago), 15 nominal species are currently recognized, but the genetic delimitation between these forms, and the knowledge on geographic distribution and natural history, are broadly scarce for several taxa. Several systematic studies have been performed on this genus, which provided advances in the alpha taxonomy; however, species occurring at the extreme south of the Atlantic Forest and in the Pampas (i.e, *O. nasutus*, *O. quaestor*, *O. delator* and *O. dasytrichus*) have been neglected, therefore, fundamental aspects of taxonomy, evolutionary history and biogeography are entirely open. This dissertation characterized patterns of genetic and morphological variation in forms of *Oxymycterus* endemic to Atlantic Forest and Pampas ecoregions, especially *Oxymycterus nasutus* and *Oxymycterus quaestor*. An integrative approach with molecular markers, skull morphometry, ecological niche models and reconstruction of ancestral areas were carried out with the objective of inferring (1) patterns of population differentiation and phylogenetic lineages, (2) influence of environmental factors on intraspecific variation, and (3) biogeographic patterns related to the evolutionary history. For *O. nasutus*, the results indicated marked genetic variation and intraspecific morphology. Six clades of mtDNA were found, which structured populations from Pampas and Atlantic Forest in distinct groups; differences in the skulls shape between lineages in the two ecoregions were detected. Considering that six clades were structured concomitantly with the last interglacial maximum, the reduction in adequate conditions during this period may have resulted in a possible vicariance process associated with isolation in refuge. It was also found that *O. nasutus* has a latitudinal gradient of variation of cranium shape and size, with the largest sizes found more to the north of the distribution (in the

Atlantic Forest domain) and the smaller ones to the south (in the Pampas). Despite of genetic and environmental influence acting together for the shape, environmental attributes significantly influenced the size of the skull. During the review of *Oxymycterus* specimens in the scientific collections a specific material associated with *O. delator* was identified as something distinct, which resulted in the description of a new species, *Oxymycterus itapeby*, which inhabits an area of transition between the Southern Cerrado and the Atlantic Forest in the South and Southeast of Brazil. *Oxymycterus itapeby* can be differentiated from other species of *Oxymycterus* by the size and shape of the skull, in particular by a combination of cranial characteristics. A Bayesian phylogenetic analysis showed that *Oxymycterus itapeby* represents a monophyletic group, related to *O. delator* and *O. amazonicus*. Finally, a taxonomic and phylogeographic approach of the '*judex* group' revealed the status for *Oxymycterus quaestor* with conspicuous boundaries relative to *O. judex* and *O. misionalis*. In addition, the data showed three associated lineages, two of which have potential status of distinct species, being the most divergent in the highlands of the state of Rio Grande do Sul, and another restricted to Serra dos Órgãos in the state of Rio de Janeiro.

CAPÍTULO 1.

INTRODUÇÃO GERAL

A ordem Rodentia (Bowdich, 1821) se destaca entre as demais ordens de mamíferos viventes por ser a maior e a mais diversa, compreendendo cerca de 42% da diversidade de mamíferos do mundo (Musser & Carleton 2005). A região Neotropical abriga uma impressionante fauna de roedores, incluindo representantes de 4 das 5 subordens do grupo: Sciuromorpha, Castorimorpha, Hystricomorpha e Myomorpha (Patton et al. 2015). A subfamília Sigmodontinae (Wagner, 1843), por exemplo, compreende a mais diversa linhagem de mamíferos das Américas, com 87 gêneros e mais de 400 espécies nominais reconhecidas (D'Elía & Pardiñas 2015; Pardiñas et al. 2016). Dentre as 11 tribos até hoje reconhecidas dos roedores de Sigmodontinae (Gonçalves et al. 2018), Akodontini é a segunda tribo mais diversa, sendo composta por 16 gêneros (D'Elia & Pardiñas 2015b; Pardiñas et al. 2016). Apesar da alta diversidade atualmente reconhecida, a sistemática envolvendo diferentes níveis taxonômicos ainda permanece incerta em sigmodontíneos (D'Elía & Pardiñas 2015).

O gênero *Oxymycterus*

O gênero *Oxymycterus* foi descrito por Waterhouse (1837), originalmente como um subgênero de *Mus*, embora Fischer tenha descrito *Mus rufus* (*Oxymycterus rufus*), em 1814, com base na descrição de Felix Azara do "*rat cinquième* ou *rat roux*" em 1801 (Contreras & Teta 2003; Oliveira & Gonçalves 2015). A espécie tipo é *Oxymycterus nasutus* (Waterhouse, 1837), descrito a partir do espécime tipo coletado por Charles Darwin durante a sua estada em Maldonado, no Uruguai (Oliveira & Gonçalves 2015). O registro fóssil mais antigo de *Oxymycterus* data para

estágio Ensenadense (0.5 – 2.1 Ma) para as chamadas glaciações Patagônicas, sendo designado a *O.* cf. *rufus* registrado nos Pampas Argentinos (Pardiñas et al. 2002). O gênero é composto por 15 espécies válidas (Oliveira & Gonçalves 2015), e tem o status de segundo gênero mais diversificado dentro da tribo Akodontini, depois do gênero *Akodon* (Meyen, 1833) com 39 representantes (Pardiñas et al. 2016). Está amplamente distribuído na América do Sul, sendo encontrado em regiões de média latitude no subcontinente Sulamericano (Figura 1), desde porção sul da bacia Amazônica, Andes do Peru e Bolívia, centro da Argentina, Uruguai, Paraguai e Brasil, em terras mais baixas (planícies), planaltos, e em elevações de até 4.000 m (Hershkovitz 1994; Oliveira & Gonçalves 2015). Dentre sua distribuição, ocupa diversas ecorregiões em diferentes fitofisionomias, tais como: Florestas de Yungas, Mata Atlântica, floresta Amazônica, Cerrado, Pampas, campos de altitude, Caatinga, Cerrado, áreas abertas e florestal montana Andinas, geralmente associado a ambientes úmidos como banhados, florestas de galeria e próximo a rios (Hinojosa et al. 1987; Hershkovitz 1994; Cueto et al. 1995; Bonvicino et al. 2008; Jayat et al. 2008; González & Martínez-Lanfranco 2010; d'Hiriart et al. 2015; Abreu-Júnior et al. 2016).

As espécies deste gênero são caracterizadas por possuirem um tamanho corporal variando entre pequeno e médio porte (comprimento cabeça-corpo [CC] de 99-197 mm e comprimento da cauda [CA] entre 70-156 mm), com cauda (aproximadamente) igual e/ou menor que o comprimento do corpo, sendo *Oxymycterus hucucha* a menor espécie, enquanto os maiores são atribuídos para *O. quaestor* (Oliveira & Gonçalves 2015). A coloração da pelagem dorsal pode variar do preto, marrom escuro, vermelho ou laranja *agouti*, possuindo o ventre mais claro. Sem limite definido com o dorso, a coloração do ventre deste gênero varia nas espécies de amarelo-acinzentado-escuro a laranja-escuro. A pelagem geralmente é densa, podendo ser em alguns casos híspida (arrepiada) e brilhosa. Algumas espécies possuem uma pelagem fortemente tracejada de preto, (Hershkovitz 1994; Bonvicino et al. 2008; Oliveira & Gonçalves 2015). A superfície superior das patas é

revestida de pelos curtos escuros, as orelhas são também recobertas por pelos curtos escuros, mais escassos na superfície externa (Bonvicino et al. 2008). A característica morfológica mais evidente do gênero são garras bem desenvolvidas e focinho longo, cauda geralmente pouco pilosa e com as escamas aparentes, pelos ungueais escuros e escassos (Bonvicino et al. 2008). Devido ao seu focinho prolongado, é denominado, de forma geral por pesquisadores de idioma hispânico como '*Hocicudo*' (= focinhudo ou narigudo, em português); em inglês, também são designados como '*Long-nosed mouse*' (= Rato-do-nariz-longo, em português). No Brasil, são rotineiramente denominados como 'Rato-do-brejo' (Hershkovitz 1994; Paise & Vieira 2006; onçalves et al. 2014).

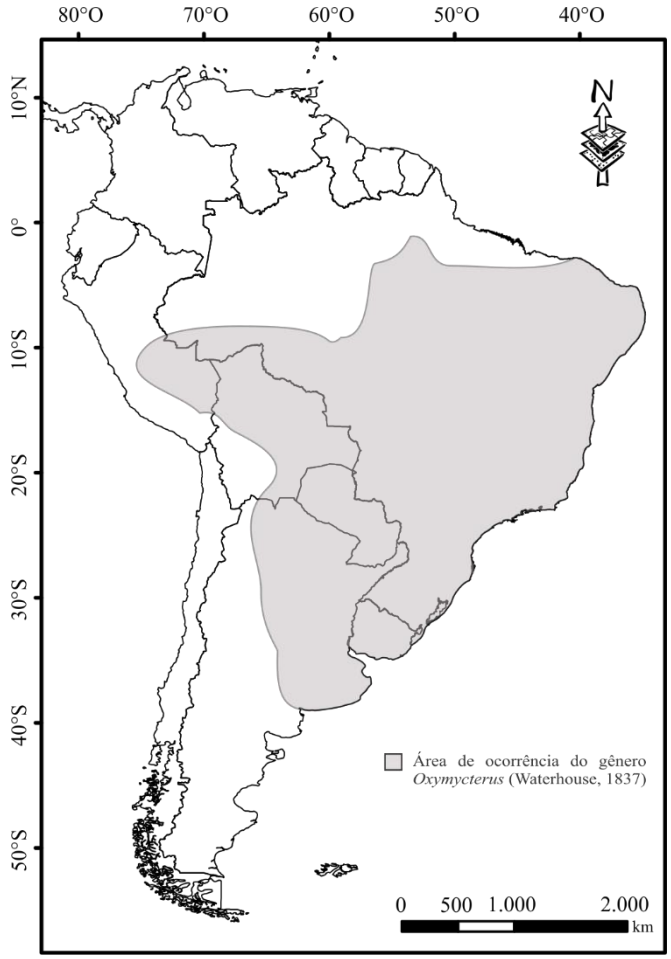

Figura 1. Distribuição geográfica do gênero *Oxymycterus* Waterhouse (1837) na América do Sul (em destaque). Adaptado de Oliveira & Gonçalves (2015).

Dados sobre o comportamento de *Oxymycterus* são escassos, e limitados a observações a poucas espécies (Barlow 1969; Alho 1982; Redford 1984; Paise & Vieira 2006). Devido à presença de longas garras, especula-se que congêneres tenham hábito fossorial (Hershkovitz 1994). Entretanto, Bonvicino et al. (2008) sugerem que o gênero possui hábitos terrestre e semi-fossorial. Há pouca disponibilidade de informações sobre hábitos alimentares. Em geral, observado em algumas espécies, a dieta é baseada em artrópodes (e.g., cupins), anelídeos, coleópteros, gastrópodes e material de origem vegetal (Hershkovitz 1994; Oliveira & Gonçalves 2015). Podem ser predados por serpentes, como as víboras *Bothrops* spp. em registros na Amazônia (Oliveira & Gonçalves 2015), pela raposa-colorada ou raposa-andina (*Lycalopex culpaeus*) nos Pampas argentinos (Pia et al. 2003), cachorro-do-mato ou graxaim (*Cerdocyon thous*) nos Pampas brasileiros (Pedó et al. 2006) e por aves de rapina em zonas de transição entre Mata Atlântica e Pampas (Scheibler & Christoff 2007) e Mata Atlântica e Cerrado (Motta-Junior 2006).

Além disso, algumas espécies são potencialmente reservatórios patogênicos de hantavírus no Uruguai e no sul do Brasil (Delfraro et al. 2008; Raboni et al. 2009; Raboni et al. 2012), embora o número de indivíduos infectados seja significativamente menor quando comparado a outros roedores. No norte do Brasil, alguns espécimes foram verificados como portadores de uma forma patogênica de *Escherichia coli* (Rocha et al. 2017).

Oxymycterus apresenta uma característica citogenética marcante. Apresenta um cariótipo quase constante (2n = 54 e NF = 62-66), variando apenas o número de braços cromossômicos e alterando seu número fundamental (Di-Nizo et al. 2017). Hershkovitz (1994) ainda menciona que o gênero aparenta ter caracteres citogenéticos monomórficos, sendo que as espécies não podem ser distinguidas citogeneticamente. Apesar da similaridade cariotípica, as linhagens de *Oxymycterus*

apresentam divergencia interespecífica nas sequências do gene mitocondrial citocromo *b* (citb) que varia em torno de 1,9 à 9,6% (Hoffmann et al. 2002).

Taxonomia e implicações

Dentre as 15 espécies de *Oxymycterus* atualmente reconhecidas (Tabela 1), quatro formas (cerca de 38% das espécies válidas) foram descritas ao longo dos últimos 25 anos (Hershkovitz 1994, Hershkovitz 1998, Hoffmann et al. 2002, Jayat et al. 2008). Apesar de revisões mais recentes de Musser & Carleton (2005) e Oliveira & Gonçalves (2015), algumas abordagens sistemáticas anteriores envolvendo do gênero *Oxymycterus* foram realizadas por Hershkovitz (1994) e Oliveira (1998), com propostas de arranjos taxonômicos e de hipóteses de diferenciação do gênero na América do Sul, entretanto, sem envolver marcadores moleculares.

Hershkovitz (1994), em uma primeira compilação taxonômica do gênero *Oxymycterus*, por exemplo, reconhece 23 formas nominais do gênero, e as subdivide em dois grupos: Atlântico e Andino, e que através de medidas externas e craniométricas, foram classificadas de tamanho pequeno, médio e grande dentro de cada grupo.

Oliveira (1998) com base em análises de medidas morfológicas e utilizando materiais tipos depositados em coleções, diverge da hipótese de dois grupos (Atlântico e Andino), e propõe a existência de 10 grupos de espécies do gênero (*angularis*, *judex*, *rufus*, *dasytrichus*, *amazonicus*, *delator*, *nasutus*, *inca*, *juliacae* e *paramensis*), e aponta algumas sinonímias, reconhecendo maior complexidade na estrutura da variabilidade morfológica do gênero. No entanto, a delimitação de espécies é fortemente apoiada por marcadores moleculares, devido às dificuldades em detectar descontinuidades em caracteres morfológicos e/ou citogenéticos (Hershkovitz,1994; Hoffmann et al. 2002; Gonçalves & Oliveira, 2004).

Tabela 1. Espécies de *Oxymycterus* listadas por Oliveira e Gonçalves (2015).

Oxymycterus
- *nasutus* Waterhouse, 1837
- *amazonicus* Hershkovitz, 1994
- *caparaoe* Hershkovitz, 1998
- *dasytrichus* Schinz, 1821
- *delator* Thomas, 1903
- *hiska* Hinojosa, Anderson & Patton, 1987
- *hucucha* Hinojosa, Anderson & Patton, 1987
- *inca* Thomas, 1900
- *paramensis* Thomas, 1902
- *quaestor* Thomas, 1903
- *rufus* Fischer, 1814
- *wayku* Jayat, 2008
- *josei* Hoffman, Lessa & Smith, 2002
- *juliacae* Allen, 1900
- *nigrifrons* Osgood, 1944

As revisões de Musser & Carleton (2005) e Oliveira & Gonçalves (2015), assim como outros trabalhos de levantamentos de diversidade, apesar dos avanços, têm apontado a existência de questões taxonômicas relevantes a serem elucidadas, como: (1) espécies consideradas sinônimas (formas nominais como coespecíficas), como por exemplo o caso de sinonímia de *Oxymycterus judex* Thomas, 1909 e *O. misonalis* Sanborn, 1931 [= *O. quaestor* Thomas, 1903], *Oxymycterus akodontius* Thomas, 1921 e *Oxymycterus paramensis jacentior* Thomas, 1925 [= *Oxymycterus paramensis* Thomas, 1902]; (2) espécies descritas / conhecidas para poucas localidades ou mesmo apenas pela localidade tipo (*Oxymycterus nigrifrons* Osgood, 1944, *Oxymycterus hucucha* Hinojosa et al. 1987, *Oxymycterus caparaoe* Hershkovitz, 1998); (3) espécies com distribuição disjunta (lacunas na faixa de distribuição geográfica), como apresentado pelas espécies *O. quaestor* Thomas, 1903 e *O. rufus* Fischer, 1814); (4) Filogenias apontando status parafilético, como o caso de *Oxymycterus paramensis* Thomas, 1903 ou mesmo constituindo um complexo de espécies em *O. paramensis* (Hinojosa et al. 1987; Hershkovitz, 1994, 1998; Gonçalves & Oliveira, 2004; Musser & Carleton, 2005; D'Elía et al. 2008; Bonvicino et al. 2008; Jayat et al. 2008). Embora estudos

prévios tenham utilizado distintas abordagens sistemáticas, a diversidade de espécies e área de distribuição permanecem pouco documentadas. Assim, mesmo a taxonomia alfa do gênero ainda apresenta lacunas (Oliveira & Gonçalves 2015).

Relações filogenéticas e problemática

Reconstruções filogenéticas do gênero *Oxymycterus* através de máxima verossimilhança e parcimônia, têm sido realizadas com base em marcadores moleculares mitocondriais (i.e. citb), concomitante com análises craniométricas (Hoffmann et al. 2002; Gonçalves & Oliveira 2004; Jayat et al. 2008). Estes estudos integrativos, relacionando morfologia (craniometria) e marcadores moleculares vêm fornecendo novas informações sobre o grupo. Os marcadores moleculares, em especial o citb (mtDNA), têm se mostrado como um robusto método de identificação de espécies, levantando inclusive, questões como a expansão da distribuição geográfica de algumas espécies, sinalização da existência de linhagens, indicativo de sinonímias e novas espécies (Smith & Patton 1999; Hoffmann et al. 2002; Gonçalves & Oliveira, 2004; Jayat et al. 2008; Peçanha et al. 2016).

Abordagens multilócus baseadas em inferência bayesiana e calibrações fósseis, apesar de incorporar representantes do gênero disponíveis em banco de dados (e.g. Genbank), fazem parte de filogenias de grupos maiores, como padrões da Ordem Rodentia (Fabre et al. 2012), da Superfamília Muroidea (Steppan & Schenk 2017) e da Subfamília Sigmodontinae (Parada et al. 2015), embora apresentem estimativas no tempo de diversificação do grupo. Contudo, outros estudos multilócus apresentam alguns aspectos das relações interespecíficas, como a formação de uma linhagem irmã altamente suportado com o gênero *Juscelinomys* (D'Elía 2003; Salazar-Bravo et al. 2013; Leite et al. 2014, Parada et al. 2015). No entanto, as propostas utilizando abordagens multilócus, estão passíveis de erros para a linhagem *Oxymycterus* em nível intraespecífico, devido

não incorporar todas as espécies do gênero ou mesmo incorporando dados passíveis de erros em banco de dados. Dessa forma, a problemática é devido provavelmente a duas principais causas:

1- Caracteres de identificação citogenética e morfológica contínuos.

Embora o gênero possua características intrínsecas de identificação, a maioria das espécies do gênero compartilha similaridade morfológica, restritas a caracteres específicos sutis de modo geral. Em destaque, Oliveira e Gonçalves (2015) descrevem que a mais notável característica morfológica (craniométrica) que as distinguem é a largura da raiz do zigomático inferior, na curvatura formada pela margem anterior das placas zigomáticos. A coloração dos pelos, assim como o tamanho entre as espécies também podem ser considerados, entretanto, nesse aspecto morfológico, espécimes juvenis amostrados podem apresentar conflitos de identificação (Bonvicino et al. 2008; Oliveira & Gonçalves, 2015) o que torna a identificação de espécies imprecisa, deixando muitas vezes a classificação de forma genérica aos espécimes deste táxon em coleções científicas. Nesse mesmo contexto, a identificação via técnicas citogenéticas também não apresentam poder de distinção entre as espécies, devido à similaridade cariotípica e número diploide constante (Hershkovitz, 1994). O gênero apresenta em seu cariótipo 2n = 54 e NF = 62-66 (Sbalqueiro, 1989; Svartman e Almeida, 1993; Bonvicino *et al.* 2005; Di-Nizo et al. 2017). Tal padrão cariotípico, do gênero *Oxymycterus*, é algo peculiar, em especial, dentro do grupo dos Sigmodontíneos, visto que a diversificação altamente específica é observada em toda subfamília Sigmodontinae presente em todas as suas tribos, e é caracterizada por uma notável variabilidade de números diploides, que variam de 2n = 16 a 86 em Oryzomyini, e 2n = 10 a 70 em Akodontini (Patton et al. 2000; Gonçalves et al. 2005; Silva et al. 2006).

2- Limites genéticos pouco explorados.

Nos últimos anos, autores que têm realizado trabalhos com o gênero, tem aliado mensurações crânio-dentárias e marcadores moleculares, em especial o gene mitocondrial citb, e têm avançado

consideravelmente a compreensão da taxonomia e filogenia do gênero *Oxymycterus* (e.g. Hoffmann et al. 2002; Gonçalves & Oliveira 2004; D'Elia et al. 2008; Jayat et al. 2008). No entanto, dados disponíveis em banco de dados (e.g. Genbank e BOLD Systems) são limitados, além de serem passíveis de erros na identificação. Este problema dá-se possivelmente a erros de identificação via caracteres morfológicos e possíveis sinonímias para algumas espécies. Apesar das inferências filogenéticas e propostas para estimativas de divergências interespecíficas entre linhagens (Baker & Bradley 2006), as abordagens baseiam-se em sequências depositadas nestes bancos de dados, sendo que nem todas as espécies do gênero possuem sequências depositadas (e.g. *Oxymycterus caparaoe*, *O. hucucha*, *O. inca*), o que acaba reduzindo o poder de inferência filogenética das propostas existentes. Desta forma, os limites genéticos entre as espécies do gênero *Oxymycterus*, ainda são pouco explorados.

Espécies do sul do Brasil e territórios adjacentes

De acordo com a revisão de Oliveira & Gonçalves (2015), quatro espécies do gênero *Oxymycterus* (*O. dasytrichus*, *O. quaestor*, *O. nasutus* e *O. delator*) possuem distribuição geográfica no sul do Brasil (Figura 2). Estas distribuiçãoes, inclui extensões de distribuição aos territórios da Argentina (*O. quaestor*), Paraguai (*O. delator*) e Uruguai (*O. nasutus*), através das fitofisionomias da Mata Atlântica (Densa, Mista e Estacional), Cerrado e dos Campos Sulinos (Pampas e campos de altitude), respectivamente. Em exceção, *O. dasytrichus* é a única espécie que possui distribuição geográfica exclusiva em território brasileiro, dos estados do Paraná a Pernambuco, pelas florestas de interiores e principalmente florestas costeiras (Oliveira & Gonçalves 2015). Ainda *O. delator*, apesar ter sua distribuição do leste do Paraguai ao Brasil central, principalmente pelo Cerrado brasileiro, verifica-se registros aos domínios do Cerrado mais ao sul do

Brasil, incluindo os estados do Paraná e São Paulo (Bonvicino et al. 2008; Oliveira & Gonçalves 2015).

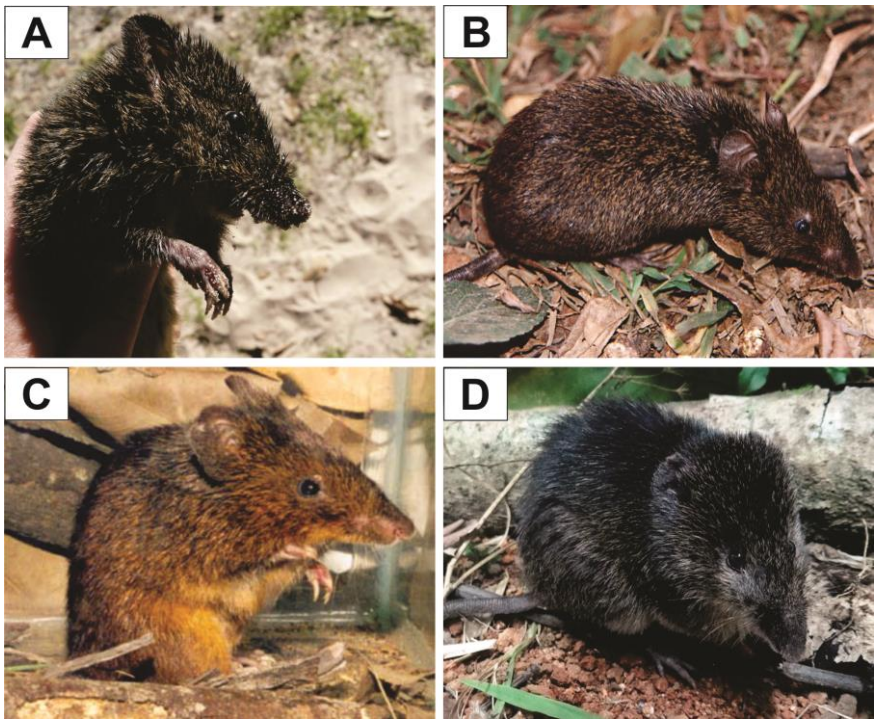

Figura 2. Representantes do gênero *Oxymycterus* presentes no sul da Mata atlântica e Pampas: (A) *O. delator* [1], (B) *O. dasytrichus* [2], (C) *O. quaestor* [3], e (D) *O. nasutus* [4].

Apesar da ampla distribuição destas espécies, as inferências filogenéticas, geralmente pouco utilizam espécies ocorrentes no sul do Brasil, e são desenvolvidos em conjunto com dados craniométricos via morfometria linear (=clássica), comparando-as com poucos espécimes (inclusive poucas localidades) e geralmente com congêneres de "distribuição restrita" e simpátrica, sem que tenha um amplo espectro amostral (e.g. Gonçalves & Oliveira 2004; Jayat et al. 2008). Apesar da morfometria geométrica em sigmodontíneos ainda ser pouco explorada (Martinez & Cola 2011;

[1]Imagem autorizada por Karina Atkinson e Disponível em: http://www.faunaparaguay.com/oxymycterusdelator.html Acesso em fev. 2019. [2]Imagem cedida por Pablo Rodrigues Gonçalves e Disponível em: https://animaldiversity.org/collections/contributors/pablo_goncalves/O.dasytrichus_a/ Acesso em fev. 2019. [3]Imagem autorizada por Cibele Rodrigues Bonvicino. Fonte: Bonvicino et al. 2008, p. 50. [4]Imagem autorizada por Fernando Marques Quintela. Fonte: Gonçalves et al. 2014, p. 79.

Quintela et al. 2016; Maestri et al. 2016; Boroni et al. 2017), estudos demonstram que essa técnica se apresenta como uma promissora ferramenta em estudos inter e intraespecíficos, revelando padrões que não são observados via técnicas de morfometria clássica. Assim, as distâncias morfológicas e principalmente genéticas, de modo intra- e interespecífica ainda não são conhecidas para os táxons dessa região geográfica (i.e. domínios da Mata Atlântica Sul e Pampas), de forma que possam ser comparados e discutidos os limites de forma clara.

Também, o conhecimento vago das formas nominais do sul do Brasil, originalmente proposto como parte de um grupo de espécies, como por exemplo o grupo '*judex*' (Oliveira 1998), ainda não foi explorado. Neste sentido, apesar da IUCN *Red List of Threatened Species* categorizar o status de conservação das espécies supracitadas como pouco preocupante [*Least Concern* – LC, em inglês] (D'Elía & Teta 2016; D'Elía & Pardiñas 2016; Patterson et al. 2016; Patterson & D'Elía 2016; Bonvicino 2016; Bonvicino et al. 2016; Patton et al. 2016), tais considerações categóricas devem ser vistas com cautela, devido à presença de formas nominais e incompatibilidade de distribuição geográfica com revisões mais recentes do gênero. Dessa forma, há um amplo desconhecimento sobre a história evolutiva envolvendo a biogeografia de *Oxymycterus* no sul do Brasil, incluindo padrões filogeográficos e morfológicos para os taxa reconhecidos.

OBJETIVO

O objetivo central do presente trabalho é investigar a variação genética e morfológica em espécies de *Oxymycterus* que ocupam distintas fitofisionomias, como áreas abertas e florestais, utilizando abordagem sistemática, filogeográfica e macroevolutiva. Abaixo são apresentados os objetivos específicos que abrangem esse estudo.

1) Investigar padrões de variação genética e morfológica intraespecífica em *Oxymycterus nasutus* de forma a testar a hipótese de estruturação geográfica Mata Atlântica vs. Pampas;

2) Testar a existência de estruturação geográfica vicariante Planície (Pampa) vs. Planalto Meridional (Floresta Atlântica) na forma e tamanho do crânio em *O. nasutus*, e analisar fatores influentes (i.e., ambiente e genética);

3) Descrever e comparar a variação genética e morfológica de *Oxymycterus* sp. e espécies simpátricas provenientes da região de Cerrado de São Paulo e do Paraná, de forma a delimitar linhagens filogenéticas distintas;

4) Caracterizar a variação genética e morfológica dentro do 'grupo judex' (proposto por Oliveira, 1998) (*Oxymycterus quaestor*, *O. judex* e *O. misionalis*) e propor limites conspícuos para as espécies.

REFERÊNCIAS BIBLIOGRÁFICAS

Abreu-Júnior, E.F., M.A. Freitas, M.J. Lapenta, N.M. Venâncio, D.P.F. França, A.R. Percequillo. (2016). Marsupials and rodents (Didelphimorphia and Rodentia) of upper Rio Acre, with new data on *Oxymycterus inca* Thomas, 1900 from Brazil. Check List, 12: 1956.

Alho CJR. (1982) Brazilian Rodents: Their Habitats and Habits. *In:* Mares, M. A. & H. H. Genoways (eds.). Mamalian Biology in South America. Special Publication Series, vol. 6, Pittsburgh, University of Pittsburgh, pp 143-166.

Baker RJ, Bradley RD. (2006). Speciation in mammals and the genetic species concept. Journal of Mammalogy, 87(4), 643-662.

Barlow JC. (1969). Observations on the biology of rodents in Uruguay. Life sci. contrib., Royal Ontario Museum, 75:1–59.

Bonvicino CR, Lemos B, Weksler M. (2005) Small mammals of chapada dos Veadeiros National Park (Cerrado of Central Brazil): Ecologic, Karyologic, and Taxonomic Considerations. Brazilian Journal of Biology, 65 (3): 395- 406.

Bonvicino CR, Oliveira JA, D'Andrea OS. (2008) Guia dos roedores do Brasil, com chaves para gêneros baseadas em caracteres externos. Centro Pan-Americano de Febre Aftosa - OPAS/OMS.

Bonvicino CR, Weksler M, Percequillo A. (2016) *Oxymycterus hispidus* (errata version published in 2017). *The IUCN Red List of Threatened Species* 2016: e.T15785A115129629. http://dx.doi.org/10.2305/IUCN.UK.20163.RLTS.T15785A22378344.en. Downloaded on 07 March 2019.

Bonvicino CR. (2016) *Oxymycterus dasytrichus*. *The IUCN Red List of Threatened Species* 2016: e.T136813A22378179. http://dx.doi.org/10.2305/IUCN.UK.20162.RLTS.T136813A22378179.en. Downloaded on 07 March 2019.

Boroni NL, Lobo LS, Romano PSR, Lessa G. (2017) Taxonomic identification using geometric morphometric approach and limited data: an example using the upper molars of two sympatric species of Calomys (Cricetidae: Rodentia).Zoologia, 34: 1-11.

Contreras JR, Teta P. (2003) Acerca del estatus taxonómico y de la localidad típica de *Oxymycterus rufus* (Fisher, 1814) (Rodentia: Muridae: Sigmodontinae). Nótulas Faunísticas, 14:1-5.

Cueto VR, Piantanida MJ, Cagnoni, M. (1995) Population demography of *Oxymycterus rufus* (Rodentia: Cricetidae) inhabiting a patchy environment of the delta of the Paraná River, Argentina. Acta Theriologica, 40: 123-130.

D'Elía G, Mora I, Myers P, Owen RD. (2008) New and noteworthy records of Rodentia (Erethizontidae, Sciuridae, and Cricetidae) from Paraguay. Zootaxa, 1784: 39–57.

D'Elía G, Pardiñas UFJ. (2015) Subfamily Sigmodontinae Wagner, 1843 *In*: Mammals of South America, Volume 2: Rodents. Edited by Patton JL, Pardiñas UFJ, D'Elía G. Chicago: University Of Chicago Press, pp 63-70.

D'Elía G, Pardiñas UFJ. (2015b) Tribe Akodontini Vorontzov, 1959. *In:* Mammals of South America, Volume 2: Rodents. Edited by Patton JL, Pardiñas UFJ, D'Elía G. Chicago: University Of Chicago Press, pp 140-144.

Delfraro A, Tomé L, D'Elía G, Clara M, Achával F, Russi JC, Arbiza Rodonz JR. (2008) Juquitiba-like hantavirus from 2 nonrelated rodent species, Uruguay. Emerging infectious diseases, 14(9): 1447-51.

D'Elía G, Pardinas U. (2016) *Oxymycterus quaestor* (errata version published in 2017). *The IUCN Red List of Threatened Species* 2016: e.T136613A115210389. http://dx.doi.org/10.2305/IUCN.UK.20163.RLTS.T136613A22378632.en.Downloaded on 07 March 2019.

D'Elía G, Teta P. (2016). *Oxymycterus nasutus* (errata version published in 2017). *The IUCN Red List of Threatened Species* 2016: e.T15789A115129860. http://dx.doi.org/10.2305/IUCN.UK.2016-3.RLTS.T15789A22377924.en. Downloaded on 07 March 2019.

D'Elía G. (2003) Phylogenetics of Sigmodontinae (Rodentia, Muroidea, Cricetidae), with special reference to the Akodont group, and with additional comments on historical Biogeography. Cladistics, (19):307-323.

d'Hiriart S, Russo C, Ortiz P, Jayat J (2015) Range extension of *Oxymycterus wayku* (Mammalia: Rodentia: Cricetidae), an endemic species from austral Yungas, and first record for Catamarca province, northwestern Argentina. Check List 11(5): 1738.

Di-Nizo CB, Banci KRS, Sato-Kuwabara Y, Silva MJJ. (2017) Advances in cytogenetics of Brazilian rodents: cytotaxonomy, chromosome evolution and new karyotypic data. Comparative Cytogenetics 11(4): 833–892.

Fabre P-H, Hautier L, Dimitrov D, Douzery EJP. (2012) A glimpse on the pattern of rodent diversification: a phylogenetic approach. BMC Evolutionary Biology, 12:88.

Gonçalves LG, Quintela FM, Freitas TRO. (2014) Mamíferos do Rio Grande do Sul. Porto Alegre: Pacartes, 212 p.

Gonçalves PR, Christoff AU, Machado LF, Bonvicino CR, Peters FB. (2018) Unraveling Deep Branches of the Sigmodontinae Tree (Rodentia: Cricetidae) in Eastern South America. Journal of Mammalian Evolution, 1–22.

Gonçalves PR, Oliveira JA. (2004) Morphological and Genetic Variation between Two Sympatric Forms of *Oxymycterus* (Rodentia: Sigmodontinae): An Evaluation of Hypotheses of Differentiation within the Genus. Journal of Mammalogy, 85(1):148-161.

Gonçalves, PR, Oliveira JA, Corrêa MO, Pessôa. LM. (2005) Morphological and cytogenetic analyses of *Bibimys labiosus* (Winge, 1887) (Rodentia, Sigmodontinae): implications for its affinities with the Scapteromyine Group; pp. 175–209, *In*: E. Lacey e P. Myers (ed.). Mammalian Diversification – From Chromosomes to Phylogeography (A celebration of the career of James L. Patton). Volume 133. Berkeley: University of California Publication on Zoology.

González, E.M., & Martinez-Lanfranco, J.A. (2010) Mamíferos de Uruguay. Guía de campo e introducción a su estúdio y conservación. Banda Oriental, Museo Nacional de Historia Natural, Vida Silvestre Uruguay, Montevideo, 463 pp.

Grazzini G, Mochi-Junior CM, Oliveira Heloisa, Pontes JS, Gatto-Almeida F, Tiepolo LM. (2015) Identidade, riqueza e abundãncia de pequenos mamíferos (Rodentia e Didelphimorphia) de área de Floresta com Araucária no estado do Paraná, Brasil. Papéis Avulsos de Zoologia, Museu de Zoologia da Universidade de São Paulo, 55(15): 217-230.

Hershkovitz P. (1994) The description of a new species of South American hocicudo, or long-nose mouse genus *Oxymycterus* (Sigmodontinae, Muroidea), with a critical review of the generic content. Fieldiana: Zoology (New Series), 1460 (79):1–43.

Hershkovitz P. (1998) Report on some sigmodontinae rodents collected in southeastern Brazil with descriptions of a new genus and six new species. Bonner zoologische Beiträge**,** 47: 193-256.

Hinojosa PF, Anderson S, Patton JL. (1987) Two new species of *Oxymycterus* (Rodentia) from Peru and Bolivia. American Museum Novitates, 2898: 1–17.

Hoffmann FG, Lessa EP, Smith MF. (2002) Systematics of *Oxymycterus* with description of a new species from Uruguay. Journal of Mammalogy**,** 83(2): 408-420.

Jayat JP, D'Elía G, Pardiñas UFJ, Miotti MD, Ortiz PE. (2008) A new species of the genus *Oxymycterus* (Mammalia: Rodentia: Cricetidae) from the vanishing Yungas of Argentina. Zootaxa, 1911: 31–51.

Leite RN, Kolokotronis S-O, Almeida FC, Werneck FP, Rogers DS, Weksler M. (2014) In the Wake of Invasion: Tracing the Historical Biogeography of the South American Cricetid Radiation (Rodentia, Sigmodontinae). PLoS One, 9(6): e100687.

Maestri R, Fornel R, Gonçalves GL, Geise L, TRO, AC. (2016) Predictors of intraspecific morphological variability in a tropical hotspot: comparing the influence of random and non-random factors. Journal of Biogeography, 43: 2160–2172.

Martínez JJ, Di Cola V. (2011) Geographic distribution and phenetic skull variation in two close species of *Graomys* (Rodentia, Cricetidae, Sigmodontinae). Zoologischer Anzeiger 250: 175-194.

Motta-Junior, JC. (2006) Relações tróficas entre cinco Strigiformes simpátricas na região central do Estado de São Paulo, Brasil. Revista Brasileira de Ornitologia, 14 (4): 359-377.

Musser GG, Carleton MD (2005) Superfamily Muroidea, pp 894–1531. *In:* Wilson DE, Reeder DM (eds.) Mammal Species of the World: a taxonomic and geographic reference 3. ed. Baltimore: The Johns Hopkins University Press, 2142 pp.

Oliveira JA. (1998) Morphometric assessment of species groups in the South American rodent genus *Oxymycterus* (Sigmodontinae), with taxonomic notes base on the analysis of type material. Tese de doutorado, Texas Tech University, 320 p.

Oliveira, JA, Gonçalves PR. (2015) Suborder Myomorpha: Family Cricetidae: Subfamily Sigmodontinae. Genus *Oxymycterus In:* Patton JL, Pardiñas UFJ, D'Elía G. (eds.). Mammals of South America 2: Rodents. Chicago: University of Chicago Press, pp. 247-268.

Paise G, Vieira EM. (2006) Daily activity of a neotropical rodent (*Oxymycterus nasutus*): seasonal changes and influence of environmental factors. Journal of Mammalogy, 87(4):733–739.

Parada A, D'Elía G, Palma ED. (2015) The influence of ecological and geographical context in the radiation of Neotropical sigmodontine rodents. BMC Evolutionary Biology, 15:172.

Pardiñas UFJ, D'Elia G, Ortiz PE. (2002) Sigmodontinos fósiles (rodentia, muroidea, sigmodontinae) de América del sur: estado actual de su conocimiento y prospectiva. Mastozoología Neotropical / J. Neotrop. Mammal, 9(2):209-252.

Pardiñas, U. F. J., Teta, P., Alvarado-Serrano, D., Geise, L., Jayat, J. P., Ortiz, P. E., Golçalves, P. R. & Délia, G. Genus *Akodon*. Pp 475-645 in Patton J.L. Pardiñas, U.F.J & D'Elia, G. (Eds.) Mammals of South America, Volume 2: Rodents, University of Press, Chicago.

Pardiñas UFJ, Geise L, Ventura K, Lessa G. (2016) A new genus for *Habrothrix angustidens* and *Akodon serrensis* (Rodentia, Cricetidae): again paleontology meets neontology in the legacy of lund. Mastozoología neotropical, 23(1), 93-115.

Patterson B, D'Elía G, Pardinas U, Teta P. (2016) *Oxymycterus delator* (errata version published in 2017). *The IUCN Red List of Threatened Species* 2016: e.T15784A115129513. http://dx.doi.org/10.2305/IUCN.UK.20163.RLTS.T15784A22377764.en. Downloaded on 07 March 2019.

Patterson B, D'Elía G. (2016) *Oxymycterus roberti* (errata version published in 2017). *The IUCN Red List of Threatened Species* 2016: e.T15791A115130098. http://dx.doi.org/10.2305/IUCN.UK.20163.RLTS.T15791A22378104.en. Downloaded on 07 March 2019.

Patton JL, da Silva MNF, Malcolm JR. (2000) Mammals of the rio Juruá and the evolutionary and ecological diversification of Amazonia. Bull Am Mus Nat Hist. 244:1–306.

Patton J, Catzeflis F, Weksler M, Percequillo M. (2016) *Oxymycterus angularis* (errata version published in 2017). *The IUCN Red List of Threatened Species* 2016: e.T15783A115129406. http://dx.doi.org/10.2305/IUCN.UK.20163.RLTS.T15783A22377695.en. Downloaded on 07 March 2019.

Patton JL. (2015) Suborder Myomorpha: Family Cricetidae G. Fischer, 1817 *In:* Patton JL, Pardiñas UFJ, D′Elía G. (eds.). Mammals of South America 2: Rodents. Chicago: University of Chicago Press, pp 58-60.

Peçanha WT, Gonçalves GL, Althoff SL, Freitas TRO, Hass I. (2016) Range extension of the Atlantic Forest Hocicudo *Oxymycterus dasytrichus* (Schinz, 1821) to the state of Santa Catarina, southern Brazil. CheckList, 12(1): 1847.

Pedó E, Tomazzoni AC, Hartz SM, Christoff AU. (2006) Diet of crab-eating fox, Cerdocyon thous (Linnaeus) (Carnivora, Canidae), in a suburban area of southern Brazil. Revista Brasileira de Zoologia, 23(3), 637-641.

Pia MV, Lopez MS, Novaro AJ. (2003) Effects of livestock on the feeding ecology of endemic culpeo foxes (*Pseudalopex culpaeus smithersi*) in central Argentina. Revista Chilena de Historia Natural 76(2):313-321.

Quintela FM, Fornel R, Freitas TRO. (2016) Geographic variation in skull shape of the water rat Scapteromys tumidus (Cricetidae, Sigmodontinae): isolation-by-distance plus environmental and geographic barrier effects? Anais da Academia Brasileira de Ciências, 88 (Suppl. 1), 451-466.

Raboni SM, Delfraro A, de Borba L, Teixeira BR, Stella V, de Araujo MR, Carstensen S, Rubio G, Maron A, Lemos ER, D'Andrea PS, Duarte dos Santos CN. (2012) Hantavirus infection prevalence in wild rodents and human antihantavirus serological profiles from different

geographic areas of South Brazil. American Journal of Tropical Medicine and Hygiene, 87 (2): 371–378.

Raboni SM, Hoffmann FG, Oliveira RC, Teixeira BR, Bonvicino CR, Stella V, Carstensen S, Bordignon J, D'Andrea PS, Lemos ER, Duarte dos Santos CN. (2009) Phylogenetic characterization of hantaviruses from wild rodents and hantavirus pulmonary syndrome cases in the state of Parana (southern Brazil). Journal of General Virology, 90: 2166-2171.

Redford KH. (1984) Mammalian predation on termites: tests with the burrowing mouse (*Oxymycterus roberti*) and its prey. Oecologia, 65(1):145-152.

Rocha DCC, Marinho ANR, Santos SD, Loureiro ECB. (2018) Molecular characterization of atypical enteropathogenic *Escherichia coli* in wild animals captured in the Amazon Region. Revista Pan-Amazônica de Saúde, 8(1): 9-16.

Salazar-Bravo J, Pardiñas UFJ, D'Elía G. (2013) A phylogenetic appraisal of Sigmodontinae (Rodentia, Cricetidae) with emphasis on phyllotine genera: systematics and biogeography. Zoologica Scripta, 42 (3): 250-261.

Sbalqueiro IJ. (1989) Análises cromossômicas e filogenéticas em algumas espécies de roedores da Região Sul. Porto Alegre, Tese de Doutorado, Universidade Federal do Rio Grande do Sul. 296p.

Scheibler DR, Christoff AU. (2007) Habitat associations of small mammals in southern Brazil and use of regurgitated pellets of birds of prey for inventorying a local fauna. Brazilian Journal of Biology, 67(4), 619-625.

Silva MJJ, Patton JL, Yonenaga-Yassuda Y. (2006) Phylogenetic relationships and karyotype evolution in the Sigmodontine rodent *Akodon* (2n = 10 and 2n = 16) from Brazil. Genet Mol Biol. 2006, 3:469–474.

Smith MF, Patton JL. (1999) Phylogenetic relationships and the radiation of sigmodontine rodents in South America: evidence from cytochrome b. Journal of Mammalian Evolution, 6 (2):89–128.

Steppan SJ, Schenk JJ. (2017) Muroid rodent phylogenetics: 900-species tree reveals increasing diversification rates. PLoS One. 12(8): e0183070.

Svartman M, Almeida EJC. (1993) The karyotype of *Oxymycterus* sp (Cricetidae, Rodentia) from Central Brazil. Journal Experientia, 49 (8):718-720.

.

CAPÍTULO 2.

Pleistocene climatic oscillations in Neotropical open areas: Refuge isolation in the rodent *Oxymycterus nasutus* endemic to grasslands

Willian T. Peçanha, Sergio L. Althoff, Daniel Galiano, Fernando M. Quintela, Renan Maestri, Gislene L. Gonçalves, Thales R. O. Freitas

Submetido: 21 de Agosto, 2017

Aceito: 17 de Outubro, 2017

Publicado: 27 de Novembro, 2017

PLoS ONE 12(11): e0187329.

https://doi.org/10.1371/journal.pone.0187329

PLOS ONE

RESEARCH ARTICLE

Pleistocene climatic oscillations in Neotropical open areas: Refuge isolation in the rodent *Oxymycterus nasutus* endemic to grasslands

Willian T. Peçanha[1], Sergio L. Althoff[2], Daniel Galiano[3], Fernando M. Quintela[4], Renan Maestri[5], Gislene L. Gonçalves[1,6]*, Thales R. O. Freitas[1]

1 Programa de Pós-Graduação em Genética e Biologia Molecular, Universidade Federal do Rio Grande do Sul, Rio Grande do Sul, Brazil, **2** Departamento de Ciências Naturais, Laboratório de Biologia Animal, Universidade Regional de Blumenau, Blumenau, SC, Brazil, **3** Pós-graduação em Ciências Ambientais, Area de Ciências Exatas e Ambientais, Unochapecó, Santa Catarina, Brazil, **4** Programa de Pós-Graduação em Biologia de Ambientes Aquáticos Continentais, Instituto de Ciências Biológicas, Universidade Federal do Rio Grande, Rio Grande do Sul, Brazil, **5** Programa de Pós-Graduação em Biologia Animal, Departamento de Zoologia, Universidade Federal do Rio Grande do Sul, Rio Grande do Sul, Brazil, **6** Departamento de Recursos Ambientales, Facultad de Ciencias Agronómicas, Universidad de Tarapacá, Arica, Chile

* lopes.goncalves@ufrgs.br

Citation: Peçanha WT, Althoff SL, Galiano D, Quintela FM, Maestri R, Gonçalves GL, et al. (2017) Pleistocene climatic oscillations in Neotropical open areas: Refuge isolation in the rodent *Oxymycterus nasutus* endemic to grasslands. PLoS ONE 12(11): e0187329. https://doi.org/10.1371/journal.pone.0187329

Editor: Riccardo Castiglia, Universita degli Studi di Roma La Sapienza, ITALY

Received: August 21, 2017

Accepted: October 17, 2017

Published: November 27, 2017

Data Availability Statement: All sequence files are available from the Genbank database, accessions numbers MF766110 to MF766188 (Cytb) and MF766189 to MF766256 (Fgb-I7).

Funding: This research was supported by the Coordenadoria de Aperfeiçoamento Pessoal (CAPES), Fundação de Amparo à Pesquisa do Estado do Rio Grande do Sul (FAPERGS) and Conselho Nacional de Desenvolvimento Científico e Tecnológico (CNPq). G.L. Gonçalves and R.

Abstract

Pleistocene climatic oscillations favoured the expansion of grassland ecosystems and open vegetation landscapes throughout the Neotropics, and influenced the evolutionary history of species adapted to such environments. In this study, we sampled populations of the rodent *Oxymycterus nasutus* endemic to open areas in the Pampas and Atlantic Forest biomes to assess the tempo and mode of population divergence using an integrative approach, including coalescence theory, ecological niche models, and morphometry. Our results indicated that these *O. nasutus* populations exhibited high levels of genetic structure. Six major mtDNA clades were found, structuring these biomes into distinct groups. Estimates of their divergence times was indicated to be 0.571 myr. The high degree of genetic structure is reflected in the analyses of geometric morphometric; skull differences between lineages in the two ecoregions were detected. During the last glacial maximum, there was a strong increase in suitable abiotic conditions for *O. nasutus*. Distinct molecular markers revealed a population expansion over time, with a possible demographic retraction during the post-glacial period. Considering that all clades coalesce with the last interglacial maximum, our results indicated that reduction in suitable conditions during this period may have resulted in a possible vicariance associated with refuge isolation.

Introduction

The glaciations occurred in the Pleistocene (2.58–0.01 million years ago [myr]), a period of climatic history that is known with near accuracy [1], which led to the migrations and reductions in the population sizes of several species, followed by recolonization and population expansion as glaciers retreated [2–4]. Therefore, the divergence promoted by glaciers have probably affected populations distributed in allopatry, which could be detected in genealogies, as observed in typical glacial refuges [5].

Maestri received fellowship from FAPERGS (16/2551-0000485-4) and CNPq (150391/2017-0), respectively. The funders had no role in study design, data collection and analysis, decision to publish, or preparation of the manuscript.

Competing interests: The authors have declared that no competing interests exist.

In the recent years, some regions in the Neotropics have been systematically studied [6], as the high biological diversity provides an opportunity to test refuge hypotheses associated with climatic oscillations in the Quaternary Epoch, especially in complex ecoregions such as the Atlantic Forest [7,8]. A remarkable landscape in South America are the open areas, such as the Pampas biome, the largest temperate grasslands in the world [9], which are excellent environments to evaluate the influence of historical climatic fluctuations on the origin and evolutionary dynamics of species. The cool and dry weather during the glaciations allowed grassland ecosystems and open vegetation landscapes to expand over much of South America [10], which created new 'suitable' areas. Thus, it is expected that a species endemic to open areas respond to Pleistocene climatic oscillations in a different way than a species adapted to forest environments, [11–15], particularly, those that occupy heterogeneous grasslands ecoregions such as the Akodontine rodent *Oxymycterus nasutus* (Waterhouse, 1837).

O. nasutus is an abundant species adapted to wet areas, thriving at sea level in the southernmost Uruguay and Rio Grande do Sul State, Brazil, to higher elevations (up to 900 m) on the Santa Catarina and Parana States, Brazil, where it is restricted by the coastal mountains [16–17] (Fig 1). It inhabits coastal sandbanks, wet grasslands, steppes, and other phytophysiognomies of the Pampas, a biome that dominate Uruguay and the plains of southernmost Brazil. Moreover, it is highly dispersed throughout the southern Brazilian plateau in high-elevation field domains, and is probably the most abundant small mammal in the high-elevation grasslands in the states of Rio Grande do Sul and Santa Catarina (Atlantic Forest domain) [17–19].

The relationship between the grasslands and the forests during the late Quaternary is well documented in the studies on pollen records in the South and Southeast Brazil [20, 10]. Overall, general patterns of grasslands distributions up to the last glacial period in the Pleistocene (42,000–10,000 years BP) is linked with the rise of vegetation formations in the late Holocene [21]. In Southern Brazil, the expansion of grasslands was promoted by cold weather conditions and dry climate owing to the glaciation periods, with a mean decrease of temperature between 5–7˚C in high-altitude (Meridional Plateau) areas [10, 21]. In addition, during the Last Glacial Maximum ([LGM] ~21,000 years BP), grasslands were also present abundantly in the coastal lowlands and on the exposed continental shelf, where forests were almost absent [22–23,10].

Since *O. nasutus* is intrinsically related to the grasslands and is abundantly found in these habitats [17–19], cyclic events of the dynamic expansion and retraction of open areas and forests that occurred during glacial and interglacial periods have probably influenced the evolutionary history of this species. Accordingly, to understand the tempo and mode of population divergence and to contribute insights into the aspects of the biogeographic history of the South America, we analysed the phylogeography, population genetics, and skull morphometry across the entire distributional range. We characterized the geographical patterns of genetic and morphological variation and used these data to investigate whether glacial and interglacial periods influenced the extant distribution of *O. nasutus* in distinct biomes, hypothesizing the existence of significant divergence between Pampas and Atlantic Forest lineages. Additionally, we estimated the current and historical potential distribution area of *O. nasutus* based on paleoclimatic models to allow a detailed evaluation of the demographic history and phylogeographical patterns.

Materials and methods

Ethics statement

Skull and tissue samples of *O. nasutus* surveyed in the study were obtained from the specimens deposited in the scientific collections (Museo Nacional de Historia Natural [MNHN], Museu de História Natural Capão da Imbuía [MHNCI], Museu de História Natural of the Universidade

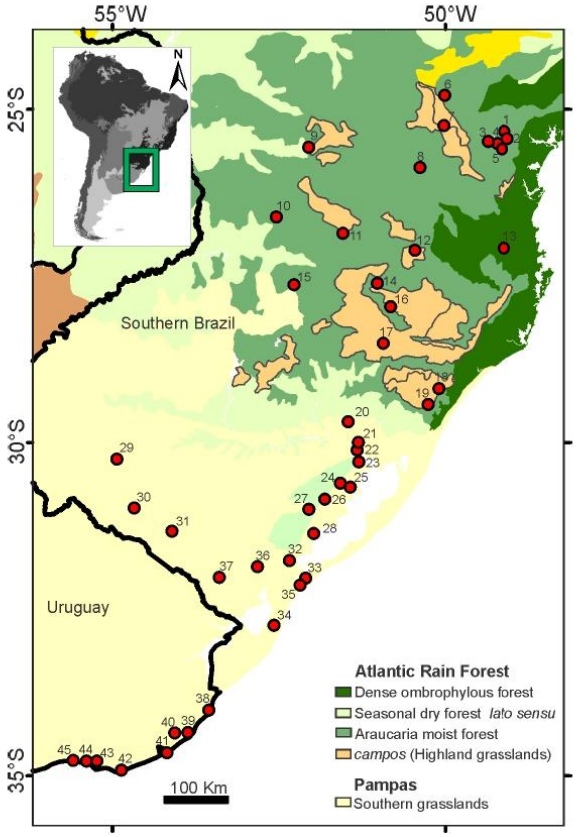

Fig 1. Geographic distribution of *O. nasutus* and sampling sites in Southern Brazil and Uruguay. The map includes the ecoregion where the species is located. Details of site numbers are found in the Table 1. The map were obtained from Ecoregions2017Resolve (available at: http://ecoregions2017.appspot.com/). Any rights in individual contents of the database are licensed under the Database Contents License: https://creativecommons.org/licenses/by/4.0/), and edited with ArcMap 10.3 software.

https://doi.org/10.1371/journal.pone.0187329.g001

Luterana do Brasil [MCNU], Fundação Zoobotânica-Museu de Ciências Naturais [FZB-MCN], Universidade Federal do Paraná [UFPR] and Universidade Regional de Blumenau [FURB]), who kindly lent the specimens for use in this study. Specimens deposited in the Universidade Federal do Rio Grande do Sul [UFRGS] were collected (previously) by our research group with the license issued by the Brazil Government authorities.

Sample collection

A total of 135 specimens of *O. nasutus* from 45 localities covering the entire known distribution of this species (Fig 1; Table 1) were surveyed. Field collection (permits granted by the Ministério do Meio Ambiente, Brazil—SISBIO 30204–1, 52650–1 and 29358–1) followed the guidelines of the American Society of Mammalogists for the use of wild mammals in research (https://www.mammalsociety.org/committees/animal-care-and-use). Specimens

were euthanized via overdoses of isofluorane and cervical dislocation, procedures authorized by The Animal Care and Use Committee of the Institute of Biological Sciences at UFRGS, Brazil, for this study Specimens trapped were deposited both in the mammal collections of UFRGS and MCNU.

Phylogenetic relationships

DNA was isolated from 107 specimens using the PureLink Genomic DNA extraction kit (Invitrogen, Life Technologies), following the manufacturer's instructions. Polymerase chain reaction (PCR) was performed to amplify the mitochondrial DNA (mtDNA) cytochrome *b* (*Cytb*) gene (801 bp) and the nuclear locus beta-fibrinogen, intron 7 (*Fgb*-I7) (408 bp) according to the method described by Smith and Patton [24] and Matocq et al. [25]. The nuclear marker was chosen as it represents a single-copy locus, and is informative and evolving at a different rate compared to the mtDNA [26]. PCR products were stained with GelRed (Biotium) and checked on 1% agarose gel, purified with enzymatic method (Exonuclease and Alkaline Phosphatase; Amersham Biosciences, Piscataway, NJ) and sequenced with Sanger method using both primers (forward and reverse). All sequences obtained were deposited in GenBank under the accession numbers: *Cyt b*, MF766110 to MF766188 and *Fgb*-I7, MF766189 to MF766256.

Alignment and editing of the mtDNA *Cytb* sequences was performed in the Clustal W algorithm using the MEGA 7 software. For the nuclear *Fgb-I7*, sequences were aligned using MAFFT v.7.245 [26] with the auto setting. Variable sites of this nuclear marker were assessed in the original chromatograms to ensure correct identification of the heterozygotes. Heterozygous sites were identified when two different nucleotides were indicated at the same position in the chromatograms, with the weakest peak reaching at least 25% of the strongest signal. The IUPAC symbols were applied for coding the double peaks. The gametic phase of each haplotype was identified computationally using the program PHASE v2.1 [27, 28] as implemented in DnaSP v5.10 [29] to reconstruct putative alleles of the nuclear marker for use in downstream haplotype-based analyses. The program was ran with 500 burn-in steps and 500 iterations, including the allowed intragenic recombination for the given data set. We also used a 0.6 output probability threshold for haplotypes and genotypes, as this was shown to reduce the number of unidentified genotypes with or without slight increase in the number of false positives [30].

The most appropriate substitution model for mtDNA phylogeny from the haplotypic data was the HKY+G that was determined based on the Akaike Information Criterion in the jModelTest v2.1.10 software [31]. The phylogeny was reconstructed using Bayesian Inference (BI) in the software BEAST 1.8.4 [32]. Two independent Markov Chain Monte Carlo (MCMC) runs, each with four streams per 25 million steps of the MCMC, sampled every 1000 generations, and discarding 2.5 million burn-in (about 10% trees discarded), starting the initial trees with randomness, without restriction were performed. Speciation tree prior was modelled on Birth-Death Process using the BEAST software. Parameter convergence was checked in Tracer v1.5 [33] as to whether effective sample sizes (ESS) reached 200. The remaining trees were used to calculate the posterior probabilities for each node.

The burn-in was determined in Tracer v1.6 based on the trajectory parameters, and 10% of the initial trees were removed and summarized in TreeAnnotator. The consensus tree generated was visualized and edited in Figtree v1.4.3 (http://tree.bio.ed.ac.uk/software/figtree/). There were no fossils for *Oxymycterus* that could be used for a specific estimate of the substitution rate. Hence, we used an evolutionary rate already published [34] of 2.37% per million years (Myr^{-1}) for the genus. Accordingly, the divergence times were estimated in BEAST assuming an uncorrelated relaxed clock model and a normal distribution for the substitution

rate, with a mean of 2.37% Myr-1, and a standard deviation of 0.25% Myr-1, to allow some uncertainty in the evolutionary rate. One representative sequence for each haplotype was used. Sequences of *Oxymycterus delator* (U03525), *Oxymycterus dasytrichus* (AF454768), *Oxymycterus amazonicus* (AF454765), and sister lineages of *O. nasutus* [35], were included in the analysis. The time of the most recent common ancestor (TMRCA) for relevant nodes and major mitochondrial clades was reported as the mean value of node height with 95% highest posterior density interval (HPD). The nodes were supported with the posterior probability (PP) of $\geq$ 90% [36]. We also reconstructed the phylogenetic tree among nuclear DNA (nDNA) haplotypes (Fgb-I7) data set with phased alleles and single-copy sequences using BI in BEAST. However, due to the low variability and lack of support, we performed downstream analysis based on the haplogroups inferred by mtDNA. The topology obtained from *Fgb*-I7 evolutionary tree is shown in S1 Fig.

The evolutionary relationships between the haplotypes for each data set (i.e. mtDNA and nDNA) were estimated using the median-joining method implemented in the Network v5.0 [37] (http://www.fluxus-engineering.com). For assessing the evolutionary relationships of the *Fgb*-I7 gene, haplotypes were identified by coalescent-based Bayesian method implemented in PHASE v2.1. Missing/gaps sites were verified and invariant sites were removed from the dataset. Indels were treated as single mutational events.

Intraspecific variation and historical demography

Statistical parameters of diversity, such as the number of variable sites (S), number of haplotypes (h), haplotype diversity (Hd), nucleotide diversity (π), and average number of nucleotide differences (k) were measured using DNASP v5.10 [29]). We calculated the genetic distance between the recognized haplogroups of *Cytb* (average distances) using p-distance model with 1000 bootstrap replications using MEGA v7 [38]. The defined clades were assumed based on the phylogeny obtained through Bayesian analysis.

Historical demographic changes such as signatures of demographic expansion, and equilibrium or decline were examined for the species and for each haplogroup using neutrality tests, such as Tajima's D [39] and Fu's Fs [40] statistics, employing the software DNASP v5.10. Pairwise mismatch distribution was performed in DNASP v.5.10 to infer the historical demography of *O. nasutus*, calculated with the expected frequency based on a population growth-decline model. The sum of squared deviations (SSDs) between the observed and expected mismatch distribution and the raggedness index (r) were calculated to test the null hypothesis of spatial expansion using ARLEQUIN v3.5 [41]. In addition, we performed a Bayesian skyline plot (BSP) analysis, which does not assume a priori any growth model and infers the effective population size through time based on coalescent theory [42]. The BSP was used to estimate the dynamics of alterations in the overall population size over time for the *O. nasutus* dataset. BEAST v1.8.4 [32] was used for estimating the BSP of mtDNA as described above, with minor alterations in the number of parameters sampled at every 10,000 steps. For nDNA, a posterior distribution model of effective population size through time was generated using a MCMC sampling scheme. Two independent analyses were ran for 40 x 10^7 generations (sampling at every 10,000 and 10% burn in) under a HKY+G substitution model (obtained through the jModelTest 2 software), assuming a relaxed molecular clock model. However, we used the substitution rates and dates estimated from previous studies to calibrate a relaxed molecular clock and approximate divergence times for the main phylogroups retrieved in our study. We implemented a lognormal prior distribution based on the substitution rate for the cricetid genus *Peromyscus* (0.006 ± 0.003 substitution/site/million years) for the *Fgb*-I7 data set [43]. Skyline reconstruction was performed in Tracer v1.5, and the median and 95% credibility interval were plotted as a function of time.

Ancestral area reconstruction

Aiming to reconstruct the ancestral range of *O. nasutus*, we performed a Statistical dispersal–vicariance analysis (S–DIVA) on the maximum clade credibility tree generated from the BEAST analysis using the software RASP 3.02 [44–46]. The DIVA method [44] develops an approach based on parsimony events and reconstructs ancestral distributions based on a simple biogeographic model and a three-dimensional cost matrix. Penalties are not assigned when speciation is the result of vicariance; however, dispersal and extinction events have a penalty of one per unit area added to or deleted from a distribution. S-DIVA method rectified the problems in DIVA analysis and suggested possible ancestral ranges at each node and also calculated the probabilities for each ancestral range at the nodes. Due to the current area of occurrence and based on historical aspects of the region (expansion and retreat of forest formations), we reconstructed the ancestral areas only within the Pampas (A) and Atlantic Forest/grassland mosaic (B) regions. According to the results obtained by BI and the presence of restricted haplogroups in a single ecoregion, the clades recognized in *O. nasutus* were categorized in these areas. We used the output files generated by BEAST (total and condensed trees) for the analysis.

Morphological analyses

Digital photographs were taken from the dorsal, lateral, and ventral views of the skull of 89 specimens of *O. nasutus* (Table 1). Only adult specimens were photographed to minimize the ontogenetic effects (the complete eruption of the third molar was the criterion to separate juveniles from adults). Two-dimensional digital images were taken using a Canon PowerShot G10 camera with 14.7 megapixels resolution (4416 x 3312) in the macro function of the automatic mode and without flash or zoom. The pictures were taken from a standard distance of 127 mm for all the specimens. A total of 17 landmarks were digitized in the dorsal view, 16 landmarks in the lateral view, and 32 landmarks in the ventral view (S2 Fig), using the TpsDig2 software [47]. The same person (WTP) conducted the digitization. The choice of landmarks was based on previous studies with sigmodontines [48,49]. In the dorsal and ventral view, all individuals were marked on both sides of skull. The description of all the landmarks employed is given in S1 Appendix. After digitization, a Generalized Procrustes Analysis (GPA) was conducted on the matrix of landmark coordinates to remove the effects of scale, position, and orientation [50]. The centroid size, derived by the square root of the sum of squared distances of each landmark from the centroid of the configuration [51], was used as a measure of size. We appended the natural log-transformed centroid size into the matrix of shape coordinates to work in the form of space for further analyses.

Our goal was to investigate whether morphology is divergent among the haplogroups found in the genetic analyses (Northwest, Central, Eastern, Steppes Plain, Southern, and Taim Wetland), and also between physiognomies or "environmental groups" (Pampas versus Atlantic Forest). First, we conducted a principal component analysis (PCA) in the form matrix for each view. The number of PCs necessary to achieve 100% variation in each view (16 PCs for dorsal view, 31 PCs for ventral view, and 29 PCs for lateral view) were used as response variables for downstream analyses. We performed multivariate analyses of variance (MANOVA) and discriminant analyses with Jackknife cross validation (DA) to investigate how morphology was structured among the six genetic haplogroups (first predictor) and the two environmental groups (second predictor). MANOVAs and DAs were performed independently for each predictor and for each skull view. All procedures were carried out in the software R [52]), with the packages geomorph [53] and Morpho [54]. Visualization of shape changes was made by comparing the shapes among groups using discriminant functions implemented in MorphoJ [55].

Table 1. Sampling localities of *Oxymycterus nasutus* in Southern Brazil and Uruguay.

					Haplotype			
#	Sample site[a]	Lat. (S), Long. (W)	N	Voucher[b]	*Cytb*	*Fgb*-I7	Haplogroup	Skull
1	BR: PR, Quatro Barras	-25.3658, -49.0769	4	MHNCI 4605,4607,4608,4595	H1	H3, H15, H24	Eastern	+
2	BR: PR, Piraquara	-25.4419, -49.0627	8	UFPR-P42,53,54,56,59,60,62,65	H1-H5	H3, H17	Eastern	-
3	BR: PR, Curitiba	-25.4789, -49.3307	1	UFPR-P86	H1	-	Eastern	-
4	BR: PR, Curitiba, Parque Regional do Iguaçu	-25.5229, -49.2229	1	MHNCI 3433	H1	H1	Eastern	+
5	BR: SC, São José dos Pinhais	-25.5799, -49.1753	11	UFPR-P969, 995*,1008*,1018*,1019*,1039*,1049*,1051*,1053*,1055,1061	H1	H3, H18, H19	Eastern	+
6	BR: SC, Castro	-24.7908, -50.0120	4	MHNCI 816–818, 0821	-	-	Central	+
7	BR: SC, Ponta Grossa	-25.2440, -50.0227	7	UFPR-P76, MHNCI 642, 657, 709, 723, 838, 839	H6	-	Central	+
8	BR: SC, São Mateus do Sul	-25.8738, -50.3827	1	MHNCI 3192	H7	-	Northwest	+
9	BR: SC, Candói,	-25.5708, -52.0527	1	CZFURB 18228	H8	H1; H2	Northwest	+
10	BR: SC, São Domingos	-26.6163, -52.5388	2	CZFURB 18119, 18153	H11	H8, H11, H12	Central	+
11	BR: SC, Agua Doce	-26.9977, -51.5558	2	CZFURB 9365, 9856	H12, H13	H1, H3-5	Central	+
12	BR: SC, Ponta Alta do Norte	-27.1153, -50.4577	2	MHNCI 4951, 4596	H9, H10	H1; H10	Northwest	+
13	BR: SC, Indaial	-27.0830, -49.1166	1	CZFURB 9825	H10	H15; H15	Central	+
14	BR: SC, Abdon Batista	-27.6108, -51.0227	1	CZFURB 20520	H2	H13; H14	Central	+
15	BR: RS, Erechim	-27.6338, -52.2738	2	CMLCE-UFRGS HFE 2, 4	H2	H1; H6, H7	Central	-
16	BR: RS, Campo Belo do Sul	-27.9625, -50.8231	4	CZFURB 15106*, 15109, 15140, 15154*	H2	H8; H9	Central	+
17	BR: RS, Vacaria	-28.511944, -50.933889	1	MCNU 2498	H2	-	Central	-
18	BR: RS, Cambará do Sul	-29.191667, -50.0975	2	CMLCE-UFRGS AS5, 17	H14	H1, H14, H20	Eastern	-
19	BR: RS, São Francisco de Paula	-29.428322, -50.259444	10	MCNU 3043, 3210, 3658, 3656*, 3657*; CMLCE-UFRGS PM 100, 104, 74, 79, 86	H14, H15	H1, H8, H16-17, H21-24	Eastern	+
20	BR: RS, Montenegro	-29.682555, -51.466450	1	FZB-MCN 547	-	-	Steppes Plain	+

(*Continued*)

Table 1. (*Continued*)

					Haplotype			
#	Sample site[a]	Lat. (S), Long. (W)	N	Voucher[b]	*Cytb*	*Fgb*-I7	Haplogroup	Skull
21	BR: RS, Eldorado do Sul	-29.997139, -51.307861	1	FZB-MCN 675	-	-	Steppes Plain	+
22	BR: RS, Guaíba	-30.113889, -51.325	11	MCNU 3211, 3652, 3228, 3119, 3009, 3141, 3146*, 3142, 3149, 3212, 3653	H16	H1, H3, H24, H26, H33-34	Steppes Plain	+
23	BR: RS, Barra do Ribeiro	-30.290833, -51.300833	6	MCNU 3144, 3654*, 3147, 3230, 3039, 3135	H16, H17, H18	H1, H33-35	Steppes Plain	+
24	BR: RS, Sentinela do Sul	-30.610833, -51.578889	1	MCNU 314	H19	H1; H29	Steppes Plain	+
25	BR: RS, Tapes	-30.669849, -51.429707	1	MCNU 3132	H19	-	Steppes Plain	+
26	BR: RS, Camaquã	-30.850833, -51.811944	10	CMLCE-UFRGS FQ 47; MCNU 3011, 3012, 3110, 3116, 3122, 3124, 3133, 3214, 3227; CZFURB 6249*,6250	H20-H24	-	Steppes Plain	+
27	BR: RS, Cristal	-31.002778, -52.050	3	MCNU 4331; CMLCE-UFRGS FQ 63, 72	H22	H1; H30		+
28	BR: RS, São Lourenço do Sul	-31.365, -51.977778	5	MCNU 3225, 3109, 3123, 3115, 3010	H19, H26	H1, H26; H31	Steppes Plain	+
29	BR: RS, Rosário do Sul	-30.247938, -54.924036	1	FZB-MCN 648	-	-	Steppes Plain	+
30	BR: RS, Dom Pedrito	-30.975882, -54.666567	2	FZB-MCN 710, 1011	-	-	Steppes Plain	+
31	BR: RS, Bagé	-31.330833, -54.106944	2	CMLCE-UFRGS ALL 12, 13	H25	H1, H25-27	Steppes Plain	-
32	BR: RS, Pelotas	-31.771944, -52.342778	4	CMLCE-UFRGS PL 300; MCNU 3223, 3041,3042	H19, H27	H1, H28-30	Steppes Plain	+
33	BR: RS, Rio Grande	-32.035, -52.098889	2	CMLCE-UFRGS MEV 01; MCNU 3014	H31	H31	Taim Wetland	-
34	BR: RS, Rio Grande, ESEC Taim	-32.7425, -52.574444	3	MCNU 3661*, 3131, 3660	H32, H33	H31	Taim Wetland	+
35	BR: RS, Rio Grande, ÁPA Lagoa Verde	-32.139934, -52.181064	1	MCNU 3660	H33	-	Taim Wetland	+
36	BR: RS, Pedro Osório	-31.863889, -52.822778	4	CMLCE-UFRGS POS 18, 20, 25, 27	H28, H29	H26; H36	Southern	-
37	BR: RS, Herval	-32.023889, -53.395833	1	CMLCE-UFRGS HL 01	H30	H31; H37	Southern	-
38	UY: Rocha, Parque Santa Teresa	-34.008180, -53.552735	1	MNHN SN EMG1809	-	H3; H3	Southern	-

(*Continued*)

Table 1. (*Continued*)

#	Sample site[a]	Lat. (S), Long. (W)	N	Voucher[b]	Haplotype		Haplogroup	Skull
					Cytb	*Fgb*-I7		
39	UY: Rocha, Laguna de Castillos	-34.35, -53.866667	2	MNHN SN SCV 108, 110	H34	H38, H29; H30 H39	Southern	-
40	UY: Rocha, Route 9 km 304.800	-34.357743, -54.064845	1	MNHN SN GD 577**	H35	-	Southern	-
41	UY: Rocha, La Paloma, La Palma	-34.655896, -54.181969	2	MNHN SN CA 614, 617*	H34	H24; H24	Southern	+
42	UY: Maldonado, San Carlos	-34.915632, -54.865456	2	MNHN SN GD 723; MVZ 182701 (CA458)**	H37, H38	H3; H31	Southern	-
43	UY: Maldonado, Pan de Azucar	-34.779218, -55.232399	1	MNHN SN CA 680*	-	-	Southern	+
44	UY: Maldonado, Solís Grande	-34.783273, -55.334011	1	MNHN SN CA 695**	H37	-	Southern	+
45	UY: Canelones, La Floresta	-34.770278, -55.588333	1	MNHN 5615 (EMG1567)	H36	H26; H31	Southern	-

Localities (#) are mapped in Fig 1. Vouchers, Cytb/Fgb-I7 haplotypes and presence (+)/absence (-) of skull samples per site are presented.

[a]: Abreviations: BR: Brazil, UY: Uruguay; PR, Paraná; SC, Santa Catarina; RS, Rio Grande do Sul states.

[b]: Acronyms of collections: UFPR-P, Scientific Collection of the Cytogenetic and Conservation Laboratory at the Universidade Federal do Paraná; MHNCI, Museu de História Natural Capão da Imbuía; CZFURB, Zoological Collection of the Universidade Regional de Blumenau; CMLCE-UFRGS, Mastozoological Collection of the Cytogenetic Laboratory and Evolution at the Universidade Federal do Rio Grande do Sul; MCNU, Museu de História Natural of the Universidade Luterana do Brasil; MNHN, Museo Nacional de Historia Natural (Uruguay); FZB-MCN, Fundação Zoobotânica-Museu de Ciências Naturais; MVZ, Museum of Vertebrate Zoology at the University of California/Berkeley.

*Vouchers presenting only skulls.

**Data obtained from NIH genetic sequence database (Genbank; https://www.ncbi.nlm.nih.gov/genbank/)

https://doi.org/10.1371/journal.pone.0187329.t001

Geographic distribution maps and modelling

Ecological niche modelling (ENM) was carried out in MAXENT v 3.3.3e [56] to predict suitable present and past potential distribution areas of *O. nasutus* based on climatic variables. Such modelling has been performed favourably compared to other analytical alternatives for presence-only data [56–59]. Information on the geographic distribution of the species was based on 51 occurrence records obtained from literature and collections (S2 Appendix). We verified the accuracy of the geo-referenced data in ArcGIS v 10.0. To avoid data clustering [60], we limited our database to a single record per km^2. For modelling settings, the function 'Auto features' was selected, and the distributions were modelled through the 'cross-validate' parameter, applying a maximum number of iterations at 500. We verified model performance using the area under the 'Receiver Operating Characteristic (ROC) Curve' (AUC) calculated by MAXENT. Values between 0.7 and 0.9 indicated good discrimination [61].

Projections for the past climatic conditions were developed for three periods: LGM c. 21 ka; Last IinterGlacial (LIG) c. 120–140 ka; and mid-Holocene c. 6 ka. Current and past distributions were modelled using 19 bioclimatic data layers available from the WorldClim database (http://www.worldclim.org) at 30 arc-sec resolution (~1 km^2), with the exception of the layers

from the LGM period, which were available in 2.5 arc-min resolution (~5 km^2). Climatic variables for the present study represented the average climate changes from 1950 to 2000. Projections for the LGM and mid-Holocene were derived from the CCSM4 [62] atmosphere-ocean general circulation models (AOGCM). All the analyses were performed in QuantumGIS 2.18 software.

Results

Intraspecific genetic variation and evolutionary patterns

We identified 73 variable sites in the mtDNA dataset resulting in 38 haplotypes and 32 variable sites in the *Fgb*-I7 locus resulting in 40 haplotypes (with one 2-bp indel) (Tables 1 and 2). Standard diversity indices (haplotype diversity, nucleotide diversity, mean number of pairwise differences) for both the markers are presented in Table 2.

Bayesian consensus tree based on mtDNA dataset depicted six highly supported (BPP > 0.90) haplogroups corresponding to two distinct biomes: Northwest, Central, and Eastern clades are distributed along the Atlantic Forest biome, and Steppes Plain, Taim Wetland, and Southern clades assigned to the Pampas biome. However, the relationship between these groups was not entirely clear, considering that they did not cluster in major clades exclusive to each of the two biomes (Fig 2). The haplotype network based on the mtDNA also supported such tree structure. Nonetheless, despite the several mutational steps between haplogroups, the haplotype network showed several median vectors indicating non-sampled or extinct ancestral sequences (Fig 3). The two main widespread haplogroups were Central and Southern clades. The Central clade occurred throughout the domain of Atlantic Forest, mainly dispersed over the Araucaria forests and the mosaic of forest/highland grasslands (Fig 2). This clade was

Table 2. Geneticvariability of *O. nasutus* using mitochondrial (*Cytb*) and nuclear (*Fgb*-I7) markers.

Group		S	N_H	Hd ± SD	π ± SD	k	Fu-Fs (P-value)	Tajima's D (P-value)
Cytb:								
Northwest	4	12	4	1.0000 ± 0.1768	0.00885 ± 0.00256	6.83	-0.12436 (0.2570)	0.44358 (0.7550)
Central	13	10	6	0.6282 ± 0.1431	0.00229 ± 0.00093	1.76	-0.36009 (0.3760)	-1.80161 (0.0160)*
Eastern	18	8	7	0.7451 ± 0.0790	0.00280 ± 0.00037	2.16	-0.24573 (0.4710)	-0.24280 (0.4240)
Steppes Plain	30	18	12	0.8874 ± 0.0329	0.00379 ± 0.00047	2.92	-3.34189 (0.0670)	-1.22763 (0.1100)
Southern	13	11	8	0.9103 ± 0.0559	0.00422 ± 0.00065	3.25	-1.96098 (0.1040)	-0.32877 (0.4000)
Taim Wetland	4	6	3	0.8333 ± 0.2224	0.00410 ± 0.00172	3.16	0.81143 (0.5720)	-0.31446 (0.5510)
All	82	73	38	0.9624 ± 0.0083	0.01190 ± 0.00066	9.18	-11.24103 (0.0070)**	-1.23865 (0.0720)
Fgb-I7:								
Northwest	3	8	5	0.9333 ± 0.1217	0.00640 ± 0.00123	3.66	-0.90493 (0.2050)	-0.06042 (0.4550)
Central	8	14	14	0.9500 ± 0.0364	0.00606 ± 0.00062	3.45	-4.51905 (0.0060)**	-1.22325 (0.1120)
Eastern	16	13	14	0.8407 ± 0.0557	0.00481 ± 0.00053	2.92	-5.23937 (0.0140)*	-0.90384 (0.1990)
Steppes Plain	29	11	14	0.7629 ± 0.0538	0.00293 ± 0.00052	2.00	-5.31470 (0.0160)*	-1.05889 (0.1440)
Southern	9	13	11	0.9216 ± 0.0417	0.00639 ± 0.00098	3.53	-3.67515 (0.0280)	-0.68862 (0.2940)
Taim Wetland	3	0	1	-	-	-	-	-
All	68	32	40	0.8778 ± 0.0225	0.00497 ± 0.00034	2.98	-26.44071(0.00)**	-1.93728 (0.0050)**

Groups are based on *Cytb* phylogenetic inferences (see Fig 2). Neutrality tests are indicated by Fu' Fs and Tajima's D.

N_{ind}: Number of individuals sequenced, S: Number of segregating sites, N_H: number of haplotypes; Hd: Haplotype diversity, **π**: Nucleotide diversity, SD: Standard deviation; k = Mean number of pairwise differences.

*P<0.02 or

**P<0.01 for Fu's FS or Tajima's D, respectively.

https://doi.org/10.1371/journal.pone.0187329.t002

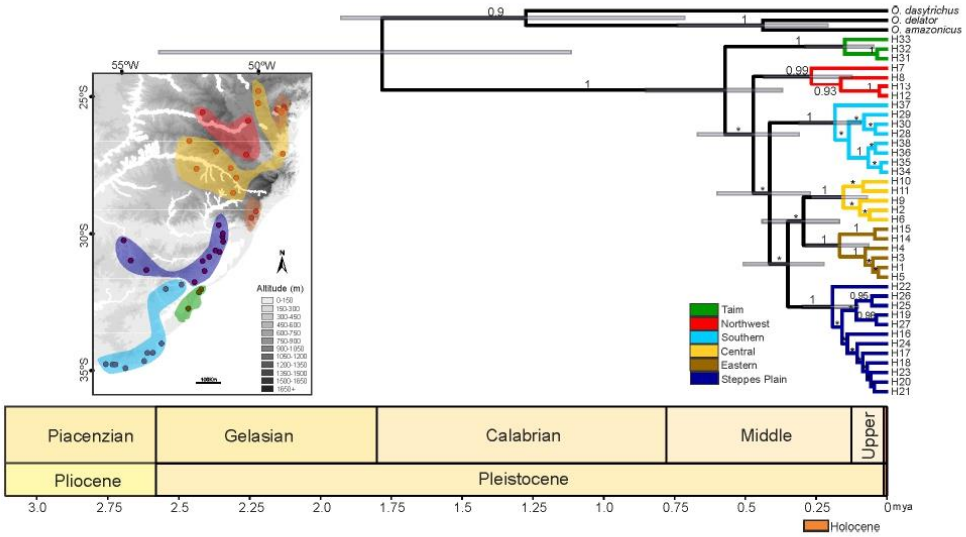

Fig 2. Bayesian consensus time-tree of *O. nasutus* based on 801 bp of the *Cytb* mtDNA sequences. Values above nodes correspond to posterior probabilities > 0.90. The 95% credible intervals for node ages are shown with transparent bars to denote the time of the most recent ancestor (TMRCA) to selected branches. Scale bars were plotted with a geological time scale using the strap package in R. The map depicted clades into a geographic context, highlighting distinct altitudes.

https://doi.org/10.1371/journal.pone.0187329.g002

distributed across the entire extension of the Araucaria Forest coverage. The Southern clade was dispersed along the Pampas biome in Uruguay and the southernmost of Brazil, a region dominated by steppes or grassland. The other haplogroups were isolated and covered smaller areas when compared to Central or Southern haplogroups, except for Eastern clade with two isolated zones of occurrence. The most diversified haplogroup was the Steppes Plain, including 12 distinct haplotypes dispersed throughout the state of Rio Grande do Sul, Brazil (Table 1). Only Piraquara locality in Parana state, Brazil, comprised haplotypes from two distinct mtDNA clades (Fig 1). nDNA network revealed 36 low-frequency haplotypic variants, with a reticulate evolutionary relationship.

The majority of haplotypes differed by one substitution site. None of the six major clades in the mitochondrial tree was recovered for the *Fgb*-I7 sequences. However, nuclear haplotype H1 was present in almost all mtDNA clades (except Taim Wetland). All mtDNA clades showed the presence of unique alleles, but Taim Wetland group shared the haplotype 31 with Steppes Plain and Southern clades.

The genetic distances between the Bayesian clades ranged from 1% to 2.5% for mtDNA, whereas it was close to 0 for *Fgb*-I7 (S1 Table).

The most common ancestor for all clades of *O. nasutus* was estimated to the middle Pleistocene (0.5715 myr; 95% HPDs = 0.3657–0.8471 mya) (Fig 2, Table 3). The mtDNA haplotypes (n = 38) clustered into six lineages; individual clades diverged between 265.8 and 147.3 myr (HPDs = 0.438.8–0.046.7 myr). The ancestral haplotype could not be inferred for this marker due to the presence of several median vectors in the network. However, the BEAST-derived tree indicated H7 (Northwest clade) as the oldest clade. Tajima's D and Fu's Fs tests were negative and non-significant for both mtDNA and nDNA markers, indicating that *O. nasutus* might have experienced a recent population expansion (Table 2).

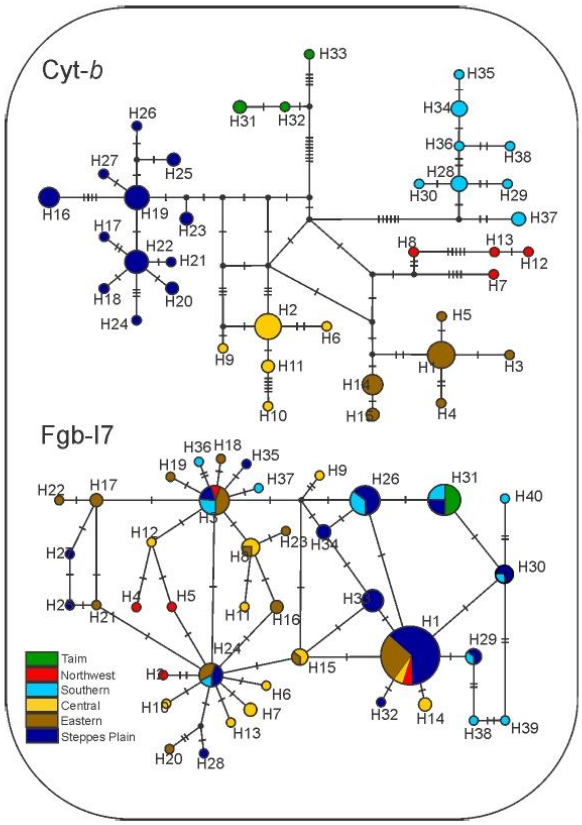

Fig 3. Evolutionary relationship of *O. nasutus* haplotypes. Median joining network based on the mitochondrial *Cytb* fragment and the nuclear *Fgb*-I7 locus. Color coding denotes the major mtDNA clades obtained in the Bayesian dated phylogeny (see Fig 2).

https://doi.org/10.1371/journal.pone.0187329.g003

Only Fu's Fs test showed significant P values for mtDNA ($P < 0.01$). Considering the mtDNA, only the Central haplogroup depicted significant P values in Tajima's D test (-1.80161, P = 0.0160), indicating an undergoing demographic expansion or mutational selection (too many

Table 3. Estimates of the time to the most recent common ancestor (TMRCA) for the nodes addressed in this study using unique haplotypes for each of the mitochondrial and overall clades for *O. nasutus*.

Clade	TMRCA (Ma)	95% HPD
Northwest	0.2658	0.1275–0.4388
Central	0.1529	0.0691–0.2675
Eastern	0.1658	0.0689–0.2894
Steppes Plain	0.1911	0.1057–0.3017
Southern	0.1822	0.0905–0.3087
Taim Wetland	0.1473	0.0467–0.2902
All	0.5715	0.3657–0.8471

https://doi.org/10.1371/journal.pone.0187329.t003

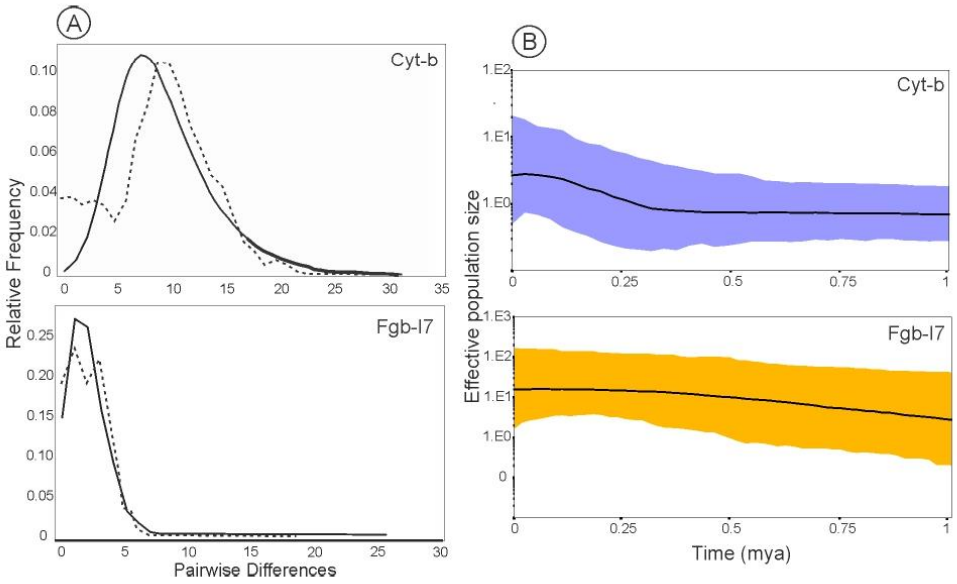

Fig 4. Demographic history of *O. nasutus* with signatures for population expansion. A, mismatch distributions of pairwise differences of *Cytb* and *Fgb*-I7 haplotypes obtained under a model allowing expansion. B, Bayesian Skyline Plot for *Cytb* and *Fgb*-I7 datasets. Bold lines indicate the median of effective population size through time and the coloured lines represent the 95% highest posterior densities over the median estimates along the coalescent history of the species.

https://doi.org/10.1371/journal.pone.0187329.g004

segregating sites/too few pairwise differences). On the other hand, Northwest haplogroup showed positive values for Tajima's D test (0.44358, P = 0.7550), which could be an indicator for a contraction (too few segregating sites/too many pairwise differences). Central, Eastern, and Steppes Plain clades showed significant P values for Fu's Fs tests performed on nDNA marker, as expected from a recent population expansion. This indicated recent demographic expansion or departure from the null hypothesis of selective neutrality and population equilibrium. Nonetheless, a unique haplotype for nDNA was found in Taim Wetland mtDNA clade, which did not allow neutrality tests to be performed. This clade also showed positive values for the Fu's Fs test for mtDNA, thereby suggesting recent population bottleneck for this lineage (Table 2).

The results of the mismatch distribution for mtDNA and nDNA analysis was approximately unimodal (Fig 4). Non-significant SSD statistic (SSD = 0.00112542, P = 0.944) and raggedness index value (r: 0.0032, P = 0.9770) under the spatial expansion models failed to reject the spatial expansion model. Similar patterns suggested demographic expansion for nDNA (SSD = 0.00322295, P = 0.570; r: 0.01631205, P = 0.780). Strong evidence of demographic expansion came from the BSP. The results showed different patterns between the mitochondrial and the nuclear datasets. For the mtDNA, a constant population size was noted over the last 0.375–1 mya after a long phase of demographic stability; the population then appeared to have experienced an accelerated demographic expansion phase approximately 0.030–0.300 myr, followed by a decrease in population size after 0.030 myr. For the nDNA marker, results showed a slow growth in the effective population size across time (0.400–1.2 mya), demographic stability for 30–400 myr, with smooth decrease posteriorly (Fig 4).

Skull morphometric variation

The occupation of different physiognomies, or environmental groups (Atlantic Forest or Pampas) explained 17.3% of the variation in the dorsal view (Wilk's $\Lambda = 0.271$, $p < 0.001$), 17.9% in the ventral view (Wilk's $\Lambda = 0.23$, $p < 0.001$) (Fig 5), and 15.4% in the lateral view (Wilk's $\Lambda = 0.31$, $p < 0.001$) of the *O. nasutus* skull (S3 Fig). Genetic haplogroups indicated 24.7% of the variation in the dorsal view (Wilk's $\Lambda = 0.084$, $p < 0.001$), 26.3% in the ventral view (Wilk's $\Lambda = 0.014$, $p < 0.001$) (Fig 5), and 23.5% in the lateral view (Wilk's $\Lambda = 0.021$, $p < 0.001$) of the *O. nasutus* skull (S3 Fig). The percentage of correct classification among the haplogroups were: 62.92% for the dorsal view, 65.16% for the ventral view, and 55.05% for the lateral view. Among the environmental groups, the percentages of correct classification were: 93.25% for the dorsal view, 82.02% for the ventral view, and 80.89% for the lateral view. The percentages of correct classification were similar between the genetic and the environmental haplogroups, considering the total number of groups in each one (i.e. six haplogroups would result in ~16% of the correct classification by chance, while with two groups this percentage will rise to 50%; deviations from the random classification are similar between the predictors). Detailed results of discriminant analyses can be found in the S2 and S3 Tables.

Ecological niche modelling and ancestral area reconstruction

Relatively high AUC values showed an excellent predictive power of the ENMs (current, AUC: 0.952; MID-HOL, mean AUC: 0.952; LGM, mean AUC: 0.952; LIG, AUC value: 0.958). The

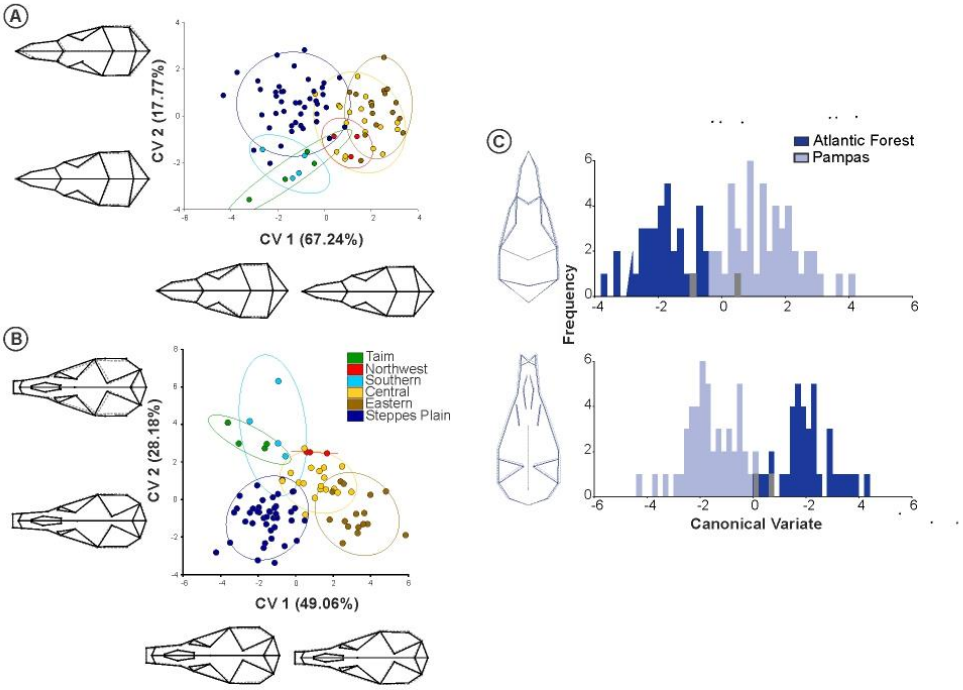

Fig 5. Scatter plot of the first Canonical Variate axis of the *O. nasutus* skull at the dorsal and ventral views, with groups following the genetic haplogroups (A, B), and the physiognomies (C). Changes in the shape for each axis are given; solid lines indicate positive scores and dashed lines indicate negative ones.

https://doi.org/10.1371/journal.pone.0187329.g005

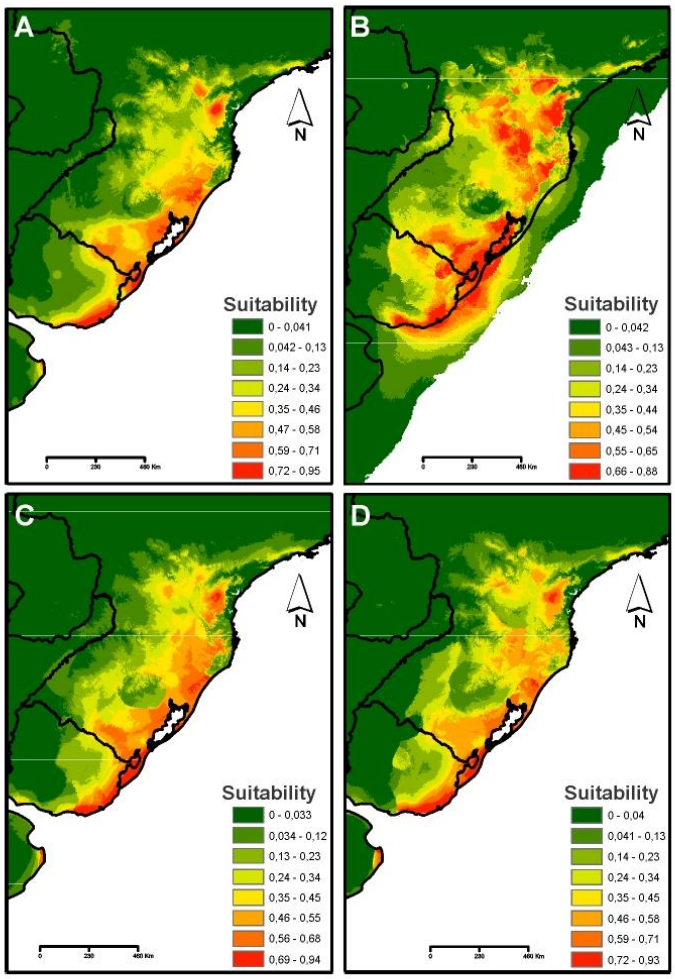

Fig 6. Predictive distribution models for *O. nasutus*. Warmer colours depict areas of higher predicted suitability. (A) Last Interglacial "LIG" ~120–140 kya. (B) Last Glacial Maximum "LGM" ~21 kya. (C) Mid-Holocene ~6 kya. (D) Current conditions. Maps were obtained from "OpenStreetMap contributors" (available at: www.openstreetmap.org; Open Street Map is made available under the Open Database License: http://opendatacommons.org/licenses/odbl/1.0/. Any rights in individual contents of the database are licensed under the Database Contents License: http://opendatacommons.org/licenses/dbcl/1.0/), and edited with QGis 2.18 software. The images were also edited using Corel Draw graphics Suite (X5).

https://doi.org/10.1371/journal.pone.0187329.g006

ENM results (Fig 6) and the potential LGM distributions were more widespread. On the other hand, the potential distribution of MID-HOL was reduced, which showed more similarities with the current conditions. The potential distributions of the LIG were the most restricted of all the ENMs. Suitable habitats in the LGM showed a great expansion in relation to the LIG. However, in all the models tested, areas of low suitability present between the Pampas and

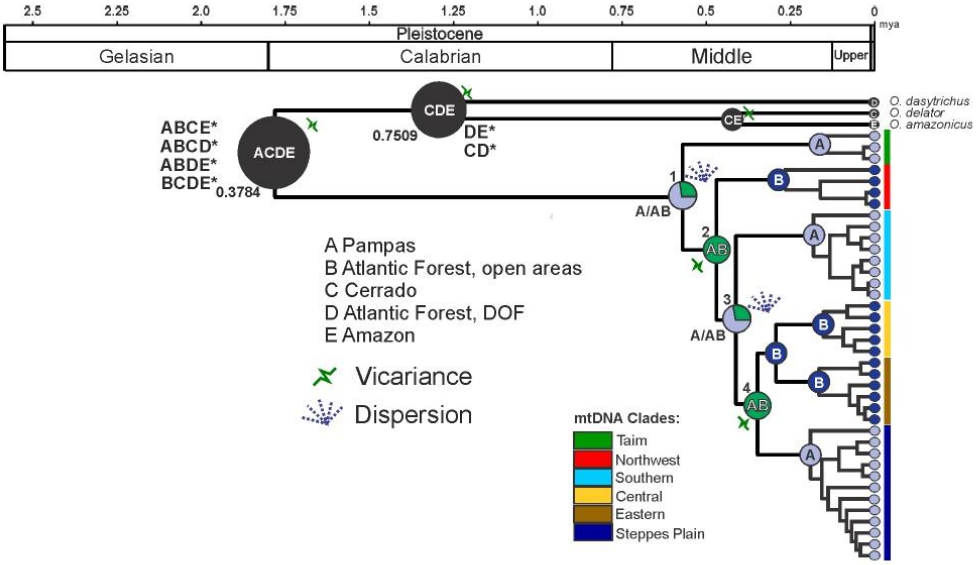

Fig 7. BEAST–derived phylogenetic relationships of 38 mtDNA haplotypes, divergence dating, and ancestral area reconstruction of *O. nasutus* clades. Larger pie diagrams on the nodes indicate the ancestral distributions inferred by S-DIVA methods using RASP. Asterisk represents the occurrence of less frequent inferences. Symbols indicate dispersion or vicariance. The clades are denoted according to Bayesian clades. Area codes: A-Pampas; B- Southern Atlantic Forest; C-Cerrado; D-Ombrophylous Dense Forest; E-Amazon.

https://doi.org/10.1371/journal.pone.0187329.g007

Atlantic Forest domains were identified, as well as in the western part of the territory of Uruguay. In addition, the coastal areas did not have suitable conditions during the LGM.

According to S-DIVA analysis (Fig 7), Pampas ecoregion (A/AB, node 1) was the most likely region for the origin of the dispersal of *O. nasutus*. Dispersal events probably progressed from Pampas domain (A) to areas that are currently translocated into the Atlantic Forest domains (B) and also ranging to other regions of the Pampas. Vicariance signals, detected on node 2 (AB), indicated that vicariance events occurred between the Northwest clade and the other haplogroups that had dispersed between the Pampas and the Atlantic Forest. A new dispersion event was detected on node 3 (A/AB), scattering the haplogroups (Southern, Steppes Plain, Central, and Eastern) along the Pampas and the current Atlantic Forest areas. Finally, on node 4, a new vicariance was verified between the haplogroups that were present on the Atlantic Forest areas (Central and Eastern) and the Pampas (Steppes Plain).

Discussion

Genetic and morphological variation in the Pampas and Atlantic Forest

The absence of *Cytb* haplotypes that was common to Atlantic Forest and Pampas groups was intriguing. However, the scenario was intricate, as a lack of further structuring between the two biomes in the Bayesian and median-joining network analysis was evident. This pattern indicated a possible isolation following the historical scenario of gene flow, as depicted by the *Fgb*-I7 network. Patterns of skull form were also roughly in agreement with the molecular findings. The differentiation between the physiognomies of *O. nasutus* populations were

evident in the classification after the cross-validation. Subtle differences in the skull shape of *O. nasutus* populations were also depicted among the environments. Such skull differences might be related to genetic grouping or with environmental factors, exerting some form of local selection and/or guiding phenotypic plasticity in each physiognomy [8]. Similarly, studies on haplogroups of sympatric akodonts (e.g., *Deltamys kempi* [63, 64] and *Scapteromys* spp. [65, 66]). were also divergent in the geometric or linear morphometric analysis of the skull.

A conspicuous geomorphological feature of the connection among the southern Atlantic Forest and Pampas landscapes is the escarpment of Serra Geral (Meridional Plateau), which might have acted as a long-term barrier to gene flow between the Pampas and the current Atlantic Forest open areas at the eastern point of contact of these two biomes. Thus, the altitudinal gradient formed might have influenced certain level of differentiation, thereby rendering a group of lineages dispersing across the highlands of the Meridional Plateau, and others through the sedimentary lowlands of the Paraná basin, and later spreading along the coastal plain. Mountain ranges and ridges have been considered as topographic elements associated with speciation processes in akodontine rodents [67–71]. Since the differentiation in *O. nasutus* populations is recent (time-tree revealed that the diversification probably began in the Middle Pleistocene) and the divergence process seems incomplete, it can be considered at the population-level and not at species-level yet.

The population structure of *O. nasutus* was quite complex; therefore, it is possible that the recent expansion of forest formations of the South Atlantic Forest, such as the Araucaria Forest and the seasonally dry Forest lato sensu [21], along with the escarpment of Serra Geral have created a new geographical barrier that separated the Atlantic Forest and Pampas lineages. Hence, divergence in the mtDNA clades suggested that the lineages have persisted in isolation across time, characterizing an 'grassland refuge' pattern. Accordingly, the species adapted to dry and/or cold environments and restricted to small areas surrounded by unsuitable habitats can persist through interglacial microrefugium [72].

Phylogeographic patterns

The phylogenetic tree revealed a more complex evolutionary history in the open areas of Pampas and Atlantic Forest instead of simple reciprocally monophyletic groups. Six major mtDNA clades were observed, which fall within the range of intraspecific divergence described for the Akodontini tribe [63, 64, 71, 73]. The mtDNA haplotype network analysis in this study was congruent with such tree structure, representing the six haplogroups separated by several mutational steps, and inserted in specific ecoregions. However, median joining vectors present in the network did not rule out the hypothesis of non-sampled or possibly extinct haplotypes. Although differentiation was less evident, patterns found in nDNA haplotypes provided indication of a demographic expansion event. Similarly, results of mtDNA analysis also suggested demographic growth. In addition, intraspecific *Fgb*-I7 variability was conspicuously lower than *Cytb* variability, as reported in other studies [43, 63,74]. Molecular markers such as mtDNA and nDNA generally show different phylogeographic patterns for the same biogeographical history owing to differentiation in effective population sizes, recombination, and mutation rates [75, 76].

The estimates of genetic distances for the mtDNA clades were moderately high (up to 2%). This might be the result of an ongoing process of isolation, and because mtDNA accumulates substitutions 5–10 times faster than the single-copy nuclear DNA [75]. The highest distances were observed among Taim Wetland versus other clades and between Southern and Northwest clades; however, none of these genetic distances were recovered for the nuclear locus (divergence close to zero). The highest genetic distance observed for these clades (Taim

Wetland, Northwest, and South) might relate to the ancestral condition of these groups, as depicted by BI and mtDNA network, along with the fact that they are geographically distant from each other. According to the S-DIVA analysis, tandem dispersion events followed by vicariance might have probably influenced the phylogenetic pattern of mtDNA observed in the study.

The Northwest clade was the northernmost lineage; so, the effects of the dynamics of forest formations/open areas might have reached earlier in this group, making it more suitable to environmental pressure. Positive values for the Tajima's D test (0.44358, P = 0.7550) for this clade (from mtDNA) and other negative but non-significant values (for both markers), indicated a possible contraction effect on this lineage. The divergence between the Steppes Plain and Central and Eastern clades dates back to 0.350 myr (0.220–0.505 myr). Moreover, some forest formation similar to Seasonal Forest, which at present is adjacent to the escarpment of the Serra Geral might have acted concomitantly. This hypothesis was supported by the results of the ENM that indicated an area of very low suitability between the zone of contact of these two ecoregions. This is consistent with the escarpment of Serra Geral, which might have corroborated mainly due to the vicariance between the Steppes Plain and Central and Eastern clades, as detected by S-DIVA analyses. Similarly, a strong phylogenetic break in this region was evident for other akodonts recently described, such as *Scapteromys meridionalis* [71] and *Deltamys araucaria* [64]. An evident pattern is the genetic divergence within the Southern clade in the Pampas ecoregion (Uruguay). In this study, ENM supported up to a limited dispersion, indicating a possible historical barrier acting in this region. In this case, the Rio Negro could be possibly acting as a barrier for Southern clade, wherein areas of low suitability were identified in all the prediction models. Southern clade was one of the most spread throughout the Pampas ecoregion. Although neutrality test indicated expansion, Southern clade was the only clade where suitable areas were identified mainly in the coastal regions and continental shelf, according to the LGM niche models.

A remarkable phylogeographic aspect was the genetic divergence of the Taim Wetland clade. The mtDNA dataset revealed a statistically supported phylogenetic break between the Taim Wetland clade and other clades, indicating a possible historical barrier acting in this region. This lineage originated about 0.147 myr (95% HPD = 0.047–0.290 myr) and was the first to have dispersed in the S-DIVA analysis. This clade was inserted on the plains of southernmost Brazil (RS), where climatic oscillations occurred during the middle Pleistocene and Holocene, resulting in marine transgressions and regressions of relative sea level that shaped the South Atlantic Coastal Plain (SACP). The formation of the SACP is related to the sedimentary processes associated with the sea transgressive events known as 'Barriers', which occurred in the middle Pleistocene with the formation of Barrier I (~ 0.400 myr), Barrier II (~ 0.325 myr), Barrier III (~ 0.120 myr), and Holocene, when Barrier IV (~0.005 myr) was established [77]. Possibly, this clade accessed this region after the formation of barriers II and III, between 0.325 and 0.120 myr, respectively. The geological evolution of the "Barriers" also formed the Patos-Mirim complex, the largest lagoon-barrier system in South America [77]. In addition, three paleochannels related to the Jacuí, Camaquã, and Jaguarão rivers were identified in the middle and southern coastal zone of RS [78]. These paleochannels were associated with the large persistent hydrographic elements such as Mirim Lagoon, São Gonçalo Channel, and the Patos Lagoon estuarine channel, which might have possibly contributed to the isolation of this lineage in the southernmost domains of the SACP. Similarly, recent studies show a strong phylogenetic break in the same region for *Scapteromys tumidus* [65] and *Deltamys kempi* [64]. Thus, major elements of Patos-Mirim lagunar complex might constitute a geographical barrier for the historical gene flow.

Climate change and landscape

Overall, substantial demographic changes associated with Pleistocene climatic oscillations were observed in more than half of the biota investigated in South America. Considering only the taxa to be associated with open vegetation, a total of 68% of the studied species experienced population expansion during the glacial periods [6]. The historical biogeographic approach presented herein appeared to corroborate this pattern detected for the open areas-dwelling species.

All divergence times within *O. nasutus* populations estimated by BEAST occurred during the Middle Pleistocene, wherein a minimum of eight glaciations occurred in the Middle–Late Pliocene in the southern Andes of South America [79]. However, the greatest glaciations occurred during the early Pleistocene, such as the Great Patagonian Glaciations, between 1.16 and 1.01 mya, when the glaciers advanced up to 200 km east of the Andes mountains, and stretching along the Pacific and south of Atlantic coast [79,80]. After the Great Patagonian Glaciations, 13 minor glacial and interglacial periods were recorded for this region in the Early-Middle Pleistocene that reached a maximum around 25,000 and 16,000 years BP (see [79]).

Although the emergence of *O. nasutus* occurred in the earlier periods (ca. 500 kyr), the patterns showed by the present and past niche models depicted expansion of high probability areas during the LGM (~21,000 years BP), favouring its distribution. Probably, a pattern similar to LGM might have occurred during the Great Patagonian Glaciations, where the effects of glaciations might have increased the open areas and retracted the forest formations. The areas of Southern Atlantic Forest were dominated by grasslands between 42,000–10,000 years BP; the period comprising the LGM. Forest elements were restricted to sites in deep river valleys and in coastal lowlands, indicating a cold and dry climate [21]. In general, grasslands adapted to cold conditions prevailed in the southern and southeastern Brazil until around 11,500 years BP [81]. Since *O. nasutus* is intrinsically related to open areas and is abundantly found in these habitats [17–19], cyclic events of the dynamic expansion and retraction of open areas and forests that occurred during glacial and interglacial periods have probably caused species dispersal and historical distribution. Such expansions of open areas promoted by glaciations made the environment more suitable for establishment of new areas, which was detected by S-DIVA analysis. It was interesting to reveal that no suitable areas in the coastal zone were increased during LGM according to the niche model. Palynological studies on the coasts of the states of Santa Catarina and Paraná indicated that fields were abundant in this region and also on the exposed continental shelf during the LGM period, whereas tropical tree species were practically absent [23]. The continental shelf during LGM presented a dry climate, hampering the colonization by any species adapted to humid/wet habitats. Areas of moderate suitability were found in the coastal region of southern Brazil and Uruguay during the LIG, Middle Holocene, and current models, with a reduction of suitability in the inland areas. Thus, the coastal regions in the Pampas ecoregion might have served as a refuge for *O. nasutus* during the interglacial periods.

O. nasutus is known to inhabit the subtropical grassland in wet or flooded seasons [17]. Accordingly, the species is adapted to humid environments, being found in bunch grass and in tall grass near the streams and rivers [82], sandbanks near wet lands across coastal semi-fossorial habit [19], and coastal vegetation in the South Atlantic Coastal Plain [83]. Thus, in addition to grassland, *O. nasutus* might have followed river routes in search of humid environments. Such habitat specialization might reflect the dispersion ability to more extensive regions during the glacial periods.

In this context, we suggest that the two major rivers in Rio Grande do Sul state (the Jacuí and Ibicuí) might have acted (and still be acting) as river barrier for the Steppes Plain clade. The haplotypes of this clade are distributed across the western edge of the Patos Lagoon and the

interior of the plains of southern Brazil. Therefore, ENM suggested that these areas might be unsuitable for the restriction caused mainly by the river Jacuí. Others rivers could have affected the limits of dispersion in *O. nasutus*. Rivers Uruguay and Paraná also might have acted in limiting the dispersion during the glacial periods. The paleoecological niche modelling suggested that at LGM, the River Uruguay limited the dispersion for Steppes Plain and Southern clades in Uruguay and Southern Brazil to reach new areas to the west. Similarly, the River Paraná limited the dispersion for Northwest and Central Clade in highlands. Finally, Paraná, and Paranapanema rivers might have acted as physical barriers in the dispersion to the north, mainly for the Northwest clade, due to their amplitude and water volume. These inferences were based on the ENM results, wherein areas of low suitability were verified in all the prediction models.

Supporting information

S1 Fig. Bayesian consensus time-tree based on the *Fgb*-I7 sequences. Values above nodes correspond to posterior probabilities > 0.90.
(TIF)

S2 Fig. Position of the landmarks (circles) digitized on the dorsal, ventral, and lateral views of the *O. nasutus* skull. A description of each landmark is presented in S1 Appendix.
(TIF)

S3 Fig. Scatter plot of the first Canonical Variate axis for the skull of *O. nasutus* in the lateral view, with groups following the genetic haplogroups (A, B) and the physiognomies (C). Changes in the shape for each axis are given. Solid lines indicate positive scores and dashed lines indicate negative ones.
(TIF)

S1 Appendix. Definition of the landmarks positioned at the three skull views of *O. nasutus* analysed specimens (see. S2 Fig).
(DOCX)

S2 Appendix. Additional localities retrieved from the literature for the spatial distribution modelling analysis.
(DOCX)

S1 Table. Genetic divergence (using *p*-distance) between pairs of *Cytb* haplotypes recovered from different clades of *O. nasutus* determined by the Bayesian phylogeny.
(DOCX)

S2 Table. Percentage of correct classification by discriminant analysis, using Jackknife cross-validation, for the dorsal, ventral, and lateral views of the *O. nasutus* skull for the mtDNA clades.
(DOCX)

S3 Table. Percentage of correct classification by discriminant analysis, using Jackknife Cross-validation, for the dorsal, ventral, and lateral views of the *O. nasutus* skull for the two ecoregions.
(DOCX)

Acknowledgments

We are grateful to Enrique M. Gonzalez (Museo Nacional de Historia Natural, MNHN), Enrique P. Lessa (Universidad de la República), Alexandre U. Christoff (Museu de Ciencias

Naturais da Universidade de Luterana do Brasil, MCNU), Andre L. Luza (UFRGS), Iris Hass (UFPR), Ives J. Sbalqueiro (UFPR), Antenor Silva and Sebastiao Pereira (Museu de História Natural "Capão da Imbuia", MHNCI) for loan tissue/skull samples. Thanks also to Andres Parada (Universidade Austral de Chile) for helping with the substitution rate for time-tree estimates and Elizabeth Rachenberg (FURB) for helping with the curatorial work of the material. Geraldo Mader, Andrea Turchetto-Zolet (PPGBM-UFRGS) and two anonymous reviewers made suggestions on earlier drafts of the manuscript that helped improve and clarify the text. This research was supported by the Coordenadoria de Aperfeiçoamento Pessoal (CAPES), Fundação de Amparo à Pesquisa do Estado do Rio Grande do Sul (FAPERGS) and Conselho Nacional de Desenvolvimento Científico e Tecnológico (CNPq). G.L. Gonçalves and R. Maestri received fellowships from FAPERGS (16/2551-0000485-4) and CNPq (150391/2017-0), respectively.

Author Contributions

Conceptualization: Willian T. Peçanha, Fernando M. Quintela, Gislene L. Gonçalves, Thales R. O. Freitas.

Data curation: Willian T. Peçanha, Sergio L. Althoff, Fernando M. Quintela, Gislene L. Gonçalves.

Formal analysis: Willian T. Peçanha, Daniel Galiano, Renan Maestri.

Funding acquisition: Thales R. O. Freitas.

Investigation: Willian T. Peçanha, Fernando M. Quintela, Gislene L. Gonçalves, Thales R. O. Freitas.

Methodology: Willian T. Peçanha, Sergio L. Althoff, Daniel Galiano, Fernando M. Quintela, Renan Maestri, Gislene L. Gonçalves, Thales R. O. Freitas.

Project administration: Gislene L. Gonçalves, Thales R. O. Freitas.

Resources: Thales R. O. Freitas.

Supervision: Gislene L. Gonçalves, Thales R. O. Freitas.

Validation: Gislene L. Gonçalves, Thales R. O. Freitas.

Visualization: Thales R. O. Freitas.

Writing – original draft: Willian T. Peçanha, Gislene L. Gonçalves.

Writing – review & editing: Willian T. Peçanha, Sergio L. Althoff, Daniel Galiano, Fernando M. Quintela, Renan Maestri, Gislene L. Gonçalves, Thales R. O. Freitas.

References

1. Lisiecki LE, Raymo ME. Plio-Pleistocene climate evolution: Trends and transitions in glacial cycle dynamics. Quaternary Sci Rev. 2007; 26, 56–69. https://doi.org/10.1016/j.quascirev.2006.09.005
2. Hewitt GM. Some genetic consequences of ice ages, and their role in divergence and speciation. Biol. J. Linn. Soc. 1996; 58: 247–276.
3. Hewitt G. The genetic legacy of the Quaternary ice ages. Nature. 2000; 405: 907–913. https://doi.org/10.1038/35016000 PMID: 10879524
4. Hewitt G. Genetic consequences of climatic oscillations in the Quaternary. Philos. Trans. R. Soc. Lond. B: Biol. Sci. 2004; 359: 183–195. https://doi.org/10.1098/rstb.2003.1388
5. Avise JC. Phylogeography: the history and formation of species. Cambridge, Harvard University Press; 2000.

6. Turchetto-Zolet AC, Pinheiro F, Salgueiro F, Palma-Silva C. Phylogeographical patterns shed light on evolutionary process in South America. Mol Ecol. 2013; 22: 1193–1213. https://doi.org/10.1111/mec.12164 PMID: 23279129
7. Carnaval AC, Moritz C. Historical climate modelling predicts patterns of current biodiversity in the Brazilian Atlantic forest. J Biogeogr. 2008; 35: 1187–1201. https://doi.org/10.1111/j.1365-2699.2007.01870.x
8. Maestri R, Fornel R, Gonçalves GL, Geise L, Freitas TRO, Carnaval AC. Predictors of intraspecific morphological variability in a tropical hotspot: comparing the influence of random and non-random factors. J Biogeogr. 2016; 43: 2160–2172. https://doi.org/10.1111/jbi.12815
9. Bilenca DN, Miñarro FO. Identificación de áreas valiosas de pastizal en las pampas y campos de Argentina, Uruguay y sur de Brasil. Buenos Aires: Fundación Vida Silvestre Argentina. 323 p. 2004
10. Behling H. South and southeast Brazilian grasslands during Late Quaternary times: a synthesis. Palaeogeogr Palaeocl. 2002; 177: 19–27. https://doi.org/10.1016/S0031-0182(01)00349-2
11. Mapelli F, Mora MS, Mirol PM, Kittlein M. Effects of Quaternary climatic changes on the phylogeography and historical demography of the subterranean rodent *Ctenomys porteousi*.J Zool. 2012; 286: 48–57. https://doi.org/10.1111/j.1469-7998.2011.00849.x
12. Mora MS, Cutrera AP, Lessa EP, Vassallo AI, D'Anatro A, Mapelli FJ. Phylogeography and population genetic structure of the Talas tuco-tuco (*Ctenomys talarum*): integrating demographic and habitat histories. J Mammal. 2013; 94: 459–476. https://doi.org/10.1644/11-MAMM-A-242.1
13. Fregonezi JN, Turchetto C, Bonatto SL, Freitas LB. Biogeographical history and diversification of *Petunia* and *Calibrachoa* (Solanaceae) in the Neotropical Pampas grassland. Bot J Linn Soc. 2013; 171: 140–153. https://doi.org/10.1111/j.1095-8339.2012.01292.x
14. Felappi JF, Vieira RC, Fagundes NJR, Verrastro LV. So Far Away, Yet So Close: Strong Genetic Structure in *Homonota uruguayensis* (Squamata, Phyllodactylidae), a Species with Restricted Geographic Distribution in the Brazilian and Uruguayan Pampas. PLoS One. 2015; 10(2): e0118162. https://doi.org/10.1371/journal.pone.0118162 PMID: 25692471
15. Cristiano MP, Cardoso DC, Fernandes-Salomão TM, Heinze J. Integrating Paleodistribution Models and Phylogeography in the Grass-Cutting Ant *D1* (Hymenoptera: Formicidae) in Southern Lowlands of South America. PLoS One. 2016; 11(1): e0146734. https://doi.org/10.1371/journal.pone.0146734 PMID: 26734939
16. Bonvicino CR, Oliveira JA, D'Andrea PS. Guia dos Roedores do Brasil, com chaves para gêneros baseadas em caracteres externos. Rio de Janeiro: Centro Pan-Americano de Febre Aftosa—OPAS/OMS; 2008.
17. Oliveira JA, Gonçalves PR. Suborder Myomorpha: Family Cricetidae: Subfamily Sigmodontinae. Genus *Oxymycterus*; pp. 247–268 in: Patton J.L., Pardiñas U.F.J. and D'Elía G. (eds.). Mammals of South America 2: Rodents. Chicago: University of Chicago Press; 2015.
18. Paise G, Vieira EM. Daily activity of a Neotropical Rodent (*Oxymycterus nasutus*): seasonal changes and influence of Environmental factors. J Mammal. 2006; 87 (4): 733–739. https://doi.org/10.1644/05-MAMM-A-158R5.1
19. González EM.Guía de campo de los mamíferos de Uruguay. Introducción al estudio de los mamíferos. Montevideo: Vida Silvestre 339p, 2001.
20. Behling H, Bauermann SG, Neves PCP. Holocene environmental changes in the São Francisco de Paula region, southern Brazil. J S Am Earth Sci. 2001; 14: 631–639. https://doi.org/10.1016/S0895-9811(01)00040-2
21. Overbeck GE, Muller SC, Fidelis A, Pfadenhauer J, Pillar VD, Blanco CC, et al. Brazil's neglected biome: The South Brazilian Campos. Perspect Plant Ecol. 2007; 9: 101–116. https://doi.org/10.1016/j.ppees.2007.07.005
22. Behling H, Pillar VD. Late Quaternary vegetation, biodiversity and fire dynamics on the southern Brazilian highland and their implication for conservation and management of modern Araucaria forest and grassland ecosystems. Philos T R Soc B. 2007; 362: 243–251. https://doi.org/10.1098/rstb.2006.1984
23. Behling H, Negrelle RRB. Tropical Rain Forest and Climate Dynamics of the Atlantic Lowland, Southern Brazil, during the Late Quaternary. Quaternary Res. 2001; 56:3, 383–389. https://doi.org/10.1006/qres.2001.2264
24. Smith MF, Patton JL. The diversification of South American murid rodents: evidence from mitochondrial DNA sequence data for the akodontine tribe. Biol J Linn Soc. 1993; 50: 149–177. https://doi.org/10.1006/bijl.1993.1052
25. Matocq MD, Shurtliff QR, Feldman CR. Phylogenetics of the woodrat genus *Neotoma* (Rodentia: Muridae): implications for the evolution of phenotypic variation in male external genitalia. Mol Phylogenet Evol. 2007; 42:637–652. https://doi.org/10.1016/j.ympev.2006.08.011 PMID: 17208019

26. Katoh K, Standley DM.MAFFT Multiple Sequence Alignment Software Version 7: Improvements in Performance and Usability. Mol Biol Evol. 2013; 30: 772–780. https://doi.org/10.1093/molbev/mst010 PMID: 23329690

27. Stephens M, Smith NJ, Donnelly P. A new statistical method for haplotype reconstruction from population data. Am. J. Hum. Genet. 2001; 68: 978–989. https://doi.org/10.1086/319501 PMID: 11254454

28. Stephens M, Donnelly P. A comparison of Bayesian methods for haplotype reconstruction from population genotype data. Am J Hum Genet. 2003; 73:1162–1169. https://doi.org/10.1086/379378 PMID: 14574645

29. Librado P, Rozas J. DnaSP v5: A software for comprehensive analysis of DNA polymorphism data. Bioinformatics. 2009; 25: 1451–1452. https://doi.org/10.1093/bioinformatics/btp187 PMID: 19346325

30. Garrick RC, Sunnucks P, Dyer RJ. Nuclear gene phylogeography using PHASE: dealing with unresolved genotypes, lost alleles, and systematic bias in parameter estimation. BMC Evol. Biol. 2010; 10: 118. https://doi.org/10.1186/1471-2148-10-118 PMID: 20429950

31. Darriba D, Taboada GL, Doallo R, Posada D. jModelTest 2: more models, new heuristics and parallel computing. Nat Methods. 2012; 30: 772. https://doi.org/10.1038/nmeth.2109

32. Drummond AJ, Suchard MA, Xie D, Rambaut A. Bayesian phylogenetics with BEAUti and the BEAST 1.7. Mol Biol Evol. 2012; 29:1969–73. https://doi.org/10.1093/molbev/mss075 PMID: 22367748

33. Rambaut A, Drummond AJ. Tracer version 1.5 [computer program]. http://beast.bio.ed.ac.uk. 2009.

34. Parada A D'Elía G, Palma R. The influence of ecological and geographical context in the radiation of Neotropical sigmodontine rodents. BMC Evol Biol. 2015; 15:172. https://doi.org/10.1186/s12862-015-0440-z PMID: 26307442

35. Hoffmann FG, Lessa EP, Smith MF. Systematics of *Oxymycterus* with description of a new species from Uruguay. J Mammal. 2002; 83: 408–420.

36. Alfaro ME, Zoller S, Lutzoni F. Bayes or bootstrap? A simulation study comparing the performance of Bayesian Markov chain Monte Carlo sampling and bootstrapping in assessing phylogenetic confidence. Mol Biol Evol. 2003; 20: 255–266. https://doi.org/10.1093/molbev/msg028 PMID: 12598693

37. Bandelt HJ, Forster P, Röhl A. Median-joining networks for inferring intraspecific phylogenies. Mol. Biol. Evol. 1999; 16:37–48. https://doi.org/10.1093/oxfordjournals.molbev.a026036 PMID: 10331250

38. Kumar S, Stecher G, Tamura K. MEGA7: Molecular Evolutionary Genetics Analysis version 7.0 for bigger datasets. Mol Biol Evol. 2016; 33: 1870–1874. https://doi.org/10.1093/molbev/msw054 PMID: 27004904

39. Tajima F. Statistical method for testing the neutral mutation hypothesis by DNA polymorphism. Genetics. 1989; 123: 585–595 PMID: 2513255

40. Fu Y-X. Statistical tests of neutrality of mutations against population growth, hitchhiking and background selection. Genetics. 1997; 147: 915–925. PMID: 9335623

41. Excoffier L, Lischer HEL. Arlequin suite ver 3.5: a new series of programs to perform population genetics analyses under Linux and Windows. Mol Ecol Resour. 2010; 10 (3): 564–567. https://doi.org/10.1111/j.1755-0998.2010.02847.x PMID: 21565059

42. Drummond AJ, Rambaut A, Shapiro B, Pybus OG. Bayesian Coalescent Inference of Past Population Dynamics from Molecular Sequences. Mol Biol Evol. 2005; 22: 1185–1192. https://doi.org/10.1093/molbev/msi103 PMID: 15703244

43. Platt RN, Amman BR, Keith MS, Thompson CW, Bradley RD. What Is *Peromyscus*? Evidence from nuclear and mitochondrial DNA sequences suggests the need for a new classification. J Mammal. 2015; 96: 708–719. https://doi.org/10.1093/jmammal/gyv067 PMID: 26937047

44. Ronquist F. Dispersal-Vicariance analysis: a new approach to the quantification of historical biogeography. Syst Biol. 1997; 46: 195–203. https://doi.org/10.1093/sysbio/46.1.195

45. Yu Y, Harris AJ, He. S-DIVA (Statistical Dispersal-Vicariance Analysis): a tool for inferring biogeographic histories. Mol Phylogenet Evol. X 2010; 56: 848–850. https://doi.org/10.1016/j.ympev.2010.04.011 PMID: 20399277

46. Yu Y, Harris AJ, Blair C, He XJ. RASP (Reconstruct Ancestral State in Phylogenies): a tool for historical biogeography. Mol Phylogenet Evol. 2015; 87: 46–49. https://doi.org/10.1016/j.ympev.2015.03.008 PMID: 25819445

47. Rohlf FJ. The tps series of software. Hystrix. 2015; 26:9–12. https://doi.org/10.4404/hystrix-26.1–11264

48. Martınez JJ, Di Cola V. Geographic distribution and phenetic skull variation in two close species of *Graomys* (Rodentia, Cricetidae, Sigmodontinae). Zool Anz, 2011; 250: 175–194. https://doi.org/10.1016/j.jcz.2011.03.001

49. Maestri R, Fornel R, Galiano D, de Freitas TRO. Niche Suitability Affects Development: Skull Asymmetry Increases in Less Suitable Areas. PLoS One. 2015; 10(4): e0122412. https://doi.org/10.1371/journal.pone.0122412 PMID: 25874364

50. Rohlf FJ, Slice D. Extensions of the Procrustes method for the optimal superimposition of landmarks. Syst. Zool. 1990; 39: 40–59.

51. Bookstein FL. Morphometric tools for landmark data: geometry and biology. Cambridge, Cambridge University Press, UK; 1991.

52. R Core Team. R: a language and environment for statistical computing. R Foundation for Statistical Computing, Vienna, Austria; (2014)

53. Adams DC, Otárola-Castillo E. geomorph: and R package for the collection and analysis of geometric morphometric shape data.–Methods Ecol. Evol. 2013; 4: 393–399. https://doi.org/10.1111/2041-210X.12035

54. Schlager S. "Morpho and Rvcg—Shape Analysis in R." In: Zheng G, Li S and Szekely G (editors), Statistical Shape and Deformation Analysis, pp. 217–256. Academic Press; 2017.

55. Klingenberg CP. MorphoJ: an integrated software package for geometric morphometrics. Mol Ecol Res. 2011; 11: 353–357. https://doi.org/10.1111/j.1755-0998.2010.02924.x

56. Phillips SJ, Anderson RP, Schapire RE. Maximum entropy modeling of species geographic distributions. Ecol Model. 2006; 190, 231–259. https://doi.org/10.1016/j.ecolmodel.2005.03.026

57. Elith J, Graham CH, Anderson RP, Dudík M, Ferrier S, Guisan S. et al. Novel methods improve prediction of species' distributions from occurrence data. Ecography. 2006; 29: 129–151. https://doi.org/10.1111/j.2006.0906–7590.04596.x

58. Peterson AT, Papes M, Eaton M. Transferibility and model evaluation in ecological niche modeling: a comparison of GARP and Maxent. Ecography. 2007; 30: 550–560. https://doi.org/10.1016/j.ecolmodel.2007.11.008

59. Peterson AT, Papes M, Soberón J. Rethinking receiver operating characteristic analysis applications in ecological niche modeling. Ecol. Model. 2008; 213: 63–72.

60. Hernandez PA, Graham CH, Master LL, Albert DL. The effect of sample size and species characteristics on performance of different species distribution modeling methods. Ecography. 2006; 29: 773–785. https://doi.org/10.1111/j.0906-7590.2006.04700.x

61. Swets JA. Measuring the accuracy of diagnostic systems. Science. 1988; 240: 1285–1293 PMID: 3287615

62. Gent PR, Danabasoglu G, Donner LJ, Holland MM, Hunke EC, Jayne SR et al. The Community Climate System Model version 4. J. Climate, 2011; 24: 4973–4991. https://doi.org/10.1175/2011JCLI4083.1

63. Montes MA, Oliveira LFB, Bonatto SL, Callegari-Jacques SM, Mattevi MS. DNA sequence analysis and the phylogeographical history of the rodent *Deltamys kempi* (Sigmodontinae, Cricetidae) on the Atlantic Coastal Plain of south of Brazil. J Evol Biol. 2008; 26: 1823–1835. https://doi.org/10.1111/j.1420-9101.2008.01586.x

64. Quintela FM, Bertuol F, González EM, Cordeiro-Estrela P, Freitas TRO, Gonçalves GL. A new species of *Deltamys* Thomas, 1917 (Rodentia: Cricetidae:) endemic to the southern Brazilian Araucaria Forest and notes on the expanded phylogeographic scenario of *D. kempi*. Zootaxa. 2017; 4294: 071–092. https://doi.org/10.11646/zootaxa.4294.1.3

65. Quintela FM, Gonçalves GL, Bertuol F, González EM, Freitas TRO. Genetic diversity of the swamp rat in South America: Population expansion after transgressive-regressive marine events in the Late Quaternary. Mamm Biol. 2015; 80: 510–517. https://doi.org/10.1016/j.mambio.2015.08.003

66. Quintela FM, Fornel R, Freitas TRO. Geographic variation in skull shape of the water rat *Scapteromys tumidus* (Cricetidae, Sigmodontinae): isolation-by-distance plus environmental and geographic barrier effects?. An. Acad. Bras. Ciênc. 2016; 88: 451–466. https://doi.org/10.1590/0001-3765201620140631 PMID: 27142549

67. Reig OA. Distribuição geográfica e história evolutiva dos roedores muroideos sulamericanos (Cricetidae: Sigmodontinae). *Rev Bras Genet*. 1984; 7: 333–365

68. Geise L, Smith MF, Patton JL. Diversification in the genus *Akodon* (Rodentia: Sigmodontinae) in southeastern South America: mitochondrial DNA sequence analysis. J Mamm. 2001; 82: 92–101.

69. Gonçalves PR, Myers P, Vilela JF, Oliveira JA. Systematics of species of the genus *Akodon* (Rodentia: Sigmodontinae) in southeastern Brazil and implications for the biogeography of the Campos de Altitude. Misc. publ.—Mus. Zool., Univ. Mich.2007; 197: 1–24.

70. Gonçalves PR, Oliveira JA. An integrative appraisal of the diversification in the Atlantic forest genus *Delomys* (Rodentia: Cricetidae: Sigmodontinae) with the description of a new species. Zootaxa. 2014; 3760:1–38. https://doi.org/10.11646/zootaxa.3760.1.1 PMID: 24870069

71. Quintela FM, Gonçalves GL, Althoff SL, Sbalqueiro IJ, Oliveira LFB, Freitas TRO. A new species of swamp rat of the genus *Scapteromys* Waterhouse, 1837 (Rodentia: Sigmodontinae) endemic to *Araucaria angustifolia* Forest in Southern Brazil. Zootaxa. 2014; 3811:207–225. https://doi.org/10.11646/zootaxa.3811.2.3

72. Rull V. Microrefugia. J Biogeogr. 2009; 36: 481–484. https://doi.org/10.1111/j.1365-2699.2008.02023.x

73. D'Elía G, Pardiñas UFJ. Systematics of Argentinean, Paraguayan, and Uruguayan swamp rats of the genus *Scapteromys* (Rodentia, Cricetidae, Sigmodontinae). J Mammal. 2004; 85: 897–910. https://doi.org/10.1644/BRB-201

74. D'Elía G, Hanson JD, Mauldin MR, Teta P, Pardiñas UFJ. Molecular systematics of South American marsh rats of the genus *Holochilus* (Muroidea, Cricetidae, Sigmodontinae). J Mammal. 2015; 96: 1081–1094. https://doi.org/10.1093/jmammal/gyv115

75. Avise JC. Phylogeography: retrospect and prospect. J Biogeog. 2009; 36: 3–15. https://doi.org/10.1111/j.1365-2699.2008.02032.x

76. Toews DPL, Brelsford A. The biogeography of mitochondrial and nuclear discordance in animals. Mol Ecol. 2012; 21:3907–3930. https://doi.org/10.1111/j.1365-294X.2012.05664.x PMID: 22738314

77. Tomazelli LJ, Villwock JA. Mapeamento geológico de planícies costeiras: o exemplo da costa do Rio Grande do Sul. Gravel. 2005; 3:109–115.

78. Weschenfelder J, Correa ICS, Aliotta S, Baitelli R. Paleochannels related to late Quaternary sea-level changes in Southern Brazil. Braz J Oceanogr. 2010; 58:35–44. https://doi.org/10.1590/S1679-87592010000600005

79. Rabassa J, Coronato A, Salemme M. Chronology of the Late Cenozoic Patagonian glaciations and their correlation with biostratigraphic units of the Pampean region (Argentina). J S Am Earth Sci. 2005; 20: 81–103. https://doi.org/10.1016/j.jsames.2005.07.004

80. Rabassa J, Clapperton C (1990) Quaternary glaciations of the southern Andes. Quaternary Sci Rev. 1990; 9:153–174. https://doi.org/10.1016/0277-3791(90)90016-4

81. Behling H, Jeske-Pieruschka V, Schüler L, Pillar VP. Campos Sulinos, conservação e uso sustentável da biodiversidade. In: Pillar VP, Müller SC, Castilhos ZMS, Jacques AVA, editors. Ministério do Meio Ambiente, Brasília, Brazil, 2009.

82. Barlow JC. Observations on the biology of rodents in Uruguay. Life sci. contrib., R. Ont. Mus. 1969; 75:1–59.

83. Quintela FM, Santos MB, Christoff AU, Gava A. Pequenos mamíferos não-voadores (Didelphimorphia, Rodentia) em dois fragmentos de mata de restinga de Rio Grande, Planície Costeira do Rio Grande do Sul. Biota Neotrop. 2012; 12:261–266.

Supporting information

S1 Fig. Bayesian consensus time-tree based on the *Fgb*-I7 sequences. Values above nodes correspond to posterior probabilities > 0.90.

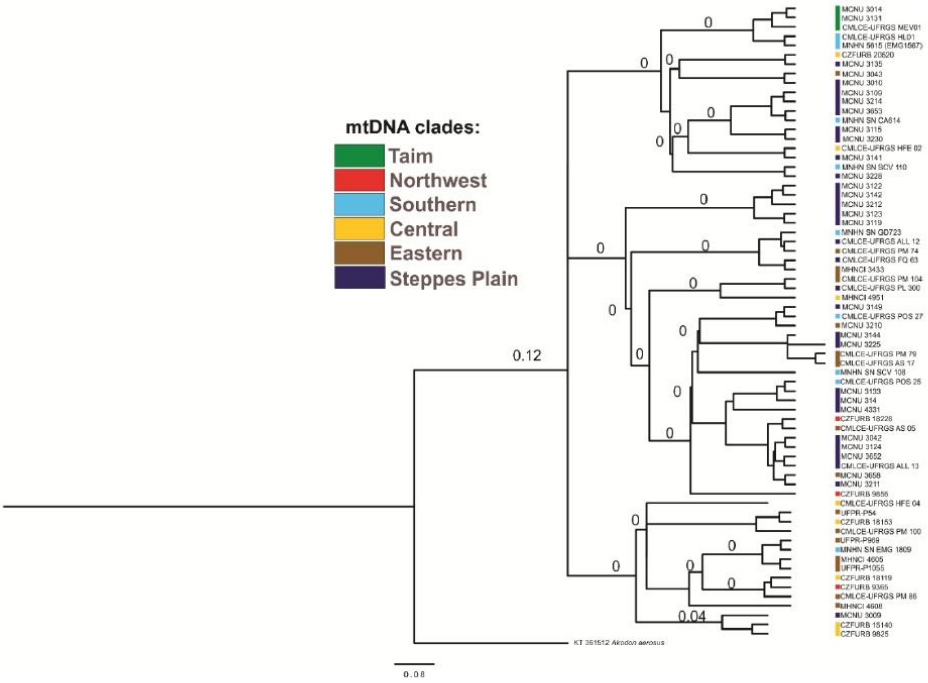

Supporting information

S2 Fig. Position of the landmarks (circles) digitized on the dorsal, ventral, and lateral views of the *O. nasutus* skull. A description of each landmark is presented in S1 Appendix. (TIF)

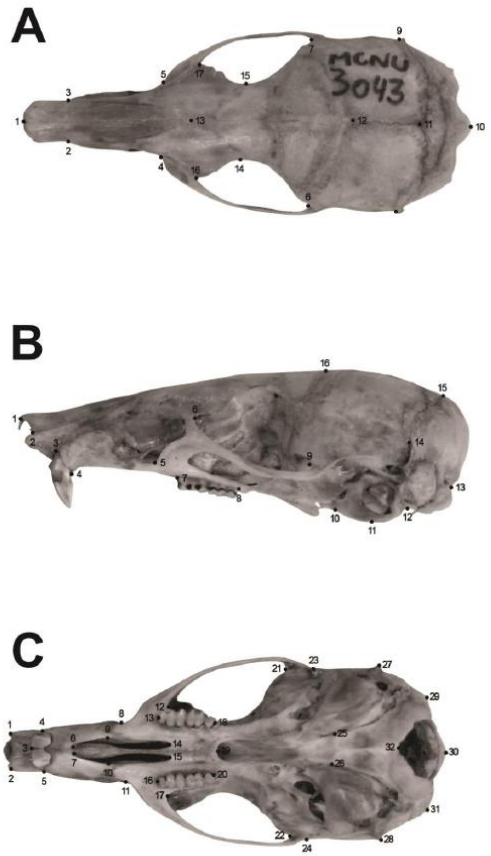

Fig S2 Peçanha et al. PONE

Supporting information

S3 Fig. Scatter plot of the first Canonical Variate axis for the skull of *O. nasutus* in the lateral view, with groups following the genetic haplogroups (A, B) and the physiognomies (C).Changes in the shape for each axis are given. Solid lines indicate positive scores and dashed lines indicate negative ones. (TIF)

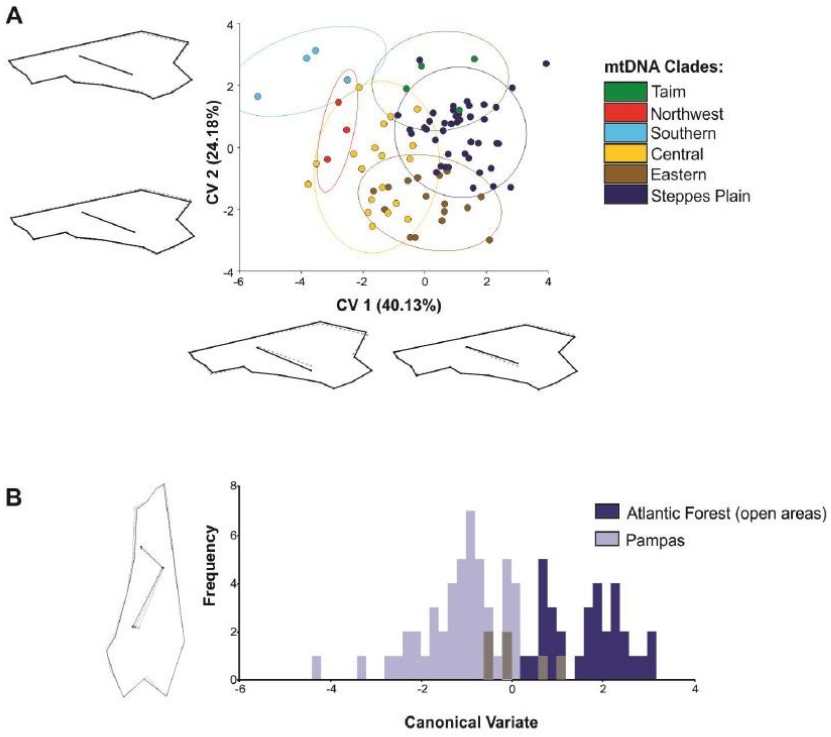

Fig S3 Peçanha et al. PONE

Supporting information

S1 Appendix. Definition of the landmarks positioned at the three skull views of *O. nasutus* analysed specimens (see. S2 Fig). **(DOCX)**

Description of landmarks of skull-ventral view:

1-2: Longest point parallel between nasal; **3:** Midpoint of upper incisors**; 4-5:** lateralmost point of the alveolus of the incisor; **6-7:** anteriormost margin of incisive foramen; **8-11:** anteriormost margin of zygomaticplate; **9-10:** posteriormost point of suture between premaxilla and maxilla; **12-17:** anteriormost margin of the maximum zygomatic plate posterior constriction; **14-15:** posteriormost margin of incisive foramen; **13-16:** anteriormost margin of first molar alveolus; **18-20:** posteriormost margin of third molar; **19:** posteriormost point of suture between palatines; **21-22:** posteriormost margin of the maximum anterior constriction of squamosal root of zygomatic; **23-24:** posterior end of squamosal root of zygomatic bar; **25-26:** basis length of suture between basisphenoid and basiocciptal; **27-28:** superiormost margin of tympanic bulla (ectotympanic); **29-31:** midpoint margin of occipital condyle; **30:** posteriormost point of superior margin of foramen magnum; **32:** anteriormost point of inferior margin of foramen Magnum.

Description of landmarks of skull dorsal view:

1: anteriormost point of suture between nasals; **2-3:** anteriormost point of suture between nasal and premaxilla; **4-5:** anteriormost point of zygomatic plate; **6-7:** anteriormost margin of the maximum constriction of squamosal root of zygomatic arch; **8-9:** superiormost point of suture between parietal and occipital; **10:** posteriormost point of occipital margin; **11:** suture between parietals and interparietal; **12:** suture between frontals and parietals; **13:** suture between nasals and frontals; **14-15:** length margim of maximum constriction of interorbital region (frontal); **16-17:** posteriormost margin of maximum constriction of antorbital bridge.

Description of landmarks of skull lateral view:

1: anteriormost point of nasal; **2:** anteriormost point of the suture between the nasal and the premaxilla; **3:** posteriormost point of incisor alveolus; **4:** inferiormost point of incisor alveolus; **5:** ventral extent of infraorbital foramen; **6:** point of maximum posterior constriction of antorbital bridge; **7:** anteriormost point of the molar row; **8:** posteriormost point of the molar row; **9**: point of maximum anterior constriction of squamosal root of zygomatic arch; **10:** anteroventral limit of the tympanic bulla; **11:** ventralmost point at the middle of the tympanic bulla; **12:** inferior extremity on the boundary between the occipital condyle and the tympanic bulla; **13:** curvature at the limit between the occipital condyle and the occipital bone; **14:** suture between parietal, squamosal and occipital; **15:** superiormost point of suture between pariental and interparietal; **16:** superiormost point of suture between frontal and parietal.

Supporting information

S2 Appendix. Additional localities retrieved from the literature for the spatial distribution modelling analysis. (DOCX)

S2 Appendix. Table Additional localities of *Oxymycterus nasutus* recover by Literature for Spatial Distribuition Modelling. *Geographical coordinates were estimated based on the municipality and/or location available.

Reference	Country	State/Dept	Municipality/Locality	Lat. (S), Long (W).
Grazzini et al. 2015	BR	PR	Piraí do Sul, Floresta Nacional de Piraí do Sul	-24.577163, -49.918777
Oliveira and Gonçalves 2015	UR	Canelones	*Salinas, Arroyo Tropa Vieja	-34.775663, -55.875237
Oliveira and Gonçalves 2015	UR	Cerro Largo	*Melo, 6km ao SE	-32.414957, -54.133716
Oliveira and Gonçalves 2015	UR	Rocha	*Lascano, 22km ao SE	-33.790417, -54.068686
Oliveira and Gonçalves 2015	UR	Maldonado	*San Carlos, 15km ao Norte	-34.751549, -54.924380
Hoffmann et al. 2002	UR	Cerro Largo	*Rio Tacuari, 20 km SE Melo	-32.519200, -54.028395

References

Grazzini G, Mochi-Junior CM, Oliveira H, Pontes JS, Gatto-Almeida F, Tiepolo LM. Identidade, riqueza e abundância de pequenos mamíferos (Rodentia e Didelphimorphia) de área de Floresta com Araucária no estado do Paraná, Brasil. Papéis Avulsos de de Zoologia (MZUSP). Volume 55(15):217-230, 2015. http://dx.doi.org/10.1590/00311049.2015.55.15.

Oliveira JA, Gonçalves PR (2015) Suborder Myomorpha: Family Cricetidae: Subfamily Sigmodontinae. Genus *Oxymycterus*; pp. 247–268 in: J.L. Patton, U.F.J. Pardiñas and G. D'Elía (eds.). Mammals of South America 2: Rodents. Chicago: University of Chicago Press. doi: 10.7208/chicago/9780226169606.001.0001

Hoffmann, F.G., E.P. Lessa and M.F. Smith. 2002. Systematics of *Oxymycterus* with description of a new species from Uruguay. Journal of Mammalogy 83(2): 408–420. doi: 10.1644/1545-1542

Supporting information

S1 Table. Genetic divergence (using *p*-distance) between pairs of *Cytb* haplotypes recovered from different clades of *O. nasutus* determined by the Bayesian phylogeny. (DOCX)

Table S1. Genetic divergence (using *p*-distance) between pairs of *Cytb* haplotypes recovered from different clades of *O. nasutus* determined by the Bayesian phylogeny.

Clades	Northwest	Central	Eastern	Coastal Plain	Southern	Within mean group distance
Northwest	-					0.009
Central	0.016	-				0.002
Eastern	0.013	0.010	-			0.003
Steppes Plain	0.016	0.012	0.012	-		0.004
Southern	0.019	0.014	0.016	0.015	-	0.004
Taim	0.023	0.020	0.020	0.021	0.025	0.004

Supporting information

S2 Table. Percentage of correct classification by discriminant analysis, using Jackknife cross-validation, for the dorsal, ventral, and lateral views of the *O. nasutus* skull for the mtDNA clades. (DOCX)

Table S2. Percentage of correct classification from discriminant analysis, using Jackknife Cross-validation, for form in dorsal, ventral, and lateral view of the skull for two Ecorregions where is inserts the *Oxymycterus nasutus*.

Groups	Predicted group membership		
	Pampas	Atlantic Forest	Overall %
Dorsal view of skull			
Pampas (N=51)	94.1176	5.8824	94.11
Atlantic Forest (N=38)	7.8947	92.1053	92.10
Ventral view of skull			
Pampas (N=50)	82	18	82
Atlantic Forest (N=38)	17.949	82.051	82.05
Lateral view of skull			
Pampas (N=50)	86	14	86
Atlantic Forest (N=38)	25.641	74.359	82.05

Supporting information

S3 Table. Percentage of correct classification by discriminant analysis, using Jackknife Cross-validation, for the dorsal, ventral, and lateral views of the *O. nasutus* skull for the two ecoregions. (DOCX)

S3 Table. Percentage of correct classification from discriminant analysis, using Jackknife Cross-validation, for form in dorsal, ventral, and lateral view of the skull for phylogenetic clades of *Oxymycterus nasutus*.

Dorsal View	Southern	Central	Steppes Plain	Taim	Eastern	Northwest	Overall
Southern	50	0	50	0	0	0	50
Central	0	47.3684	15.7895	0	31.5789	5.2632	47.36
Steppes Plain	2.3256	4.6512	86.0465	4.6512	2.3256	0	86.04
Taim	50	0	50	0	0	0	0
Eastern	0	43.75	0	0	50	6.25	50
Northwest	0	66.6667	0	0	33.3333	0	0

Ventral View	Southern	Central	Steppes Plain	Taim	Eastern	Northwest	Overall
Southern	25	0	75	0	0	0	25
Central	0	61.9048	14.2857	9.5238	4.7619	9.5238	61.90
Steppes Plain	0	16.6667	78.5714	2.38	0	2.3810	78.57
Taim	25	25	50	0	0	0	0
Eastern	0	13.3333	0	0	73.3333	13.3333	73.33
Northwest	0	66.6667	0	0	33.3333	0	0

Lateral View	Southern	Central	Steppes Plain	Taim	Eastern	Northwest	Overall
Southern	25	0	25	25	0	25	25
Central	4.7619	47.6190	14.2857	0	28.5714	4.7619	47.61
Steppes Plain	0	2.3810	76.1905	7.1429	14.2857	0	76.19
Taim	0	0	75	25	0	0	25
Eastern	0	40	26.6667	0	33.3333	0	33.33
Northwest	0	100	0	0	0	0	0

CAPÍTULO 3.

Clinal variation on skull size and shape in Darwin's Hocicudo rat (Rodentia: Cricetidae: *Oxymycterus*) and the relative influence of genetic and environmental factors

Willian T. Peçanha, Fernando M. Quintela, Sergio L. Althoff, Luiz E. J. Ribas, Renan Maestri, Gislene L. Gonçalves, Thales R. O. Freitas.

Artigo em preparação: ***Journal of Biogeography***

Clinal variation on skull size and shape in the Darwin's Hocicudo rat (Rodentia: Cricetidae: *Oxymycterus*) and the relative influence of genetic and environmental factors

Willian T. Peçanha*, Fernando M. Quintela, Sergio L. Althoff, Luiz E. J. Ribas, Renan Maestri, Gislene L. Gonçalves, Thales R. O. Freitas.

Programa de Pós-graduação em Genética e Biologia Molecular, Departamento de Genética, Universidade Federal do Rio Grande do Sul, CP 15007, Porto Alegre, RS 91501-970, Brazil.

Programa de Pós-Graduação em Biologia de Ambientes Aquáticos Continentais, Universidade Federal do Rio Grande, Campus Carreiros, Rio Grande, RS 96203-900, Brazil.

Departamento de Ciências Naturais, Universidade Regional de Blumenau, Campus 1, Blumenau, SC 89012-900, Brazil.

Programa de Pós-graduação em Ecologia, Universidade Federal do Rio Grande do Sul, CP 15007, Porto Alegre, RS 91501-970, Brazil.

Departamento de Recursos Ambientales, Facultad de Ciencias Agronómicas, Universidad de Tarapacá, Arica, Chile.

*Correspondence: wthomaz90@gmail.com

ABSTRACT

Aim We aimed to evaluate the relative role of environmental attributes and genetic influence on size and shape of skulls in a small rodent, *Oxymycterus nasutus.*

Location South America

Methods We reveal the patterns of skull size and shape variation using 188 individuals from 47 localities for geometric morphometrics analyses, along with another sub dataset with 47 sampling points with genetic information by cytochrome-*b* gene (61 localities sampling). We extract information from five environmental variables, topography, net primary productivity, annual mean precipitation, mean temperature of the warmest and coldest quarter for the same sampling points. Using the matrix of environmental attributes and genetic distance as predictor components, we estimated the relative importance of genetic and environmental distances on the spatial structure of skull size and shape using variance partitioning analysis.

Results We found a latitudinal gradient of morphologic differentiation for both skull size and shape. Differences in size and shape between females and males were detected, but the sexual dimorphism is uniform among the populations. According to the variation partitioning results, the importance of predictors varied for shape and size. Both genetic and environmental predictors were important to explain the shape gradient (dorsal and ventral view, $P < 0.05$). On the other hand, environmental predictors ($P < 0.01$) were more important to explain size variation than genetic influence.

Main conclusions Measurements of genetic distance and environmental attributes seem to influence in a balanced way the shape of the skull. However, the size of the skull is strongly influenced by environmental attributes. A pattern of morphologic differentiation along a north–south axis is verified on species, with larger organisms to the north (Atlantic Forest domains) and smaller towards to the south (on Pampas). At least this species, the influence of environmental features of each ecoregion seems to overcome the Bergmann's rule to explain the size pattern.

Keywords

Bergmann’s rule, Sigmodontinae, cytochrome-*b*, environmental variables, geographical variation, geometric morphometrics, Pampa, Atlantic Forest

INTRODUCTION

Morphological variation among individuals are found in all lineages of mammals, commonly described in terms of gradual changes in the size and shape of skulls (Cardini *et al.*, 2007, Martínez & Di Cola, 2011), teeth (McGuire, 2010; Ledevin *et al.*, 2010a) or mandibles (Renaud & Millien, 2001) across a species' geographic distribution. Such differences are expected to become more pronounced over time in populations that remain genetically and geographically isolated, as a result of neutral and selective processes (Gould, 1972). However, geographic variation in morphological phenotypes may not coincide with gene flow along environmental gradients (Endler, 1973). Accordingly, other factors in addition to restriction of gene flow, as evolutionary adaptation (e.g. Endler, 1995; Ims, 1997), phenotypic plasticity (e.g. Meyer, 1987; Peres-Neto & Magnan, 2004) and genetic drift are known to account for geographic morphological differences within species. These processes are non-exclusive, and the morphology of individuals in a population might reflect an interaction between them (Renaud & Michaux, 2003; Ackermann & Cheverud, 2004; Ledevin & Millien, 2013). Environmental factors have been suggested to contribute to intraspecific morphological variation in mammals (e.g., Cardini *et al.*, 2007; Cardini & Elton, 2009; Morales *et al.*, 2016), in particular, clinal variation in skull shape and size have been identified in rodents (e.g., Renaud & Millien 2001; Monteiro *et al.*, 2003; Maestri *et al.*, 2016; Peçanha *et al.*, 2017). Gradients of morphological variation often mirror floristic and thermal gradients, leading to empirical generalizations as ecogeographical rules (Souto-Lima & Millien 2014). A classic example is the Bergmann's rule, i.e., in endotherms heat generation capacity increases with body volume, whereas heat loss increases with surface area; larger organisms, with relatively lower surface area, are therefore favoured in cooler environments (Mayr, 1956).

Considering the wide geographic distribution, its abundance and ability to thrive in distinct environments, the Neotropical Darwin's hocicudo (*Oxymycterus nasutus*) provides a good model to

investigate the effects of environmental factors on skull size and shape variation in small mammals. This cricetidae rodent inhabit grasslands, coastal sandbanks and steppes in the Pampas biome at southernmost Brazil and Uruguay (González, 2001; Bonvicino *et al.*, 2008; Oliveira & Gonçalves, 2015), and Atlantic Forest in elevations higher than 1,700 m in southern Brazil (Paise & Vieira, 2006; Oliveira & Gonçalves, 2015).

A recent integrative phylogeographic approach of *O. nasutus* using 2D cranial geometric morphometrics, ecological niche modeling and multilocus DNA sequences analysis revealed patterns of genetic and morphological structure coincident to the biomes of its occurrence, Pampa and Atlantic Forest (Peçanha *et al.*, 2017). Genetic haplogroups explained about 23.5 – 26.3% of the variation in skull shape, whereas the occupation on distinct biomes (Atlantic Forest or Pampa) accounted for 15.4 – 17.9% of such variation (Peçanha *et al.*, 2017). Accordingly, one expected other factors than genetics and biomes structuring to be influencing phenotypic differentiation within *O. nasutus*. The southern Atlantic Forest and Pampas are spatially heterogeneous considering geomorphology, vegetation and climatic conditions (Overbeck *et al.*, 2007; Dantas *et al.*, 2010). Thus, we hypothesize that fine-scale variations on environmental attributes within these biomes might contribute substantially to skull variation in *O. nasutus*. Recent advances in modeling and the integration of phenotypic data to DNA sequencing analyses have allowed to identify and quantify the biological mechanisms that partition genetic and phenotypic variation among populations, and ultimately generate diversity (Edwards *et al.*, 2016; Papadopoulou & Knowles, 2016; Thomé & Carstens, 2016).

Thus, in this study we investigated two aspects concerning the intraspecific differences in the skull morphology of *O. nasutus*. First, we characterize variation in size and shape across the whole distributional range and examined whether a putative clinal pattern conform to the Bergmann's rule (i.e. decreased temperatures lead to increased size in endotherms). Since previous

studies using close related species did not found larger sizes of skull in greater latitudes areas (Maestri *et al.*, 2016; Quintela *et al.*, 2016), we did not expected it for *O. nasutus*. Second, we explicitly quantify the influence of other environmental attributes (i.e. topography, precipitation, net primary productivity and others) and genetic structure on the intraspecific variation of skull morphology (size and shape). *Oxymycterus* species are considered semi-fossorial rodents (Bonvicino *et al.*, 2008; González & Martínez-Lanfranco, 2010). *O. nasutus* forage in the litter, where it digs with the help of the well-developed forefeet claws and muzzle (González & Martínez-Lanfranco, 2010). Accordingly, we predict that factors related to plant coverage (primary productivity, rainfall) might have influence on the geographical variation of the skull shape and size of *O. nasutus*. We expect that patterns of variation among populations (both genotypic and phenotypic) are driven by environmental differences rather than historical process responsible for restricted gene flow. Finally, we quantified the relative influence of genetic structure and environmental attributes on skull morphology.

MATERIAL AND METHODS

Sampling and study area

We obtained 267 specimens from scientific collections (Supporting information, Appendix S1) that include 61 localities, covering almost all the species range in the Atlantic Forest and Pampas biomes (Figure 1). In total, 188 specimens from 47 localities were used for the analyzes of morphological variation of skull. Only adults were included, defined by the presence of a functional third molar. Based on results of sexual dimorphism we pooled males and females in the analyses. The sample size per locality ranged from 2 to 11 individuals. For genetic analyses we used 153

specimens from 47 locations, with data both generated for this study and obtained from Genbank (Appendix S1). Specimens were grouped into eight populations defined as: Paraná [PR], Santa Catarina [SC], Serra Geral [SG], Central Depression-Northern Shield [CDNS], Patos Lagoon West Coast [PLWC], Southern Shield-Campanha [SSC], Southern Coastal Plain [SCP] and Uruguay [UY]), according to traits as ecoregion, geology, major rivers (putative geographic barriers) and evolutionary history inferred by Peçanha *et al.*, (2017). Specimens used for morphological and genetic analyses from each population is presented in Table S1.

Morphometric Analyses

We obtained 2D images of the skulls in two views (dorsal and ventral). Images were captured using a standard protocol for all specimens. We digitized a total of 41 landmarks – 15 in dorsal and 26 in ventral views of the skull, using TPS Dig2 (Rohlf, 2015) (S1 Figure). The description of all the landmarks employed is given in Appendix S2. After, we applied a Generalized Procrustes Analysis (GPA), to remove the effects of isometric size, orientation and position (Rohlf & Slice, 1990). Both ventral and dorsal views were rendered symmetrical to avoid noise caused by bilateral asymmetry. The GPA produces variables that retain all the information about the shape of the structures, which were used in the analyses of geographical variation in shape. We used the centroid size (CS) as a measure of size, which is the square root of the sum of squared distances of each landmark from the centroid of the configuration (Bookstein, 1991). This measure of size from the ventral view was used in the analyses of geographic variation.

We investigated the magnitude of shape and size differences among the eight pre-established populations. A principal component analysis (PCA) in the shape matrix for dorsal and ventral views was generated. The number of PCs necessary to achieve 100% variation in each view

(13 PCs for dorsal view and 24 PCs for ventral view) were used as response variables for downstream analyses.

We tested the existence of significant differences in skull shape among the clusters though a multivariate analysis of variance (MANOVA) for each view, following by a pairwise MANOVA (10,000 interactions), aiming to identify the pairs of clusters that showed significant differences in shape. To investigate how morphology (shape) was structured among the clusters, and its adequacy to the isolation-by-distance model, we created a morphological tree using Mahalanobis distances among populations (Mahalanobis, 1936) and the Neighbor-Joining algorithm of clustering (Saitou & Nei, 1987) for each view. To evaluate geographic variation in skull size, we compared populations with an analysis of variance (ANOVA) on centroid sizes. The Tukey's test was also performed aiming to verify significant differences in skull size between population pairs. ANOVA and Tukey's test were based only in ventral view.

The sexual dimorphism in centroid size was evaluated for only a subset of male and female specimens of all populations (about 90% of all sampling), because not all specimens presented sex information. The existence of significant differences in the logarithm of skull size between sexes for each view was tested with an ANOVA, including population (geographic clusters) as a second predictor to evaluate if sexual dimorphism varied among populations. The existence of significant differences in skull shape between sexes for each view was tested with a MANOVA on shape variables, also considering the interaction of sex with a second predictor describing the populations. We performed a linear discriminant analysis (LDA) calculated on a subset of PC's (12 and 23 for dorsal and ventral views, respectively) using a leave-one-out cross-validation procedure to calculate the percentages of correct classification for sexes for each skull view. All statistical analyses and graphs were generated in R 3.3.3 (R Core Team, 2017) using the libraries: ape (Popescu *et al.*,

2012), geomorph (Adams & Otárola-Castillo, 2013), MASS (Venables & Ripley, 2002), stats (R Development Core Team) and phytools (Revell, 2012).

Sequence Data Analyses

The genetic data used in our analyses consist in 153 partial sequences of cytochrome-*b* (*Cyt-b*) mitochondrial gene of *O. nasutus*. DNA was isolated from 71 specimens using the PureLink Genomic DNA extraction kit (Invitrogen, Life Technologies), following the manufacturer's instructions. The initial 801 bp of *Cyt-b* was amplified by using primers MVZ05 and MVZ16 using conditions as described by Smith & Patton (1993). In addition to the specimens sequenced, others haplotypes from *O. nasutus* available in Genbank were included in the analysis (Appendix S1). The alignment was performed in the Clustal W algorithm implemented in MEGA7 (Kumar *et al.*, 2016). As a proxy for pRDA analysis, mtDNA genetic distances among the eight populations were estimated using the *p*-distance as model of evolution (Table S2), implemented in MEGA7. Standard errors were calculated using the bootstrap method with 1000 replicates.

Analyses of molecular variance (AMOVA) were performed for the clusters grouped by groups defined by ecoregions (1-Atlantic Forest, PR, SC and SG vs 2- Pampas, CDNS, PLWC, SSC, SCP and UY). Two AMOVAs were carried out to examine the partition of genetic variance into (a) ‘among-clusters’ and ‘within-populations’ component, and (b) ’among-ecoregions’, ‘among-clusters within ecoregion’, and ‘within-populations’ components. The significance of Φ-statistics parameters was assessed by permutation tests with 10,000 replicates as implemented in Arlequin v. 3.5.1.2 (Excoffier *et al.*, 2005). To explore the population differentiation, we calculated pairwise F_{ST} between all site pairs using 10,000 random permutations in Arlequin v. 3.5.1.2. Additionally, to determine if genetic and geographic distances between clusters were significantly correlated, isolation by distance (IBD) was employed by testing the correlation between pairwise

F_{ST} and geographical distance using a Mantel test (Mantel, 1967). Geographical distances between the clusters were measured as the shortest along-distribution distances using the path tool in Google Earth Pro v. 7.3.0.3832. The isolation-by-distance test were done in GENEPOP on the Web version 4.0.10. For testing of statistical significance, 10,000 permutations in Mantel tests were used to test the null hypothesis that genetic distance and geographical distance were independent.

Environmental Variables

To describe present-day climatic conditions, we extracted environmental data at each locality (Figure 1) based on maps at 30 arc second resolution. The following five environmental variables were used: mean temperature of the warmest and coldest quarter, mean annual precipitation (obtained from the Worldclim bioclimatic database available at http://www.worldclim.org/download), net primary productivity (from the Atlas of the Biosphere; http://nelson.wisc.edu/sage/data-and-models/atlas/) and topography (from ESA GlobCover, available at http://www.esa.int/ESA). After extract environmental data on ArcMap 10.3 software, we averaged the environmental information based on the sampling localities of each population (Table 1). In this work we choose these variables from evidences in other studies with rodents that presents influence from these variables in skull morphology (Monteiro *et al.,* 2003; Martinez & Cola 2011; Maestri *et al.,* 2016). The description of all the environmental attributes used in each sampling is present in Appendix S3.

Comparing morphological, genetic and environmental data

We used a variance-partitioning analysis (Borcard *et al.,* 1992) to estimate the relative contribution of genetic distances and environmental variables on skull shape and size. Matrices of

shape (dorsal and ventral view) and size distances among populations entered as response variables in three independent analyses. Predictor variables were main descriptors of genetic distances and environmental variables. To reduce dimensionality in both predictors, a PCoA was conducted on each, and a Horn's parallel analysis was performed to select the optimal numbers of dimensions (2 for genetic distances, 1 for environmental distances) that entered as predictors in the variance partitioning analyses. R packages vegan (Oksanen *et al.*, 2013) and paran (Dinno, 2012) were used to conduct the analyses.

RESULTS

Skull morphology: sexual dimorphism, size and shape variation

Sexual dimorphism in size was statistically significant for both dorsal (F = 11.2, P < 0.01) and ventral (F = 13.71, P < 0.001) views; however, sex × population interactions were not significant (P > 0.05). For shape, differences between males and females were significant for dorsal (MANOVA Wilks'λ = 0.81815, F = 2.6501, P < 0.01) and ventral views (MANOVA Wilks'λ = 0.685, F = 2.7591, P < 0.001). However, sex × population interactions were not significant (P > 0.05). The percentage of correct classification for sexes was 60.95% and 65.68% for dorsal and ventral views, respectively. Since the interaction between factors were not significant (i.e., sexual dimorphism is uniform across assumed populations) and considering the low percentage of correct classification), we pooled all adult individuals from the same locality in subsequent analyses.

We found significant differences (F = 6.532; P < 0.001) in the centroid size for ventral view among populations (Figure 2). The Tukey HSD test for pairwise comparisons indicated eight significant differences for skull size (Appendix S4). The Paraná [PR] differs from Patos Lagoon West Coast [PLWC], Southern Shield Campanha [SSC], Southern Coastal Plain [SCP] and

Uruguay [UY] ($P < 0.05$). Furthermore, Serra Geral [SG] differs from Patos Lagoon West Coast [PLWC], Southern Coastal Plain [SCP] and Uruguay [UY] ($P < 0.05$), while Santa Catarina [SC] was statistically different only in relation to Uruguay [UY] ($P < 0.05$). All significant differences in skull size were between populations from different biomes (Atlantic Forest and Pampas).

Similarly, significant differences were identified in skull shape among populations for both dorsal (MANOVA Wilks'λ = 0.10188, $F = 5.1338$, $P < 0.001$) and Ventral (MANOVA Wilks'λ = 0.052524, $F = 3.4902$, $P < 0.001$) views. Populations explained 17.64% and 16.17% of variation in dorsal and ventral views, respectively. The pairwise MANOVA showed significant differences in 26 of 28 on dorsal; and 22 of 28 on ventral comparisons among 8 populations. The R^2 and F values and significance levels are showed in Table S3.

The unrooted neighbour-joining tree of Mahalanobis distances for the dorsal and ventral views placed populations PR, SC and SG and the clusters SCP and UY as the most divergent (Figure 3). The CDNS, PLWC and SSC clusters (placed at the center of the species geographical distribution) appeared as morphologically intermediate between the two divergent groups.

Population Genetic Structure

Considering the ungrouped data set, the AMOVA results showed that greater proportions of mtDNA variations occurred both within (38.80%) and among populations (61.20%) (Table 2); strong genetic differentiation was found among groups ($\Phi_{ST} = 0.61201$, $P < 0.001$). The hierarchical AMOVA revealed that only 21.02% of the total variance was distributed among the ecoregion clusters (21.02%, $\Phi_{CT} = 0.21020$, $P < 0.05$), whereas the molecular variance 'among clusters within ecoregions' was slightly higher than 'within populations' accounted for 43.31% and 35.67%, respectively. In addition, most of the pairwise comparisons showed significant F_{ST} values (Table S4), indicating strong genetic differentiation among populations. The values of pairwise F_{ST} range

from 0.0265 to 0.9304. Overall, of the 28 comparisons, 26 were significant ($P < 0.05$). Therefore, CDNS vs. PLWC and SSC populations showed low and non-significant genetic differentiation.

A weak correlation between that F_{ST} and geographic distances was identified ($R^2 = 0.1225$; $P = 0.05$) in the Mantel test, revealing a marginally significant isolation by distance (IBD) pattern (S2 Figure).

Factors influencing skull shape and size

The set of exploratory predictors matrices herein used (environmental attributes and genetic distances) accounted for approximately ~ 85% of the variation in skull shape and size (Figure 4). Considering the shape, these components act in a balanced way to explain the variation observed. In general, the genetic influence explained 41% of the variation in the dorsal view and 32% in ventral view (Figure 4a, 4b). The environmental attributes explain 47% and 30% for the dorsal and ventral view, respectively. Furthermore, for the ventral view, there is a joint fraction of explanation between genetic distance and environmental attributes, encompassing 18%. The residuals components comprised about 20% in ventral and 12% for dorsal view. All these components were significant ($P < 0.05$). Performing the partitioning of environmental attributes variables applied to skull shape variation, only three fractions presents high significance; topography ($P < 0.01$), net primary productivity and annual precipitation ($P < 0.001$).

In contrast to shapes, the environmental variables better explained the variation in the size accounting for 62% of this variation ($P < 0.01$) (Figure 4c). Two environmental variables fractions (mean temperature of warmest quarter and mean temperature of coldest quarter) were not significant ($P > 0.05$). In addition, the genetic influence was the lowest (and non-significant) component obtained for size variation in this analysis (about 4%), although there is a joint variation portion (genetic and Environmental attributes together) of 21%. On the other hand, net primary

productivity ($P < 0.05$), topography ($P < 0.01$) and annual precipitation ($P < 0.001$) appeared as the most influential fractions from the environmental attributes related to the size variation. Mean temperature of warmest quarter and mean temperatures of the coldest quarter were not significant, both for shape and size ($P > 0.05$).

DISCUSSION

Variation of shape and size along spatial distribution

A marked pattern of phenotypic differentiation on size and shape of skulls was identified along a north–south axis of the geographic distribution of the Darwin's hocicudo. The Neighbor-joining tree of Mahalanobis distances (phenogram) generated from both dorsal and ventral views showed spatially structured morphological relationships in cline, where the greatest distance was between Atlantic Forest populations (PR, SC and SG) and the populations from Pampas (UY and SCP), located in the far north and extreme southern parts of the species' range, respectively. Similarly, this pattern parallel for size. For the shape, recent studies on Sigmodontine rodents reveal comparable patterns of spatially structured morphological relationships in relation to a north–south axis along their respective distributions in Pampa (Quintela *et al.*, 2016) and Atlantic Forest (Maestri *et al.*, 2016). However, the present study suggest that the phenotypic variation found in *O. nasutus* might not be only neutral and provide support that traits in skull shape are undergo by random and non-random factors (gene flow and environmental attributes).

Previous study of *O. nasutus* phylogeography pointed out morphological differentiation related to ecological variables, such as altitudinal gradient or different physiognomies, and phylogenetic clusters (used as predictors variables) explained a considerable part percentage (~25%) of skull shape variation (Peçanha *et al.*, 2017). Geoclimatic variables are partly associated

to intraspecific variation of shape skull of other studied small rodents such as genus *Graomys* (Martínez & Cola, 2011) and *Neotoma cinerea* (Cordero & Epps, 2012). Overall, AMOVA showed that most of the variation arose from variability among clusters (61.20% and 43.31% in both grouping criterion, respectively), suggesting that geographical isolation may represent the main reason which resulted in the genetic differentiation. Additionally, an apparent low gene flow, considering the matrilineal origin (mtDNA) may reinforce the genetic structure ($\Phi_{ST} = 0.61201$, $P < 0.001$).

We found association between CS and net primary productivity (NPP), indicating that *O. nasutus* have larger skulls in regions where there is the highest average NPP. The populations with the largest skulls are present on regions with higher values for NPP in open areas of the Atlantic Forest (north of geographic distribution, lower latitudes), while the smallest ones occurs in the south of the species distribution in Pampas biome (where minor values are observed for NPP). Furthermore, the mean of precipitation and altitude corroborate with pattern reveal by NPP. Thus, the variation in cline, although not all populations on the north-south axis were significantly different, suggest that the influence of environmental features of each ecoregion it seems to overcome the Bergmann's rule (Bergmann, 1847; Meiri, 2011) to explain the size.

Our results coincide to that of Maestri *et al.* (2016b) in which environmental gradients interact with historical processes to determine body size variation in assemblages of sigmodontines rodents. In *O. nasutus*, significant differences in skull size were found between populations from different biomes (Atlantic Forest vs Pampas), but not between populations of same biome. In fact, despite of gene flow being geographically structured, our results indicated correspondence with spatial patterns of variation in size, since pairwise F_{ST} analysis showed higher values in populations in the extreme of the distribution (in general), but also in close populations included in the same ecoregion (Table S4). It coincides with the results presented by Tukey HSD test for multiple

comparisons, and also to corroborate with Mantel test that shown weak positive spatial autocorrelation. Accordingly, we found a slight correspondence between geographic patterns of mitochondrial structure and spatial patterns of variation in size, which does not seems to be driven by gene flow (that seems to prevent isolation). Similarly, as well as studies with *Akodon cursor*, in the northernmost domains of the Atlantic Forest (Maestri et al. 2016a), our results reveal spatial patterns of variation of size likely determined by others environmental variables.

Relative effect of environmental attributes and genetics

According to variation partitioning analysis, our results suggest varied contribution of predictors of skull shape and size variation. Regarding shape, the pRDA demonstrate that the predictors (i.e. genetic distance, altitude, precipitation and net primary productive, mainly) act in a balanced way to explain the variation, but slightly differ for dorsal and ventral views. Peçanha *et al.,* (2017) evidenced that 26.3% of the ventral view variation was attributed to haplogroups and 17.9% to environmental groups (Atlantic Forest and Pampas). Although the present study does not have a phylogenetic focus, our data resemble the previous investigation within *O. nasutus* (Peçanha *et al.,* 2017), considering the 16.17% of the variation of the ventral view attributed by the populations herein assumed. However, some previous studies take into account similar predictors to shape variation not completely concordant. Maestri *et al.* (2016a) inferred that differences in skull shape are best explain by random factors (e.g. genetic drift) than non-random in *Akodon cursor*, while Alvarado-Serrano *et al.,* (2013) demonstrated limited morphological differentiation related to ecological and genetic variables for *Akodon mollis.*

We identified that environmental variables were relevant to explain variation in size, accounting the highest explanatory power (62% of the variation ($P < 0.01$). The pRDA also confirm that, in addition to altitude ($P < 0.01$), others environmental attributes such as precipitation ($P <$

0.001) and net primary productive ($P < 0.05$) have influence on the skull size. Thus, these results partially corroborates the patterns found in other mammals of tropical regions, where precipitation and primary production were important contributors to the skull size pattern (Cardini *et al.,* 2007; Medina *et al.,* 2007; Maestri *et al.,* 2016). The positive correlation between size and altitude, however, was not observed for *Graomys* spp. (Martínez & Cola, 2011) and *Akodon cursor* (Maestri *et al.,* 2016). However, this pattern goes against the results of *Graomys* spp. and refutes the idea of precipitation as a productivity proxy does not apply to small mammals in the same way as to large mammals (Martínez & Cola, 2011), but we must take into account that these species (i.e. *Graomys* spp.) occur in a drier environment (Chaco ecoregion) and in this sense, the temperature was one of the variables most related to the size. Thus, considering this inverse pattern, the mean temperature warmest and coldest quarter were variables not correlated with of centroid size variation to our dataset. It is worth emphasizing that *O. nasutus* is distributed predominantly in grasslands of southern Brazil and Uruguay, and rainfall is the main condition for the plant growth. Thus, variations of this factor likely affect net primary productivity in terrestrial ecosystems (Knapp & Smith 2001, Del Grosso *et al.,* 2008). In this way, the differences, mainly in the size, across environments might also arise as an indirect effect of changes in performance under different conditions (e.g., increased energy available for investment in growth) (Yom-Tov & Yom-Tov, 2004). However, considering geographically structured gene flow and evidences for low influence (and non-significant) for genetic component for size (4%), herein is suggested the influence of non-random factors as local selection pressures acting as an evolutionary force of change in size.

Finally, the area of occurrence of *O. nasutus* is within a well-documented region in which Late Pleistocene effects of glaciations resulted in the predominance of grasslands until 11,500 kyr (with dry and cold climate), and the emergence of forest formations occurred only in the Holocene (Behling, 2002; Behling *et al.,* 2009). Peçanha *et al.,* (2017) showed through predictive distribution

models that this species experienced an expansion in its geographic distribution on the Last Glacial Maximum (around 21 kyr), suggesting affinity with cold climates. Consequently, due lack of correlation of the size with the environmental attributes mean temperature of the colder quarter, the concept of adaptation to cold environments seems to contrast due to the non-significance ($P > 0.05$) in relation to the environmental attributes selected for temperature. Although it occupies grassland, *O. nasutus* is distributed through humid (not dry) conditions, found along riverbanks and wetlands. This reinforce the significance with primary net productivity and precipitation (rainfall) found, for both shape and size. Indeed, we found influence significant for environmental attributes, however, since evaluate whether these effects are phenotypic plasticity or local adaptation to size or shape still seems to be a challenge.

CONCLUSIONS

Our study used variation partitioning analysis to examine the contribution of environmental variables and genetic indices to size and skull shape in a sigmodontine rodents present in different biomes, in our case the Atlantic Forest and Pampas. Some studies have investigated the effects of environmental and genetic factors influencing skull morphology separately, but relatively few have attempted to separate the relative contribution of both factors in small rodents in South America (Alvarado-Serrano *et al.,* 2013; Maestri *et al.,* 2016). Here, we have demonstrated that shape variation in *Oxymycterus nasutus* is influenced by random and non-random factors such as genetic and environmental components. The shape presents a clinal variation along to Atlantic Forest and Pampa biomes, influenced by genetic distance and environmental attributes, such as topograghy, net productivity primary and precipitation. Similarly to shape, the size also presented a cline pattern, with a trend of larger skulls northward of the distribution (in patches of grasslands of the Atlantic Forest) and smaller more southward of its geographical distribution (Pampas), which was not in

conformity with Bergmann's rule, as expected for the sigmodontines rodents (Maestri *et al.*, 2016b). However, differently from shape findings, the environmental attributes appears to have more influence in size than genetic ones, although presenting a considerable fraction of jointly explanation. Our results also demonstrated that gene flow is geographically structured in these populations.

REFERENCES

Ackermann, R. R., & J. M. Cheverud. (2004) Detecting genetic drift versus selection in human evolution. *Proceedings of the National Academy of Sciences USA*, **101**, 17946 – 17951.

Adams, D.C., & Otarola-Castillo, E. (2013) geomorph: an R package for the collection and analysis of geometric morphometric shape data. *Methods in Ecology and Evolution*, **4**, 393-399.

Alvarado-Serrano, D.F., Luna, L. & Knowles, L.L. (2013) Localized versus generalist phenotypes in a broadly distributed tropical mammal: how is intraspecific variation distributed across disparate environments? *BMC Evolutionary Biology*, **13**, 160.

Behling, H. (2002) South and southeast Brazilian grassland during Late Quaternary times: a synthesis. *Palaegeography, Palaeclimatology, Palaeoecology*, **177**, 19-27.

Behling, H., Jeske-Pieruschka, V., Schüler, L., & Pillar, V. (2009) Dinâmica dos campos no sul do Brasil durante o Quaternário Tardio. In: Pillar, V; Müller, S. C.; Souza Castilhos, Z. M. & Jacques, A. V. A. eds. Campos Sulinos – Conservação e Uso Sustentável da Biodiversidade. Brasília, Ministério do Meio Ambiente, p. 13-25.

Bergmann, C. (1847) Über die Verhältnisse der Wärmeokönomie der Thiere zu ihrer Grösse. *Göttinger Studien*, **3**, 595–708.

Bonvicino, C.R., Oliveira, J. A. & D'Andrea, P.S. (2008) Guia dos Roedores do Brasil, com chaves para gêneros baseadas em caracteres externos. Rio de Janeiro, Centro Pan-Americano de Febre Aftosa – OPAS/OMS.

Bookstein, F.L. (1991) Morphometric tools for landmark data: geometry and biology. Cambridge University Press, Cambridge, UK.

Borcard, D., Legendre, P. & Drapeau, P. (1992) Partialling out the spatial component of ecological variation. *Ecology*, **73**, 1045–1055.

Cardini, A. & Elton, S. (2009) Geographical and taxonomic influences on cranial variation in red colobus monkeys (Primates, Colobinae): introducing a new approach to 'morph' monkeys. *Global Ecology and Biogeography*, **18**,248–263.

Cardini, A., Jansson, A. & Elton, S. (2007) A geometric morphometric approach to the study of ecogeographical and clinal variation in vervet monkeys. *Journal of Biogeography*, **34**, 1663–1678.

Cordero, G.A., & Epps, C.W. (2012) From desert to rainforest: phenotypic variation in functionally important traits of bushy-tailed woodrats (*Neotoma cinerea*) across two climatic extremes. *Journal of Mammalian Evolution*, **19**, 135–153.

Dantas, M. E., Viero, A.C., Silva, D.R.A. (2010) Origem das Paisagens. *In:* VIERO, A.C., SILVA, D.R.A. (orgs.) Geodiversidade do estado do Rio Grande do Sul. Porto Alegre: CPRM, 2010.

Del Grosso, S., Parton, W. & Stohlgren, T. (2008) Global potential net primary production predicted from vegetation class, precipitation, and temperature. *Ecology*, **89**, 2117–2126.

Dinno, A. (2012) paran: Horn's test of principal components/factors. R package version 1.5.1. http://CRAN.R-project.org/package=paran.

Edwards, S.V. (2016) Phylogenomic subsampling: a brief review. *Zoologica Scripta*, **45**, 63-74.

Endler, J.A. (1995) Multiple-trait coevolution and environmental gradients in guppies. *Trends in Ecology & Evolution*, **10,** 22-29.

Endler, J.Á. (1973) Gene flow and population differentiation. *Science*, **179** (4070):243–250.

Excoffier, L., Laval, G. & Schneider, S. (2005) Arlequin (version 3.0): an integrated software package for population genetics data analysis. *Evolutionary Bioinformatics Online*, **1**, 47–50.

González, E.M. (2001) Guía de campo de los mamíferos de Uruguay: Introducción al estudio de los mamíferos. Montevideo: Vida Silvestre, 339p.

González, E.M., & Martinez-Lanfranco, J.A. (2010) Mamíferos de Uruguay. Guía de campo e introducción a su estúdio y conservación. Banda Oriental, Museo Nacional de Historia Natural, Vida Silvestre Uruguay, Montevideo, 463 pp.

Gould, S.J., & Johnston, R.F. (1972) Geographic variation. *Annual Review of Ecology and Systematics*, **3**, 457–498.

Ims, R.A. (1997) Determinants of geographic variation in growth and reproductive traits in the root vole. *Ecology*, **78**, 461–470.

Knapp, A.K., & Smith, M.D. (2001) Variation among biomes in temporal dynamics of aboveground primary production. *Science*, **291**, 481-484.

Kumar, S., Stecher, G & Tamura K. (2016) MEGA7: Molecular Evolutionary Genetics Analysis. version 7.0 for bigger datasets. *Molecular Biology and Evolution*, **33**, 1870-1874.

Ledevin, R., & Millien, V. (2013) Congruent morphological and genetic differentiation as asignature of range expansion in a fragmented landscape. *Ecology and Evolution*, **3**(12): 4172 – 4182.

Ledevin, R., Michaux J. R., Deffontaine, V., Henttonen, H., & and Renaud. S. (2010) Evolutionary history of the bank vole *Myodes glareolus*: a morphometric perspective. *Biological Journal of the Linnean Society*, **100**, 681–694.

Ledevin, R., Quéré, J-P., & Renaud, S. (2010b) Morphometrics as an Insight into Processes Beyond Tooth Shape Variation in a Bank Vole Population. *PLoS ONE*, **5**(11): e15470.

Maestri, R., Fornel, R., Gonçalves, G.L., Geise, L., Freitas, T.R.O. & Carnaval, A.C. (2016) Predictors of intraspecific morphological variability in a tropical hotspot: comparing the influence of random and non-random factors. *Journal of Biogeography*, 43, 2160–2172.

Maestri, R., Luza, A.L., Barros, L.D., Hartz, S.M., Ferrari, A., Freitas, T.R.O., & Duarte, L.D.S. (2016b) Geographical variation of body size in sigmodontine rodents depends on both environment and phylogenetic composition of communities. *Journal of Biogeography*, **43**, 1192–1202.

Mahalanobis, P.C. (1936) On the generalized distance in statistics. *Proceedings of the National Institute of Sciences of India*, **2**, 49–55.

Mantel N. (1967) The detection of disease clustering and a generalized regression approach. *Cancer Research*, 27, 209–220.

Martínez, J.J. & Cola, V.D. (2011) Geographic distribution and phonetic skull variation in two close species of *Graomys* (Rodentia, Cricetidae, Sigmodontinae). *Zoologischer Anzeiger*, **250**, 175–194.

Mayr, E. (1956) Geographical character gradients and climatic adaptation. *Evolution*, 10: 105–108.

McGuire, J. (2010) Geometric morphometrics of vole (*Microtus californicus*) dentition as a new paleoclimate proxy: shape change along geographic and climatic clines. *Quaternary International*, **212**, 198–205.

Medina, A.I., Martí, D.A. & Bidau, C.J. (2007) Subterranean rodents of the genus *Ctenomys* (Caviomorpha, Ctenomyidae) follow the converse to Bergmann's rule. *Journal of Biogeography*, **34**, 1439–1454.

Meiri, S. (2011) Bergmann's Rule – what's in name? *Global Ecology and Biogeography*, **20**, 203–207.

Meyer, A. (1987) Phenotypic Plasticity and Heterochrony in Cichlasoma managuense (Pisces, Chichlidae) and their Implications for Speciation in Cichlid Fishes. *Evolution*, **41**, 1357-1369.

Monteiro, L.R., Duarte, L.C. & Reis, S.F. (2003) Environmental correlates of geographical variation in skull and mandible shape of the punar_e rat Thrichomys apereoides (Rodentia, Echimyidae). *Journal of Zoology*, **261**, 47–57.

Morales, A., Villalobos, F., Velazco, P.M., Simmons, N.B., & Piñero, D. (2016) Environmental niche drives genetic and morphometric structure in a widespread bat. *Journal of Biogeography*, **43**, 1057–1068.

Oksanen, J., Blanchet, F.G., Kindt, R., Legendre, P., Minchin, P.R., O'Hara, R.B., Simpson, G.L., Solymos, P., Stevens, M.H.H. & Wagner, H. (2013) Vegan: Community Ecology package. R package version 2.0-10.

Oliveira, J.A. & Gonçalves, P.R. (2015) Suborder Myomorpha: Family Cricetidae: Subfamily Sigmodontinae. Genus *Oxymycterus*; pp. 247–268 in Mammals of South America, volume 2—rodents (J. M. Patton, G. D'Elía, and U. F. J. Pardiñas, eds.). University of Chicago Press, Chicago, Illinois and London, United Kingdom.

Overbeck, G.E., Müller, S.C., Fidelis, A., Pfadenhauer, J., Pillar, V.D., Blanco, C.C., Boldrini, I.I., Both, R., & Forneck, E.D. (2007) Brazil's neglected biome: the south brazilian campos. *Perspectives In Plant Ecology, Evolution And Systematics*, **9**, 101-116.

Paise, G. & Vieira, E.M. (2006) Daily activity of a Neotropical Rodent (*Oxymycterus nasutus*): seasonal changes and influence of Environmental factors. *Journal of Mammalogy*, 87 (4): 733–739.

Papadopoulou, A., & Knowles, L.L. (2016) Toward a paradigm shift in comparative phylogeography driven by trait-based hypotheses. *Proceedings of the National Academy of Sciences USA*, **113**, 8018–8024.

Peçanha, W.T., Althoff, S.L., Galiano, D., Quintela, F.M., Maestri, R., Gonçalves, G.L., & Freitas, T.R.O. (2017) Pleistocene climatic oscillations in Neotropical open areas: Refuge isolation in the rodent *Oxymycterus nasutus* endemic to grasslands. *PLoS ONE*, **12**(11): e0187329.

Peres-Neto, P.R., & Magnan, P. (2004) The influence of swimming demand on phenotypic plasticity and morphological integration: a comparison of two polymorphic charr species. *Oecologia*, **140**, 36-45.

Popescu, A.A., Huber, K.T., & Paradis, E. (2012) ape 3.0: new tools for distance- based phylogenetics and evolutionary analysis in R. *Bioinformatics*, **28**, 1536–1537.

Quintela, F.M., Fornel, R. & Freitas T.R.O. (2016) Geographic variation in skull shape of the water rat *Scapteromys tumidus* (Cricetidae, Sigmodontinae): isolation-by-distance plus environmental and geographic barrier effects? *Anais da Academia Brasileira de Ciências*, **88**, 451-466.

R Core Team (2017) R: A language for statistical computing. R Foundation for Statistical Computing, Vienna, Austria. Available at: http://www.R-project.org/. Accessed on 15 jun 2018.

Renaud, S., & Michaux, J.R. (2003) Adaptive latitudinal trends in the mandible shape of *Apodemus* wood mice. *Journal of Biogeography*, **30**, 1617–1628.

Renaud, S., & Millien, V. (2001) Intra and interspecific morphological variation in the field mouse species *Apodemus argenteus* and *A. speciosus* in the Japanese archipelago: the role of insular isolation and biogeographic gradients. *Biological Journal of the Linnean Society*, **74**, 557–569.

Revell, L. J. (2012) phytools: an R package for phylogenetic comparative biology (and other things). *Methods in Ecology and Evolution*, **3**, 217–223.

Rohlf, F.J. & Slice, D. (1990) Extensions of the Procrustes method for the optimal superimposition of landmarks. *Systematic Zoology*, 39, 40–59.

Rohlf, F.J. (2015) The tps series of software. *Hystrix*, **26**, 9–12.

Saitou, N. & Nei, M. (1987) The Neighbor-joining method: a new method for reconstructing phylogenetic trees. *Molecular Biology and Evolution*, **4**, 406–425.

Smith, M.F., & Patton, J.L. (1993) The diversification of South American murid rodents: Evidence from mitochondrial DNA sequence data for the akodontine tribe. *Biological Journal of the Linnean Society*, **50**, 149-177.

Souto-Lima, R.B., & Millien, V. (2014) The influence of environmental factors on the morphology of red-backed voles *Myodes gapperi* (Rodentia, Arvicolinae) in Québec and western Labrador. *Biological Journal of the Linnean Society*, **112**, 204–218.

Thomé, M.T., & Carstens, B.C. (2016) Phylogeographic model selection leads to insight into the evolutionary history of four-eyed frogs. *Proceedings of the National Academy of Sciences USA*, **113**, 8010-8017.

Venables, W. N., & Ripley, B. D. (2002). Modern Applied Statistics with S. New York: Springer.

Yom-Tov, Y., & Yom-Tov, S. (2004) Climatic change and body size in two species of Japanese rodents. *Biological Journal of the Linnean Society*, **82**, 263-267.

Supporting Information

Appendix S1. Detailed table of all specimens used in this work.

Appendix S2. Description of landmarks digitized used in skulls for dorsal and ventral view.

Appendix S3. Description of all the environmental attributes used in each sampling point in this work.

Appendix S4. Description of all Tukey's test on Ventral – Size.

S1 Figure. Position of the landmarks (circles) digitized on the dorsal (A) and ventral (B), views of the *O. nasutus* skull. A description of each landmark is presented in Appendix S2.

S2 Figure. Isolation by distance among *O. nasutus* clusters.

Table S1. Description of each population sampling from skulls and mtDNA sequences evaluated in this study.

Table S2. Genetic divergence (using *p*-distance) between pairs of *Cytb* haplotypes recovered from eight population of *Oxymycterus nasutus*

Table S3. Pairwise MANOVA analysis of variation in *Oxymycterus nasutus* skull shape among eight populations in southern Brazil and Uruguay, for dorsal and ventral views

Table S4. Matrix of pairwise F_{ST} among eight populations of *Oxymycterus nasutus* in South America grasslands.

TABLES

Table 1. Environmental variables extracted to distribution range geographic of *Oxymycterus nasutus* based on mean on each population for five attributes.

Population	Topography (m)	Net primary productivity (NPP)	Annual precipitation (mm)	M.T. Warmest Quarter °C	M.T. Coldest Quarter °C
1. PR	897.88	1.116333333	1478.77	203.88	133.44
2. SC	788.5	1.122666667	1762.83	205.83	129.66
3. SG	707.14	1.118857143	1809.85	202.57	129.42
4. CDNS	133.75	1.08425	1406.25	228.50	148.25
5. PLWC	31.25	1.037181818	1362.81	228.45	140.27
6. SSC	147.37	0.994625	1436.12	229.62	136.75
7. UY	38.66	0.988454545	1106.83	216.08	116.91
8. SCP	8	1.017	1212.75	223	130.75

Table 2. Analysis of molecular variance (AMOVA) estimated for the *Oxymycterus nasutus Cyt-b* sequences using two hierarchical models: two-level model includes only populations and three-level model includes all populations distributed in the two biogeographical areas observed (Atlantic Forest and Pampas).

Grouping criterion	Source of variation	df	% of variance	Φ -statistics	*P* value
unstructured	Among populations	7	61.20	Φ_{ST} = 0.61201*	*P* < 0.001
	Within populations	145	38.80		
two ecoregions	Among ecoregions	1	21.02	Φ_{CT} = 0.21020**	P = 0.01584
	Among populations within ecoregions	6	43.31	Φ_{SC} = 0.54842*	*P* < 0.001
	Within populations	145	35.67	Φ_{ST} = 0.64334*	*P* < 0.001

Φ -statistics probability level after 10,000 permutations. * *P* < 0.001. ***P* < 0.05.

FIGURES

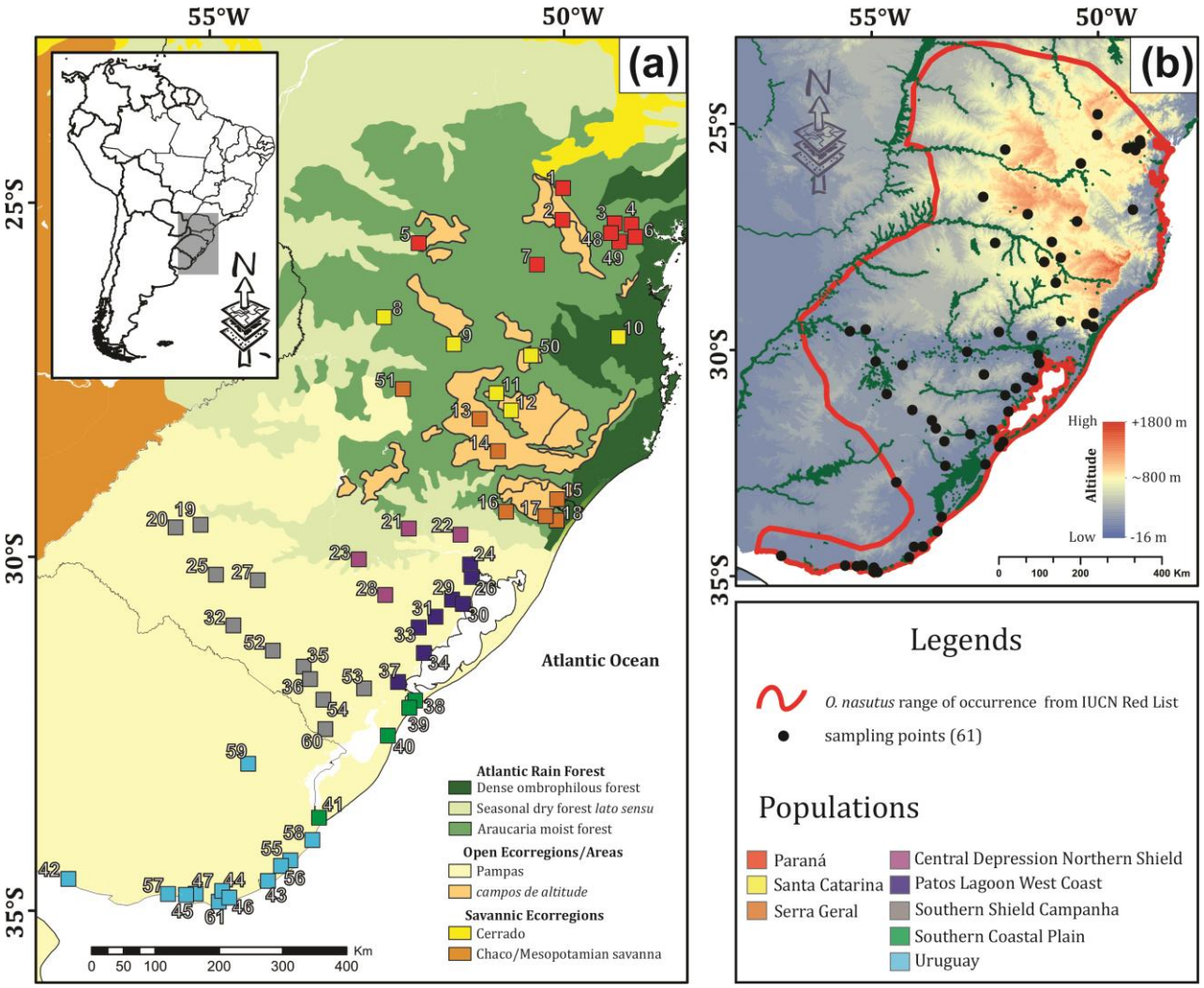

Figure 1. Distribution of the 61 sampling localities points of *Oxymycterus nasutus*. (a) The eight populations estimated in this study scattered out mainly in campos de altitude and Pampas ecoregion in the South America. The colors from each population are indicated in the legends (squares). For a description of each locality, see Appendix S1. (b) Map showing the topography and the main rivers (shown in green) from southern Brazil and Uruguay. The *Oxymycterus nasutus* range of occurrence from IUCN Red List is shown by red line perimeter.

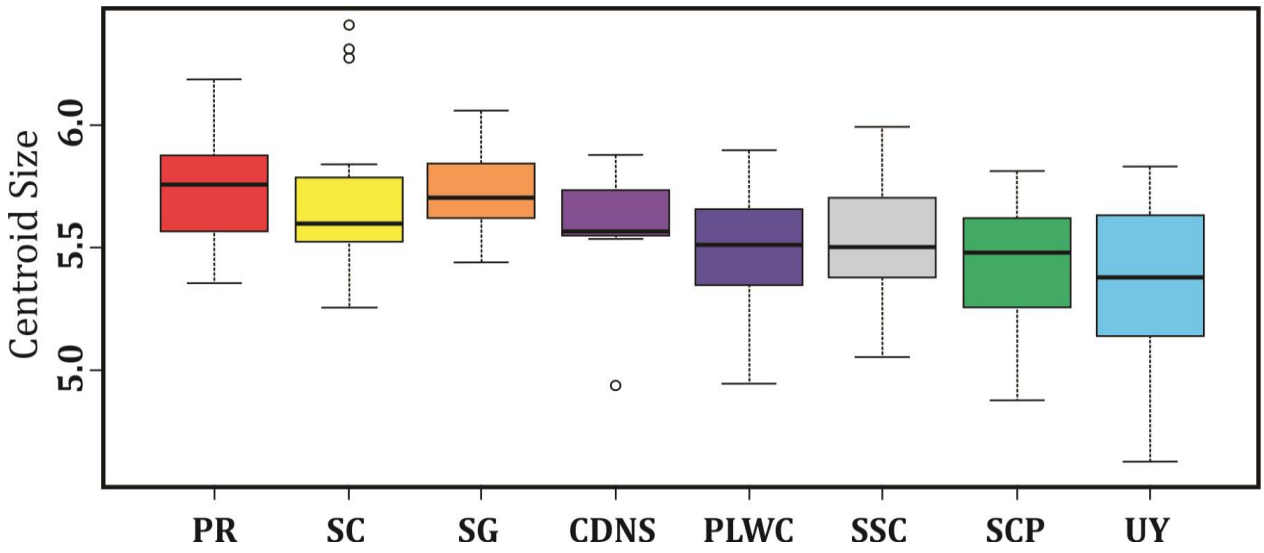

Figure 2. Box plot showing variability of centroid size among population of *Oxymycterus nasutus* for the sum of logarithms transformed centroid size for ventral views skull. The horizontal line represents the mean, box margins are at the 25th and 75th percentiles, bars extend to the 5th and 95th percentiles, and circles are outliers.

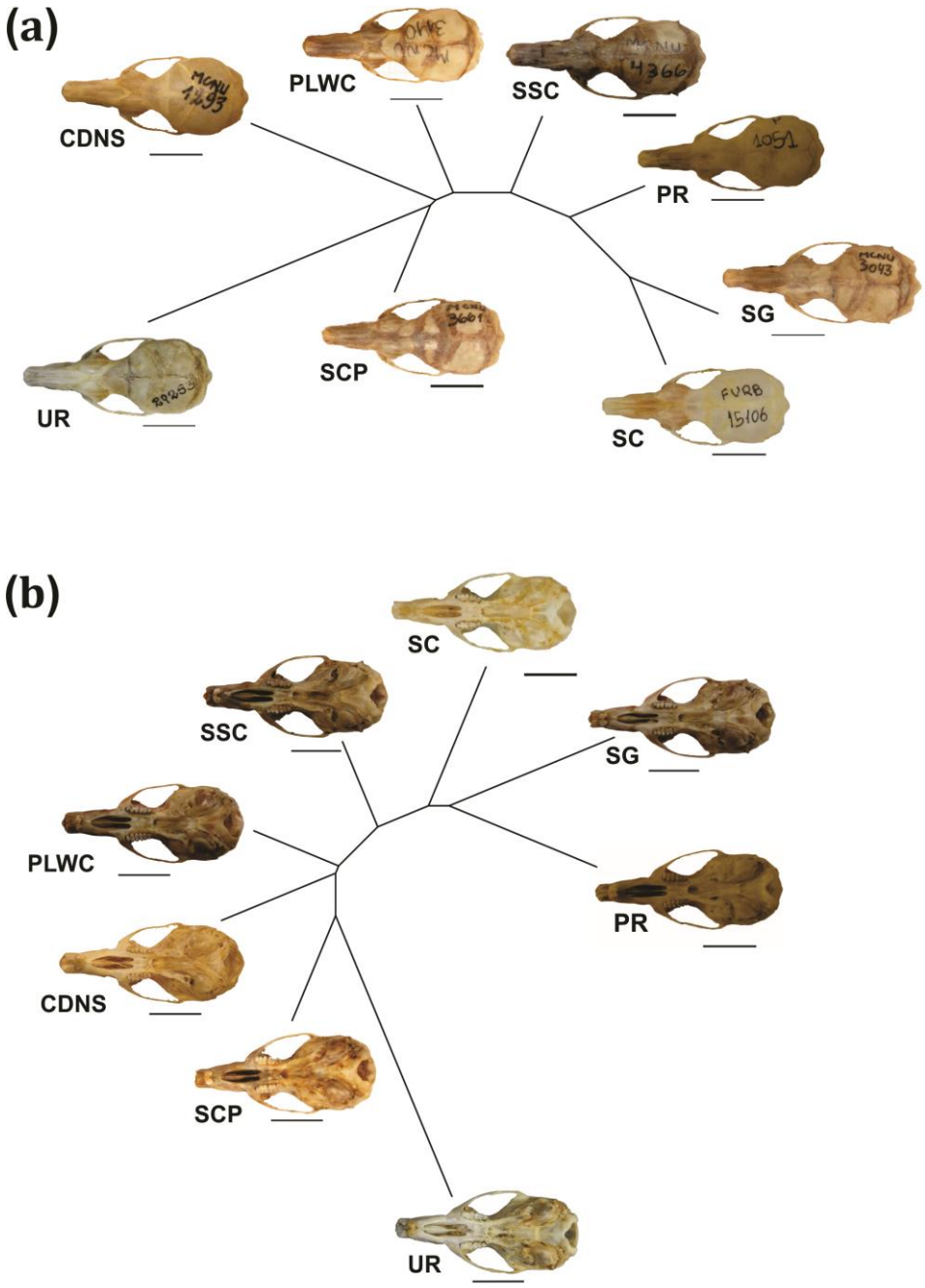

Figure 3. Neighbor-joining phenograms generated from Mahalanobis distances for dorsal (a) and ventral (b) views of the skull of *Oxymycterus nasutus*. Acronyms correspond to geographic clusters. Shape visualization made from mean skull shape for each cluster. Scale bar = 10 mm.

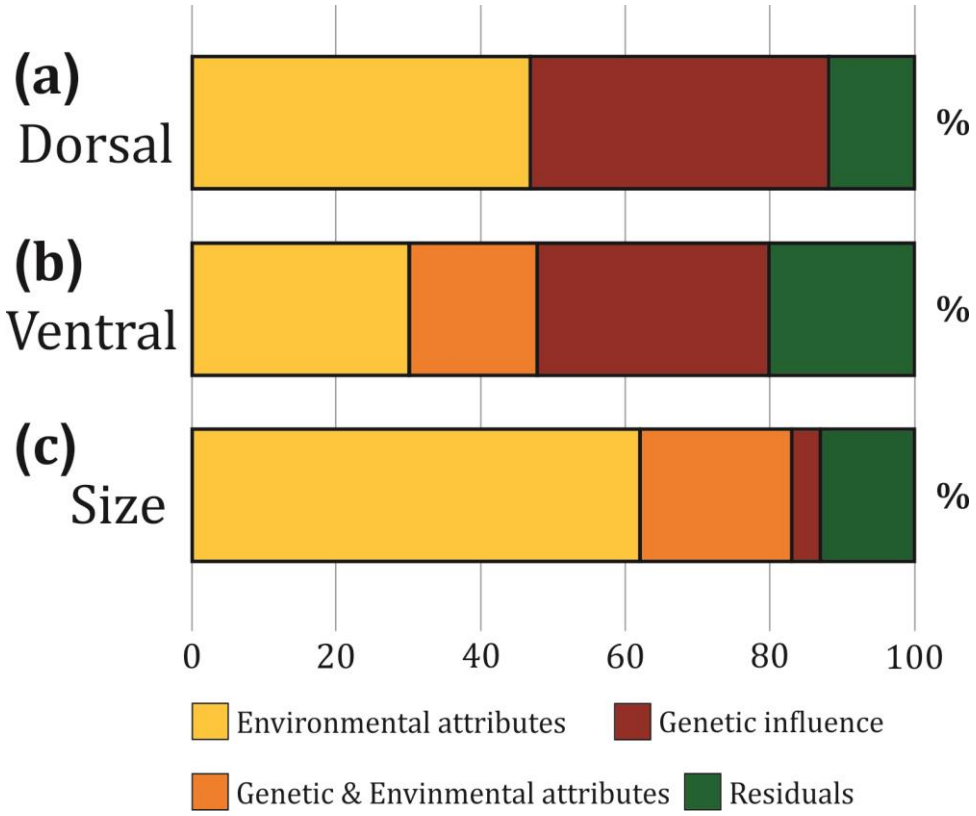

Figure 4. Results from partial redundancy analysis for (a) dorsal shape, (b) ventral shape and (c) size. Horizontal colored bars shown are the relative contributions (percentage of explanation) of environmental attributes (yellow) and genetic influence (red), as well as the shared components explaining variation (orange). The residuals (green) are understood as inexplicable components. The percentage values shown are from adjusted R^2 for each fraction.

Appendix S1. Detailed table of all specimens used in this work. Field numbers are uses when museums or scientific collections numbers were not available. Localities and geographic coordinates are listed after voucher ID. M and F are assigned for males and females. The presence (+)/absence (-) of mtDNA sequences and skull samples per site. 'Code' and 'Pop', numbers and acronyms respectively, are refer to the total sample and population used evidenced in maps (Figure 1). GenBank accession numbers for the cytochrome *b* (*cytb*) generated in this study indicated in bold. Abbreviation. Acronym: MHNCI, Museu de História Natural "Capão da Imbuía", Curitiba (Brazil); UFPR, Departmento de Genética da Universidade Federal do Paraná, Curitiba (Brazil); MCNU Museu de Ciências Naturais da Universidade Luterana do Brasil, Canoas (Brazil); FZB-MCN, Fundação Zoobotânica/Museu de Ciências Naturais, Porto Alegre (Brazil); DZUP/CCMZ, Departamento de Zoologia da Universidade Federal do Paraná/ Coleção Científica De Mastozoologia, Curitiba (Brazil); CZFURB Coleção Zoológica da Universidade Regional de Blumenau, Blumenau (Brazil); CMLCE-UFRGS, Mastozoological Collection of the Cytogenetic Laboratory and Evolution at the Universidade Federal do Rio Grande do Sul, Porto Alegre (Brazil); FMNH, Field Museum of Natural History, Chicago (USA); MVZ, Museum of Vertebrate Zoology, University of California at Berkeley, Berkeley (USA); MNHN, Museo Nacional de Historia Natural [of Uruguay], Montevideo (Uruguay). Country: BRA, Brazil; URU, Uruguay. Brazilian States: PR, Paraná; SC, Santa Catarina; RS, Rio Grande do Sul.

Voucher #	Localities	Coordinates	Sex	*Cytb*	Skull	Code	Pop	GenBank ID
MHNCI 0816	BRA:PR, Castro, Parque Florestal de Caxambu	-24.790891, -50.012062	M	-	+	01	PR	-
MHNCI 0818	BRA:PR, Castro, Parque Florestal de Caxambu	-24.790891, -50.012062	F	-	+	01	PR	-
MHNCI 0821	BRA:PR, Castro, Parque Florestal de Caxambu	-24.790891, -50.012062	-	-	+	01	PR	-
MHCNI 0642	BRA:PR, Ponta Grossa, Parque Estadual de Vila Velha	-25.244064, -50.022787	-	-	+	02	PR	-
MHCNI 0657	BRA:PR, Ponta Grossa, Parque Estadual de Vila Velha	-25.244064, -50.022787	M	-	+	02	PR	-
MHNCI 0709	BRA:PR, Ponta Grossa, Parque Estadual de Vila Velha	-25.244064, -50.022787	F	-	+	02	PR	-
MHNCI 0723	BRA:PR, Ponta Grossa, Parque Estadual de Vila Velha	-25.244064, -50.022787	F	-	+	02	PR	-
MHNCI 0839	BRA:PR, Ponta Grossa, Parque Estadual de Vila Velha	-25.244064, -50.022787	M	-	+	02	PR	-
UFPR-P76	BRA:PR, Ponta Grossa, Parque Estadual de Vila Velha	-25.244064, -50.022787	F	+	-	02	PR	MF766123
MHCNI 3433	BRA:PR, Curitiba, Parque Regional do Iguaçu	-25.522947, -49.222987	M	+	+	03	PR	MF766120
UFPR SCB-P86	BRA:PR, Curitiba*, Reserva Biológica do Cambuí	-25.522947, -49.222987	F	+	-	03	PR	MF766119
MHNCI 2148	BRA:PR, Araucária*, Thomaz Coelho	-25.540142, -49.355415	M	-	+	04	PR	-
DZUP/CCMZ 181	BRA:PR, Araucária, Repar	-25.540142, -49.355415	M	-	+	04	PR	-
DZUP/CCMZ 207	BRA:PR, Araucária, Repar	-25.540142, -49.355415	-	-	+	04	PR	-
DZUP/CCMZ 547	BRA:PR, Araucária, Repar	-25.540142, -49.355415	M	-	+	04	PR	-
CZFURB 18228	BRA:PR, Candói, UHE Santa Clara	-25.570833, -52.052778	M	+	+	05	PR	MF766125
UFPR-SCB P995	BRA:PR, São José dos Pinhais, Barro Preto	-25.5799, -49.175373	F	+	+	06	PR	

UFPR-SCB P1008	BRA:PR, São José dos Pinhais, Barro Preto	-25.5799, -49.175373	M	+	+	06	PR	
UFPR-SCB P1018	BRA:PR, São José dos Pinhais, Barro Preto	-25.5799, -49.175373	M	+	+	06	PR	
UFPR-SCB P1019	BRA:PR, São José dos Pinhais, Barro Preto	-25.5799, -49.175373	M	+	+	06	PR	
UFPR-SCB P1039	BRA:PR, São José dos Pinhais, Barro Preto	-25.5799, -49.175373	M	+	+	06	PR	
UFPR-SCB P1049	BRA:PR, São José dos Pinhais, Barro Preto	-25.5799, -49.175373	M	+	+	06	PR	
UFPR-SCB P1051	BRA:PR, São José dos Pinhais, Barro Preto	-25.5799, -49.175373	M	+	+	06	PR	
UFPR-SCB P1053	BRA:PR, São José dos Pinhais, Barro Preto	-25.5799, -49.175373	F	+	+	06	PR	
UFPR-SCB P1055	BRA:PR, São José dos Pinhais, Barro Preto	-25.5799, -49.175373	M	+	+	06	PR	MF766121
UFPR-SCB P1061	BRA:PR, São José dos Pinhais, Barro Preto	-25.5799, -49.175373	M	+	+	06	PR	MF766122
UFPR SCB-P969	BRA:PR, São José dos Pinhais, Barro Preto	-25.5799, -49.175373	F	+	-	06	PR	
UFPR SCB-P970	BRA:PR, São José dos Pinhais, Barro Preto	-25.5799, -49.175373	M	+	-	06	PR	
UFPR SCB-P973	BRA:PR, São José dos Pinhais, Barro Preto	-25.5799, -49.175373	F	+	-	06	PR	
UFPR SCB-P980	BRA:PR, São José dos Pinhais, Barro Preto	-25.5799, -49.175373	F	+	-	06	PR	
UFPR SCB-P1099	BRA:PR, São José dos Pinhais, Barro Preto	-25.5799, -49.175373	F	+	-	06	PR	
MHNCI 3192	BRA:PR, São Matheus do Sul, Fazenda do Durgo	-25.873889, -50.382778	-	+	+	07	PR	MF766124
CZFURB 6855	BRA:SC, São Domingos, Aheqq	-26.616388, -52.538866	F	-	+	08	SC	-
CZFURB 9253	BRA:SC, São Domingos, Aheqq	-26.616388, -52.538866	-	-	+	08	SC	-
CZFURB 9254	BRA:SC, São Domingos, Aheqq	-26.616388, -52.538866	F	-	+	08	SC	-
CZFURB 18119	BRA:SC, São Domingos, PCH Luzia Alto	-26.616388, -52.538866	F	+	+	08	SC	MF766126
CZFURB 18153	BRA:SC, São Domingos, PCH Luzia Alto	-26.616388, -52.538866	M	+	+	08	SC	MF766127
CZFURB 9364	BRA:SC, Água Doce, Campo Eólico	-26.997778, -51.555833	M	-	+	09	SC	-
CZFURB 9366	BRA:SC, Água Doce, Campo Eólico	-26.997778, -51.555833	M	-	+	09	SC	-
CZFURB 9969	BRA:SC, Água Doce, Campo Eólico	-26.997778, -51.555833	F	-	+	09	SC	-
CZFURB 9365	BRA:SC, Água Doce, Campo Eólico	-26.997778, -51.555833	M	+	-	09	SC	MF766128
CZFURB 9856	BRA:SC, Água Doce, Campo Eólico	-26.997778, -51.555833	-	+	-	09	SC	MF766129
CZFURB 6086	BRA:SC, Indaial, Parque Nacional da Serra do Itajaí	-26.897778, -49.231944	F	-	+	10	SC	-
CZFURB 9112	BRA:SC, Indaial, Parque Nacional da Serra do Itajaí	-26.897778, -49.231944	-	-	+	10	SC	-
CZFURB 9825	BRA:SC, Indaial, Parque Nacional da Serra do Itajaí	-26.897778, -49.231944	-	+	+	10	SC	MF766131
CZFURB 20520	BRA:SC, Abdon Batista, UHE Garibaldi	-27.610833, -51.022778	-	+	+	11	SC	MF766132
CZFURB 20541	BRA:SC, Abdon Batista, UHE Garibaldi	-27.610833, -51.022778	-	+	+	11	SC	
CZFURB 15102	BRA:SC, Campo Belo do Sul, Fazenda dos Gateados	-27.962555, -50.823104	M	-	+	12	SC	-
CZFURB 15106	BRA:SC, Campo Belo do Sul, Fazenda dos Gateados	-27.962555, -50.823104	M	+	+	12	SC	
CZFURB 15109	BRA:SC, Campo Belo do Sul, Fazenda dos Gateados	-27.962555, -50.823104	M	+	+	12	SC	MF766135
CZFURB 15112	BRA:SC, Campo Belo do Sul, Fazenda dos Gateados	-27.962555, -50.823104	M	-	+	12	SC	-
CZFURB 15113	BRA:SC, Campo Belo do Sul, Fazenda dos	-27.962555, -50.823104	M	-	+	12	SC	-

	Gateados							
CZFURB 15136	BRA:SC, Campo Belo do Sul, Fazenda dos Gateados	-27.962555, -50.823104	F	-	+	12	SC	-
CZFURB 15139	BRA:SC, Campo Belo do Sul, Fazenda dos Gateados	-27.962555, -50.823104	M	-	+	12	SC	-
CZFURB 15140	BRA:SC, Campo Belo do Sul, Fazenda dos Gateados	-27.962555, -50.823104	M	+	+	12	SC	MF766136
CZFURB 15154	BRA:SC, Campo Belo do Sul, Fazenda dos Gateados	-27.962555, -50.823104	-	+	+	12	SC	
CZFURB 15155	BRA:SC, Campo Belo do Sul, Fazenda dos Gateados	-27.962555, -50.823104	M	-	+	12	SC	-
MCNU 276	BRA:RS, Esmeralda	-28.053889, -51.19	M	-	+	13	SG	-
MCNU 277	BRA:RS, Esmeralda	-28.053889, -51.19	M	-	+	13	SG	-
MCNU 1458	BRA:RS, Esmeralda	-28.053889, -51.19	F	+	+	13	SG	
MCNU 1459	BRA:RS, Esmeralda	-28.053889, -51.19	M	+	+	13	SG	
MCNU 2498	BRA:RS, Vacaria	-28.511944, -50.933889	M	+	+	14	SG	MF766137
MCNU 260	BRA:RS, Cambará do Sul, Parque Nacional Aparados da Serra	-29.191667, -50.0975	M	-	+	15	SG	-
MCNU 264	BRA:RS, Cambará do Sul, Parque Nacional Aparados da Serra	-29.191667, -50.0975	-	-	+	15	SG	-
MCNU 265	BRA:RS, Cambará do Sul, Parque Nacional Aparados da Serra	-29.191667, -50.0975	M	-	+	15	SG	-
MCNU 266	BRA:RS, Cambará do Sul, Parque Nacional Aparados da Serra	-29.191667, -50.0975	M	-	+	15	SG	-
MCNU 269	BRA:RS, Cambará do Sul, Parque Nacional Aparados da Serra	-29.191667, -50.0975	F	-	+	15	SG	-
MCNU 270	BRA:RS, Cambará do Sul, Parque Nacional Aparados da Serra	-29.191667, -50.0975	F	-	+	15	SG	-
MCNU 271	BRA:RS, Cambará do Sul, Parque Nacional Aparados da Serra	-29.191667, -50.0975	M	-	+	15	SG	-
MCNU 272	BRA:RS, Cambará do Sul, Parque Nacional Aparados da Serra	-29.191667, -50.0975	M	-	+	15	SG	-
MCNU 1447	BRA:RS, Cambará do Sul, Parque Nacional Aparados da Serra	-29.191667, -50.0975	M	-	+	15	SG	-
MCNU 1448	BRA:RS, Cambará do Sul, Parque Nacional Aparados da Serra	-29.191667, -50.0975	M	-	+	15	SG	-
CMLCE-UFRGSAS 05	BRA:RS, Cambará do Sul, Parque Nacional Aparados da Serra	-29.191667, -50.0975	-	+	-	15	SG	MF766138
CMLCE-UFRGSAS 17	BRA:RS, Cambará do Sul, Parque Nacional Aparados da Serra	-29.191667, -50.0975	-	+	-	15	SG	MF766139
MCNU 262	BRA:RS, Canela	-29.365833, -50.815833	M	-	+	16	SG	-
MCNU 278	BRA:RS, Canela	-29.365833, -50.815833	-	-	+	16	SG	-
MCNU 3043	BRA:RS, São Francisco de Paula, Pró-Mata	-29.428322, -50.259444	M	+	+	17	SG	MF766140
MCNU 3658	BRA:RS, São Francisco de Paula, Pró-Mata	-29.428322, -50.259444	M	+	+	17	SG	MF766142
MCNU 3656	BRA:RS, São Francisco de Paula, Pró-Mata	-29.428322, -50.259444	M	-	+	17	SG	-
MCNU 3657	BRA:RS, São Francisco de Paula, Pró-Mata	-29.428322, -50.259444	M	-	+	17	SG	-
MCNU 275	BRA:RS, São Francisco de Paula, Pró-Mata	-29.428322, -50.259444	M	-	+	17	SG	-

MCNU 623	BRA:RS, São Francisco de Paula, Pró-Mata	-29.428322, -50.259444	M	-	+	17	SG	-
MCNU 3006	BRA:RS, São Francisco de Paula, Pró-Mata	-29.428322, -50.259444	M	-	+	17	SG	-
MCNU 3154	BRA:RS, São Francisco de Paula, Pró-Mata	-29.428322, -50.259444	M	-	+	17	SG	-
MCNU 3210	BRA:RS, São Francisco de Paula, Pró-Mata	-29.428322, -50.259444	F	+	-	17	SG	MF766141
CMLCE-UFRGSPM 104	BRA:RS, São Francisco de Paula, Pró-Mata	-29.428322, -50.259444	-	+	-	17	SG	MF766143
CMLCE-UFRGSPM 100	BRA:RS, São Francisco de Paula, Pró-Mata	-29.428322, -50.259444	-	+	-	17	SG	
CMLCE-UFRGSPM 86	BRA:RS, São Francisco de Paula, Pró-Mata	-29.428322, -50.259444	-	+	-	17	SG	
CMLCE-UFRGSPM 79	BRA:RS, São Francisco de Paula, Pró-Mata	-29.428322, -50.259444	-	+	-	17	SG	MF766144
CMLCE-UFRGSPM 74	BRA:RS, São Francisco de Paula, Pró-Mata	-29.428322, -50.259444	-	+	-	17	SG	
CMLCE-UFRGSPM 47	BRA:RS, São Francisco de Paula, Pró-Mata	-29.428322, -50.259444	-	+	-	17	SG	
CMLCE-UFRGSPM 65	BRA:RS, São Francisco de Paula, Pró-Mata	-29.428322, -50.259444	-	+	-	17	SG	
CMLCE-UFRGSPM 66	BRA:RS, São Francisco de Paula, Pró-Mata	-29.428322, -50.259444	-	+	-	17	SG	KJ936958*
CMLCE-UFRGSPM 70	BRA:RS, São Francisco de Paula, Pró-Mata	-29.428322, -50.259444	-	+	-	17	SG	
CMLCE-UFRGSPM 76	BRA:RS, São Francisco de Paula, Pró-Mata	-29.428322, -50.259444	-	+	-	17	SG	
CMLCE-UFRGSPM 80	BRA:RS, São Francisco de Paula, Pró-Mata	-29.428322, -50.259444	-	+	-	17	SG	
CMLCE-UFRGSPM 87	BRA:RS, São Francisco de Paula, Pró-Mata	-29.428322, -50.259444	-	+	-	17	SG	
CMLCE-UFRGSPM 91	BRA:RS, São Francisco de Paula, Pró-Mata	-29.428322, -50.259444	-	+	-	17	SG	
CMLCE-UFRGSPM 99	BRA:RS, São Francisco de Paula, Pró-Mata	-29.428322, -50.259444	-	+	-	17	SG	
MCNU 2805	BRA:RS, Itati	-29.488889, -50.105	F	-	+	18	SG	-
MCNU 1454	BRA:RS, São Francisco de Assis, Fazendo Trevo	-29.55, -55.130833	M	-	+	19	SSC	-
MCNU 1455	BRA:RS, São Francisco de Assis, Fazendo Trevo	-29.55, -55.130833	M	-	+	19	SSC	-
MCNU 1456	BRA:RS, São Francisco de Assis, Fazendo Trevo	-29.55, -55.130833	F	-	+	19	SSC	-
MCNU 1457	BRA:RS, São Francisco de Assis, Fazendo Trevo	-29.55, -55.130833	M	-	+	19	SSC	-
MCNU 786	BRA:RS, Manoel Viana	-29.588889, -55.482778	F	+	+	20	SSC	
MCNU 129	BRA:RS, Venâncio Aires	-29.605833, -52.191944	F	-	+	21	CDNS	-
MCNU 200	BRA:RS, Venâncio Aires	-29.605833, -52.191944	M	-	+	21	CDNS	-
MCNU 309	BRA:RS, Venâncio Aires	-29.605833, -52.191944	M	+	+	21	CDNS	
MCNU 311	BRA:RS, Venâncio Aires	-29.605833, -52.191944	F	-	+	21	CDNS	-
FZB-MCN 547	BRA:RS, Montenegro, Nova Paris	-29.688889, -51.460833	-	-	+	22	CDNS	-
MCNU 320	BRA:RS, Cachoeira do Sul	-30.038889, -52.893889	M	-	+	23	CDNS	-
MCNU 3211	BRA:RS, Guaíba	-30.113889, -51.325	F	+	+	24	PLWC	
MCNU 3652	BRA:RS, Guaíba	-30.113889, -51.325	M	+	+	24	PLWC	MF766145
MCNU 3119	BRA:RS, Guaíba	-30.113889, -51.325	M	+	+	24	PLWC	
MCNU 3009	BRA:RS, Guaíba	-30.113889, -51.325	F	+	+	24	PLWC	MF766146
MCNU 3141	BRA:RS, Guaíba	-30.113889, -51.325	F	+	+	24	PLWC	MF766147
MCNU 3146	BRA:RS, Guaíba	-30.113889, -51.325	M	+	+	24	PLWC	

MCNU 3142	BRA:RS, Guaíba	-30.113889, -51.325	M	+	+	24	PLWC	
MCNU 3212	BRA:RS, Guaíba	-30.113889, -51.325	M	+	+	24	PLWC	
MCNU 3040	BRA:RS, Guaíba	-30.113889, -51.325	M	-	+	24	PLWC	-
MCNU 3229	BRA:RS, Guaíba	-30.113889, -51.325	F	-	+	24	PLWC	-
MCNU 4336	BRA:RS, Guaíba	-30.113889, -51.325	M	-	+	24	PLWC	-
MCNU 3228	BRA:RS, Guaíba	-30.113889, -51.325	M	+	-	24	PLWC	
MCNU 3149	BRA:RS, Guaíba	-30.113889, -51.325	M	+	-	24	PLWC	
MCNU 3653	BRA:RS, Guaíba	-30.113889, -51.325	F	+	-	24	PLWC	
CMLCE-UFRGS GUA19	BRA:RS, Guaíba	-30.113889, -51.325	-	+	-	24	PLWC	
MCNU 1453	BRA:RS, Rosário do Sul	-30.257778, -54.913889	F	-	+	25	SSC	-
MCNU 3144	BRA:RS, Barra do Ribeiro	-30.290833, -51.300833	M	+	+	26	PLWC	
MCNU 3654	BRA:RS, Barra do Ribeiro	-30.290833, -51.300833	M	+	+	26	PLWC	
MCNU 3147	BRA:RS, Barra do Ribeiro	-30.290833, -51.300833	F	+	+	26	PLWC	MF766148
MCNU 3230	BRA:RS, Barra do Ribeiro	-30.290833, -51.300833	M	+	+	26	PLWC	MF766149
MCNU 3039	BRA:RS, Barra do Ribeiro	-30.290833, -51.300833	M	+	+	26	PLWC	MF766150
MCNU 3004	BRA:RS, Barra do Ribeiro	-30.290833, -51.300833	M	+	+	26	PLWC	
MCNU 3140	BRA:RS, Barra do Ribeiro	-30.290833, -51.300833	M	-	+	26	PLWC	-
MCNU 3655	BRA:RS, Barra do Ribeiro	-30.290833, -51.300833	F	-	+	26	PLWC	-
MCNU 4329	BRA:RS, Barra do Ribeiro	-30.290833, -51.300833	F	-	+	26	PLWC	-
MCNU 4330	BRA:RS, Barra do Ribeiro	-30.290833, -51.300833	M	-	+	26	PLWC	-
MCNU 4335	BRA:RS, Barra do Ribeiro	-30.290833, -51.300833	F	-	+	26	PLWC	-
MCNU 3135	BRA:RS, Barra do Ribeiro	-30.290833, -51.300833	M	+	-	26	PLWC	MF766151
MCNU 2166	BRA:RS, São Gabriel	-30.335833, -54.32	F	+	+	27	SSC	
MCNU 1293	BRA:RS, Encruzilhada do Sul	-30.543889, -52.521944	F	+	+	28	CDNS	
MCNU 302	BRA:RS, Sentinela do Sul	-30.610833, -51.578889	M	-	+	29	PLWC	-
MCNU 304	BRA:RS, Sentinela do Sul	-30.610833, -51.578889	M	-	+	29	PLWC	-
MCNU 305	BRA:RS, Sentinela do Sul	-30.610833, -51.578889	F	+	+	29	PLWC	
MCNU 306	BRA:RS, Sentinela do Sul	-30.610833, -51.578889	F	-	+	29	PLWC	-
MCNU 308	BRA:RS, Sentinela do Sul	-30.610833, -51.578889	F	-	+	29	PLWC	-
MCNU 312	BRA:RS, Sentinela do Sul	-30.610833, -51.578889	F	-	+	29	PLWC	-
MCNU 313	BRA:RS, Sentinela do Sul	-30.610833, -51.578889	M	-	+	29	PLWC	-
MCNU 314	BRA:RS, Sentinela do Sul	-30.610833, -51.578889	F	+	+	29	PLWC	MF766152
MCNU 3132	BRA:RS, Tapes	-30.669849, -51.429707	M	+	+	30	PLWC	MF766153
MCNU 3110	BRA:RS, Camaquã	-30.850833, -51.811944	F	+	+	31	PLWC	MF766156
MCNU 3116	BRA:RS, Camaquã	-30.850833, -51.811944	F	+	+	31	PLWC	MF766157
MCNU 3214	BRA:RS, Camaquã	-30.850833, -51.811944	M	+	+	31	PLWC	MF766159
MCNU 3227	BRA:RS, Camaquã	-30.850833, -51.811944	F	+	+	31	PLWC	MF766160
MCNU 3113	BRA:RS, Camaquã	-30.850833, -51.811944	F	-	+	31	PLWC	-

MCNU 3117	BRA:RS, Camaquã	-30.850833, -51.811944	F	-	+	31	PLWC	-
MCNU 3128	BRA:RS, Camaquã	-30.850833, -51.811944	F	-	+	31	PLWC	-
MCNU 3130	BRA:RS, Camaquã	-30.850833, -51.811944	F	-	+	31	PLWC	-
MCNU 3145	BRA:RS, Camaquã	-30.850833, -51.811944	M	-	+	31	PLWC	-
MCNU 3219	BRA:RS, Camaquã	-30.850833, -51.811944	M	-	+	31	PLWC	-
MCNU 4038	BRA:RS, Camaquã	-30.850833, -51.811944	F	-	+	31	PLWC	-
CMLCE-UFRGSFQ 47	BRA:RS, Camaquã	-30.850833, -51.811944	F	+	-	31	PLWC	MF766154
CMLCE-UFRGSFQ 30	BRA:RS, Camaquã	-30.850833, -51.811944	M	+	-	31	PLWC	
MCNU 3011	BRA:RS, Camaquã	-30.850833, -51.811944	F	+	-	31	PLWC	MF766161
MCNU 3012	BRA:RS, Camaquã	-30.850833, -51.811944	F	+	-	31	PLWC	MF766155
MCNU 3122	BRA:RS, Camaquã	-30.850833, -51.811944	M	+	-	31	PLWC	MF766158
MCNU 3124	BRA:RS, Camaquã	-30.850833, -51.811944	F	+	-	31	PLWC	
MCNU 3133	BRA:RS, Camaquã	-30.850833, -51.811944	M	+	-	31	PLWC	
CZFURB 6250	BRA:RS, Camaquã	-30.850833, -51.811944	F	+	-	31	PLWC	MF766162
CZFURB 6249	BRA:RS, Camaquã	-30.850833, -51.811944	F	+	-	31	PLWC	
FZB-MCN 710	BRA:RS, Dom Pedrito, Fazenda São Martinho	-30.975882, -54.666567	-	-	+	32	SSC	-
FZB-MCN 1011	BRA:RS, Dom Pedrito, Fazenda São Martinho	-30.975882, -54.666567	F	-	+	32	SSC	-
MCNU 4331	BRA:RS, Cristal	-31.002778, -52.050	M	+	+	33	PLWC	MF766163
MCNU 4334	BRA:RS, Cristal	-31.002778, -52.050	F	-	+	33	PLWC	-
CMLCE-UFRGSFQ 63	BRA:RS, Cristal	-31.002778, -52.050	M	+	-	33	PLWC	MF766164
CMLCE-UFRGSFQ 72	BRA:RS, Cristal	-31.002778, -52.050	M	+	-	33	PLWC	MF766165
MCNU 3109	BRA:RS, São Lourenço do Sul	-31.365, -51.977778	F	+	+	34	PLWC	MF766167
MCNU 3123	BRA:RS, São Lourenço do Sul	-31.365, -51.977778	F	-	+	34	PLWC	-
MCNU 3115	BRA:RS, São Lourenço do Sul	-31.365, -51.977778	M	+	+	34	PLWC	MF766168
MCNU 3005	BRA:RS, São Lourenço do Sul	-31.365, -51.977778	M	-	+	34	PLWC	-
MCNU 3010	BRA:RS, São Lourenço do Sul	-31.365, -51.977778	-	+	+	34	PLWC	MF766169
MCNU 3112	BRA:RS, São Lourenço do Sul	-31.365, -51.977778	F	-	+	34	PLWC	-
MCNU 3121	BRA:RS, São Lourenço do Sul	-31.365, -51.977778	F	-	+	34	PLWC	-
MCNU 3134	BRA:RS, São Lourenço do Sul	-31.365, -51.977778	M	-	+	34	PLWC	-
MCNU 3148	BRA:RS, São Lourenço do Sul	-31.365, -51.977778	F	-	+	34	PLWC	-
MCNU 3225	BRA:RS, São Lourenço do Sul	-31.365, -51.977778	M	+	+	34	PLWC	MF766166
MCNU 3226	BRA:RS, São Lourenço do Sul	-31.365, -51.977778	F	-	+	34	PLWC	-
MCNU 2386	BRA:RS, Candiota	-31.557778, -53.672778	M	-	+	35	SSC	-
MCNU 4366	BRA:RS, Candiota	-31.557778, -53.672778	M	-	+	35	SSC	-
MCNU 4367	BRA:RS, Candiota	-31.557778, -53.672778	F	-	+	35	SSC	-
MCNU 4381	BRA:RS, Candiota	-31.557778, -53.672778	M	-	+	35	SSC	-
MCNU 4387	BRA:RS, Candiota	-31.557778, -53.672778	M	-	+	35	SSC	-
MCNU 1352	BRA:RS, Pedras Altas	-31.732778, -53.583889	M	+	+	36	SSC	
MCNU 1353	BRA:RS, Pedras Altas	-31.732778, -53.583889	M	+	+	36	SSC	

MCNU 1354	BRA:RS, Pedras Altas	-31.732778, -53.583889	F	+	+	36	SSC	
MCNU 1355	BRA:RS, Pedras Altas	-31.732778, -53.583889	F	+	+	36	SSC	
MCNU 1356	BRA:RS, Pedras Altas	-31.732778, -53.583889	M	+	+	36	SSC	
MCNU 1357	BRA:RS, Pedras Altas	-31.732778, -53.583889	F	+	+	36	SSC	
MCNU 1358	BRA:RS, Pedras Altas	-31.732778, -53.583889	M	+	+	36	SSC	
MCNU 1359	BRA:RS, Pedras Altas	-31.732778, -53.583889	F	+	+	36	SSC	
MCNU 3223	BRA:RS, Pelotas, Horto-Botânico Irmão Teodoro Luís	-31.771944, -52.342778	M	+	+	37	PLWC	MF766172
MCNU 3041	BRA:RS, Pelotas, Horto-Botânico Irmão Teodoro Luís	-31.771944, -52.342778	M	+	+	37	PLWC	MF766173
MCNU 3042	BRA:RS, Pelotas, Horto-Botânico Irmão Teodoro Luís	-31.771944, -52.342778	F	+	+	37	PLWC	MF766174
MCNU 3176	BRA:RS, Pelotas, Horto-Botânico Irmão Teodoro Luís	-31.771944, -52.342778	M	-	+	37	PLWC	-
CMLCE-UFRGS PL300	BRA:RS, Pelotas, Horto-Botânico Irmão Teodoro Luís	-31.771944, -52.342778	-	+	-	37	PLWC	
CMLCE-UFRGS PL200	BRA:RS, Pelotas, Horto-Botânico Irmão Teodoro Luís	-31.771944, -52.342778	-	+	-	37	PLWC	
MCNU 3014	BRA:RS, Rio Grande, Mata da Estrada Velha	-32.035, -52.098889	F	+	+	38	SCP	MF766176
MCNU 1467	BRA:RS, Rio Grande, Mata da Estrada Velha	-32.035, -52.098889	M	-	+	38	SCP	-
MCNU 1737	BRA:RS, Rio Grande, Mata da Estrada Velha	-32.035, -52.098889	F	-	+	38	SCP	-
MCNU 1739	BRA:RS, Rio Grande, Mata da Estrada Velha	-32.035, -52.098889	M	-	+	38	SCP	-
MCNU 1795	BRA:RS, Rio Grande, Mata da Estrada Velha	-32.035, -52.098889	M	-	+	38	SCP	-
MCNU 1796	BRA:RS, Rio Grande, Mata da Estrada Velha	-32.035, -52.098889	M	-	+	38	SCP	-
MCNU 1798	BRA:RS, Rio Grande, Mata da Estrada Velha	-32.035, -52.098889	F	-	+	38	SCP	-
MCNU 1799	BRA:RS, Rio Grande, Mata da Estrada Velha	-32.035, -52.098889	F	-	+	38	SCP	-
CMLCE-UFRGSMEV 01	BRA:RS, Rio Grande, Mata da Estrada Velha	-32.035, -52.098889	M	+	-	38	SCP	MF766175
MCNU 3660	BRA:RS, Rio Grande, APA Lagoa Verde	-32.139934, -52.181064	M	+	+	39	SCP	MF766178
MCNU 3661	BRA:RS, Rio Grande, Estação Ecológica do Taim	-32.532753, -52.486550	M	-	+	40	SCP	-
MCNU 3131	BRA:RS, Rio Grande, Estação Ecológica do Taim	-32.532753, -52.486550	M	+	+	40	SCP	MF766177
MCNU 4368	BRA:RS, Chuí	-33.690833, -53.456944	M	-	+	41	SCP	-
MCNU 4369	BRA:RS, Chuí	-33.690833, -53.456944	F	-	+	41	SCP	-
MCNU 4370	BRA:RS, Chuí	-33.690833, -53.456944	M	-	+	41	SCP	-
MCNU 4372	BRA:RS, Chuí	-33.690833, -53.456944	F	-	+	41	SCP	-
MCNU 4382	BRA:RS, Chuí	-33.690833, -53.456944	M	-	+	41	SCP	-
MCNU 4384	BRA:RS, Chuí	-33.690833, -53.456944	F	-	+	41	SCP	-
MCNU 4386	BRA:RS, Chuí	-33.690833, -53.456944	M	-	+	41	SCP	-
FMNH 27652	URU:San Jose, Azarati, Ecilda (South)	-34.555727, -56.995273	M	-	+	42	UY	-
MNHN SN CA 614	URU:Rocha, Ruta 15 km 10 Arroyo la Paloma	-34.583004, -54.178482	-	+	+	43	UY	MF766186
MNHN SN CA 617	URU:Rocha, Ruta 15 km 10 Arroyo la Paloma	-34.583004, -54.178482	-	-	+	43	UY	-

MNHN 4281 CA 680	URU:Maldonado, El Renegado, 3 km E Pan de Azúcar	-34.766667, -55.200000	-	-	+	44	UY	-
MNHN 3855 CA 695	URU:Maldonado, Las Flores, Arroyo Tararias	-34.783273, -55.334011	-	+	+	45	UY	AF175287
FMNH 29250	URU:Maldonado, San Fernando de Maldonado	-34.908825, -54.958086	M	-	+	46	UY	-
FMNH 29253	URU:Maldonado, San Fernando de Maldonado	-34.908825, -54.958086	F	-	+	46	UY	-
MVZ 182701 CA459	URU:Maldonado, Km 10 on Ruta 39 N of Maldonado, El Penasco	-34.816670, -54.950000	F	+	+	47	UY	AF175286
MHNCI 4605	BRA:PR, Quatro Barras, Fazenda Três Pinheiros	-25.365833, -49.076944	M	+	-	48	PR	
MHNCI 4607	BRA:PR, Quatro Barras, Fazenda Três Pinheiros	-25.365833, -49.076944	F	+	-	48	PR	MF766110
MHNCI 4608	BRA:PR, Quatro Barras, Fazenda Três Pinheiros	-25.365833, -49.076944	F	+	-	48	PR	MF766111
UFPR SCB-P42	BRA:PR, Piraquara	-25.441944, -49.062778	F	+	-	49	PR	MF766112
UFPR SCB-P50	BRA:PR, Piraquara	-25.441944, -49.062778	M	+	-	49	PR	
UFPR SCB-P53	BRA:PR, Piraquara	-25.441944, -49.062778	M	+	-	49	PR	MF766113
UFPR SCB-P54	BRA:PR, Piraquara	-25.441944, -49.062778	F	+	-	49	PR	
UFPR SCB-P56	BRA:PR, Piraquara	-25.441944, -49.062778	M	+	-	49	PR	MF766114
UFPR SCB-P59	BRA:PR, Piraquara	-25.441944, -49.062778	F	+	-	49	PR	MF766115
UFPR SCB-P60	BRA:PR, Piraquara	-25.441944, -49.062778	F	+	-	49	PR	MF766116
UFPR SCB-P62	BRA:PR, Piraquara	-25.441944, -49.062778	M	+	-	49	PR	MF766117
UFPR SCB-P65	BRA:PR, Piraquara	-25.441944, -49.062778	M	+	-	49	PR	MF766118
MHNCI 4951	BRA:SC, Ponta Alta do Norte, Fazenda Rio das Pedras	-27.157778, -50.463889	M	+	-	50	SC	MF766130
CMLCE-UFRGSHFE 02	BRA:RS, Erechim	-27.633889, -52.273889	F	+	-	51	SG	MF766133
CMLCE-UFRGSHFE 03	BRA:RS, Erechim	-27.633889, -52.273889	F	+	-	51	SG	
CMLCE-UFRGSHFE 04	BRA:RS, Erechim	-27.633889, -52.273889	M	+	-	51	SG	MF766134
CMLCE-UFRGSHFE 05	BRA:RS, Erechim	-27.633889, -52.273889	M	+	-	51	SG	
CMLCE-UFRGSALL12	BRA:RS, Bagé	-31.330833, -54.106944	-	+	-	52	SSC	MF766170
CMLCE-UFRGSALL13	BRA:RS, Bagé	-31.330833, -54.106944	-	+	-	52	SSC	MF766171
CMLCE-UFRGSPOS 18	BRA:RS, Pedro Osório, Arroio Moreira	-31.863889, -52.822778	F	+	-	53	SSC	MF766179
CMLCE-UFRGSPOS 20	BRA:RS, Pedro Osório, Arroio Moreira	-31.863889, -52.822778	M	+	-	53	SSC	MF766180
CMLCE-UFRGSPOS 25	BRA:RS, Pedro Osório, Arroio Moreira	-31.863889, -52.822778	F	+	-	53	SSC	MF766181
CMLCE-UFRGSPOS 27	BRA:RS, Pedro Osório, Arroio Moreira	-31.863889, -52.822778	F	+	-	53	SSC	MF766182
CMLCE-UFRGSHL 01	BRA:RS, Herval	-32.023889, -53.395833	-	+	-	54	SSC	MF766183
MNHN SN SCV 108	URU:Rocha, Refugio de Fauna Laguna de Castillos	-34.35, -53.866667	F	+	-	55	UY	MF766184

MNHN SN SCV 110	URU:Rocha, Refugio de Fauna Laguna de Castillos	-34.35, -53.866667	M	+	-	55	UY	MF766185
MNHN SN GD 577	URU:Rocha, Route 9, km304.800	-34.357743, -54.064845	-	+	-	56	UY	DQ518258
MNHN 5615 (EMG1567)	URU:Canelones, Balnerio San Luis	-34.770278, -55.588333	M	+	-	57	UY	MF766188
MNHN 5617 (EMG1571)	URU:Canelones, Balnerio San Luis	-34.770278, -55.588333	M	+	-	57	UY	
MNHN SN EMG 1809	URU:Rocha, Parque Santa Teresa, Playa Grande	-34.008180, -53.552735	F	+	-	58	UY	
MNHN SN EMG 1096	URU:Treinta y Tres, Quebrada de Los Cuervos	-32.9275, -54.456944	F	+	-	59	UY	
MNHN SN EMG 1097	URU:Treinta y Tres, Quebrada de Los Cuervos	-32.9275, -54.456944	M	+	-	59	UY	
MCNU 1321	BRA:RS, Jaguarão	-32.565833, -53.375833	M	+	-	60	SSC	
MNHN SN GD 723	URU:Maldonado, La Barra, Barra del Arroyo Maldonado	-34.915632, -54.865456	M	+	-	61	UY	MF766187

Appendix S2. Description of landmarks digitized used in skulls for dorsal and ventral view.

Description of landmarks of skull dorsal view:
1: anteriormost point of suture between nasals;
2-3: anteriormost point of suture between nasal and premaxilla;
4-5: anteriormost margin of the maximum constriction of squamosal root of zygomatic arch;
6-7: lateralmost point of the Anterolateral tip of interparietal bone sutures;
8: posteriormost point of occipital margin;
9: suture between parietals and interparietal;
10: suture between frontals and parietals;
11: suture between nasals and frontals;
12-13: length margim of maximum constriction of interorbital region (frontal);
14-15: posteriormost margin of maximum constriction of antorbital bridge.

Description of landmarks of skull-ventral view:
1: anteriormost point of the suture between nasals;
2-3: lateralmost point of the alveolus of the incisor;
4-5: anterodorsal tip of zygomatic plate;
6-7: anteriormost margin of the maximum zygomatic plate posterior constriction;
8-9: posteriormost margin of the maximum anterior constriction of squamosal root of zygomatic;
10-11: anteriormost margin of the occipital condyle;
12: posteriormost point of foramen magnum;
13: anteriormost point of inferior margin of foramen Magnum.
14-15: basis length of suture between basisphenoid and basiocciptal;
16: posteriormost point of suture between palatines and anterior border of mesopterygoid fossa;
17-18: posteriormost margin of third molar;
19-20: anteriormost margin of first molar alveolus;
21-22: posteriormost margin of incisive foramen;
23-24: anteriormost margin of incisive foramen;
25-26: posteriormost margin of the masseteric tubercle.

Appendix S3. Description of all the environmental attributes used in each sampling point in this work. Abbreviations: sampling points (P), topography (m), net primary productivity (NPP), BIO12 = annual precipitation (mm), BIO10 = mean temperature warmest quarter, BIO11 = mean temperature coldest quarter. N/A: not available.

P	Localities	Approximate Coordinates	(m)	(NPP)	BIO12 (mm)	BIO10 (°C)	BIO11 (°C)
1	BRA:PR, Castro, Parque Florestal de Caxambu	-24..790891, -50.012062	1045	1,085000	1539	20	13,4
2	BRA:PR, Ponta Grossa, Parque Estadual de Vila Velha	-25.24.4064, -50.022787	841	1,098000	1475	21,3	14,3
3	BRA:PR, Curitiba*, Pq. Reg. do Iguaçu/Res. Bio. do Cambuí	-25.522947, -49.222987	897	1,126000	1296	20	13,2
4	BRA:PR, Araucária*, Thomaz Coelho/Repar	-25.540142, -49.355415	901	1,126000	1327	20,1	13,1
5	BRA:PR, Candói, UHE Santa Clara	-25.570833, -52.052778	830	1,136000	1775	21	13,4
6	BRA:PR, São José dos Pinhais, Barro Preto	-25.5799, -49.175373	897	1,126000	1296	20	13,2
7	BRA:PR, São Matheus do Sul, Fazenda do Durgo	-25.873889, -50.382778	788	1,098000	1487	20,9	12,9
8	BRA:SC, São Domingos*, Aheqq/PCH Luzia Alto	-26.616388, -52.538866	623	1,126000	2083	22	14,1
9	BRA:SC, Água Doce, Campo Eólico	-26.997778, -51.555833	1105	1,111000	1889	193	11,6
10	BRA:SC, Indaial, Parque Nacional da Serra do Itajaí	-26.897778, -49.23.1944	179	1,116000	1601	23,5	16,3
11	BRA:SC, Abdon Batista, UHE Garibaldi	-27.610833, -51.022778	836	1,111000	1739	20,2	12,3
12	BRA:SC, Campo Belo do Sul, Fazenda dos Gateados	-27.962555, -50.823.104	943	1,136000	1629	19,8	12,2
13	BRA:RS, Esmeralda	-28.053889, -51.19	879	1,138000	1750	20,1	12,6
14	BRA:RS, Vacaria	-28.511944, -50.933889	877	1,164000	1782	19,8	12,6
15	BRA:RS, Cambará do Sul, Parque Nacional Aparados da Serra	-29.191667, -50.0975	672	1,109000	1781	19,8	12,7
16	BRA:RS, Canela	-29.365833, -50.815833	514	1,109000	1829	21	13,5
17	BRA:RS, São Francisco de Paula, Pró-Mata	-29.428322, -50.259444	751	1,109000	1922	19,5	12,2
18	BRA:RS, Itati	-29.488889, -50.105	563	1,109000	1749	20,2	13
19	BRA:RS, São Francisco de Assis, Fazendo Trevo	-29.55, -55.130833	136	1,016000	1705	24,1	14,3
20	BRA:RS, Manoel Viana	-29.588889, -55.482778	98	1,016000	1689	24,2	14
21	BRA:RS, Venâncio Aires	-29.605833, -52.191944	103	1,052000	1298	23,2	152
22	BRA:RS, Montenegro, Nova Paris	-29.688889, -51.460833	32	1,079000	1404	23,4	153
23	BRA:RS, Cachoeira do Sul	-30.038889, -52.893889	44	1,103000	1412	23,2	152
24	BRA:RS, Guaíba	-30.113889, -51.325	34	1,060000	1409	23,3	150
25	BRA:RS, Rosário do Sul	-30.257778, -54.913889	107	0,976000	1534	23,8	14,1
26	BRA:RS, Barra do Ribeiro	-30.290833, -51.300833	5	1,060000	1395	23,5	15,0
27	BRA:RS, São Gabriel	-30.335833, -54.32	148	0,976000	1483	23,1	14,3
28	BRA:RS, Encruzilhada do Sul	-30.543889, -52.521944	356	1,103000	1511	21,6	13,6
29	BRA:RS, Sentinela do Sul	-30.610833, -51.578889	102	1,060000	1402	22,8	14,5
30	BRA:RS, Tapes	-30.669849, -51.429707	9	1,060000	1391	23,2	14,7
31	BRA:RS, Camaquã	-30.850833, -51.811944	22	1,060000	1375	23,1	14,6

32	BRA:RS, Dom Pedrito, Fazenda São Martinho	-30.975882, -54.666567	191	0,976000	1343	22,7	13,7
33	BRA:RS, Cristal	-31.002778, -52.050	53	1,039000	1391	23	14,2
34	BRA:RS, São Lourenço do Sul	-31.365, -51.977778	7	1,039000	1359	23,2	14
35	BRA:RS, Candiota	-31.557778, -53.672778	186	1,000000	1228	22	13,4
36	BRA:RS, Pedras Altas	-31.732778, -53.583889	296	1,000000	1287	21,5	12,7
37	BRA:RS, Pelotas, Horto-Botânico Irmão Teodoro Luís	-31.771944, -52.342778	18	1,039000	1382	22,8	13,3
38	BRA:RS, Rio Grande, Mata da Estrada Velha	-32.035, -52.098889	4	N/A	1212	23,1	13,5
39	BRA:RS, Rio Grande, APA Lagoa Verde	-32.139934, -52.181064	6	N/A	1251	22,9	13,3
40	BRA:RS, Rio Grande, Estação Ecológica do Taim	-32.532753, -52.486550	12	N/A	1222	22,3	13,1
41	BRA:RS, Chuí	-33.690833, -53.456944	10	1,017000	1166	20,9	12,4
42	URU:San Jose, Azarati, Ecilda (South)	-34.555727, -56.995273	19	0,905000	1091	22,7	11,2
43	URU:Rocha, Ruta 15 km 10 Arroyo la Palma	-34.583004, -54.178482	12	1,027000	1091	21,1	11,5
44	URU:Maldonado, El Renegado 3 km E, Pan de Azucar	-34.766667, -55.200000	82	0,933000	1107	21,6	11,6
45	URU:Maldonado, Las Flores [Tararias]	-34.783273, -55.334011	40	0,933000	1100	22	11,7
46	URU:Maldonado, San Fernando de Maldonado	-34.908825, -54.958086	15	1,027000	1043	21,4	11,9
47	URU:Maldonado, Km 10 on Ruta 39 N of Maldonado, El Penasco	-34.816670, -54.950000	30	1,027000	1089	21,5	11,8
48	BRA:PR, Quatro Barras, Fazenda Três Pinheiros	-25.365833, -49.076944	941	1,126000	1557	20,1	13,3
49	BRA:PR, Piraquara	-25.441944, -49.062778	941	1,126000	1557	20,1	13,3
50	BRA:SC, Ponta Alta do Norte, Fazenda Rio das Pedras	-27.157778, -50.463889	1045	1,136000	1636	18,7	11,3
51	BRA:RS, Erechim	-27.633889, -52.273889	694	1,094000	1856	21,4	14
52	BRA:RS, Bagé	-31.330833, -54.106944	175	0,956000	1283	22	13,2
53	BRA:RS, Pedro Osório, Arroio Moreira	-31.863889, -52.822778	33	1,039000	1325	22,7	13,3
54	BRA:RS, Herval	-32.023.889, -53.395833	207	0,997000	1279	21,7	12,5
55	URU:Rocha, Refugio de Fauna Laguna de Castillos	-34.35, -53.866667	7	N/A	1113	21	11,8
56	URU:Rocha, Route 9, km304.800	-34.357743, -54.064845	18	1,027000	1112	21,1	11,6
57	URU:Canelones, Balnerio San Luis	-34.770278, -55.588333	38	0,933000	1091	22,1	11,5
58	URU:Rocha, Parque Santa Teresa, Playa Grande	-34.008180, -53.552735	18	1,017000	1142	20,9	12,2
59	URU:Treinta y Tres, Quebrada de Los Cuervos	-32.9275, -54.456944	170	1,017000	1260	22,5	11,6
60	BRA:RS, Jaguarão	-32.565833, -53.375833	17	0,997000	1220	22,3	12,9
61	URU:Maldonado, La Barra, Barra del Arroyo Maldonado	-34.915632, -54.865456	15	1,027000	1043	21,4	11,9

Appendix S4. Description of all Tukey's test on Ventral – Size.

***P* =<0.05; *****P* =<0.10.**

Population	differences	lower	upper	*P* adj
PR-CDNS	0.225396006	-0.0907795673	0.5415715798	0.3649583
PLWC-CDNS	-0.015812821	-0.3113889058	0.2797632638	0.9999998
SC-CDNS	0.165114291	-0.1540542218	0.4842828032	0.7577746
SG-CDNS	0.209631924	-0.1052107750	0.5244746221	0.4567409
SCP-CDNS	-0.065857983	-0.3952075390	0.2634915726	0.9986694
SSC-CDNS	0.009115505	-0.3117411037	0.3299721135	1
UY-CDNS	-0.172235918	-0.5549055213	0.2104336854	0.8651026
***PLWC-PR**	**-0.241208827**	**-0.4176565196**	**-0.0647611348**	**0.0011061**
SC-PR	-0.060281716	-0.2739101445	0.1533467133	0.9886855
SG-PR	-0.015764083	-0.2228739355	0.1913457701	0.9999980
***SCP-PR**	**-0.291253989**	**-0.5198140388**	**-0.0626939401**	**0.0032441**
***SSC-PR**	**-0.216280501**	**-0.4324228839**	**-0.0001381187**	**0.0497255**
***UY-PR**	**-0.397631924**	**-0.6979727166**	**-0.0972911317**	**0.0018396**
****SC-PLWC**	**0.180927112**	**-0.0008291379**	**0.3626833611**	**0.0519977**
***SG-PLWC**	**0.225444745**	**0.0513967060**	**0.3994927830**	**0.0025581**
SCP-PLWC	-0.050045162	-0.2491379164	0.1490475919	0.9943716
SSC-PLWC	0.024928326	-0.1597761898	0.2096328416	0.9999012
UY-PLWC	-0.156423097	-0.4349959245	0.1221497305	0.6728533
SG-SC	0.044517633	-0.1671331105	0.2561683763	0.9981593
****SCP-SC**	**-0.230972274**	**-0.4636549811**	**0.0017104333**	**0.0532523**
SSC-SC	-0.155998786	-0.3764961227	0.0644985512	0.3750500
***UY-SC**	**-0.337350209**	**-0.6408401387**	**-0.0338602785**	**0.0179287**
***SCP-SG**	**-0.275489907**	**-0.5022025612**	**-0.0487772523**	**0.0062072**
SSC-SG	-0.200516419	-0.4147043293	0.0136714921	0.0847232
***UY-SG**	**-0.381867841**	**-0.6808051646**	**-0.0829305184**	**0.0031324**
SSC-SCP	0.074973488	-0.1600194184	0.3099663947	0.9769462
UY-SCP	-0.106377935	-0.4205573870	0.2078015175	0.9678819
UY-SSC	-0.181351423	-0.4866161630	0.1239133173	0.6060006

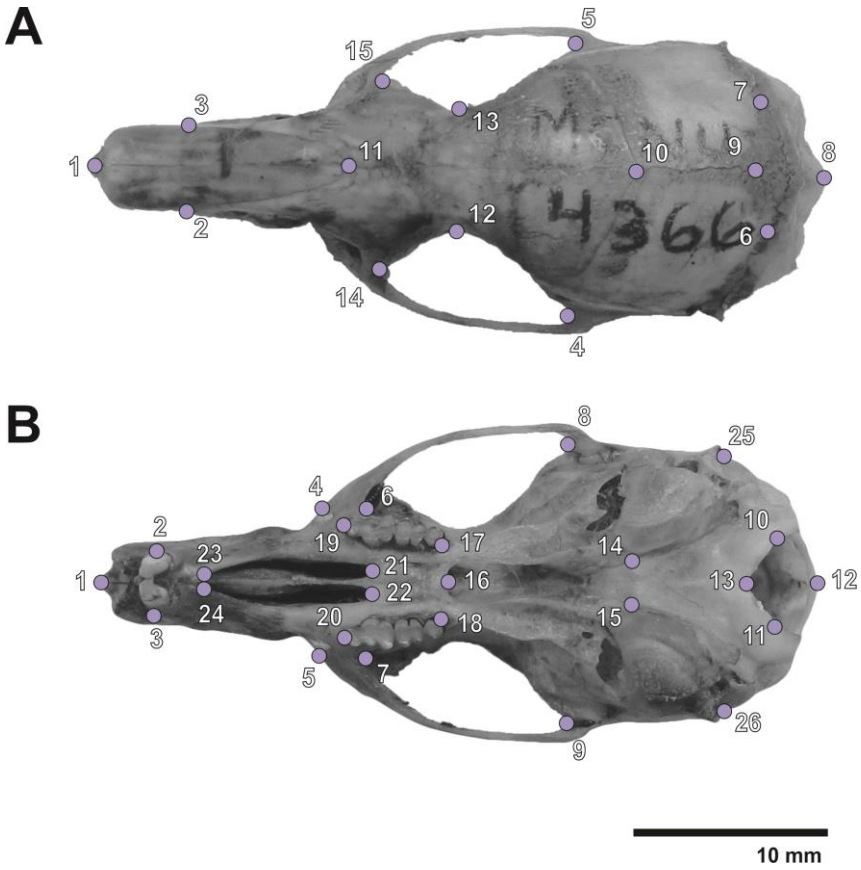

S1 Figure. Position of the landmarks (circles) digitized on the dorsal (A) and ventral (B), views of the *O. nasutus* skull. A description of each landmark is presented in Appendix S2.

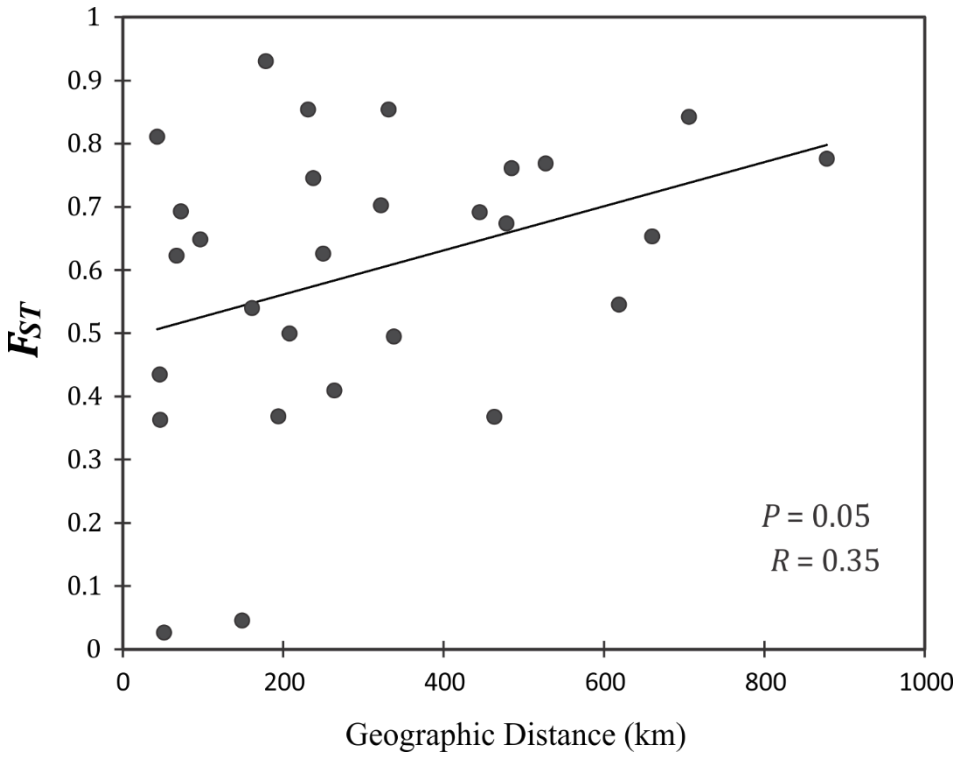

S2 Figure. Isolation by distance among *O. nasutus* clusters (R^2 = 0.1225). Isolation by distance for eight populations defined of Darwin's Hocicudo analyzed, as shown by the correlation of genetic distances (F_{ST}) and geographic distances (Mantel test).

Table S1. Description of each population sampling from skulls and mtDNA sequences evaluated in this study.

Population (N total)	**Skulls (N)**	***Cytb* haplotypes (N)**
Paraná N = 44	25	32
Santa Catarina N = 26	23	12
Serra Geral N = 47	26	26
Central Depression Northern Shield N = 07	07	02
Patos Lagoon West Coast N = 77	59	47
Southern Shield Campanha N = 30	22	18
Uruguay N = 17	08	12
Southern Coastal Plain N = 19	18	04
Total N = 267	188	153

Table S2. Genetic divergence (using *p*-distance) between pairs of *Cytb* haplotypes recovered from eight population of *Oxymycterus nasutus.*

Population	1	2	3	4	5	6	7
1. PR	—						
2. SC	0.0108	—					
3. SG	0.0055	0.0071	—				
4. CDNS	0.0130	0.0105	0.0097	—			
5. PLWC	0.0137	0.0123	0.0106	0.0039	—		
6. SSC	0.0162	0.0137	0.013	0.0084	0.0104	—	
7. UY	0.0202	0.0178	0.017	0.0151	0.0171	0.0119	—
8. SCP	0.0165	0.0144	0.0133	0.0163	0.0181	0.0182	0.0233

Table S3. R^2 (upper), F (bottom) values and significance levels of pairwise MANOVA analysis of variation in *Oxymycterus nasutus* skull shape among eight populations in southern Brazil and Uruguay, for dorsal and ventral views (*P < 0.05; **P < 0.01; ***P < 0.001).

DORSAL	**PR**	**SC**	**SG**	**CDNS**	**PLWC**	**SSC**	**SCP**
PR	-						
SC	0.075519 3.7576 **	-					
SG	0.056153 2.9152 *	0.043548 2.1399 *	-				
CDNS	0.11193 3.7813 **	0.16825 5.6638 ***	0.1635 6.059 ***	-			
PLWC	0.074351 6.5865 ***	0.092718 8.1755 ***	0.11623 10.916 ***	0.035551 2.3592 *	-		
SSC	0.043187 2.0311	0.13267 6.5774 ***	0.11556 6.0101 ***	0.11706 3.5795 ***	0.052884 4.4111 **	-	
SCP	0.11459 5.3061 ***	0.19298 9.3259 ***	0.19142 9.9427 ***	0.077657 1.9365	0.030298 2.3434 *	0.078197 3.2236 **	-
UY	0.12998 4.6312 **	0.27586 11.047 ***	0.25123 10.737 ***	0.21003 3.4564 **	0.081535 5.7702 ***	0.12206 3.893 **	0.13354 3.6989 **

VENTRAL	**PR**	**SC**	**SG**	**CDNS**	**PLWC**	**SSC**	**SCP**
PR	-						
SC	0.066963 3.3014 **	-					
SG	0.081355 4.3395 ***	0.094561 4.9085 ***	-				
CDNS	0.057095 1.8166	0.063979 1.9139	0.09685 3.3243 **	-			
PLWC	0.076432 6.7861 ***	0.078267 6.793 ***	0.14222 13.761 ***	0.01661 1.0813	-		
SSC	0.097181 4.8439 ***	0.056792 2.5891 *	0.093395 4.7388 ***	0.04718 1.337	0.044764 3.702 **	-	
SCP	0.15722 7.6485 ***	0.1222 5.4291 ***	0.19183 9.9693 ***	0.06429 1.5802	0.051181 4.0457 ***	0.058577 2.3644 *	-
UY	0.18168 6.8825 ***	0.19285 6.9289 ***	0.28007 12.449 ***	0.10677 1.554	0.0667 4.6453 ***	0.15253 5.0396 ***	0.11299 3.0572 **

Table S4. Matrix of pairwise F_{ST} (below diagonal) and *P* significance (above diagonal) among eight populations of *Oxymycterus nasutus* in South America grasslands.

Populations	PR	SC	SG	CDNS	PLWC	SSC	SCP	UY
PR	*	+	+	+	+	+	+	+
SC	0.53964	*	+	+	+	+	+	+
SG	0.40920	0.43461	*	+	+	+	+	+
CDNS	0.69180	0.49953	0.69296	*	-	-	-	+
PLWC	0.67358	0.62591	0.64827	0.02657	*	+	+	+
SSC	0.54508	0.36793	0.49478	0.04519	0.36297	*	+	+
SCP	0.84262	0.76119	0.85387	0.93043	0.81073	0.61969	*	+
UY	0.77622	0.65315	0.76891	0.70233	0.74533	0.36870	0.85395	*

(+) = $P < 0.05$; *(-)* = non-significant.

CAPÍTULO 4.

A new species of *Oxymycterus* (Rodentia: Cricetidae: Sigmodontinae) from a transitional area of Cerrado - Atlantic Forest in Southeastern Brazil

Willian T. Peçanha, Sergio L. Althoff, Daniel Galiano, Fernando M. Quintela, Renan Maestri, Gislene L. Gonçalves, Thales R. O. Freitas

Submetido: 25 de outubro, 2018

Aceito: 28 de fevereiro, 2019

Publicado: 24 de Abril, 2019

Journal of Mammalogy, 100(2):578–598, 2019

DOI:10.1093/jmammal/gyz060

Journal of Mammalogy, 100(2):578–598, 2019
DOI:10.1093/jmammal/gyz060
Version of Record, first published online 24 April 2019, with fixed content and layout in compliance with Art. 8.1.3.2 ICZN.

A new species of *Oxymycterus* (Rodentia: Cricetidae: Sigmodontinae) from a transitional area of Cerrado – Atlantic Forest in southeastern Brazil

Willian Thomaz Peçanha, Fernando Marques Quintela, Luiz Eduardo Jorge Ribas, Sérgio Luiz Althoff, Renan Maestri, Gislene Lopes Gonçalves,* and Thales R. O. de Freitas

Departamento de Genética, Universidade Federal do Rio Grande do Sul, Porto Alegre, RS 91501–970, Brazil (WTP, LEJR, GLG, TROF)
Universidade Federal do Rio Grande, Programa de Pós-Graduação em Biologia de Ambientes Aquáticos Continentais. Av. Itália km 8, Rio Grande, RS, Brazil (FMQ)
Departamento de Ciências Naturais, Universidade Regional de Blumenau, CEP Blumenau, SC 89012–900, Brazil (SLA)
Departamento de Ecologia, Universidade Federal do Rio Grande do Sul, Porto Alegre, RS 91501–970, Brazil (RM)
Departamento de Recursos Ambientales, Facultad de Ciencias Agronómicas, Universidad de Tarapacá, Arica, Chile (GLG)

* *Correspondent: lopes.goncalves@ufrgs.br*

We describe a new species of the cricetid rodent *Oxymycterus* (Sigmodontinae), which inhabits a transitional area between the southern Cerrado and the Atlantic Forest in south-southeastern Brazil. Compared to other *Oxymycterus*, the new species is large-sized with a tawny-brown pelage coloration. The new species could be differentiated from other *Oxymycterus* species by a combination of cranial characteristics that includes markedly large and inflated auditory bulla; a narrow rostrum and large incisive foramen, with the posterior extremity reaching the posterior region of the M1 protocone or hypoflexus; a wide parapterygoid fossa; the presence of a foramen ovale in the posterior region of the parapterygoid plate; and a thin hamular process of the squamosal. Bayesian analysis based on the mitochondrial and nuclear genes (cytochrome-*b* and acid phosphatase type V—Intron 2, respectively) recovered from the *Oxymycterus* sp. nov. showed it to be phylogenetically closely related to *O. amazonicus* and *O. delator,* all three species associated with open vegetation. The lineage leading to this clade likely emerged around 1.14 million years ago during the Early-Middle Pleistocene. Genetic distances between the new taxa and these two species calculated from comparison of cytochrome-*b* sequences are 3.7% and 4.1%, respectively. Currently, *Oxymycterus* sp. nov. is known from only two unprotected sites, with the type locality inserted in an area under the process of conurbation. Our study raises the number of living species in the genus to 16.

Descrevemos uma nova espécie de roedor cricetídeo *Oxymycterus* (Sigmodontinae), que habita uma área de transição entre o Cerrado Meridional e a Mata Atlântica no Sudeste do Brasil. Comparativamente aos demais *Oxymycterus,* a nova espécie possui tamanho médio e coloração marrom-avermelhada. A nova espécie também pode ser diferenciada dos demais *Oxymycterus* pelo tamanho e forma do crânio. Em particular por uma combinação de características cranianas, que incluem a bula auditiva acentuadamente grande e inflada, um rostro estreito e um grande forame incisivo, com a extremidade posterior alcançando a região posterior do protocone ou hipoflexus do M1; fossa parapterigóide larga; a presença de um forame oval na região posterior da placa parapteritóide; e um estreito processo hamular do esquamosal. Uma análise bayesiana reconstruída com base em genes mitocondriais e nucleares (citocromo-*b* e o íntron 2 do fosfatase ácida tipo V, respectivamente) demostrou que *Oxymycterus* sp. nov. é filogeneticamente relacionada a *O. amazonicus* e *O. delator*, todas as três espécies associadas a formações savânicas. A linhagem que deu origem a esse clado surgiu, provavelmente, há cerca de 1,14 milhão de anos (MIA) durante o Pleistoceno Médio-Antigo. A distância genética entre o novo táxon e estas duas espécies, calculadas a partir da comparação de sequências do gene citocromo-*b,* foram de 3.7% e 4.1%, respectivamente. *Oxymycterus*

sp. nov. é conhecido apenas em duas localidades não protegidas, e a localidade tipo encontra-se em uma área em processo de conurbação. Nosso estudo eleva para 16 o número de espécies descritas para o gênero.

Key words: acid phosphatase type V, Akodontini, Cerrado, cytochrome *b*, *Oxymycterus delator*

The Neotropical region presents an impressively diverse rodent fauna (Patton et al. 2015). The subfamily Sigmodontinae (family Cricetidae) is the largest lineage, including 438 species (Pardiñas et al. 2017; Hurtado and D'Elia 2018). In the last 10 years, 26 new species have been described (Jayat et al. 2008, 2016; Percequillo et al. 2008, 2011; Pardiñas et al. 2009, 2013, 2014, 2016; Carleton et al. 2009; Bonvicino et al. 2010, 2014; Braun et al. 2010; Andrade-Costa et al. 2011; Tavares et al. 2011; Gonçalves and Oliveira 2014; Quintela et al. 2014, 2017; D'Elía et al. 2015a; Hanson et al. 2015; Christoff et al. 2016; Teta and D'Elía 2016; Brito 2017; Palma and Rodríguez-Serrano 2017; Hurtado and D'Elía 2018; Timm et al. 2018) and a number of phylogenetic units, i.e., lineages divergent at the species level based on at least one molecular marker, were identified (e.g., Ventura et al. 2011; D'Elía et al. 2015b; Suárez-Villota et al. 2017). Despite this high taxonomic diversity, the alpha taxonomy remains uncertain in several groups, for example, within the tribe Akodontini in the genus *Oxymycterus* Waterhouse, 1837 (Oliveira and Gonçalves 2015).

Oxymycterus is composed of 15 species distributed across a wide geographic range in South America, including strikingly distinct ecoregions, such as forest borders in the Atlantic and Amazon Forests, open areas in the Caatinga (restricted to fertile regions), Cerrado (Bonvicino et al. 2008), Pampas (Peçanha et al. 2017), Yungas Montane Forests (Jayat et al. 2008), and regions with elevations above 4,000 m in the Andean Mountains (Hershkovitz 1994). This group also includes terrestrial species with marked habitat preferences, particularly wet grasslands, tall grass, woodland, and near edges of streams or rocky outcroppings (Hershkovitz 1994). It has a conserved karyotype, with a constant diploid number (2n = 54), and a variable number of autosomal arms (NF = 62–64), in particular due to the X chromosomes with submetacentric or subtelocentric morphologies or the Y chromosome being acrocentric or metacentric (Kajon et al. 1984; Vitullo et al. 1986; Sbalqueiro 1989; Svartman and Almeida 1993; Bonvicino et al. 2005; Moreira et al. 2009). In addition, most of the species are conspicuously divergent regarding DNA sequences based on the mitochondrial cytochrome *b* gene (*Cytb*), showing an average genetic distance of approximately 7.5% (Hoffmann et al. 2002).

Phylogenetic inferences in *Oxymycterus* have been made with a combination of molecular and craniometric analyses (Hoffmann et al. 2002; Gonçalves and Oliveira 2004; Jayat et al. 2008), and multilocus sequence data (e.g., Fabre et al. 2012; Parada et al. 2015). However, overall species boundaries have only been delimited through DNA polymorphisms, due to difficulties in detecting discontinuities in cytogenetic and morphological characteristics in this sigmodontine group (Hoffmann et al. 2002; Gonçalves and Oliveira 2004).

The genus still presents a confusing taxonomy, for example, the specific status of *Oxymycterus judex* Thomas, 1909, *O. misionalis* Sanborn, 1931, [= *O. quaestor* Thomas, 1903], and *Oxymycterus akodontius* Thomas, 1921 [= *Oxymycterus paramensis* Thomas, 1902], cases of putative synonyms (Oliveira and Gonçalves 2015). Additionally, some species are described and known only from a few localities or only from the type locality (e.g., *Oxymycterus nigrifrons* Osgood, 1944, *Oxymycterus hucucha* Hinojosa et al. 1987, and *Oxymycterus caparaoe* Hershkovitz, 1998) whereas *O. quaestor* Thomas, 1903 is disjointly distributed and poorly known. A striking case is *Oxymycterus paramensis* Thomas, 1903, recovered by Jayat et al. (2008) as composed of more than one specific lineage.

As part of an ongoing study on the taxonomy and evolution of small mammals from the Atlantic Forest, we have accessed specimens of sigmodontines throughout museum collections. A distinct morphotype of *Oxymycterus* collected in a transitional zone of the Atlantic Forest and Cerrado in south-southeastern Brazil (Fig. 1) was recognized. In this study, we compared this form to other *Oxymycterus*, particularly sympatric species, using an integrative morphological and molecular approach. Phylogenetic relationships of the genus are reviewed and discussed in the light of new information generated by a time-calibrated tree.

Materials and Methods

Specimens used, DNA extraction, and molecular markers.—Two specimens of *Oxymycterus* sp. nov. were detected from the Museu de História Natural "Capão da Imbuía" (MHNCI 3595 and MHNCI 3593) located in Curitiba, Paraná, Brazil, consisting of skin, skull, and tissue. Tissues of another three specimens not available for morphological analysis (MHNCI 1704, MHNCI 5140, and MHNCI 5141) were used for genetic analysis.

Genomic DNA was extracted from kidney and muscle tissues from five samples (stored at −20°C or 70% ethanol) using the PureLink Genomic DNA extraction kit (Thermo Fisher Scientific, Carlsbad, California), following the manufacturer's instructions. Two loci including a total of 1,580 base pairs (bp) in length were amplified through a polymerase chain reaction (PCR): the cytochrome-*b* (*Cytb*) gene of the mitochondrial genome and the Intron 2 and parts of the exons 2 and 3 of the Acid Phosphatase type V autosomal nuclear gene (*Acp5*-I2). For *Cytb*, we used the primers MVZ05 and MVZ16 (or MVZ26), and MVZ23 and MVZ14 as external primers following conditions proposed by Smith and Patton (1993), whereas for *Acp5*-I2, we used the primers AP5-564rev and AP5-120fwd, following conditions proposed by DeBry and Seshadri (2001). All PCR products were checked in 1% agarose gel stained with GelRed (Biotium, Fremont, California), further purified with Alkaline phosphatase and Exonuclease I (Amersham Biosciences, Little Chalfont, United Kingdom), and sequenced

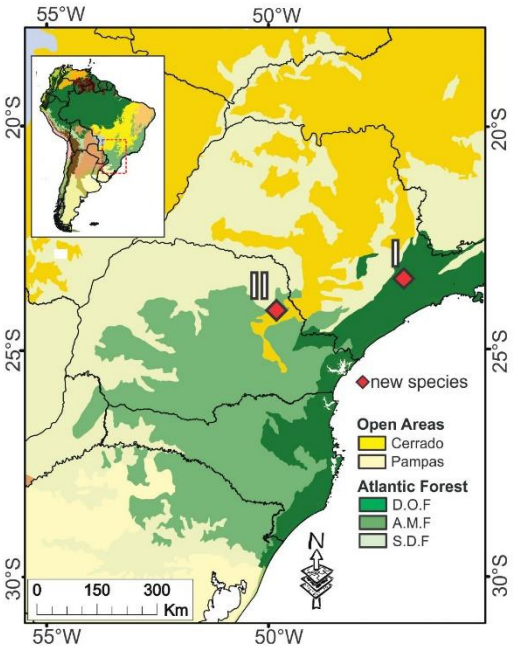

Fig. 1.—Map including South American biomes and ecoregions (adapted), and sampling localities of *Oxymycterus* sp. nov. in transitional areas of the Cerrado and Atlantic Forest of south and southeastern Brazil. I. Type locality: Itapevi County, Transurb condominium (São Paulo State); II. Jaguariaíva County (Paraná State). The maps were obtained and generated from Ecoregions 2017 Resolve (available at: http://ecoregions2017.appspot.com/). Any rights regarding the individual contents of the database are licensed under the Database Contents License: https://creativecommons.org/licenses/by/4.0/) and edited with the ArcMap 10.3 software. D.O.F, Dense Ombrophilous Forest; A.M.F, Araucaria Moist Forest; S.D.F, Seasonal Dry Forest.

using ABI chemistry. In addition, we sequenced the entire *Cytb* (1,140 bp) gene of a specimen of each of *O. josei*, *O. delator, O. dasytrichus, O. quaestor*, and *O. nasutus* aiming to explore the overall intra-specific distance. All sequences generated in this study were deposited in the GenBank (*Cytb*, MK331133-MK331147; *Acp5*-I2, MK331148– MK331151).

Phylogenetic analyses and distance.—Our analyses included data from the new species and 10 other *Oxymycterus* (Oliveira and Gonçalves 2015; Table 1). The tree was rooted with representative species of Akodontini based on topology proposed by Parada et al. (2015) and Salazar-Bravo et al. (2016; Table 1). From those species where no nuclear data were available, the matrix was completed with missing state characters. The mtDNA and nuclear sequences were aligned and manually adjusted using the Clustal W algorithm and default value parameters within MEGA v7 (Kumar et al. 2016). All polymorphic positions in the nuclear loci were verified using Bioedit v7.2.5 (Hall 1999) to ensure correct and consistent identification of double peaks in heterozygotes. Contiguous insertion-deletion (indels or gaps) events involving more than one base pair were coded and treated as one mutational event (Simmons and Ochoterena 2000).

The jModelTest v2.1.10 software (Darriba et al. 2012) was used to determine the substitution model HKY + I + G and HKY + I for *Cytb* and *Acp5*-I2, respectively, based on the Akaike information criterion. The phylogeny was reconstructed using Bayesian inference (BI) through the software BEAST v1.8.4 (Drummond et al. 2016) under three datasets: 1) only *Cytb* sequenced; 2) concatenated tree using *Cytb* and *Acp5*-I2; and 3) *Cytb* sequenced + sequences available from GenBank. We used the evolutionary rate estimated by Parada et al. (2015) for *Oxymycterus* as 2.37% per million years (Myr^{-1}) and a standard deviation of 0.25% Myr^{-1}. We performed six independent Markov Chain Monte Carlo (MCMC) runs, each one with four streams per 20 million steps of the MCMC, sampled every 1,000 generations and discarding the four million burn-in (about 20% discarded), starting the initial trees with randomness, without restriction. Runs were performed under an uncorrelated lognormal relaxed-clock model; speciation was modeled on a birth-death process with estimated base frequencies and four gamma rate categories, using an initial random tree, and other priors set as default. All parameter convergences were checked for convergence in Tracer v1.5 (Rambaut and Drummond 2009). All posterior parameter estimates had effective sample sizes (ESS) above 200 and the remaining trees were used to calculate posterior probabilities for each node. The burn-in was determined in Tracer based on trajectory parameters, and 20% of the first trees were then removed and summarized in TreeAnnotator in BEAST. For the concatenated dataset trees and logs, files were combined using LogCombiner in BEAST for concatenated phylogeny, and 20% of the first trees were then removed (10 million) and summarized in TreeAnnotator. The tree consensus generated was visualized and edited in Figtree v1.4.3 (http://tree.bio.ed.ac.uk/software/figtree/). The *p*-distance parameter model of evolution was used to calculate genetic distances for mtDNA and nDNA. These values were then used to assess levels of genetic divergence among and within the species of *Oxymycterus* following the criteria outlined by Baker and Bradley (2006). All Genbank accession numbers used for intra-specific phylogenetic reconstruction and genetic distances are listed in Supplementary Data SD1.

Morphological analysis.—We directly examined the skull and skin for diagnostic characters to distinguish the new species from congenerics distributed in Brazil, Paraguay, Argentina, and Uruguay, which included *Oxymycterus amazonicus, O. caparaoe, O. dasytrichus, O. delator, O. josei, O. nasutus, O. quaestor, O. rufus*, and *O. wayku* (Oliveira and Gonçalves 2015). We transcribed the external measurements (Table 2) of total length (TL), head-body length (HB), length of tail (LT), height of ear (Ear), and hindfoot length (including claws; HF) from specimen tags. We calculated HB by subtracting LT from TL. External measurements are given to the nearest millimeter (mm). The external morphological terminology used by Brown (1971) and Brown and Yalden (1973); the cranial terminology used by Hershkovitz (1962, 1994), Voss (1988) and Gonçalves and Oliveira (2004); and the molar terminology used by Reig (1977) were used here.

Table 1.—Demonstrative table containing the species, voucher origin, Genbank accession number, and location of the sequences of the cytochrome *b* (*Cytb*) and acid phosphatase type V (*Acp5-I2*) genes used for phylogenetic reconstruction of the genus *Oxymycterus*. The acronyms used are from the respective collections: CML, Colección de Mamíferos "Lillo," Universidad Nacional de Tucumán, San Miguel de Tucumán. CZFURB, Coleção Zoológica da Universidade Regional de Blumenau, Blumenau. FMNH, Field Museum of Natural History, Chicago. MHNCI, Museu de História Natural "Capão da Imbuía," Curitiba. MSB, Museum of Southwestern Biology, University of New Mexico, Albuquerque. MVZ, Museum of Vertebrate Zoology, University of California at Berkeley. MZUSP, Museu de Zoologia da Universidade de São Paulo, São Paulo. OMNHN, Sam Noble Oklahoma Museum of Natural History, University of Oklahoma, Norman. TTU, Museum of Texas Tech University, Lubbock. UMMZ, University of Michigan, Museum of Zoology, Ann Arbor. USNM, Smithsonian National Museum of Natural History, Smithsonian Institution, Washington.

Species	Voucher #	Genbank accession		Reference
		Cytb	*Acp5-I2*	
Ingroup				
Oxymycterus sp. nov.	MHNCI 3595	MK331137	MK331150	This study
Oxymycterus sp. nov.	MHNCI 3593	MK331136	MK331149	This study
Oxymycterus sp. nov.	MHNCI 1704	MK331135	MK331148	This study
Oxymycterus sp. nov.	MHNCI 5140	MK331133		This study
Oxymycterus sp. nov.	MHNCI 5141	MK331134		This study
Oxymycterus amazonicus	MZUSP 21317	AF454765		Hoffmann et al. 2002
Oxymycterus amazonicus	USNM 549815		MF110476	Steppan and Schenk 2017
Oxymycterus delator	UMMZ 137077	AF454766		Hoffmann et al. 2002
Oxymycterus delator	MVZ 197931		MF110478	Steppan and Schenk 2017
Oxymycterus dasytrichus	MVZ183126	AF454769		Hoffmann et al. 2002
Oxymycterus dasytrichus	MVZ183127		MF110477	Steppan and Schenk 2017
Oxymycterus hiska	MVZ 171518	U03542	MF110479	Smith and Patton 1993, Steppan and Schenk 2017
Oxymycterus josei	MVZ 193036	MK331138		This study
Oxymycterus josei	MVZ193035		MF110481	Steppan and Schenk 2017
Oxymycterus nasutus	MVZ 182701	KY754092	MF110482	Steppan and Schenk 2017
Oxymycterus paramensis	CML 7251	DQ518259		Jayat et al. 2008
Oxymycterus paramensis	OMNHN 34968		MF110483	Steppan and Schenk 2017
Oxymycterus paramensis	MSB 67277 (NK22836)	AY041197		Rinehart et al. 2005
Oxymycterus paramensis	UMMZ 160535	U03536		Smith and Patton 1993
Oxymycterus wayku	CML 7247	DQ518262		Jayat et al. 2008
Oxymycterus quaestor	MVZ 183128	AF454773		Hoffmann et al. 2002
Oxymycterus quaestor	CZFURB5005		MK331151	This study
Oxymycterus rufus	TTU 66589 (TK49119)	AF454776		Hoffmann et al. 2002
Oxymycterus rufus	OMNHN 30079		MF110484	Steppan and Schenk 2017
Outgroup				
Juscelinomys huanchace	USNM 584508	KY754009	MF110397	Steppan and Schenk 2017
Akodon boliviensis	MVZ 171607	M35691		Smith and Patton 1999
Akodon boliviensis	FMNH 162747		MF110304	Steppan and Schenk 2017
Brucepattersonius igniventris	MVZ 183250	KY753956	MF110334	Steppan and Schenk 2017
Thaptomys nigrita	MVZ 183040	KY754165	MF110558	Steppan and Schenk 2017
Necromys amoenus	MVZ 171563	AY273911		D'Elia 2003
Necromys amoenus	MVZ 172877		MF110436	Steppan and Schenk 2017
Scapteromys tumidus	MVZ 183269	AY275133		D'Elia 2003
Scapteromys tumidus	MVZ 183267		MF110538	Steppan and Schenk 2017
Kunsia tomentosus	USNM 584516 (LHE 1620)	AY275121	MF110398	D'Elia 2003, Steppan and Schenk 2017

Twenty craniodental measurements (greatest skull length [GSL], nasal length [NAL], rostral tube length [RTL], diastemal length [DIL], molar tooth-row length [MRL], incisive foramen length [IFL]; palatal length [PAL], palatal bridge length [PBL], rostral greatest breadth [ROB], antero-orbital greatest breadth [AGB], zygomatic arch greatest breadth [ZAB], zygomatic plate breadth [ZPB], braincase breadth [BCB], greatest length of interparietal [IPL], greatest breadth of interparietal [IPB], least interorbital breadth [LIB], auditory bulla breadth [ABB], rostral depth [ROD], braincase depth [BCD], greatest length of mandible [GLM]) were taken with a digital caliper accurate to the nearest 0.01 mm. Measurements were taken as illustrated by Gonçalves and Oliveira (2004).

Analysis of variation in skull shape.—Variability in skull shape was explored on 73 specimens from eight species of *Oxymycterus* (*O. nasutus*, *O. quaestor*, *O. delator* [including holotype], *O. amazonicus* [holotype], *O. dasytrichus*, *O. rufus*, *O. josei* [including holotype], and the new species; see Supplementary Data SD1). For geometric morphometric analyses, we photographed each skull in the ventral view, after applying a standard protocol to obtain the images (Maestri et al. 2017). To confirm the correct species identification, the identity of each specimen was cross-checked with molecular data, diagnostic characters of the skulls, and geographic distribution. Only adult specimens (third molar erupted) were used in the analyses. Thirty bilateral landmark coordinates were placed on the ventral side of the specimens (following Maestri et al. 2015; Fabre et al. 2018), using TpsDig2 (Rohlf 2015). The matrix of landmark coordinates was submitted to a generalized Procrustes analyses (Rohlf and Slice 1990) to obtain a measure of size (centroid size) and Procrustes-corrected shapes considering object symmetry (Viscozi and Cardini 2011). To visualize

Table 2.—External and cranial measurements (in millimeters) and weight (in grams) of *Oxymycterus* sp. nov. holotype (MHNCI 3595) and paratype (MHNCI 3593); ND = not determined. Refer to Materials and Methods for descriptions of acronyms.

	MHNCI 3595	MHNCI 3593
HBL	136	147
LT	80	90
Ear	19	17
HF	26	28
GSL	33.84	34.14
NAL	13.82	13.63
RTL	2.19	1.59
DIL	7.45	8.17
MRL	4.85	4.81
IFL	7.58	7.84
PAL	14.11	14.54
PBL	3.45	3.81
ROB	5.30	5.37
AGB	8.85	9.03
ZAB	14.84	ND
ZPB	2.29	2.54
BCB	13.78	13.81
IPL	2.80	3.03
IPB	8.04	7.54
LIB	5.66	5.86
ABB	4.07	4.12
ROD	6.29	6.25
BCD	10.31	10.84
GLM	17.25	17.54
Weight	58	60

major patterns of shape variation, we conducted a principal component analysis (PCA) on the Procrustes-corrected shape and compared the extreme morphologies along each PC (for the first two PCs). An analysis of variance (ANOVA) and a Tukey test were employed to test for differences in centroid size among species. We evaluated shape differences among species through a multivariate analysis of covariance (MANCOVA) using (log) the centroid size as a covariable and 10,000 iterations for significance testing. The entire shape matrix was used as a response variable in the MANCOVA, following the Procrustes distances procedure for high dimensional data (Adams et al. 2018). We also conducted MANCOVAs pairwise to investigate shape differences between the new taxon and conspecifics separately. Analyses were conducted in the software R (R Core Team 2018) using the package geomorph (Adams et al. 2018).

Results

Oxymycterus sp. nov. presents clear morphological distinctiveness in relation to other *Oxymycterys* forms. The tympanic bulla is comparatively larger and highly inflated, the parapterygoid fossa is conspicuously wider, and the petrotympanic fissure is comparatively shorter in the new species. *Oxymycterus* sp. nov. also has a comparatively less-inflated braincase and proportionally longer parietals in relation to other brownish forms (*O. dasythrichus, O. nasutus, O. josei*, and *O. caparaoe*). Detailed comparisons are provided in "Morphological comparisons."

The topology derived from both the first and second data sets (only *Cytb* and concatenated genes [*Cytb* + *Acp5*-I2]) retrieved *Oxymycterus* sp. nov. as reciprocally monophyletic to the clade formed by *O. delator* + *O. amazonicus* (Fig. 2). The main difference between the trees was the lower node support in the second dataset (Fig. 2B).

The Bayesian time-tree recovered three major groups within *Oxymycterus*: 1) (*O. nasutus* (*O. dasytrichus* (*Oxymycterus* sp. nov. (*O. amazonicus* (*O. delator*))))); 2) (*O. quaestor* (*O. rufus* (*O. josei*))); and 3) (*O. wayku* (*O. hiska* (*O. paramensis*))) (Fig. 3). The divergence of these groups was estimated to have occurred in the early Pleistocene (ca. 1.80 MYA) while the diversification within clades dates from 1.5 to 0.25 MYA. The divergence time between *Oxymycterus* sp. nov. and *O. delator* + *O. amazonicus* was estimated at 1.14 MYA (95% Highest Posterior Density [HDP]: 0.72–1.62). However, the most common ancestor for *Oxymycterus* sp. nov. appeared 0.23 MYA (95% HPD: 0.12–0.39), whereas the split into *O. delator* + *O. amazonicus* dated back to 0.66 MYA (HPD: 0.37–1.02).

Overall, the mean interspecific genetic distance calculated from *Cytb* for *Oxymycterus* was 6%. The genetic divergences observed between *Oxymycterus* sp. nov. and *O. delator* and *O. amazonicus* were 4.1% and 3.7%, respectively (Table 3). The distance between the new taxon and other *Oxymycterus* ranged from 5.5% (*O. dasytrichus*) to 8.4% (*O. rufus*). The intraspecific distance of *Oxymycterus* sp. nov. was 1% and overall intraspecific distances ranged from 0.2% (*O. josei*) to 1.8% (*O. nasutus*). In contrast, overall genetic distances based on *Acp5*-I2 were 0.8%. For this locus, relevant distances were only found between *Oxymycterus* sp. nov. and *O. hiska* (0.9%), *O. dasytrichus* (1.2%), *O. quaestor* (1.2%), and *O. paramensis* (from northwestern Argentina, 1.4%; Table 4).

Taxonomy

Oxymycterus itapeby, New Species

Holotype.—MHNCI 3595, adult male, collected on 30 May 1996 by D. M. Barros-Battesti. The specimen consists of a dried skin, poorly prepared (Fig. 4), and a cleaned skull (Fig. 5). Molars are fully erupted and show advanced wear (Fig. 6). Frozen tissue samples are deposited in the Department of Genetics of the Universidade Federal do Rio Grande do Sul (DG-UFGRS).

Type locality.—Brazil, São Paulo, Itapevi, Transurb district, "Condomínio Vila Verde" (Fig. 1). The approximate geographical coordinates are 23°35′41.474″S; 46°58′30.59″W. Itapevi is located in the Atlantic Forest biome and the vegetation in the municipality is characterized by the predominance of a dense ombrophilous forest and the occurrence of patches of mixed ombrophilous forests (Araucaria Forest). The vegetation in Transurb district is composed mainly of dense ombrophilous forest fragments and the elevation ranges from 915 to 985 m above sea level.

Paratypes.—A paratype of *O. itapeby* (MHNCI 3593, adult male) was collected on 26 September 1995 by D. M. Barros-Battesti at the type locality. The specimen consists of a dried skin (Fig. 4) and a cleaned skull with the right zygomatic arch damaged and the left jugal missing (Fig. 5). Molars are fully erupted and show advanced wear (Fig. 6). Frozen tissue samples are deposited in the Department of Genetics of the Universidade Federal do Rio Grande do Sul (DG-UFGRS).

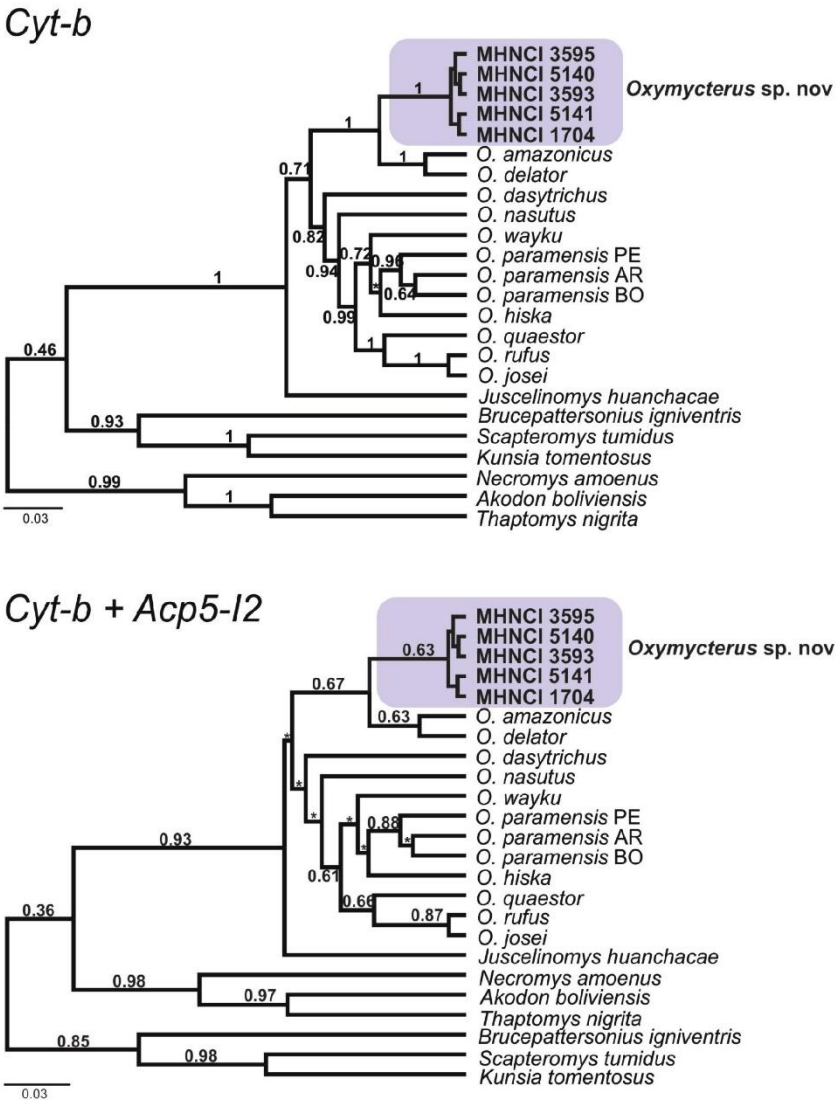

Fig. 2.—Bayesian phylogenies comparison of the ordinal topologies depicting the monophyletic status and relationships of *Oxymycterus* sp. nov. reconstructed using single complete *Cytb* sequences (1,140 bp) and concatenated genes *Cytb* and *Acp5*-I2 (1,580 bp). The analysis included 10 conspecifics of the genus *Oxymycterus* available from Genbank. The values above the nodes correspond to the posterior probabilities (PP) > 0.60. Scale bar indicates substitutions per site. AR, Argentina; BO, Bolivia; PE, Peru.

Reference material.—Three specimens not analyzed herein were collected in the Jaguariaíva Municipality, Paraná state, southern Brazil. One of these from Fazenda Chapada do Santo Antônio (Chapada do Santo Antônio farm, 24°15′43.384″S; 49°56′55.176″W) was collected on 30 July 1991 by I. J. Sbalqueiro (MHNCI 1704) and the other two were collected in Fazenda Banestado Cajurú (Banestado Cajurú farm, 24°11′56.3″S 49°36′24.7″W) on 17 December 2004 by F. G. Braga (MHNCI 5140 and 5141). Unfortunately, only tissue samples from the three specimens from Jaguariaíva were available.

Etymology.—The species name (from tupy itá-peb'y "flat stone of waters") is the nomination given by the tupy indigenous to the locality currently known as Itapevi county.

Nomenclature statement.—A life science identifier (LSID) number was obtained for the new species (*Oxymycterus itapeby*): urn:lsid:zoobank.org:pub:CC2232C4-F20D-44A7-B0C3-B24168437E50.

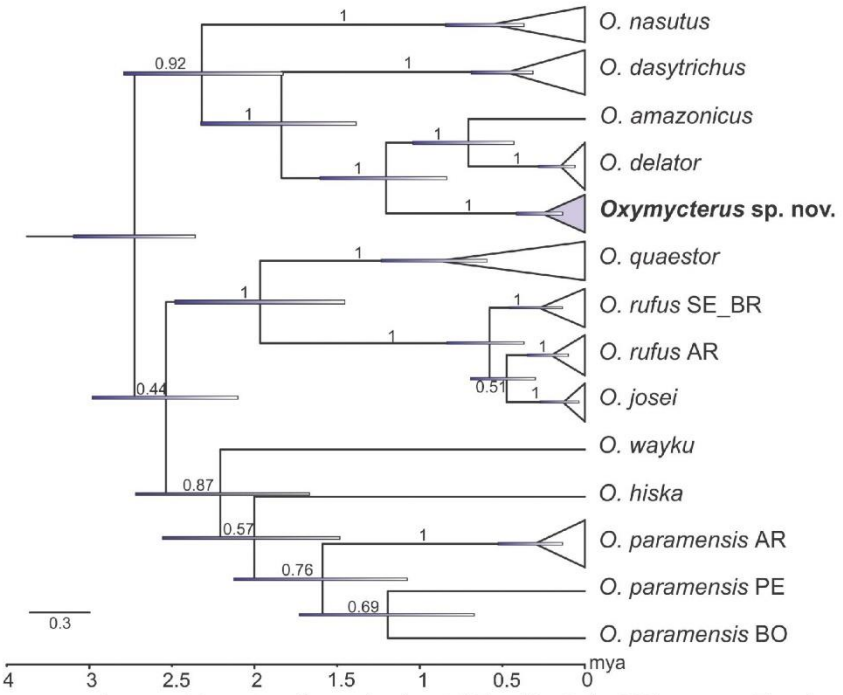

Fig. 3.—Bayesian consensus time-tree of *Oxymycterus* lineages based on 1,140 bp of the *Cytb* mtDNA sequences. The values above the nodes indicate the posterior probabilities. The 95% credible intervals for the node ages are shown with transparent bars to denote the time of the most recent ancestor (TMRCA) for the relevant nodes and represent species and nominal forms. AR, Argentina; BO, Bolivia; PE, Peru; SE BR, southeastern Brazil.

Table 3.—Pairwise genetic *p*-distances within and among species of *Oxymycterus* based on sequences of the mitochondrial cytochrome *b* gene. AR, Argentina; BO, Bolivia; PE, Peru; and SE BR, southeastern Brazil were used to indicate distinct regions of some samples.

Species	1	2	3	4	5	6	7	8	9	10	11	12	13
1 *O.* sp. nov.	[0.010]												
2 *O. amazonicus*	0.0374												
3 *O. delator*	0.0412	0.0271	[0.002]										
4 *O. dasytrichus*	0.0556	0.0541	0.0501	[0.007]									
5 *O. nasutus*	0.0610	0.0639	0.0619	0.0619	[0.018]								
6 *O. quaestor*	0.0744	0.0740	0.0717	0.0710	0.0654	[0.017]							
7 *O. josei*	0.0814	0.0824	0.0832	0.0790	0.0698	0.0642	[0.002]						
8 *O. rufus*	0.0843	0.0856	0.0856	0.0817	0.0722	0.0673	0.0165	[0.015]					
9 *O. rufus* SE BR	0.0847	0.0850	0.0860	0.0848	0.0723	0.0694	0.0206	0.0147	[0.006]				
10 *O. hiska*	0.0774	0.0813	0.0764	0.0760	0.0667	0.0736	0.0743	0.0730	0.0740				
11 *O. wayku*	0.0654	0.0699	0.0661	0.0614	0.0653	0.0805	0.0743	0.0743	0.0801	0.0699			
12 *O. paramensis* AR	0.0728	0.0802	0.0764	0.0841	0.0777	0.0815	0.0770	0.0811	0.0844	0.0667	0.0705	[0.008]	
13 *O. paramensis* BO	0.0712	0.0650	0.0607	0.0698	0.0639	0.0724	0.0824	0.0833	0.0850	0.0650	0.0667	0.0612	
14 *O. paramensis* PE	0.0563	0.0585	0.0493	0.0564	0.0588	0.0652	0.0726	0.0743	0.0801	0.0699	0.0585	0.0640	0.0472

Distribution.—Records of *O. itapeby* are restricted to two localities about ca. 285 km away from each other in the middle elevations (740 to 1,050 m asl) of the Atlantic (Itapevi) and Meridional plateaus (Jaguariaíva; Fig. 1). These localities are part of the Atlantic Forest (Itapevi) and ecotonal area between the Atlantic Forest and the southernmost Cerrado (Jaguariaíva).

Vernacular names.—We propose the following vernacular names for *O. itapeby*: Itapevi Hocicudo Rat (English), Rato-do-brejo-de-Itapevi (Portuguese), Hocicudo de Itapevi (Spanish).

Diagnosis.—According to our molecular and morphological analysis, *Oxymycterus itapeby* belongs to the Akodontini tribe, subfamily Sigmodontinae, family Cricetidae (D'Elía et al.

Table 4.—Pairwise genetic *p*-distances within and among the species of *Oxymycterus* based on sequences of the Intron 2 and parts of the exons 2 and 3 of acid phosphatase type V (*Acp5-I2*) nuclear gene. AR, Argentina.

Species	1	2	3	4	5	6	7	8	9
1 *O.* sp. nov.									
2 *O. amazonicus*	0								
3 *O. delator*	0.007	0.007							
4 *O. dasytrichus*	0.012	0.012	0.014						
5 *O. nasutus*	0.002	0.002	0.009	0.009					
6 *O. josei*	0.005	0.005	0.007	0.007	0.002				
7 *O. rufus*	0.005	0.005	0.007	0.007	0.002	0			
8 *O. hiska*	0.009	0.009	0.012	0.007	0.007	0.005	0.005		
9 *O. paramensis* AR	0.014	0.014	0.016	0.016	0.012	0.009	0.009	0.014	
10 *O. quaestor*	0.012	0.012	0.015	0	0.009	0.007	0.007	0.007	0.015

2007; Pardiñas et al. 2015). Considering the *Cytb* marker, the new species is ~4% divergent from the sister clade formed by *O. amazonicus* + *O. delator* (PP = 1).

Oxymycterus itapeby can be distinguished from other *Oxymycterus* species by the combination of the following morphological characteristics: 1) large-sized *Oxymycterus* (HB = 136–147 mm; LT = 80–90 mm; body mass = 58–60 g); 2) moderately developed rostral tube (Fig. 5); 3) auditory bullae large and inflated; 4) short petrotympanic fissure; 5) parapterygoid fossa wide; 6) narrow rostrum; 7) capsular projection of upper incisor inflated to a small degree; 8) gnathic process very reduced and rounded; 9) large incisive foramen, reaching M1 protocone or hypoflexus; 10) the posteriormost point of the frontoparietal suture trespassing the plane of the posterior border of the squamosal root of the zygomatic, from the dorsal view; 11) thin hamular process of squamosal.

Description.—Oxymycterus itapeby is a large-sized *Oxymycterus* (HB = 136–147 mm; LT = 80–90 mm; body mass = 58–60 g) with tail shorter than head-body length (58.8–61.3% of HB). The pinnae are small, reaching 11.6–13.9% of head-body length (Fig. 4). The pes (hindfoot with claws) are short, reaching 19.1% of head-body length. The overall dorsal coloration is tawny-brown, lighter in the laterals of head and upper flanks. The overall ventral coloration is tawny-gray, tawnier in chest and pubic region and grayer in the other ventral parts. The tail is paler below, dark-brown in dorsum and flanks, and lighter in venter. Four groups of vibrissae are distinguishable: mystacial, superciliary, genal, and submental; most of the vibrissae are entirely eumelanic, except some mystacial (dichromic, eumelanic on most of its length with a pheomelanic distal segment) and all submentals (entirely pheomelanic); measurements of largest vibrissae from the paratype: mystacial—21.72 mm; supraciliary—15.98 mm; genal—16.63; submental—8.58 mm. The longest mystacial does not reach the bases of the pinnae when laid back alongside head. The dorsal pelage is composed of guard-hair (Fig. 4), overhair, and underhair; guard-hair reaching about 17 mm into the middle dorsum and entirely eumelanic; overhair reaching about 11 mm into the middle dorsum and tribanded, eumelanic on most of their length, followed by a pheomelanic distal band and an eumelanic tip; underhair reaching about 8 mm into the middle dorsum and entirely eumelanic. Ventral pelage is composed of overhair and underhair; overhair reach about 7 mm and are dichromic, proximally eumelanic and distally pheomelanic, with the pheomelanic band more extensive in lighter parts of the venter; underhair reach about 7 mm and are dichromic, eumelanic on most of their length with a distal pheomelanic segment. The manus (forefeet) are tawny in the dorsum and conpiscuously lighter in the plantar surface. The dorsal manus is densely covered by thick pheomelanic hair; ungueal tufts are absent. Digit III of the manus is slightly longer than digits II and IV, which are subequal in size; digit V is conspicuously shorter than digits II and IV and slightly longer than digit I; the claws of the manus are large, reaching about 1.35× the length of digits; the hypothenar is slightly longer than the thenar pad; the thenar pad is conspicuously wider than the hypothenar pad; three distinguishable interdigitals pads subequal in size are present (Fig. 7). The pes (hindfeet) are dark brown both in dorsal and plantar surfaces. The dorsal pes is densely covered by thick eumelanic hair; ungueal tufts cover about half of the length of digits II-IV and a short proximal segment of digits I and V. Digit III of pes is slightly longer than digits II and IV, which are subequal in size; digit V is conspicuously shorter than digits II and IV and slightly longer than digit I; the claws of pes are large, reaching about 0.8× the length of digits; the hypothenar pad is well-developed, reaching 3× the length of the thenar pad; interdigital pad 3 is largest, followed in size by 2, 4, and 1 (Fig. 7). The tail is covered by thick hair arranged in triplets on each scale, with the central hair conspicuously thicker and longer, reaching three to three and a half scale bars in size, and lateral hairs reaching one to two and a half scale bars in size; central hairs of dorsal scales are entirely eumelanic; lateral hairs of dorsal scales vary from entirely eumelanic to dichromic (proximally eumelanic and distally pheomelanic) and are entirely pheomelanic; central hair of ventral scales is dichromic (proximally eumelanic and distally pheomelanic); lateral hairs of ventral scales vary from entirely pheomelanic to dichromic (proximally eumelanic and distally pheomelanic).

The skull is characterized by an elongated rostrum and a moderately developed rostral tube (Fig. 5), formed by nasal and premaxillar projection beyond the plane of the incisors; os rostri absent; rostral tube reaching about 16% of nasal length and 7% of condylo-incisive length. The gnathic process is very reduced and rounded. The nasal bones are elongated and narrow, subequal in size with the greatest length of

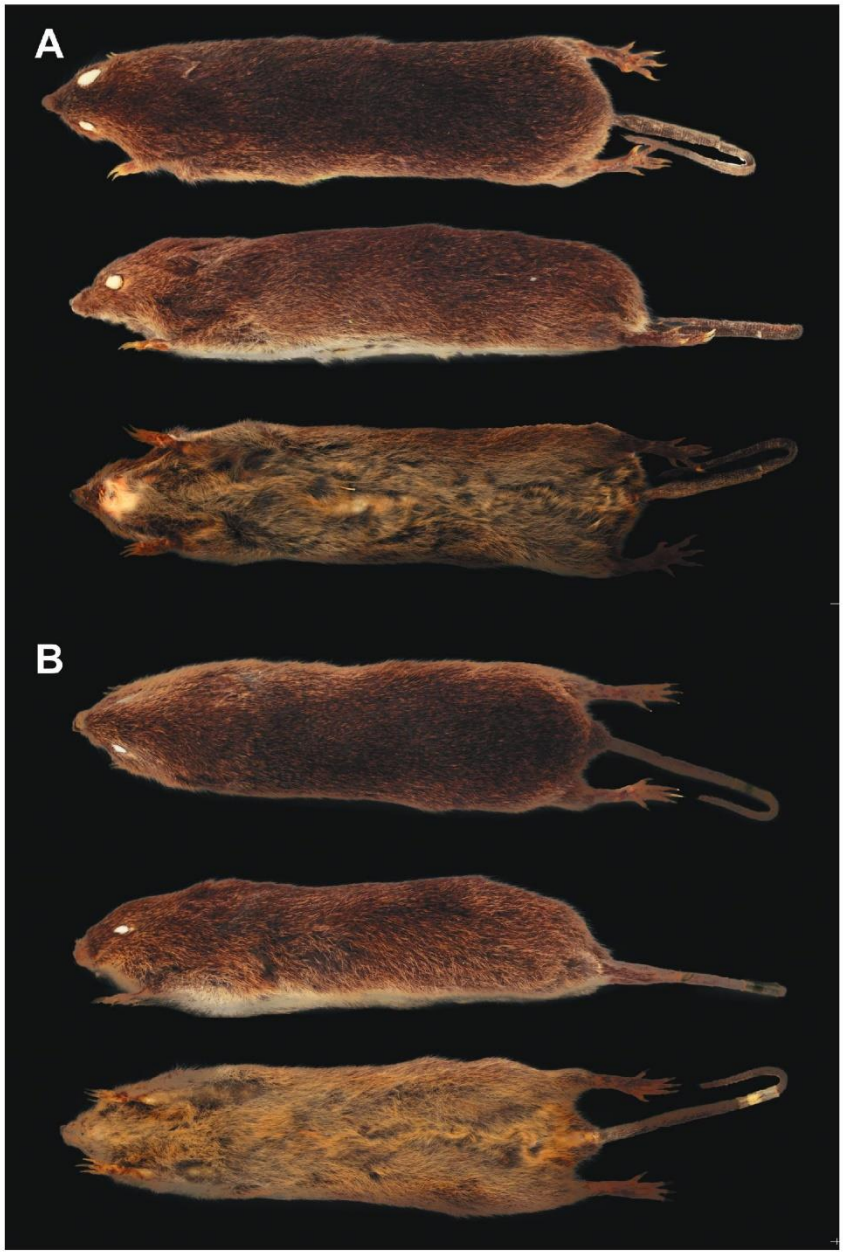

Fig. 4.—Dorsal (upper), lateral (middle), and ventral (bottom) views of the skin of *Oxymycterus itapeby* sp. nov. (A) holotype (MHNCI 3595) and (B) paratype (MHNCI 3593). Scale bar = 50 mm.

frontal bones; in frontal view, the posterior nasal extremity slightly trespasses the posterior curve of the maxillary root of the zygomatic. The nasolacrimal capsules are slightly inflated. The incisive foramen has convergent borders and its posterior extremity reaches the posterior region of the M1 protocone or hypoflexus. The nasofrontal suture is V-shaped. The lacrimal bones are large and oval, presenting a well-developed posterior projection. The nasolacrimal fissures are weakly developed

Fig. 5.—Dorsal (left), ventral (middle), and lateral (upper right) views of the skull and mandible (bottom right) of *Oxymycterus itapeby* sp. nov. (A) holotype (MHNCI 3595) and (B) paratype (MHNCI 3593). Scale bar = 10 mm.

and located far ahead of the zygomatic plate, being completely exposed from this. The zygomatic notches are shallow. The zygomatic plates are narrow and strongly curved backward. The origin of the superficial masseter is evidenced by a small oval rugosity located in the anteriormost portion of the zygomatic plate. The supraorbital foramen is reduced and visible only from the lateral view. The optic foramen is large and rounded and it is located a little behind the plane of the supraorbital foramen. The sphenopalatine foramen is conspicuous with a diameter smaller than the supraorbital foramen. The anterior lacerated foramen is large and oval, with the largest diameter similar in size to the optic foramen. The palatine bone is short and wide. A single posterior palatal foramen is present, located in the plane of the M2 hypocone. The posterior border of the palatine bone does not show a well-developed process. The mesopterygoid fossa is elongated, longer than the molar series. The parapterygoid borders are parallel on most of their extension and slightly divergent in the posterior segment. The hamular processes of the pterygoids are slightly developed and have parallel borders. The presphenoid is elongated, with a length corresponding to half the length of the pterygoid processes. The basisphenoid is slightly longer than the presphenoid, trespassing the plane of the Eustachian canal. Sphenopalatine vacuities are subequal in size and located one above and the other below the presphenoid–basisphenoid suture. The parapterygoid fossa is deep and narrower than the mesopterygoid fossa in the posterior region. A conspicuous foramen ovale is present in the posterior region of the parapterygoid fossa. A foramen ovale accessorius, with a diameter greater than the foramen ovale, is entirely or partially covered by the posterior region of the lateral edge of the parapterygoid fossa, from a ventral view. The anterior opening of the alisphenoid canal is separated from the foramen ovale accessorius by a robust alisphenoid strut. An accessory foramen is associated with the anterior opening of the alisphenoid canal, separated from this by a thin alisphenoid strut; this accessory foramen is smaller or subequal to the anterior opening of the alisphenoid canal in size and located in front or above of it (Fig. 8). The petrotympanic fissure is short, extending from the lateral extremity of the auditory bulla to its anterior region, but not reaching the Eustachian tube. The stapedial spine is well-developed, larger than half the width of the petrotympanic fissure. The auditory bulla is large, slightly greater than the molar series. The carotid canal and the stapedial foramen are conspicuous,

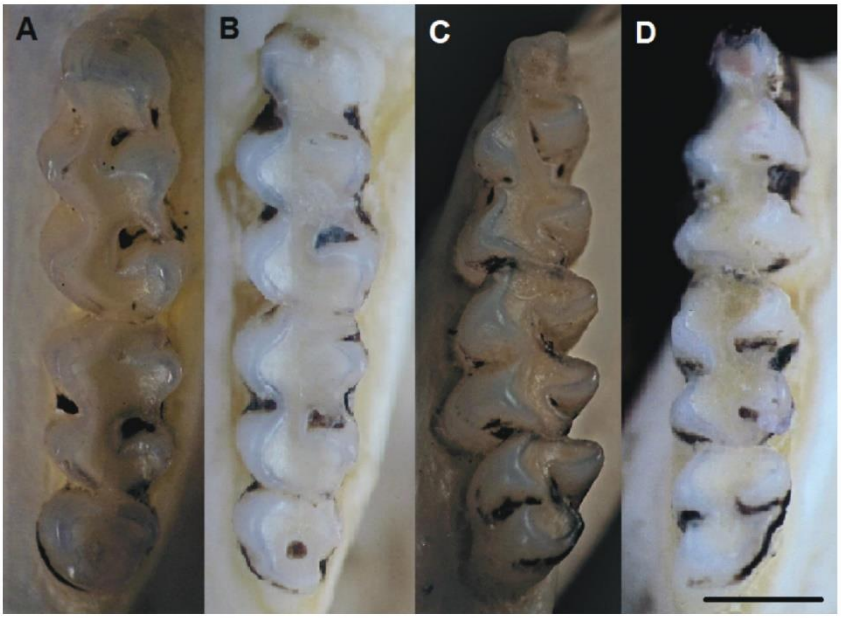

Fig. 6.—Occlusal views of the upper left (A, B) and lower left (C, D) molar series of the *Oxymycterus itapeby* sp. nov. holotype (MHNCI 3595; A, C) and paratype (MHNCI 3593; B, D). Scale bar = 1 mm.

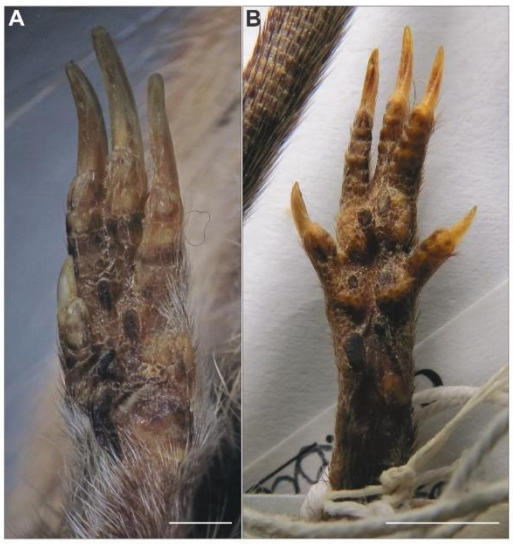

Fig. 7.—Photograph of the right forefeet (A) and left hind feet (B) of *Oxymycterus itapeby* sp. nov., taken from the MHNCI 3595 holotype. Scale bars = 0.2 and 0.5 mm, respectively.

the former being larger. The jugular and stylomastoid foramina are well-developed and similar in size. The external auditory meatus is small-sized and rounded. The malleus is very delicate, with a long and thin manubrium strongly inclined toward the interior of the external auditory meatus. The orbicular process is wide and robust. The postglenoid foramen is slightly longer than the subsquamosal foramen, trespassing or almost reaching the plane of the posterior border of the auditory meatus (Fig. 9). The hamular process of the squamosal is thin. The basioccipital is markedly depressed and presents a prominent central ridge. The hypoglossal foramen is well-developed. The foramen magnum is large, with a width similar to the length of the auditory bulla. The antorbital bridge is short and narrow. The interorbital region is hourglass-shaped, with a rounded dorsal maxillary anterolateral protuberance. The zygomatic arch is delicate and strongly convergent in the anterior segment. The jugal is well-developed, extending over 43% of the length of the zygomatic arch. The squamosal root of the zygomatic is narrow (approximately one-half the width of the zygomatic plate) and trespass the braincase in dorsal and ventral views. The glenoid fossa is deep. The frontoparietal suture is U-shaped. The fronto-parietal-squamosal suture is in the extremity of or a little behind the parietal process. The greatest length of the parietal corresponds to approximately 67% of the greatest length of the frontal. Slightly developed temporal and lambdoidal crests are present. The interparietal is well-developed; greatest length of the interparietal is larger than the least interorbital length. The exoccipital and supraoccipital are markedly inflated; exoccipital presents a conspicuous median crest. The periotic capsule of the mastoid is inflated and moderate-sized, slightly greater than the diameter of the external auditory meatus (1.1–1.3×).

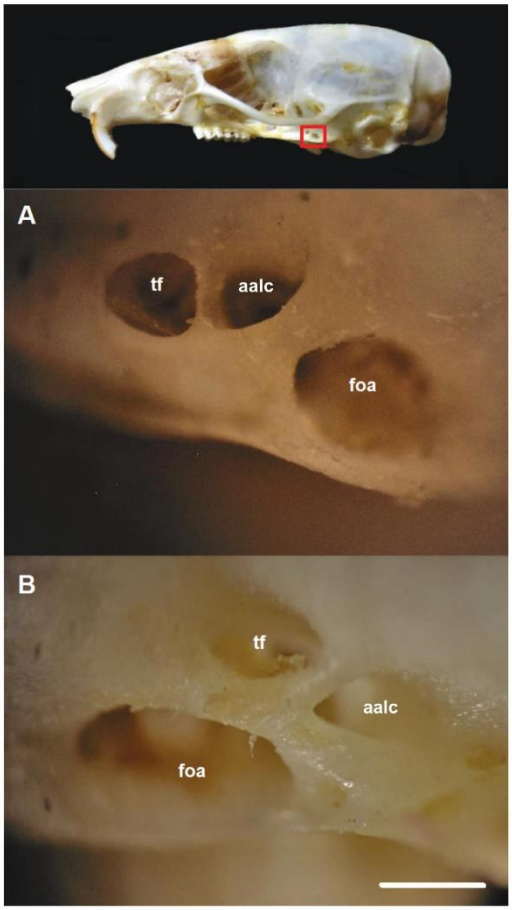

Fig. 8.—The alisphenoid region in the *Oxymycterus itapeby* sp. nov. holotype (A, MHNCI 3595; left side) and paratype (B, MHNCI 3593; right side). foa, foramen ovale accessorius; aalc, anterior opening of alisphenoid canal; tf, third foramen of alisphenoid. Scale bar = 0.5 mm.

The mandible is very elongated and slim (Fig. 5), with height about 40% of the length without the incisors. The ramus is narrow and elongated, with the anterior extremity located far above the molar root plane. The mental foramen is well-developed and visible from both occlusal and lateral views. The masseteric ridges are scarcely developed. A marked ridge extends from the region anterior to the coronoid process to the posterior extremity of the condyloid process; capsular process absent. The coronoid process is thin and elongated, and it is separated from the condyloid process by a shallow and strongly concave sigmoid notch. The condyloid process is robust, and it is separated from the narrower angular process by a shallow and slightly concave mandibular notch. The retromolar region is shallow, with a well-developed internal ridge extending from the M3 entoconid to the plane of the anterior

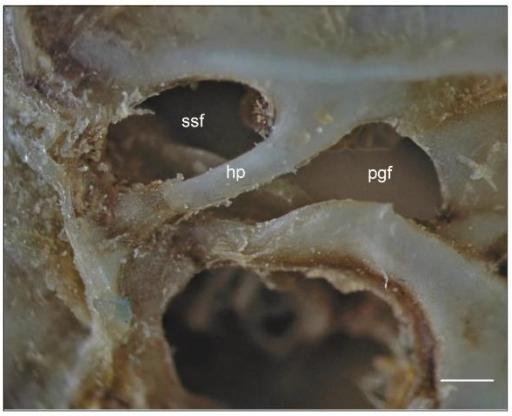

Fig. 9.—The lateral view of the temporal region in the *Oxymycterus itapeby* sp. nov. paratype (MHNCI 3593). hp, hamular process of the squamosal; pgf, postglenoid foramen; ssf, subsquamosal foramen. Scale bar = 0.5 mm.

region of the coronoid process. The mandibular foramen is large and oval.

The upper incisors are opisthodont and orange on their frontal surface; posterior and lateral surfaces are much paler. Lower incisors are moderately sized (32% of mandibular bone length) and pale; dentine fissure is slightly marked. The upper molar series is slightly divergent; molars crested; lingual cusps are higher than labial cusps; main cusps are almost opposite. The left M1 of the paratype presents a vestigial anteromedian flexus and the anterolingual conule is more developed than the anterolabial conule; the paraflexus is deep and backward curved; the protoflexus is deep and straight; the anterior mure is conspicuous and slightly diagonal; the paracone is conspicuously wider than the protocone; the mesoflexus is vestigial; a well-developed paralophule is present; the holotype presents a second paralophule in the right M1; the hypoflexus is deep and straight; the metaflexus is deep and backward curved; the metacone and hypocone are similar in size; the mediam mure is conspicuous and straight (Fig. 6). The M2 presents a well-developed anteroloph; the paraflexus is shallow and straight; the protocone is larger than the paracone; the mesoflexus is absent; a well-developed paralophule is present; the hypoflexus is shallow and straight; the metaflexus is deep and backward curved; the median mure is conspicuous and slightly diagonal; the hypocone is larger than the paracone; a vestigial posteroflexus is fused to the metacone (Fig. 6). The M3 is cylindrical; the protocone is larger than the paracone. The lower molar series are parallel; molars crested; the main cusps are alternate (Fig. 6). The m1 procingulum presents a shallow anteromedian flexid; the proconid is larger than the metaconid; the anterior murid is wide and slightly diagonal; the metaflexid is deep and strongly upward curved; an undeveloped mesolophid is present; the hypoflexid is shallow and straight; an undeveloped ectolophid is present; the median murid is short and wide; the hypoconid is larger and narrower than the entoconid; the

posteroflexid is deep and strongly upward curved; the posterolophid is well-developed and straight (Fig. 6). The main cusps of m2 are proportionally larger than the main cusps of m1; the protoconid is conspicuously larger and narrower than the metaconid; the anterior murid is narrow and diagonal; the entoflexid is deep and strongly upward curved; the hypoflexid is shallow and straight; the hypoconid is conspicuously larger and narrower than the entoconid; the posteroflexid is shallow and strongly upward curved; the posterolophid is well-developed and curved in its distal extremity (Fig. 6). Four cuspids are visible in m3 (protoconid, metaconid, hypoconid, and entoconid); the protoconid is larger and narrower than the metaconid; the entoflexid is deep and upward curved; the hypoflexid is deep and straight; the median murid is narrow strongly diagonal; the hypoconid and the entoconid are similar in size (Fig. 6).

Morphological comparisons.—*Oxymycterus itapeby* differs from *O. amazonicus* by: 1) a longer and narrower rostrum; 2) a narrower interorbital region; 3) a less-inflated braincase; 4) a longer interparietal; 5) a narrower incisive foramen; 6) a large incisive foramen, with the posterior border reaching the posterior region of the M1 protocone or hypoflexus (in *O. amazonicus* the posterior border of the incisive foramen reaches the protoflexus or anterior region of the M1 protocone); 7) the mesopterygoid fossa is longer and narrower; and 8) a longer and more-inflated auditory bulla (Fig. 10). *Oxymycterus itapeby* differs from *O. caparaoe* by: 1) a proportionally shorter rostral tube; 2) a proportionally shorter rostrum; 3) the distal extremity of nasals lacking lateral projections (lateral projections are present in nasal of *O. caparaoe*, giving the rostrum a wider appearance from the dorsal view); 4) a proportionally wider zygomatic arch, trespassing the plane of the braincase from the dorsal view (the zygomatic arch of *O. caparaoe* is narrower and more convergent, not trespassing the plane of the braincase from the dorsal view); 5) the curved borders of the anterior border of the parietals, giving the frontoparietal suture an aspect of an open "U" (the anterior borders of the *O. caparaoe* parietals are straight, giving the frontoparietal suture a "V" aspect); 6) a thinner hamular process of the squamosal; and 7) a postglenoid foramen extending over the posterior ectotympanic region (the thicker hamular process of the squamosal in *O. caparaoe* limits the postglenoid foramen to the anterior and middle ectotympanic regions). *Oxymycterus itapeby* differs from *O. dasytrichus* by: 1) a round gnathic process (in *O. dasytrichus* the gnathic process is pointed); 2) a larger incisive foramen, with the posterior border reaching the posterior region of the M1 protocone or hypoflexus (in *O. dasytrichus* the posterior border of the incisive foramen reaches the procingulum, protoflexus or anterior region of the M1 protocone); 3) the presence of

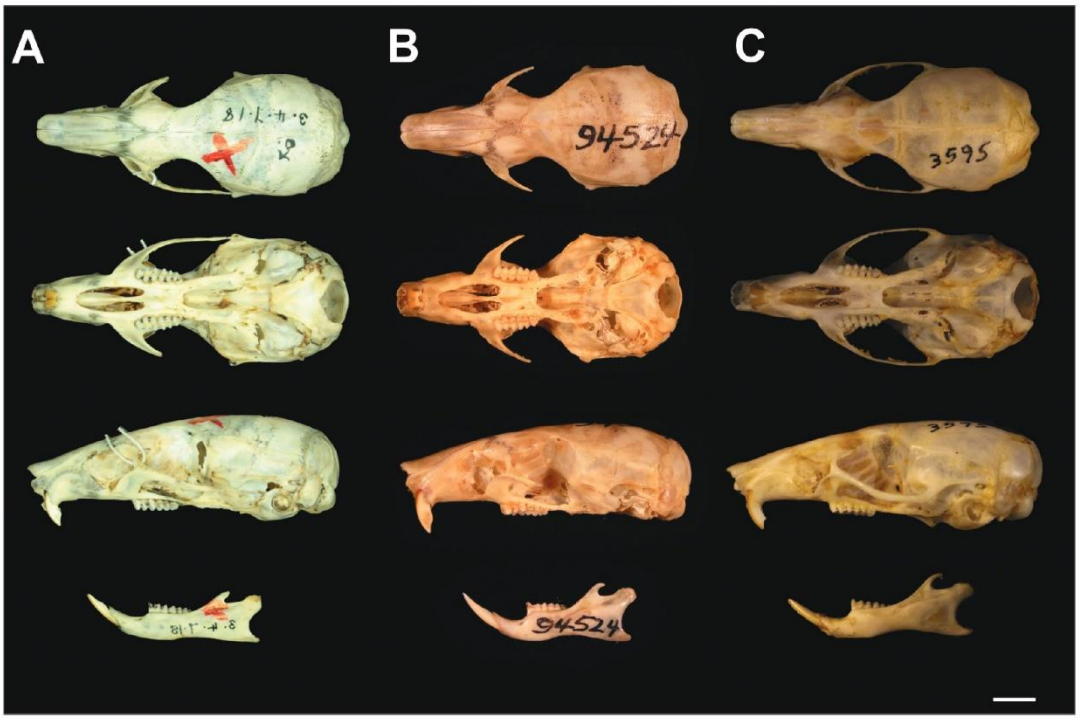

Fig. 10.—The dorsal (upper), ventral (middle), and lateral (bottom) views of the skull and mandible (bottom) of (A) *Oxymycterus delator* (British Museum Natural History 3.4.7.18; holotype), (B) *O. amazonicus* (FMNH 94524; holotype), and (C) *O. itapeby* sp. nov. (MHNCI 3595; holotype). Scale bar = 5 mm.

a foramen ovale in the posterior border of the parapterygoid plate (in *O. dasytrichus* the posterior opening of the alisphenoid canal is not enclosed by the alisphenoid bone, which is not characterized by a foramen ovale); 4) the thin hamular process of the squamosal (in *O. dasytrichus* the hamular process of the squamosal is markedly robust); and 5) the subsquamosal foramen which is comparatively larger (in *O. dasytrichus* the subsquamosal foramen is very reduced, constricted by the thick hamular process of the squamosal). *Oxymycterus itapeby* differs from *O. delator* by: 1) the tawny-brown dorsal pelage (the dorsal pelage of *O. delator* is dark brown); (2) a larger and wider auditory bulla; 3) a wider parapterygoid fossa; 4) a thin hamular process of the squamosal (in *O. delator* the hamular process of the squamosal is robust); and 5) the postglenoid foramen trespassing or almost reaching the plane of the posterior border of the auditory meatus (in *O. delator* the postglenoid foramen does not reach the plane of the posterior auditory meatus, being limited by the thicker hamular process of the squamosal) (Fig. 10). *Oxymycterus itapeby* differs from *O. josei* by: 1) the tawny-brown dorsal pelage (the pelage of *O. josei* is reddish or dark brown); 2) a proportionally narrower rostrum; 3) proportionally longer frontals; 4) a proportionally narrower zygomatic plate; 5) the posteriormost extremity of the frontoparietal suture trespassing the plane of the posterior border of the squamosal root of the zygomatic from the dorsal view (in *O. josei* the posteriormost extremity of the frontoparietal suture is aligned with the posterior border of the squamosal root of the zygomatic); 6) proportionally smaller orbits; 7) wider interparietals; 8) the presence of a foramen ovale in the posterior border of the parapterygoid plate (in *O. josei* the posterior opening of the alisphenoid canal is not enclosed by the alisphenoid bone and not characterizing a foramen ovale); and 9) a narrower petrotympanic fissure, not reaching the eustachian canal (in *O. josei* the petrotympanic fissure is conspicuously larger, trespassing the plane of the eustachian canal). *Oxymycterus itapeby* differs from *O. nasutus* by: 1) a shorter rostral tube; 2) more inflated tympanic bulla; 3) wider parapterygoid fossa; and 4) wider interparietals *Oxymycterus itapeby* differs from *O. quaestor* by: 1) its smaller size; 2) tawny-brown dorsal pelage (the dorsal pelage of *O. quaestor* varies from reddish-brown to dark brown); 3) a proportionally smaller rostral tube; 4) a proportionally shorter rostrum; 5) a proportionally wider zygomatic plate; 6) a proportionally shorter stapedial spine; 7) a more-inflated braincase; and 8) a proportionally higher interorbital region, from the lateral view. *Oxymycterus itapeby* differs from *O. rufus* by: 1) a proportionally shorter rostral tube; 2) a slightly inflated capsular projection of the upper incisor; 3) a less-inflated braincase; 4) proportionally wider and longer interparietals; and 5) a proportionally longer mesopterygoid fossa, with parallel borders (the mesopterygoid fossa of *O. rufus* is proportionally shorter and presents markedly divergent borders of the anterior region). *Oxymycterus itapeby* differs from *O. wayku* by: 1) a shorter and narrower rostral tube; 2) a narrower rostrum; 3) a larger incisive foramen, with the posterior border reaching the posterior region of the M1 protocone or hypoflexus (in *O. wayku* the posterior border of the incisive foramen reaches the M1 procingulum or protoflexus); 4) a proportionally shorter foramen ovale of the alisphenoid; and 5) a proportionally longer and narrower braincase.

Skull shape comparisons.—A principal components analysis (PCA) was performed on the shape matrix of *Oxymycterus itapeby* and seven other *Oxymycterus* species from Brazil, Paraguay, Uruguay, and Argentina, used in the molecular analysis and morphological comparisons. In the PCA, the first two components were responsible for 35.99% and 19.24% of all variation, respectively. *Oxymycterus* species differ slightly along the morphospace generated by PC1 and PC2 (Fig. 11). Positive scores along PC1 are related to a relatively shorter rostrum, shorter rostral tube, shorter incisive foramen, larger braincase, and larger foramen magnum, which set *O. quaestor* (negative PC1), *O. delator*, and *O. itapeby* apart (positive PC1). Positive scores along PC2 indicate a relatively larger rostral tube, a more inflated braincase, and a longer foramen magnum, which sets *O. nasutus* apart (positive PC2) from the rest. An overlap of the *O. amazonicus*, *O. josei,* and *O. dasytrichus* scores was observed in both PC1 and PC2. ANOVA results showed statistically significant differences in the skull centroid size among the "species" ($F = 22.5$; $P < 0.001$; Fig. 12). Tukey's test showed significant differences among several pairs of species, including *O. itapeby* versus the two largest species *O. dasytrichus* and *O. quaestor* ($P < 0.05$; Supplementary Data SD2). *Oxymycterus itapeby* was the smallest when compared with *O. dasytrichus* and *O. quaestor*. Based on our MANCOVA results, the species also differ in skull shape after considering allometry ($R^2 = 0.452$, $F = 8.915$, $P < 0.001$). Size predicted 11% of the skull shape ($R^2 = 0.111$, $F = 15.35$, $P < 0.001$) and the interaction between log (size) and species was small ($R^2 = 0.030$, $F = 0.697$, $P = 0.015$), suggesting that allometric trajectories are very similar among species. Pairwise MANCOVAs revealed statistically significant shape differences between *O. itapeby* and all other *Oxymycterus* species (Table 5, all $P < 0.015$).

Discussion

General comparisons.—The present study raises to 16 the number of *Oxymycterus* species recognized as valid. Our results based on molecular analysis support the unit of *O. itapeby* sequences, indicating that it diverges from the sister clade (*O. amazonicus* + *O. delator*) at ca. 4% while intraspecific distance is around 1%. This level of divergence fits the threshold of interspecific variation (see Baker and Bradley 2006), similar to distances previously found in *Oxymycterus* using *Cytb* (Hoffmann et al. 2002; Jayat et al. 2008). In contrast, the average genetic distances for *Acp5*-I2 indicated low levels of divergence. The lower levels of divergence for *Acp5*-I2 might be due to the nuclear genome presenting a lower mutation rate than the mitochondrial genome, or because of the longer period in which ancestral polymorphisms have been segregated (Moore 1995).

Despite the lack of an autapomorphic trait, *O. itapeby* is distinguishable from other *Oxymycterus* by a combination of

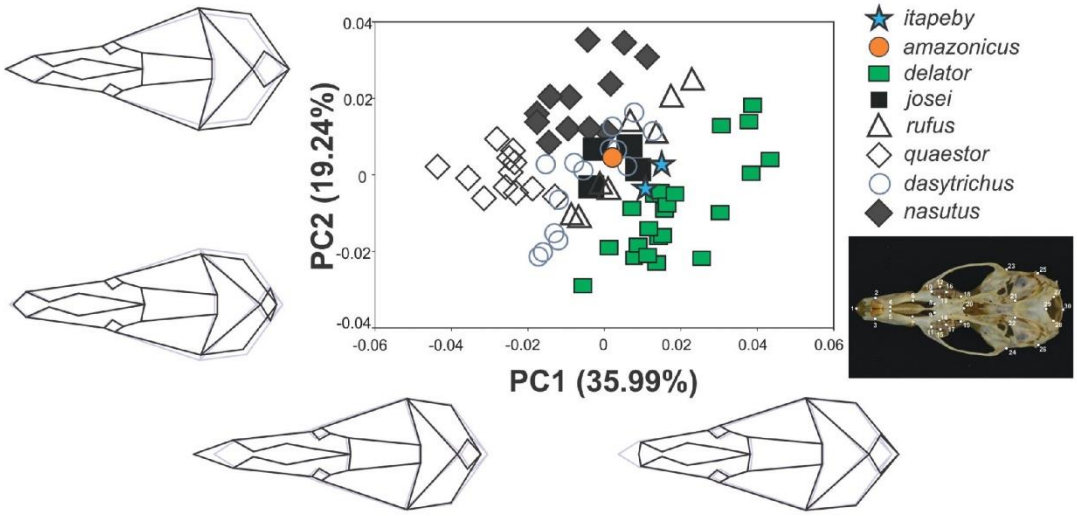

Fig. 11.—The principal components (PC) of morphological variation of the ventral view of the skulls among the *Oxymycterus* species, including the new taxon described. Shape changes in the extremes of each axis are given; gray lines indicate the average shape and black lines indicate the extreme shapes in each axis. Landmark locations on the ventral view: 1) the anteriormost point of the suture between nasals, 2–3) the lateralmost point of the alveolus of the incisor, 4–5) the anteriormost margin of the incisive foramen, 6–7) the posteriormost point of the suture between the premaxilla and maxilla, 8–9) the posteriormost margin of the incisive foramen, 10–11) the anteriormost margin of the first molar alveolus, 12–15) the lingual margin of the M1 at the level of the second lamina, 13–14) the labial margin of the M1 at the level of the second lamina, 16–17) the posterior margin of the M1, 18–19) the posteriormost margin of the third molar, 20) the posteriormost point of the suture between palatines, 21–22) the basis length of the suture between the basisphenoid and basioccipital, 23–24) the posterior end of the squamosal root of the zygomatic bar, 25–26) the superiormost margin of the tympanic bulla (ectotympanic), 27–28) the lateral margin of the foramen magnum, 29) the anteriormost point of the inferior margin of the foramen magnum, 30) the posteriormost point of the superior margin of the foramen magnum. The specimens used are listed in Supplementary Data SD1.

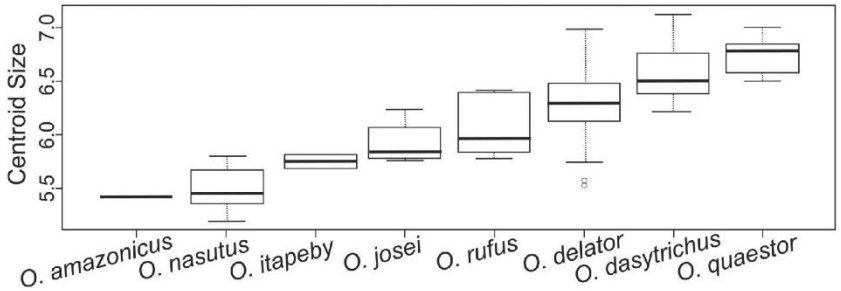

Fig. 12.—Boxplots of variability in skull centroid size among eight *Oxymycterus* species, ordered from smallest to largest. The names placed under the plots correspond to the species (see "Materials and Methods").

diagnostic characters, mainly cranial. The MANOVA also indicated that the *Oxymycterus* species differ slightly in relation to skull shape, although significant differences in the centroid size were detected. Considering the distributional ranges presented by Oliveira and Gonçalves (2015), *O. itapeby* is possibly sympatric with *O. dasytrichus*, *O delator*, *O. quaestor*, and *O. nasutus*. Externally, *O. itapeby* can be distinguished from *O. quaestor* and *O. delator* by pelage coloration. The pelage of *O. quaestor* is orange or reddish-brown and *O. delator* presents a markedly darker tonality (Oliveira and Gonçalves 2015), which clearly contrasts with the tawny-brown pelage of *O. itapeby*. In addition, *O. itapeby* is smaller than these two forms and also differs by several cranial traits. In contrast, *O. itapeby* cannot be securely distinguished from *O. dasytrichus* and *O. nasutus* based only on external attributes. All three species present paler brown pelage (darker and reddish variations are also cited for *O. dasytrichus*—Oliveira and Gonçalves 2015) and the body size measures of *O. itapeby* fall within the ranges reported for *O. dasytrichus* and *O. nasutus* (Bonvicino et al. 2008; Oliveira and Gonçalves 2015). However, *O. itapeby* clearly differs from

Table 5.—Pairwise MANCOVA comparisons of skull shape between *O. itapeby* and every other *Oxymycterus* species (see main text). The size (log of centroid size) was used as a covariable in all models. The number of iterations for significance testing was 10,000. The analysis was not conducted against *O. amazonicus* because for this species only one specimen was available.

Species	R^2	F	P
O. dasytrichus	0.128	2.455	0.014
O. delator	0.105	3.039	0.005
O. josei	0.479	4.320	0.008
O. nasutus	0.242	4.161	0.001
O. quaestor	0.191	4.288	0.001
O. rufus	0.345	3.630	0.001

the two sympatric brownish forms by cranial morphology and centroid size; it was significantly smaller when compared with *O. dasytrichus* and *O. quaestor*.

The most conspicuous differences in relation to *O. dasytrichus* are the presence of the foramen ovale in the posterior parapterygoid plate and the thinner hamular process of the squamosal. When compared to *O. nasutus*, the shorter rostral tube and the presence of a third foramen in the parapterygoid region, in addition to a buccinator-masticatory foramen and foramen ovale accessorius, are notable in *O. itapeby*. However, because these observations are based on only a few specimens comprising the *O. itapeby* type series, analysis of cranial characters along with *Cytb* sequences is recommended to distinguish the *Oxymycterus* species. Generally, the pelage color and body size of rodents are influenced by ecological factors, hampering recognition of the species (Smith et al. 2001; Gonçalves and Oliveira 2004). Hoffmann et al. (2002) also demonstrated the impossibility of distinguishing between the "brown forms" *O. nasutus* and *O. josei* based only on external characters.

Phylogenetic relationships.—Our phylogenetic results are derived from three approaches: single (*Cytb*), concatenated matrix (*Cytb* + *Acp5*-I2), and time-tree dated (all *Cytb* sequences available). All placed *O. itapeby* as a single phylogenetic unit closely related to the clade formed by *O. delator* + *O. amazonicus*. Overall, one western (Andean) and two eastern (Amazon-Cerrado and Atlantic Forest-Pampas) major clades of *Oxymycterus* were recovered in the time-calibrated tree, as the sister position of *Juscelinomys huanchacae*.

A few studies accessed interspecific relationships in *Oxymycterus* (Hoffmann et al. 2002; Gonçalves and Oliveira 2004; Jayat et al. 2008; Parada et al. 2015). Hoffmann et al. (2002) and Jayat et al. (2008) were the first to explore phylogenetic inferences of *Oxymycterus* on a broader context, using *Cytb* sequences under maximum parsimony (MP) and maximum likelihood (ML) approaches. The trees based on the MP of Hoffmann et al. (2002) and Jayat et al. (2008), using nine and 10 species, respectively, presented different topologies (with several polytomies) and both recovered the monophyly of the genus. The phylogeny derived by the ML from Jayat et al. (2008) and Hoffmann et al. (2002) resulted in a tree that included *Juscelinomys huanchacae* within the *Oxymycterus* lineage. Later, Parada et al. (2015) performed a dense taxon sampling and a Bayesian time-calibrated tree for the subfamily Sigmodontinae, based on *Cytb* and *IRBP* (interphotoreceptor retinol-binding protein exon I) genes, including 10 species of *Oxymycterus*, which recovered the monophyly of *Oxymycterus* with a strong support (PP = 0.99) while *Juscelinomys* was placed as sister of the *Oxymycterus* clade. Our Bayesian *Cytb* and *Cytb* + *Acp5*-I2 trees presented the same topology, although lower supports were found for the later in all branches. However, our tree presented differences in relation to the positions of *O. nasutus* and *O. dasytrichus*, which appeared nested in the major clade (*O. itapeby* (*O. amazonicus* (*O. delator*))). Except for the inclusion of the new taxon herein described, the topology of the time-tree is completely congruent to the *Cytb* + *IRBP* time-tree of Parada et al. (2015) (including the position of *Juscelinomys*). Contrary to that, even when considering the same marker (*Cytb*), discrepancies were found between Bayesian and MP–ML methods. Jayat et al. (2008), in opposition to our results, recovered *O. hiska* and *O. waiku* nested in the clade (*O. quaestor* (*O. rufus* (*O. josei*))) while sequences of *O. paramensis* were grouped in a single clade. The placements of *O. nasutus* and *O. dasytrichus* in Hoffmann et al. (2002) and Jayat et al. (2008) are also incongruent with our time-tree. Hence, the attainment of a congruent framework for the *Oxymycterus* phylogeny, including its relationship to *Juscelinomys*, comes up against the disparities of the results revealed by distinct methodologies.

Far beyond the main goals of this study, our results raise some questions about species boundaries within *Oxymycterus*. Despite its monophyletic condition (Figs. 2 and 3), *O. paramensis* deserves attention, considering that genetic distances between the clades from Bolivia, Peru are higher (*Cytb*) than distances between some valid species (*O. amazonicus* versus *O. delator*; *O. josei* versus *O. rufus*) with marked morphological distinction. Specimens from the Argentinean clade differ by > 6% in relation to specimens from the Bolivian and Peruvian clades which are 4.7% distant to each other. These results corroborate Jayat et al. (2008), who also detected high *Cytb* divergences between *O. paramensis* sequences from Bolivia, Peru (treated as *O. p. paramensis*), and Argentina (treated as *O. p. jacentior*). Additionally, *O. p. paramensis* was not recovered as monophyletic in the Jayat et al. (2008) analysis. Thus, these authors highlighted the existence of a complex species, which required further analysis, under the designation, *O. paramensis*. Our results reinforce that proposition and recommend a revision of *O. paramensis* including the use of molecular markers, aiming to identify independent lineages.

Oxymycterus rufus is another example of a taxon that deserves further analysis, considering its unusual distribution. A neotype for *O. rufus* selected by Oliveira and Gonçalves (2015) restricted the type locality to "Estancia San Juan Poriahú, Depto. San Miguel, Provincia Corrientes, Argentina," and most of the species' distribution includes the Argentinean provinces of Buenos Aires, Córdoba, Corrientes, and Entre Rios (Oliveira and Gonçalves 2015). However, isolated populations are reported in two localities (Ouro Preto and Viçosa municipalities) in the Minas Gerais state, southeastern Brazil (Gonçalves and Oliveira 2004; Oliveira and Gonçalves 2015). In the *Cytb*

phylogenetic analysis performed by Gonçalves and Oliveira (2004), the distance between Argentinean and Brazilian populations of *O. rufus* ranged from 1.5% to 3.1%, and these groups appeared monophyletic with a low support (PP = 54), nested with *O. josei* as a sister species (PP = 1). Nevertheless, our Bayesian time-tree analysis recovered *O. rufus* as paraphyletic in relation to *O. josei* with low support for the clade (*O. rufus* Argentina (*O. josei*)), but high support for the clade (*O. rufus* Minas Gerais (*O. rufus* Argentina (*O. josei*))). In contrast, the *Cytb* distance detected between *O. rufus* from Argentina and *O. josei* (1.65%) was higher than the distance found between the samples of *O. rufus* from Argentina and Minas Gerais (1.47%), the lowest distance among all pairwise comparisons. The distances found between *O. josei* and *O. rufus* from Argentina and Minas Gerais in our study were 1.65% and 2.06%, respectively, similar to the low values found between the two taxa in previous studies (Hoffmann et al. 2002; Gonçalves and Oliveira 2004; Jayat et al. 2008). At this point, it is surprising that the distances between two valid species, *O. rufus* and *O. josei*, are lower than the distances between the haplotypes within a single species (e.g., *O. rufus*—Gonçalves and Oliveira 2004). Hoffmann et al. (2002) commented that *O. josei* shared morphological characteristics with *O. nasutus*, although *Cytb* sequences were closer to *O. rufus*. According to our time-tree, the divergence between *O. rufus* from Argentina and *O. josei* was the most recent one within the *Oxymycterus* radiation, dating back around 400,000 years BP. Thus, considering its discrepant morphologies (see Hoffmann et al. 2002; García-Olaso 2008), it is supposed that a dynamic process of morphological evolution is involved in these two forms, which was also observed by Gonçalves and Oliveira (2004). Nevertheless, in view of our topology and the low levels of *Cytb* divergence, a broader genetic analysis is recommended, as well as integrative analysis using environmental datasets as possible predictors of morphological differentiation.

Diversification and phylogeography.—Our estimates of the diversification time indicate that the *Oxymycterus* lineage emerged in the Late Pliocene and Early Pleistocene while the clades within the genus diversified in the early Pleistocene. The lineage leading to the group *O. itapeby* and *O. amazonicus* + *O. delator* emerged around 1.14 MYA during the Early-Middle Pleistocene and all three species are associated with open formations. Despite the distribution of *O. amazonicus* in the Amazon Forest biome, the species is associated with savanna areas within this biome, denominated in Capoeiras or Cerrados amazônicos (Hershkovitz 1994; Oliveira and Gonçalves 2015). *Oxymycterus delator*, on the other hand, is mainly associated with the Cerrado biome, although part of its distribution encompasses the southern Atlantic Forest (Oliveira and Gonçalves 2015). Hoorn et al. (2017), based on geochemical and palynological data, showed evidence of savanna expansion over the areas of the Amazon basin between 2.6 and 0.8 MYA. The major lineage (*O. itapeby* (*O. delator* (*O. amazonicus*))) emerged around ca. 1.14 MYA (95% HPD: 0.72–1.62) and possibly expanded over the widespread savanna at that time. However, taking these historical contexts into consideration, we can consider this region as unstable from the Galesian–Calabrian Pleistocene (2.58–0.781 MYA) until the present, due to the absence of climatic stability in the south and east Amazon border in the Last Interglacial Period (LIG) and the possible existence of corridors linking the south Amazon with the Cerrado (Werneck et al. 2012). Other palynological approaches revealed a subtle persistence of the Cerrado–"Dry Forests" areas and Semideciduous Forests in the southeastern Amazon region during the last 30,000 years (within the temporal range of the Last Glacial Maximum [LGM]; Anhuf et al. 2006; Werneck et al. 2011), in this way, resulting in a favorable scenario for geographic isolation and divergence. The time of divergence between *O. amazonicus* and *O. delator* was estimated at 0.66 MYA (95% HPD: 0.37–1.02), a period coincident with the end of the savanna expansion, which may have promoted the isolation of *O. amazonicus* in the open-area patches within the Amazon Forest, like secondary forests and Capoeiras (areas of secondary growth brush), according to Oliveira and Gonçalves (2015). Meanwhile, the wide confidence intervals associated with the estimation of times of divergence do not allow us to infer the role of the interglacial periods on lineage divergence with security, despite the historical spatial models of Cerrado indicating the persistence of savanna patches during the LIG in several areas of Amazon (Werneck et al. 2012), which include the current distribution of *O. amazonicus*. *Oxymycterus itapeby* is distributed along the south-southeastern Brazilian Plateau, which is characterized by a mosaic of open areas (called *campos de altitude*) and the Atlantic Forest, including the southern Araucaria Forest (Behling 2002). In these regions, the grassland-forest relationship during the Late Quaternary is documented through palynological studies (Behling 2002; Behling et al. 2004, 2007) that have demonstrated the dominance of open areas (grasslands) up to the Late Pleistocene (42,000–10,000 years BP) with a rise in forest formation in the Holocene (Overbeck et al. 2007; Behling et al. 2009). Considering the possible scenario that *O. delator* and *O. amazonicus*, the most recent common ancestor of *O. itapeby*, emerged approximately 0.23 MYA in the Middle Pleistocene, it is most likely that this lineage originated in grassland conditions. Supporting this hypothesis, Costa et al. (2018) demonstrated that the northern Cerrado and the Atlantic Forest present a mosaic of stable and unstable biomes in simulations of biome stability in South America (for LGM). Also, vegetation shifts could be explained by recurrent climate-driven local extinction events followed by recolonization processes. Thus, it should be expected that the source populations persisted through climatically unfavorable periods in multiple regional microrefugia (Rull 2009). We report that until then, new species were present in localities of high elevation (Itapevi [~940 m] and Jaguariaíva municipality [~840 m]), and previous studies demonstrate that during interglacial (Forest expansion) periods, the higher sites acted as refuges to Sigmodontinae species associated with open areas (Gonçalves et al. 2007; Gonçalves and Oliveira 2014; Peçanha et al. 2017). Despite this, the geographic distribution of *O. itapeby* remains unclear; however, we suggest that these localities may have acted as

a refuge for this species, i.e., that Quaternary climatic cycles might have played a role in the diversification of this lineage, as demonstrated by others sigmodontines (e.g., Palma et al. 2005; Rodriguez-Serrano et al. 2006; Bonvicino et al. 2009; Cañón et al. 2010; Nascimento et al. 2011; Gonçalves and Oliveira 2014; Quintela et al. 2015; Peçanha et al. 2017).

Conservation.—Oxymycterus itapeby is known only from three localities situated in transitional areas between the biomes of the Atlantic Forest and Cerrado. Both of these biomes are considered global hotspots of biodiversity and have experienced an accelerated loss of diversity due to urbanization, industrialization, and agricultural expansion, which dramatically increases the vulnerability of species to extinction (Scarano and Ceotto 2015; Strassburg et al. 2017). The type locality of *O. itapeby* is a peri-urban condominium surrounded by the densely urban areas of the Itapevi, Cotia, and Vargem Grande Paulista municipalities. This region is the western limit of the Metropolitan Region of São Paulo (population estimated at 21.4 million inhabitants) and it is characterized by an ongoing conurbation process and the presence of many reduced forest fragments. The Transurb condominium preserves small forest fragments but these do not constitute legal areas of environmental protection. The single protected area in Itapevi is the Reserva Natural do Patrimônio Natural (Private Reserve of Nature Patrimony—RPPN) Sítio Ryan, a conservation unit for sustainable use comprised of only 19.5 ha located at approximately 4 km from the Transurb condominium. Another conservation unit for sustainable use, the Reserva Florestal Morro Grande (Morro Grande Reserve), is considerably larger (10,876.5 ha) and it is located ca. 7 km southward of Transurb, in the Cotia municipality. Similarly, the collection sites in Paraná (Chapada do Santo Antônio farm and Banestado Cajurú farm, Jaguariaíva municipality) do not constitute environmental protection areas. These localities are inserted in a typically rural area, where the fragments of the original physiognomies (Cerrado and Atlantic Forest patches) are considerably larger when compared to the fragments in a type locality. Additionally, the Parque Estadual do Cerrado (Cerrado State Park), an integral protection conservation unit, is located next to the collection sites of Jaguariaíva. Thus, in view of the lack of records from protected areas, sampling areas inside the Morro Redondo Reserve and Cerrado State Park are highly recommended to verify the occurrence of *O. itapeby* in these conservation units. We also recommend a morphological review and sequencing of the *Cytb* gene from the brownish *Oxymycterus* vouchers from the Atlantic Forest–Cerrado transitional areas to identify new specimens and new sites of occurrence for *O. itapeby*.

Finally, our results highlight the importance of natural history museums. Much more than repositories, scientific collections are crucial to address the rapid loss of worldwide biodiversity in an era of reduced funding (McLean et al. 2016; de la Sancha et al. 2017; Malaney and Cook 2018) and increased impediments in basic inventories in Brazil (Bockmann et al. 2018).

Acknowledgments

We thank R. Owen (Texas Tech University, Lubbock, Texas), B. Patterson (Field Museum of Natural History, Chicago, Illinois), E. González (Museo Nacional de Historia Natural, Uruguay), A. U. Christoff (Museu de Ciências Naturais ULBRA, Brazil), F. Passos (Universidade Federal do Paraná, Brazil), and A. Silva Junior (Museu de História Natural Capão da Imbuia, Brazil) for allowing us to access and photograph specimens from their collections. We are also grateful to C. Conroy and J. Patton (Museum of Vertebrate Zoology, Berkeley, California) for the loan of the tissue samples. We thank P. Cordeiro Estrela (Universidade Federal da Paraíba) and P. R. Gonçalves (Universidade Federal do Rio de Janeiro) for providing images from *Oxymycterus* holotypes; A. Parada (Universidad Austral de Chile) for helping with the substitution rate for the time-tree estimates; A. Ferrari (Universidade Federal do Rio Grande) for assisting with the stereomicroscope photographs; and E. Rachenberg (Universidade Regional de Blumenau) for helping with the laboratory work. We thank U. F. J. Pardiñas (Centro Nacional Patagónico) for reviewing the manuscript. This research was supported by the Coordenadoria de Aperfeiçoamento de Pessoal de Nível Superior (CAPES), Fundação de Amparo à Pesquisa do Estado do Rio Grande do Sul (FAPERGS-PRONEX/CNPq2015) and Conselho Nacional de Desenvolvimento Cientifico e Tecnológico (CNPq).

Supplementary Data

Supplementary data are available at *Journal of Mammalogy* online.

Supplementary Data SD1.—Specimens examined for genealogical analyses.

Supplementary Data SD2.—All pairwise Tukey's test comparisons of skull centroid size among eight *Oxymycterus* species. Gray lines show the significant comparisons ($P < 0.05$).

Literature Cited

Adams, D. C., M. L. Collyer, and A. Kaliontzopoulou. 2018. Geomorph: Software for geometric morphometric analyses. R package version 3.0.6. https://cran.r-project.org/package=geomorph. Accessed 20 June 2018.

Andrade-Costa, B. M., L. Geise, L. G. Pereira, and L. P. Costa. 2011. Phylogeography of *Rhipidomys* (Rodentia: Cricetidae: Sigmodontinae) and description of two new species from southeastern Brazil. Journal of Mammalogy 92:945–962.

Anhuf, D., et al. 2006. Paleo-environmental change in Amazonian and African rainforest during the LGM. Palaeogeography, Palaeoclimatology, Palaeoecology 239:510–527.

Baker, R. J., and R. D. Bradley. 2006. Speciation in mammals and the genetic species concept. Journal of Mammalogy 87:643–662.

Behling, H. 2002. South and southeast Brazilian grassland during Late Quaternary times: a synthesis. Palaeogeography, Palaeoclimatology, Palaeoecology 177:19–27.

Behling, H., V. Jeske-Pieruschka, L. Schüler, and V. Pillar. 2009. Dinâmica dos campos no sul do Brasil durante o Quaternário Tardio. *In*: Campos Sulinos – Conservação e Uso Sustentável da Biodiversidade (V. Pillar, S. C. Müller, Z. M. Souza Castilhos, and A. V. A. Jacques, eds.). Ministério do Meio Ambiente, Brasília 13–25.

Behling, H., V. D. Pillar, S. C. Müller, and G. E. Overbeck. 2007. Late-Holocene fire history in a forest-grassland mosaic in southern Brazil: implications for conservation. Applied Vegetation Science 10:81–90.

Behling, H., V. D. Pillar, L. Orloc, and S. G. Bauermann. 2004. Late Quatemary Araucaria forest, grassland (*Campos*), fire and climate dynamics, studied by high-resolution pollen, charcoal and multivariate analysis of the Cambara do Sul core in southern Brazil. Palaeogeography, Palaeoclimatology and Palaeoecology 203:277–297.

Bockmann, F. A., et al. 2018. Brazil's government attacks biodiversity. Science 360:865.

Bonvicino, C. R., F. Casado, and M. Weksler. 2014. A new species of *Cerradomys* (Mammalia: Rodentia: Cricetidae) from Central Brazil, with remarks on the taxonomy of the genus. Zoologia 31:525–540.

Bonvicino, C. R., P. R. Goncalves, J. A. Oliveira, L. F. Oliveira, and M. S. Mattevi. 2009. Divergence in *Zygodontomys* (Rodentia: Sigmodontinae) and distribution of Amazonian savannas. Journal of Heredity 100:322–328.

Bonvicino, C. R., B. Lemos, and M. Weksler. 2005. Small mammals of Chapada dos Veadeiros National Park (Cerrado of central Brazil): ecology, karyologic, and taxonomic considerations. Brazilian Journal of Biology 65:1–12.

Bonvicino, C. R., J. A. Oliveira, and P. S. D'Andrea. 2008. Guia dos Roedores do Brasil, com chaves para gêneros baseadas em caracteres externos. OPAS/OMS, Rio de Janeiro, Centro Pan-Americano de Febre Aftosa.

Bonvicino, C. R., J. A. Oliveira, and R. Gentile. 2010. A new species of *Cerradomys* (Rodentia: Sigmodontinae) from Eastern Brazil. Zootaxa 2336:19–25.

Braun, J. K., M. A. Mares, B. S. Coyner, and R. A. Van Den Bussche. 2010. New species of *Akodon* (Rodentia: Cricetidae: Sigmodontinae) from central Argentina. Journal of Mammalogy 91:387–400.

Brito J. M., et al. 2017. New species of arboreal rat of the genus *Rhipidomys* (Cricetidae, Sigmodontinae) from Sangay National Park, Ecuador. Neotropical Biodiversity 3:65–79.

Brown, J. C. 1971. The description of mammals 1. The external characters of the head. Mammal Review 1:151–168.

Brown, J. C., and D. W. Yalden. 1973. The description of mammals 2. Limbs and locomotion of domestic mammals. Mammal Review 3:107–134.

Cañón, C., G. D'Elía, U. F. J. Pardiñas, and E. P. Lessa. 2010. Phylogeography of *Loxodontomys micropus* with comments on the alpha taxonomy of *Loxodontomys* (Cricetidae: Sigmodontinae). Journal of Mammalogy 91:1449–1458.

Carleton, M. D., L. H. Emmons, and G. Musser. 2009. A New species of the rodent genus *Oecomys* (Cricetidae: Sigmodontinae: Oryzomyini) from Eastern Bolivia, with emended definitions of *O. concolor* (Wagner) and *O. mamorae* (Thomas). American Museum Novitates 3661:1–32.

Christoff, A. U., E. M. Vieira, L. R. Oliveira, J. W. Gonçalves, V. H. Valiati, and P. S. Tomasi. 2016. A new species of *Juliomys* (Rodentia, Cricetidae, Sigmodontinae) from the Atlantic Forest of Southern Brazil. Journal of Mammalogy 97:1469–1482.

Costa, G. C., et al. 2018. Biome stability in South America over the last 30 kyr: inferences from long-term vegetation dynamics and habitat modeling. Global Ecology and Biogeography 27:285–297.

D'Elía, G. 2003. Phylogenetics of Sigmodontinae (Rodentia, Muroidea, Cricetidae), with special reference to the akodont group, and with additional comments on historical biogeography. Cladistics 19:307–323.

D'Elía, G., J. D. Hanson, M. R. Mauldin, P. Teta, and U. F. J. Pardiñas. 2015b. Molecular systematics of South American marsh rats of the genus *Holochilus* (Muroidea, Cricetidae, Sigmodontinae). Journal of Mammalogy 96:1081–1094.

D'Elía, G., U. F. J. Pardiñas, P. Teta, and J. L. Patton. 2007. Definition and diagnosis of a new tribe of sigmodontine rodents (Cricetidae: Sigmodontinae), and a revised classification of the subfamily. Gayana 71:187–194.

D'Elía, G., P. Teta, N. S. Upham, U. F. J. Pardiñas, and B. D. Patterson. 2015a. Description of a new soft-haired mouse, genus *Abrothrix* (Sigmodontinae), from the temperate Valdivian rainforest. Journal of Mammalogy 96:839–853.

Darriba, D., G. L. Taboada, R. Doallo, and D. Posada. 2012. Jmodeltest 2: more models, new heuristics and parallel computing. Nature Methods 9:772.

Debry, R. W., and S. Seshadri 2001. Nuclear intron sequences for phylogenetics of closely related mammals: an example using the phylogeny of Mus. Journal of Mammalogy 82:280–288.

Drummond, A. J., A. Rambaut, and M. Suchard. 2016. BEAST: Bayesian evolutionary analysis sampling trees. http://beast.bio.ed.ac.uk/. Accessed 10 May 2016.

Fabre, P.-H., L. Hautier, D. Dimitrov, and E. J. P. Douzery. 2012. A glimpse on the pattern of rodent diversification: a phylogenetic approach. BMC Evolutionary Biology 12:88.

Fabre, P. H., A. H. Reeve, Y. S. Fitriana, K. P. Aplin, and K. M. Helgen. 2018. A new species of *Halmaheramys* (Rodentia: Muridae) from Bisa and Obi Islands (North Maluku Province, Indonesia). Journal of Mammalogy 99:187–208.

García-Olaso, F. 2008. Evaluación de los caracteres diagnósticos de *Oxymycterus josei* Hoffmann, Lessa y Smith, 2002 (Rodentia: Cricetidae) con comentarios sobre la Diferenciación de las especies uruguayas del género. Mastozoologia Neotropical 15:117–123.

Gonçalves, P. R., P. Myers, J. F. Vilela, and J. A. Oliveira. 2007. Systematics of species of the genus *Akodon* (Rodentia: Sigmodontinae) in southeastern Brazil and implication for the biogeography of the Campos De Altitude. Miscellaneous Publications. Museum of Zoology, University of Michigan 197:1–24.

Gonçalves, P. R., and J. A. Oliveira. 2004. Morphological and genetic variation between two sympatric forms of *Oxymycterus* (Rodentia: Sigmodontinae): an evaluation of hypotheses of differentiation within the genus. Journal of Mammalogy 85:148–161.

Gonçalves, P. R., and J. A. Oliveira. 2014. An integrative appraisal of the diversification in the Atlantic forest genus *Delomys* (Rodentia: Cricetidae: Sigmodontinae) with the description of a new species. Zootaxa 3760:001–038.

Hall, T. A. 1999. BioEdit: a user-friendly biological sequence alignment editor and analysis program for windows 95/98/NT. Nucleic Acids Symposium Series 41:95–98.

Hanson, J. D., G. D'Elía, S. B. Ayers, S. B. Cox, S. F. Burneo, and T. E. Lee-Jr. 2015. A new species of fish-eating rat, genus *Neusticomys* (Sigmodontinae), from Ecuador. Zoological Studies 54:49.

Hershkovitz, P. 1962. Evolution of Neotropical cricetine rodents (Muridae) with special reference to the phyllotine group. Fieldiana, Zoology 46:1–524.

Hershkovitz, P. 1994. The description of a new species of South American hocicudo, or long-nose mouse, genus *Oxymycterus* (Sigmodontinae, Muroidea), with a critical review of the generic content. Fieldiana: Zoology (New Series) 79:1–43.

HOFFMANN, F. G., E. P. LESSA, AND M. F. SMITH. 2002. Systematics of *Oxymycterus* with description of a new species from Uruguay. Journal of Mammalogy 83:408–420.

HOORN, C., ET AL. 2017. Amazon at sea: onset and stages of the Amazon River from a marine record, with special reference to Neogene plant turnover in the drainage basin. Global and Planetary Change 153:51–65.

HURTADO, N., AND G. D'ELÍA. 2018. A new species of long-tailed mouse, genus *oligoryzomys* bangs, 1900 (rodentia: cricetidae), from the bolivian yungas. Zootaxa 4500:341–362.

JAYAT, J. P., G. D'ELÍA, P. E. ORTIZ, AND P. TETA. 2016. A new species of the rodent genus *Necromys* Ameghino (Cricetidae: Sigmodontinae: Akodontini) from the Chaco Serrano grasslands of northwestern Argentina. Journal of Mammalogy 97:1321–1335.

JAYAT, J. P., G. D'ELÍA, U. F. J. PARDIÑAS, M. D. MIOTTI, AND P. E. ORTIZ. 2008. A new species of the genus *Oxymycterus* (Mammalia: Rodentia: Cricetidae) from the vanishing Yungas of Argentina. Zootaxa 1911:31–51.

KAJON, A. E., O. A. SCAGLIA, C. HORGAN, C. VELASQUEZ, M. S. MERAMI, AND O. A. REIG. 1984. Tres nuevos cariotipos de la tribu Akodontini (Rodentia, Cricetidae). Revista del Museo Argentino de Ciencias Naturales "Bernardino Rivadavia". Zoología 13:461–469.

KUMAR, S., G. STECHER, AND K. TAMURA. 2016. MEGA7: molecular evolutionary genetics analysis version 7.0 for bigger datasets. Molecular Biology and Evolution 33:1870–1874.

MAESTRI, R., R. FORNEL, D. GALIANO, AND T. R. DE FREITAS. 2015. Niche suitability affects development: skull asymmetry increases in less suitable areas. Plos One 10:e0122412.

MAESTRI, R., L. R. MONTEIRO, R. FORNEL, N. S. UPHAM, B. D. PATTERSON, AND T. R. O. FREITAS. 2017. The ecology of a continental evolutionary radiation: is the radiation of sigmodontine rodents adaptive? Evolution 71:610–632.

Malaney, J. L., and J. A. Cook. 2018. A perfect storm for mammalogy: declining sample availability in a period of rapid environmental degradation. Journal of Mammalogy 99:773–788.

MCLEAN, B. S., ET AL. 2016. Natural history collections-based research: progress, promise, and best practices. Journal of Mammalogy 97:287–297.

MOORE, W. S. 1995. Inferring phylogenies from mtDNA variation: mitochondrial-gene trees versus nuclear-gene trees. Evolution 49:718–726.

MOREIRA, J. C., ET AL. 2009. Small mammals from Serra do Brigadeiro state park, Minas Gerais, southeastern Brazil: species composition and elevational distribution. Arquivos do Museu Nacional, Rio de Janeiro 67:103–118.

NASCIMENTO, F. F., L. G. PEREIRA, L. GEISE, A. M. BEZERRA, P. S. D'ANDREA, AND C. R. BONVICINO. 2011. Colonization process of the brazilian common vesper mouse, *calomys expulsus* (cricetidae, sigmodontinae): a biogeographic hypothesis. The Journal of Heredity 102:260–268.

OLIVEIRA, J. A., AND P. R. GONÇALVES. 2015. Suborder myomorpha: family cricetidae: subfamily sigmodontinae. Genus *Oxymycterus*. Pp. 247–268 in Mammals of South America, volume 2—rodents (J. M. Patton, G. D'Elía, and U. F. J. Pardiñas, eds.). University of Chicago Press, Chicago, Illinois and London, United Kingdom.

OVERBECK, G. E., ET AL. 2007. Brazil's neglected biome: the South Brazilian *Campos*. Perspectives in Plant Ecology, Evolution and Systematics 9:101–116.

PALMA R. E., P. A. MARQUET, AND D. BORIC-BARGETTO. 2005. Inter and intraspecific phylogeography of small mammals in the Atacama Desert and adjacent areas of northern Chile. Journal of Biogeography 32:1931–1941.

PALMA, R. E., AND E. RODRÍGUEZ-SERRANO. 2017. Systematics of *Oligoryzomys* (Rodentia, Cricetidae, Sigmodontinae) from southern Chilean Patagonia, with the description of a new species. Journal of Zoological Systematics and Evolutionary Research 56:280–299.

PARADA, A., G. D'ELÍA, AND R. E. PALMA. 2015. The influence of ecological and geographical context in the radiation of neotropical sigmodontine rodents. BMC Evolutionary Biology 15:172.

PARDIÑAS, U. F. J., G. LESSA, P. TETA, J. SALAZAR-BRAVO, AND E. M. V. C. CÂMARA 2014. A new genus of sigmodontine rodent from eastern Brazil and the origin of the tribe Phyllotini. Journal of Mammalogy 95:201–215.

PARDIÑAS, U. F. J., ET AL. 2017. Family Cicetidae (true hamsters, voles, lemmings and New World rats and mice). Pp. 204–279 in Handbook of the mammals of the world. Vol. 7. Rodents II (D.E. Wilson, T.E. Lacher, Jr., and R.A. Mittermeier, eds.). Lynx Edicions, Barcelona, Spain.

PARDIÑAS, U. F. J., P. TETA, AND G. D'ELÍA. 2009. Taxonomy and distribution of *Abrawayaomys* (Rodentia: Cricetidae), an Atlantic Forest endemic with the description of a new species. Zootaxa 2128:39–60.

PARDIÑAS, U. F. J., P. TETA, AND J. SALAZAR-BRAVO. 2015. A New Tribe of Sigmodontinae Rodents (Cricetidae). Mastozoología Neotropical 22:171–186.

PARDIÑAS, U. F. J., P. TETA, J. SALAZAR-BRAVO, P. MYERS, AND C. A. GALLIARI. 2016. A new species of arboreal rat, genus *Oecomys* (Rodentia, Cricetidae) from Chaco. Journal of Mammalogy 97:1177–1196.

PARDIÑAS, U. F. J., P. TETA, D. VOGLINO, AND F. J. FERNÁNDEZ. 2013. Enlarging rodent diversity in west-central Argentina: a new species of the genus *Holochilus* (Cricetidae, Sigmodontinae). Journal of Mammalogy 94:231–240.

PATTON, J. L., U. F. J. PARDIÑAS, AND G. D'ELÍA. 2015. Mammals of South America. Volume 2, Rodents. University of Chicago Press, Chicago, Illinois.

PEÇANHA, W. T., ET AL. 2017. Pleistocene climatic oscillations in Neotropical open areas: refuge isolation in the rodent *Oxymycterus nasutus* endemic to grasslands. PLoS One 12:e0187329.

PERCEQUILLO, A. R., E. HINGST-ZAHER, AND C. R. BONVICINO. 2008. Systematic review of genus *Cerradomys* Weksler, Percequillo and Voss, 2006 (Rodentia: Cricetidae: Sigmodontinae: Oryzomyini), with description of two new species from Eastern Brazil. American Museum Novitates 3622:1–46.

PERCEQUILLO, A. R., M. WEKSLER, AND L. P. COSTA. 2011. A new genus and species of rodent from the Brazilian Atlantic Forest (Rodentia: Cricetidae: Sigmodontinae: Oryzomyini), with comments on oryzomyine biogeography. Zoological Journal of the Linnean Society 161:357–390.

QUINTELA, F. M., F. BERTUOL, E. M. GONZÁLEZ, P. CORDEIRO-ESTRELA, T. R. O. FREITAS, AND G. L. GONÇALVES. 2017. A new species of *Deltamys* Thomas, 1917 (Rodentia: Cricetidae) endemic to the southern Brazilian Araucaria Forest and notes on the expanded phylogeographic scenario of *D. kempi*. Zootaxa 4294:071–092.

QUINTELA F. M., G. L. GONÇALVES, S. L. ALTHOFF, I. J. SBALQUEIRO, L. F. B. OLIVEIRA, AND T. R. O. FREITAS. 2014. A new species of swamp rat of the genus *Scapteromys* Waterhouse, 1837 (Rodentia:

Sigmodontinae) endemic to *Araucaria angustifolia* Forest in Southern Brazil. Zootaxa 3811:207–225.

Quintela F. M., G. L. Gonçalves, F. Bertuol, E. M. González, and T. R. O. Freitas. 2015. Genetic diversity of the swamp rat in South America: population expansion after transgressive-regressive marine events in the Late Quaternary. Mammalian Biology 80:510–517.

R Core Team. 2018. R: a Language and Environment for Statistical Computing. https://www.R-project.org/. Accessed 20 June 2018.

Rambaut, A., and A. J. Drummond. 2009. Tracer 1.5. http://beast.bio.ed.ac.uk/Tracer. Accessed 20 June 2018.

Reig, O. A. 1977. A proposed unified nomenclature for the enameled components of the molar teeth of the Cricetidae (Rodentia). Journal of Zoology, London 181:227–241.

Rinehart, T. A., R. A. Grahn, and H. A. Wichman. 2005. SINE extinction preceded LINE extinction in sigmodontine rodents: implications for retrotranspositional dynamics and mechanisms. Cytogenetic and Genome Research 110:416–425.

Rodriguez-Serrano, E., R. A. Cancino, and E. Palma. 2006. Molecular phylogeography of *Abrothrix olivaceus* (Rodentia: Sigmodontinae) in Chile. Journal of Mammalogy 87:971–980.

Rohlf, F. J. 2015. The tps series of software. Hystrix 26:9–12.

Rohlf, F. J., and D. Slice. 1990. Extensions of the Procrustes method for the optimal superimposition of landmarks. Systematic Zoology 39:40–59.

Rull, V. 2009. Microrefugia. Journal of Biogeography 36:481–484.

Salazar-Bravo, J., U. F. J. Pardiñas, H. Zeballos, and P. Teta. 2016. Description of a new tribe of Sigmodontine rodents (Cricetidae: Sigmodontinae) with an updated summary of valid tribes and their generic contents. Occasional Papers of the Museum of Texas Tech University 338:1–24.

de la Sancha, N., A. S. Boyle., and B. D. Patterson. 2017. Getting back to the basics: museum collections and satellite imagery are critical to analyzing species diversity. BioScience 67:405–406.

Sbalqueiro, I. J. 1989. Análises cromossômicas e filogenéticas em algumas espécies de roedores da Região Sul do Brasil. Ph.D. Dissertation, Universidade Federal do Rio Grande do Sul, Porto Alegre.

Scarano, F. R., and P. Ceotto. 2015. Brazilian Atlantic Forest: impact, vulnerability, and adaptation to climate change. Biodiversity Conservation 24:2319–2331.

Simmons, M. P., and H. Ochoterena. 2000. Gaps as characters in sequence-based phylogenetic analyses. Systematic Biology 49:369–381.

Smith, M. F., D. A. Kelt, and J. L. Patton. 2001. Testing models of diversification in mice in the *Abrothrix olivaceus/xanthorhinus* complex in Chile and Argentina. Molecular Ecology 10:397–405.

Smith, M. F., and J. L. Patton. 1993. The diversification of South American murid rodents: evidence from mitochondrial DNA sequence data for the akodontine tribe. Biological Journal of the Linnean Society 50:149–177.

Smith, M. F., and J. L. Patton. 1999. Phylogenetic relationships and the radiation of sigmodontine rodents in South America: evidence from cytochrome *b*. Journal of Mammalian Evolution 6:89–128.

Steppan, S. J., and J. J. Schenk. 2017. Muroid rodent phylogenetics: 900-species tree reveals increasing diversification rates. PLoS One 12:e0183070.

Strassburg, B. B. N., et al. 2017. Moment of truth for the Cerrado hotspot. Nature Ecology and Evolution 1:099.

Suárez-Villota, E. Y., A. P. Carmignotto, M. V. Brandão, A. R. Percequillo, and M. J. J. Silva. 2017. Systematics of the genus *Oecomys* (Sigmodontinae: Oryzomyini): molecular phylogenetic, cytogenetic and morphological approaches reveal cryptic species. Zoological Journal of the Linnean Society 184:182–210.

Svartman, M., and E. J. C. Almeida. 1993. The karyotype of *Oxymycterus* sp. (Cricetidae, Rodentia) from Central Brazil. Journal Experientia. 49:718–720.

Tavares, W. C., L. M. Pessôa, and P. B. Gonçalves. 2011. New species of *Cerradomys* from coastal sandy plains of Southeastern Brazil (Cricetidae: Sigmodontinae). Journal of Mammalogy 92:645–658.

Teta, P., and G. D'Elía 2016. Taxonomical notes on the long-clawed mole mice of the genus *Geoxus* (Cricetidae), with the description of a new species from an oceanic island of southern Chile. Hystrix 27:11996.

Timm, R. M., R. H. Pine, and J. D. Hanson. 2018. A new species of *Tanyuromys* Pine, Timm, and Weksler, 2012 (Cricetidae: Oryzomyini), with comments on relationships within the Oryzomyini. Journal of Mammalogy 99:608–623.

Ventura, K., V. Fagundes, G. D'Elía, A. U. Christoff, and Y. Yonenaga-Yassuda. 2011. A new allopatric lineage of the rodent *deltamys* (rodentia: sigmodontinae) and the chromosomal evolution in *deltamys kempi* and *deltamys* sp. Cytogenetic and Genome Research 135:126–134.

Viscozi, V., and A. Cardini 2011. Leaf morphology, taxonomy and geometric morphometrics: a simplified protocol for beginners. PLoS One 6:e25630.

Vitullo, A. D., et al. 1986. Cytogenetics of South American akodont rodents (Cricetidae): new karyotypes and chromosomal banding patterns of Argentinian and Uruguayan forms. Journal of Mammalogy 67:69–80.

Voss, R. S. 1988. Systematics and ecology of ichthyomyine rodents (Muroidea): patterns of morphological evolution in a small adaptive radiation. Bulletin of the American Museum of Natural History 188:260–493.

Werneck, F. P., G. C. Costa, G. R. Colli, D. E. Prado, and J. W. SitesJr. 2011. Revisiting the seasonally dry tropical forests historical distribution: new insights based on palaeodistribution modeling and palynological evidence. Global Ecology and Biogeography 20:272–288.

Werneck, F. P., C. Nogueira, G. R. Colli, J. W. Sites, Jr., and G. C. Costa. 2012. Climatic stability in the Brazilian Cerrado: implications for biogeographical connections of South American savannas, species richness, and conservation in a biodiversity hotspot. Journal of Biogeography 39:1695–1706.

Submitted 25 September 2018. Accepted 28 February 2019.

Associate Editor was Ricardo Moratelli.

SUPPLEMENTARY DATA

Supplementary Data SD1.—Specimens examined for genealogical analyses.

Specimens examined for genealogical analyses. — The specimens examined belong to the following collections: CML, Colección de Mamíferos "Lillo", Universidad Nacional de Tucumán, San Miguel de Tucumán (Argentina); CMLCE-UFRGS, Mastozoological Collection of the Cytogenetic Laboratory and Evolution at the Universidade Federal do Rio Grande do Sul, Porto Alegre (Brazil); CNP, Colección de Mamíferos del Centro Nacional Patagónico, Puerto Madryn (Argentina); CZFURB, Coleção Zoológica da Universidade Regional de Blumenau, Blumenau (Brazil); DZUP/CCMZ, Departamento de Zoologia da Universidade Federal do Paraná, Curitiba (Brazil); FMNH, Field Museum of Natural History, Chicago (USA); BM, British Museum, London (United Kingdom); MCNU, Museu de Ciências Naturais da Universidade Luterana do Brasil, Canoas (Brazil); MHNCI, Museu de História Natural "Capão da Imbuía", Curitiba (Brazil); MLP, BAL [La Balandra], AC [Achala], PY [Papagayos] and UP [Ulyses Pardiñas], Museo de la Plata, La Plata (Argentina); MN [LG, ML, PGR], Museu Nacional, Universidade federal do Rio de Janeiro, Rio de Janeiro (Brazil); MNHNP [TK], Museo Nacional de Historia Natural del Paraguay, San Lorenzo (Paraguay); MSB [NK], Museum of Southwestern Biology, University of New Mexico, Albuquerque (USA);MVZ, Museum of Vertebrate Zoology, University of California at Berkeley, Berkeley (USA); MZUFV, Museu de Zoologia ''João Moojen de Oliveira'', Universidade Federal de Viçosa, Viçosa (Brazil); MZUSP, Museu de Zoologia da Universidade de São Paulo, São Paulo (Brazil); OMNHN, Sam Noble Oklahoma Museum of Natural History, University of Oklahoma, Norman (USA); TTU [TK], Museum of Texas Tech University, Lubbock (USA); UFES, Coleção Científica da Universidade Federal do Espírito Santo, Vitória (Brazil); MNHN, Museo Nacional de Historia Natural [of Uruguay], Montevideo (Uruguay); UFMG [LPC], Universidade Federal de Minas Gerais, Belo Horizonte (Brazil); UFPR-P, Departmento de Genética da Universidade Federal do Paraná, Curitiba (Brazil); UMMZ, University of Michigan, Museum of Zoology, Ann Arbor (USA); USNM, Smithsonian National Museum of Natural History, Smithsonian Institution, Washington (USA). Field numbers are uses when museums or scientific collections numbers were not available. Taxonomic arrangement follows Oliveira and Gonçalves (2015). Localities and specimens are listed after species assignments. Genbank accessions in brackets. Sequences generated in this study indicated in bold.

Oxymycterus amazonicus. BRAZIL: Pará (state): Cachoeira do Espelho, Rio Xingu —MZUSP 21317 [AF454765]; Altamira, 52 SSW, E Bank Rio Xingu — USNM 549815 [MF110476].

Oxymycterus delator. PARAGUAY: Canindeyu (department): 13.3km N Curuguaty by Road — MVZ 193002 [**MK331139**], UMMZ 133939 [U03525], UMMZ 137077 [AF454766]; Estancia Felicidad — UMMZ 175101 [AY275125]; Itapúa (department): Estancia San Isidro — MNHNP 2914 [DQ518256]; BRAZIL: Minas Gerais (state): Fazenda São Luis, 30 km N Barra do Garças — MVZ 197931 [MF110478]; Mato Grosso (state), Barra do Garças, 30 km N Fazenda São Luis — LPC481 [AF454767].

Oxymycterus itapeby. BRAZIL: São Paulo (state): Itapevi, Condomínio Transurb —MHNCI 3593 [**MK331136 / MK331149**], MHNCI 3595 [**MK331137 / MK331150]**; Paraná (state): Jaguariaíva, Fazenda Chapada Santo Antônio — MHNCI 1704 [**MK331135 / MK331148**]; Fazenda Banestado Cajuru — MHNCI 5140 [**MK331133**], MHNCI 5141 [**MK331134**].

Oxymycterus hiska. PERU: Puno (department); Puno, 14 km W of Yanahuaya —MVZ 171518 [U03542].

Oxymycterus dasytrichus. BRAZIL: Santa Catarina (state): Itapoá, Porto de Itapoá —CZFURB 18669 [KU161271], CZFURB 18828 [**MK331147**]; Paraná (state); Antonina, basin of the Rio Nunes — UFPR-P177 [KU161272], Guaraqueçaba, Massarapuã — UFPR-P757 [KU161275], Guaraqueçaba, Índios — UFPR-P752 [KU161273], UFPR-P754 [KU161274], UFPR-P760 [KU161276]; São Paulo (state); Capão Bonito, Fazenda Intervales, Base do Carmo — MVZ 183125 [AF454768], MVZ 183126 [AF454769], MVZ 183127 [KY754090], MVZ 193008 [KY754091]; Salesópolis, Estação Biológica de Boraceia — MVZ 193005 [AF454770]; Rio de Janeiro (state): Angra dos Reis, Ilha Grande — MN 62254 [AF516662], MN 62258 [AF516663], MN 62259 [AF516664]; Paraty, Tarituba — MN62260 [AF516665]; Espírito Santo (state): Venda Nova do Imigrante — MN65536 [AF516657]; Santa Tereza — ML125 [AF454771]; Minas Gerais (state): Viçosa — MN65534 [AF516659], MZUFV 659 [AF516658].

Oxymycterus josei. URUGUAY: Maldonado (department): Maldonado, Las Flores —MVZ 183264 [AF175288], MVZ 183265 [AF175289], MVZ 193035 [MF110481], MVZ 193036 [**MK331138**].

Oxymycterus nasutus. BRAZIL: Paraná (state): São José dos Pinhais, Barro Preto — UFPRP1055 [**MK331145**]; Santa Catarina (state); Campo Belo do Sul, Fazenda Gateados — CZFURB 15140 [**MK331141**]; Água Doce — CZFURB 9365 [**MK331142**]; Rio Grande do Sul (state): São Francisco de Paula, Pró-Mata — MCNU 3210 [**MK331143**]; Guaíba — MCNU 3228 [**MK331144**]; Rio Grande, Mata da Estrada Velha — CMLCE/MEV01 [**MK331140]**; URUGUAY: Maldonado, km 10 on Ruta 39 N of Maldonado, El Peñasco — MVZ 182701 [KY754092].

Oxymycterus quaestor. BRAZIL: Rio de Janeiro (state): Teresópolis — MN65543 [AF516661], MN 65544 [AF516660]; Nova Friburgo, Sitio Xitaca — LG41 [AF454772]; São Paulo (state): Capão Bonito, Fazenda Intervales, Base do Carmo — MVZ 183129 [AF454774], MVZ 183128 [AF454773]; Santa Catarina (state): Itá, Usina Hidrelétrica Itá — CZFURB 0901 [**MK331146**]; Indaial, Parque Nacional da Serra do Itajaí, Parque das Nascentes, Vale do Espingarda — CZFURB 5005 [**MK331150]**; PARAGUAY: Alto Paraná (department), Colonia Britez Cue — TK121751 (TTU catalogue number unavailable) [EU449517]; ARGENTINA: Misiones (province): Reserva Privada "Valle del arroyo Cuña Pirú," Balneario Arroyo Cuña Pirú — CNP 851 [DQ518257].

Oxymycterus rufus. BRAZIL: Minas Gerais (state): Viçosa — PRG1013 [AF516651], PRG903 [AF516652], MN65522 [AF516654], MZUFV713 [AF516653]; ARGENTINA: Buenos Aires (province): Ensenada — MN65538 [AF516655]; Berisso— BAL000511 (MLP) [AF454777]; Berisso, La Balandra, Club de Pesca La Terraza — CNP 5248 (UP33) [AY275127]; Córdoba (province): Río Cuarto, 2 km S Espinillo — TTU 66588 (TK49118) [AF454775], TTU 66589 (TK49119) [AF454776]; Calamuchita, Pampa de Achala — AC30 (MLP) [AF516667], MLP 24.X.01.1 (AC05) [AF516666]; Entre Ríos (province): Colón, Colonia Caraballo — MLP 31.XII.02.18 (UP AC004) [AY275126]; San Luis (province); Camping Municipal Papagayos— MLP16.X.01.3 (PY01) [AF516668], PY02 (MLP) [AF516669]; 15 km N Paso del Rey — OMNHN30079 [MF110484].

Oxymycterus paramensis. PERU: Cusco (province): Cusco, 55.4 km by road N Calea — UMMZ160535 [U03536]; BOLIVIA: Cochabamba (department): 17 km from Totora —

MSB67277 (NK22836) [AY041197]; ARGENTINA: Jujuy (province): San Francisco —CNP 850 [DQ518261]; León, Río Lozano, 3 km upwaters route 9 — CNP852 [DQ518260]; San Salvador de Jujuy 24.9 km N — OMNHN 34968 [MF110483]; Salta (province), Pampa verde ca. 8 km WSW Los Toldos and S Cerro Bravo — CML7251 [DQ518259].

Oxymycterus wayku. ARGENTINA: Tucumán (province): 10 km by road south of Hualinchay — CML7247 [DQ518262].

Specimens examined for morphological comparisons. — Specimens used in comparative analyses and geometrics morphometrics for landmarks from skull. Localities and specimens are listed after species assignments.

Oxymycterus amazonicus. BRAZIL: Pará (state): Fordlândia, right bank, lower Rio Tapajoz — FMNH 94524 (holotype).

Oxymycterus delator. BRAZIL: Mato Grosso (state): Itiguira, Fazenda Espigão — DZUP/CCMZ338; PARAGUAY: Paraguari (department), Sapucai — BM3.4.7.18 (holotype); Canindeyu (department), Reserva Natural del Bosque Mbaracayú — TK121107, TK 122190, TK122195, TK122197, TK61793, TK61815, TK61851, TK61852, TK66810, TK121098 (to be transferred at the MNHNP); Reserva de Biosfera del Bosque, Mbaracayu, Puesto Aguara Nu — TK 122347, TK122432 (to be transferred at the MNHNP); Estancia Rama III — TK121173, TK121781, TK122008, TK140322 (to be transferred at the MNHNP); Colonia Britez Cue — TK122450, TK122455, TK122466, TK130576 (to be transferred at the MNHNP).

Oxymycterus itapeby. BRAZIL: São Paulo (state): Itapevi, Condomínio Transurb — MHNCI 3593, MHNCI 3595 (holotype).

Oxymycterus dasytrichus. BRAZIL: Santa Catarina (state): Itapoá, Porto de Itapoá — CZFURB 18669, CZFURB 18828; Paraná (state): Antonina, Bairro Alto — MHNCI 1992; Antonina, Bairro Alto – Usina Hidrelétrica Parigot de Souza — MHNCI 2195; Guaraqueçaba, Paruguara — MHNCI 2055; Guaraqueçaba, Fazenda Salto Dourado —MHNCI 6465; São Paulo (state): Jacupiranga, Parque Estadual de Jacupiranga—MHNCI 3197; Ribeirão Grande, Córrego Água Limpa — MHNCI 4780; Capão Bonito, Fazenda Intervales, Base do Carmo — MVZ 183125, MVZ 183127, MVZ 183132, MVZ 183133, MVZ 183137; Espírito Santo (state): Águia Branca, Fazenda do Zequinha Manduca —UFES 281.

Oxymycterus josei. URUGUAY: Maldonado (department): Maldonado, Las Flores —MVZ 183264, MVZ 183265, MVZ 183266; Las Flores, west margin of Arroyo Tarariras — MNHN 3838 (holotype).

Oxymycterus nasutus. BRAZIL: Rio Grande do Sul (state): Encruzilhada do Sul —MCNU 1293; Pedras Altas — MCNU 1354, MCNU 1355, MCNU 1356, MCNU 1357 MCNU 1358, MCNU 1359; São Gabriel — MCNU 2166; Camaquã — MCNU 3126; Tapes — MCNU 3132; Pelotas — MCNU 3223.

Oxymycterus quaestor. BRAZIL: Santa Catarina (state): Anitápolis, Vale do IFC —CZFURB 0449, CZFURB 0510; Blumenau, Parque Nacional da Serra do Itajaí, Parque das Nascentes — CZFURB

0621; Indaial, Parque Nacional da Serra do Itajaí, Parque das Nascentes, Vale do Espingarda — CZFURB 0999, CZFURB 5014; Itá, Usina Hidrelétrica Itá — CZFURB 5047, CZFURB 0901; Rio Grande do Sul (state): Maquiné — MCNU 1619; Vila Flores — MCNU 2114; Paraná (state): Pinhão, Foz do Rio da Divisa — MHNCI 2146; Araucária, Thomaz Coelho — MHNCI 2150; São Paulo (state): Ribeirão Grande, Córrego Água Limpa — MHNCI 5539.

Oxymycterus rufus. ARGENTINA: Buenos Aires (province):25 km S Azul — MVZ 134241;35 km S Azul — MVZ 134242, MVZ 134243 — Valeriadel Mar — MVZ 134244; Mar del Tuyú, General Lavalle — FMNH 122697; Pereira, FGR — FMNH 95138; Córdoba (province): Pampa de Achala, 14km E Cura Bochero — MVZ 165833, MVZ 165832.

Oxymycterus wayku. ARGENTINA: Tucumán (province): 10 km by road south of Hualinchay — CML7247, CML 7250.

Oxymycterus caparaoe. BRAZIL: Espírito Santo (state): Dores do Rio Preto, Parque Nacional do Caparaó — UFES 1744

Supplementary Data SD2.—All pairwise Tukey's test comparisons of skull centroid size among eight *Oxymycterus* species. Gray lines show the significant comparisons ($P < 0.05$).

Species	Differences	Lower	Upper	*P* adj
dasytrichus-amazonicus	1.14913377	0.23997612	2.058291421	0.0044862
delator-amazonicus	0.8564866	-0.04158335	1.754556541	0.0722285
josei-amazonicus	0.5033086	-0.47869389	1.485311101	0.7444762
nasutus-amazonicus	0.07904513	-0.83834036	0.996430614	0.9999942
quaestor-amazonicus	1.32821984	0.41402527	2.242414414	0.0006193
rufus-amazonicus	0.65822806	-0.30393395	1.620390081	0.3987193
itapeby-amazonicus	0.33284555	-0.74288429	1.408575383	0.9770321
delator-dasytrichus	-0.29264718	-0.59293206	0.007637713	0.0613388
josei-dasytrichus	-0.64582517	-1.14379132	-0.147859014	0.0032168
nasutus-dasytrichus	-1.07008865	-1.42397778	-0.716199511	0.0000000
quaestor-dasytrichus	0.17908607	-0.166447	0.524619141	0.7336890
rufus-dasytrichus	-0.49090571	-0.94850502	-0.033306392	0.0270409
itapeby-dasytrichus	-0.81628823	-1.4802431	-0.152333356	0.0063133
josei-delator	-0.35317799	-0.83060054	0.124244554	0.2998691
nasutus-delator	-0.77744147	-1.10178622	-0.45309672	0.0000000
quaestor-delator	0.47173325	0.15652681	0.786939686	0.0003829
rufus-delator	-0.19825853	-0.63341268	0.236895614	0.8406651
itapeby-delator	-0.52364105	-1.17233055	0.12504845	0.2019125
nasutus-josei	-0.42426348	-0.93709756	0.088570599	0.1777197
quaestor-josei	0.82491124	0.31780733	1.332015146	0.0000877
rufus-josei	0.15491946	-0.43428204	0.744120957	0.9910613
itapeby-josei	-0.17046306	-0.93111892	0.590192804	0.9966330
quaestor-nasutus	1.24917472	0.8825392	1.615810237	0.0000000
rufus-nasutus	0.57918294	0.10544711	1.052918767	0.0067503
itapeby-nasutus	0.25380042	-0.42137702	0.928977857	0.9351243
rufus-quaestor	-0.66999178	-1.13751848	-0.202465075	0.0007684
itapeby-quaestor	-0.9953743	-1.66620971	-0.324538881	0.0004412
itapeby-rufus	-0.32538252	-1.0602459	0.40948086	0.8592515

CAPÍTULO 5.

Genetic and morphological variation in *Oxymycterus quaestor* Thomas, 1903 (Rodentia, Sigmodontinae): new and re-defined lineages

Willian T. Peçanha, Fernando M. Quintela, Sergio L. Althoff, Diego M. Jung, Alexandre U. Christoff, Pablo R. Gonçalves, João A. Oliveira, Gislene L. Gonçalves, Thales R. O. Freitas.

Artigo em preparação: *Journal of Mammalogy*

Genetic and morphological variation in *Oxymycterus quaestor* **Thomas, 1903 (Rodentia, Sigmodontinae): new and re-defined lineages**

Willian T. Peçanha, Fernando M. Quintela, Sergio L. Althoff, João Alves de Oliveira, Pablo R. Gonçalves, Diego M. Jung, Alexandre Uarth Christoff, Gislene L. Gonçalves*, Thales R. O. Freitas

Programa de Pós-graduação em Genética e Biologia Molecular, Departamento de Genética, Universidade Federal do Rio Grande do Sul, CP 15007, Porto Alegre, RS 91501-970, Brazil. (WTP, GLG, TROF)

Programa de Pós-Graduação em Biologia de Ambientes Aquáticos Continentais, Universidade Federal do Rio Grande, Campus Carreiros, Rio Grande, RS 96203-900, Brazil. (FMQ)

Departamento de Ciências Naturais, Universidade Regional de Blumenau, Campus 1, Blumenau, SC 89012-900, Brazil. (SLA)

Setor de Mastozoologia, Departamento de Vertebrados, Museu Nacional – Universidade Federal do Rio de Janeiro, Rio de Janeiro, RJ 20940-040, Brazil. (JAO)

Núcleo em Ecologia e Desenvolvimento Socioambiental de Macaé, Universidade Federal do Rio de Janeiro, Macaé, RJ 27965-045, Brazil. (PRG)

Laboratório de Biologia Molecular, Universidade do Vale do Rio dos Sinos, São Leopoldo, RS 93020-190, Brazil. (AUC, DMJ)

Departamento de Recursos Ambientales, Facultad de Ciencias Agronómicas, Universidad de Tarapacá, Arica, Chile. (GLG)

*Corresponding author: lopes.goncalves@ufrgs.br

ABSTRACT

Oxymycterus quaestor (Thomas, 1903) is a widely distributed species throughout the Southern Atlantic Forest that presents a complex history of synonymies with *Oxymycterus judex* (Thomas, 1909) and *Oxymycterus misionalis* (Sanborn, 1931). These originally formed the '*judex* group' of species, but further analysis proposed *O. quaestor* as the only valid name. In this study, we identified variation in skull morphology and DNA sequences (using Cytochrome b and Fgb-I7 sequences) within *O. quaestor*. By revisiting the '*judex* group' we were able to demonstrate an ongoing process of differentiation at molecular level. Holotypes assigned to *O. quaestor, O. judex* and *O. misionalis* included in the morphological analyses had no discrete characters that allow us to tell them apart. Bayesian phylogeny indicated four well-supported groups (lineages A to D) within *O. quaestor*. Lineage A was considered *O. quaestor* sensu strict as it includes the type locality; lineage B included samples from Teresópolis, Rio de Janeiro, Brazil, previously assigned as a restricted population to *O. quaestor*; lineage C was widespread in Alto Paraná Atlantic Forests, eastern Paraguay and northeast Argentina and Serra do Mar Coastal Forests and included the type locality originally assigned to *O. misionalis* and *O. judex*; and lineage D consisted of specimens from the northern Rio Grande do Sul. The time calibrated-tree suggest a recent (ca. 0.794 myr) emergence of these lineages.

KEYWORDS: Araucaria Forest, Akodontini, *campos de altitude*, species limits, systematics, taxonomy

INTRODUCTION

Species delimitation is crucial for conservation, macroecology and biogeography and has greatly benefited from recent integrative approaches combining evidence from multiple character systems (Luo et al. 2018). However, recognizing and diagnosing species in genera with ample but continuous morphological variation among populations still remains a difficult task, even with the growing use of molecular approaches.

Among Neotropical rodents of the subfamily Sigmodontinae, *Oxymycterus* probably offers one of the biggest challenges for species diagnosis and recognition due to the lack of integrative analyses for most nominal taxa. At least 26 nominal forms have been proposed acknowledging the wide morphological diversity in the genus, but only 15 are currently recognized as valid species due to difficulties in detecting discrete variation among populations (Gonçalves and Oliveira 2004; Oliveira and Gonçalves 2015). The absence of karyotype distinction and the relatively recent origin of the genus (Hershkovitz 1994; Parada et al. 2015; Di-Nizo et al. 2017) likely contribute to the taxonomy uncertainties that characterize this group. In addition, molecular genetic divergence between sister-species inferred from mitochondrial DNA markers is sometimes lower (e.g. *O. amazonicus*-*O. delator* or *O. rufus*-*O. josei* (Hoffmann et al. 2002; Jayat et al. 2008) than the threshold found for species of mammals (Bradley and Baker 2001), blurring the cut-off values commonly assumed to infer inter and intraspecific levels of variation in closely related forms.

Oxymycterus quaestor (Thomas, 1903) is an example of species in which levels of among and within lineages variation have been poorly understood. The species is distributed throughout Mixed Ombrophilous forests in northeastern Argentina, eastern Paraguay and southern Brazilian highlands, with disjoint populations in Montane Ombrophilous forests in Southeastern Brazil (Oliveira and Gonçalves 2015). Three nominal forms recurrently considered as junior synonyms of *O. quaestor* have been described based on specimens collected at close localities or at the margin of

the species range (Oliveira and Gonçalves 2015). Thomas (1903) described *O. quaestor* based on a single specimen obtained from Montane forests (1000m altitude) of Serra do Mar in the Southern Brazilian state of Paraná. Six years later, Thomas (1909) described *O. judex* from specimens from nearby coastal lowland forests in Santa Catarina state and distinguished it from *O. quaestor* by the larger general size and larger braincase. The last nominal form, *Oxymycterus misionalis*, was described by Sanborn (1931) based on specimens from Misiones province, Argentina, at the west margin of *O. quaestor* range, which were overall larger than *O. judex*. Despite the size differences among representatives of the three nominal forms emphasized in the descriptions, Cabrera (1961) considered all three forms as conspecifics, and regarded them as subspecies of *O. hispidus*, an arrangement that was followed by most subsequent authors.

The first comprehensive analyses of morphological variation among samples allocated to the group revealed that they conform to a continuum of size variation (Oliveira 1998). Furthermore, the few molecular phylogenetic assessments of *Oxymycterus* made so far revealed reduced genetic divergence (0.5-2.8% in cytochrome *b* pairwise distance) among samples from Southeastern Brazil (São Paulo and Rio de Janeiro states) assigned to *O. judex* and *O. quaestor*, and samples from Paraguay and Argentina assigned to *O. misionalis* (Hoffmann et al. 2002; Gonçalves and Oliveira 2004; D'Elía et al. 2008; Jayat et al. 2008). More recently, Oliveira and Gonçalves (2015) distinguished *O. judex*, *O. misionalis* and *O. quaestor* from *O. hispidus*, but maintained the three forms as synonyms based on the limited evidence available for species delimitation within the group, partially keeping the lumping perspective of Cabrera (1961).

In this study we quantify genetic and morphological variation in *O. quaestor* to evaluate the hypothesis of differentiation of nominal forms and to identify diversity at phylogenetic level. By using an integrative analysis we revisit the existence of '*judex* group' proposed by Oliveira (1998)

and investigate boundaries among taxonomic entities originally proposed (i.e., *O. quaestor*, *O. judex* and *O. misionalis*).

MATERIALS AND METHODS

Ethics Statement and sampling — The skulls and tissue samples assigned to *O. quaestor* used in the present study were obtained from the specimens deposited in natural history museums (or scientific institutions) and accredited zoological collections. Museums or Scientific Collections ID, general identification codes and site locations are provided in Supplementary Data 1. We analyzed 151 samples from 46 localities throughout the range of *Oxymycterus quaestor*, representing localities in Brazil, Argentina and Paraguay (Fig. 1). In overall, 114 samples were used for molecular data and, 106 skulls (for dorsal, ventral and lateral views) were used in geometric morphometric analyses.

Genetic and phylogenetic analyses — These analyses were based on DNA sequences of two loci, the mitochondrial *cytochrome b* gene (*cytb*; 1137 bp) and nuclear *fibrinogen beta chain* gene (*Fgb*-I7; ~660 bp). Sampling was both geographically and genealogically extensive for *O. quaestor* and other vouchers assigned for *O. judex* and *O. misionalis*, being sequences derived from tissue samples housed at scientific collections, including seven sequences retrieve from Genbank (Supplementary Data 2). Total genomic DNA was extracted PureLink Genomic DNA extraction kit (Invitrogen, Life Technologies), following the manufacturer's instructions from kidney and muscle tissues (stored at -20 ° C or 70% ethanol). The cyt *b* complete sequences were obtained by Polymerase Chain Reaction (PCR) using the light strand MVZ05 (5′-CGAAGCTTGATATGAAAAACCATCGTTG-3′), heavy strand MVZ16 (5′-AAATAGGAARTATCAYTCTGGTTTRAT-3′), light strand MVZ23(5′-TACTCTTCCTCCACGAAACNGGNTC-3′) and heavy strand MVZ14 (5′-

GGTCTTCATCTYHGGYTTACAAGAC-3′) primers according to thermal cycles of Smith and Patton (1993), and intron 7 of the *Fgb* gene was amplified with primers β17-mammL (5-ACCCCAGTAGTATCTGCCGTTTGGATT-3) and βfib-mammU (5'-CACAACGGCATGTTCTTCAGCAC-3') according to Matocq et al. (2007). PCR products were checked in 1% agarose gel stained with GelRed^{TM} and after, were purified with exonuclease and alkaline phosphatase (Amersham Biosciences, Piscataway, NJ) and sequenced by Macrogen, Inc. (Seoul, South Korea). All sequences have been deposited in GenBank (*Cyt-b*: xxxxx–xxxxxx, *Fgb*-I7: xxxxx– xxxxxx). The *cytb* sequences were aligned using the ClustalW algorithm implemented in MEGA v.7 (Kumar et al. 2016). The *Fgb*-I7 alignment, we used the default settings and the automatic optimization option in the online version of MAFFT v.7 (Katoh and Standley 2013). All polymorphic positions in the nuclear loci were verified using Bioedit v7.2.5 (Hall 1999) to ensure correct and consistent identification of double peaks in heterozygotes. For nuclear sequences, contiguous insertion/deletion (indels or gaps) events involving more than one base pair were coded and treated as one mutational event (Simmons and Ochoterena 2000). The IUPAC symbols were applied for coded the double peaks. Six other *Oxymycterus* species were used as outgroups (*O. delator*, *O. itapeby*, *O. nasutus*, *O. dasytrichus*, *O. rufus* and *O. josei*) and all genbank codes are listed in Supplementary Data 2. For those taxa which either no mitochondrial (4 cases) or nuclear genes (26 cases) were available, the matrix was completed with missing state characters (i.e., n). Phylogenetic trees were inferred for the different haplotypes using Bayesian inference (BI). The jModelTest v2.1.10 software (Darriba et al. 2012) selected the substitution models assigned HKY+I+G and HKY+G for *Cyt-b* and *Fgb*-I7, respectively, based on the Akaike Information Criterion (AIC). Phylogenetic relationships among species were estimated using BEAST v1.8.4 (Drummond and Rambaut 2007). The BI was performed for the concatenated data and for mitochondrial genes separately. We performed six independent Markov Chain Monte Carlo

(MCMC) runs, each one with four streams per **25** million steps of the MCMC (for mitochondrial run) and **50** million steps of the MCMC for concatenated datasets, sampled every 1000 generations and discarding the four million burn-in (about 20% discarded), starting the initial trees with randomness, without restriction. Runs were performed under an uncorrelated lognormal relaxed-clock model; speciation was modeled on a Birth-Death Process with estimated base frequencies and four gamma rate categories, using an initial random tree, and other priors set as default. MCMC convergence was also checked in Tracer v.1.6 (Rambaut et al. 2014), where we confirmed if effective sample sizes (ESS) were above 200. The burn-in was determined in Tracer-based on trajectory parameters, and 20% of the first trees were then removed and summarized in TreeAnnotator on BEAST. For the concatenated dataset, trees and logs, files were combined using LogCombiner on BEAST for concatenated phylogeny, and 20% of the first trees were then removed (10 millions) and summarized in TreeAnnotator. The tree consensus generated was visualized and edited in Figtree v1.4.3 (http://tree.bio.ed.ac.uk/software/figtree/). The *p*-distance parameter model of evolution was used to calculate genetic distances for mtDNA and nDNA. These values were then used to assess levels of genetic divergence among and within the species of *Oxymycterus* following the criteria outlined by Baker and Bradley (2006). Polymorphic sites such as indels, singletons and parsimony-informative sites were obtained with *MEGA v.7 and* DnaSP 5.10.01 (Librado and Rozas 2009).

Estimating divergence times — Divergence times among species were estimated from the combined matrix of mitochondrial sequences from all Akodontini tribe representatives (Salazar-Bravo et al. 2016). The Genbank accession nunbers used in this analysis are listed in Supplementary Data 3. The model HKY+I+G were selected using the jModelTest v2.1.10 as the best-fitting substitution results (based on AIC). We used 11 of 16 valid species of genus *Oxymycterus*, further 3 related

lineages found in previous studies (termed here as *O. paramensis* "Argentina", *O. paramensis* "Peru" and *O. rufus* "Brazil"), beyond 3 representatives sequences from 3 lineages associated to *O. quaestor* (see results). The BEAST v1.8.4 (Drummond and Rambaut 2007) was employed assuming a Birth-Death model of speciation, with empirical base frequencies (and four gamma rate categories) and an uncorrelated lognormal relaxed-clock model distribution molecular clock as tree priors. We ran MCMC chains for 50 million generations, with trees sampled every 1000 generations. The trees were summarized with TreeAnnotator (BEAST) into the maximum clade credibility tree and the first 20% of sampled trees were treated as burn-in. Burn-in and convergence of the chains were determined with TRACER v.1.6. The ESS were used to determine the Bayesian statistical significance of each parameter were above 200. The consensus tree was visualized and edited in Figtree v1.4.3. We incorporated information from a total of 3 fossils to calibrate the nodes of the phylogeny. For these points the log-normal distribution was designated as prior, since it attributes a higher probability to a nodal age older than the age of the fossil (Ho and Phillips 2009). We calibrated only well-supported nodes for those fossils that with strong paleontological evidence of Akodontini tribe membership describe and their taxonomic status. We used the following constraints: (i) the oldest fossils records of *Oxymycterus* (*O.* cf. *rufus*) described for Ensenadean Stage/Age, 0.5-2.1 Ma (Pardiñas et al. 2002) representing the most recent common ancestor (MRCA) of *Oxymycterus* (offset = 0.5, median = 0.8 and 95th percentile = 2.1); (ii) fossil record of *Scapteromys hershkovitzi* described for Sanandresian Stage/Age, 2.15-2.55 Ma (Quintana 2002) to represent split between *Scapteromys* and *Kunsia* (offset = 2.15, median = 0.2 and 95th percentile = 2.55); (iii) the *Akodon* group (affiliated respectively to *A. mollis, A. toba* and *A. cursor*) were constrained using the *Akodon lorenzinii* fossil record from Vorohuean Stage/Age, 2.55-2.85 Ma (Pardiñas et al. 2002) (offset = 2.55, meldian = 0.15 and 95th percentile = 2.85). The standard deviations of the lognormal distributions were adjusted so that the 95% quantile took each

maximum age (2.1, 2.55 and 2.85, respectively), with an approximate value of 0.496 for all constraints. We forced the monophyly only for *Akodon*. The dates of the Stage/Age were based on the timing of chronology of the Patagonian glaciations proposed by Rabassa and Coronato (2009).

Geometric morphometric procedures — To explore the variability of *O. quaestor* we analyzed 106 skulls of adult specimens for dorsal and ventral views for each sample and 104 for the lateral view. The complete eruption of the third molar was the criterion to separate juveniles from adults to minimize the ontogenetic effects. Two-dimensional digital images were obtained from each skull view, with a Canon PowerShot G10 camera with 14.7 megapixel resolution (4416 x 3312) in macro mode automatically and without flash or zoom to all samples. Twenty-one, forty-two and sixteen landmarks coordinates were placed on the dorsal, ventral and lateral views of the specimens, respectively, following previous geometric morphometric approach with rodents (Maestri et al. 2015; Peçanha et al. 2017; Fabre et al. 2018), using TpsDig2 software (Rohlf 2015). The description of all the landmarks employed is given in Supplementary Data 4. After the digitization, the matrix coordinates matrix was superimposed through a generalized analysis of Procrustes (GPA) in the MorphoJ 1.06b (Klingenberg 2011). This analysis aims to remove unrelated effects such as position, orientation and scale (Rohlf and Slice 1990). The size of each skull was estimated through the centroid size (CS): square root of the sum of the squares of the distances of each centroid frame (Bookstein 1991). This set was used in the analyses of geographic variation in the size based on ventral view. Procrustes-corrected shapes considering object symmetry (Viscozi and Cardini 2011). To visualize major patterns of shape variation we conducted a Principal Component Analysis (PCA) on the Procrustes-corrected shape and compared the extreme morphologies along each PC (for the first two PCs) in MorphoJ v1.06 software (Klingenberg 2011).

An analysis of variance (ANOVA) and a Tukey test was employed to test for centroid size differences among lineages. We performed multivariate analyses of variance (MANOVA) to investigate whether morphology was structured among the putative different species. However, due to unresolved taxonomic issues discussed below, we excluded all samples from localities of Joinville and Corupá (Fig. 1; Localities 10 and 46), including the holotype of *Oxymycterus judex* (BM 9.11.19.19). Thus, the PCA axes were used to visualize the placement of admixed individuals relative to raised groups, whether full dataset or reduced. The reduced dataset was used in a discriminant analysis (DA) in order to assess the correct classification percentages between the species were calculated through jackknife cross-validation analysis. In addition, the holotypes of *Oxymycterus quaestor* (BM 3.7.1.80) and *Oxymycterus misionalis* (FMNH 26756) were includes in geometric morphometric and statistical analyses (Fig. 2). MANOVAs and DAs were performed independently for each each skull view. All procedures were carried out in the software R (R Core team 2017), with the packages geomorph (Adams and Otárola-Castillo 2013) and Morpho (Schlager 2017).

RESULTS

Molecular phylogenetic analyses — A total of 1137 bp segment of *Cyt-b* were obtained from 110 individuals, including 103 novel sequences (Supplementary Data 2). The dataset contained 169 variable sites, 46 singletons and 123 parsimony-informative sites. We translated all *Cyt-b* sequences into amino acids, and no stop codon was detected. Length of nuclear dataset (non-coding *Fgb*-I7) of 89 individuals ranged from 658 bp to 675 bp, with three indels (2-bp, 12-bp and 27-bp, respectively). In subsequent analysis (e.g. genetic distance and phylogenetic), indels with more than one base-length were considered as a single mutation. Thus, the matrix was resumed to 651 bp, and

the adjusted matrix included 56 variable sites (three of which were due to the presence of indels), 3 singletons and 53 parsimony-informative sites. Additional information on the length of haplotypes obtained and the description of each individual analyzed is present in Supplementary Data 1.

Bayesian consensus tree based on mtDNA dataset (Fig. 3) revealed strong support for a monophyletic group containing all sequences assigned to *O. quaestor* (Posterior Probability (PP) = 0.91). Four well-supported clades (PP = 1) were identified within *O. quaestor*, hereafter lineages A to D. Lineage A, the sister group of lineage B and C, included sequences from Piraquara County (Paraná State, Brazil), type locality of *O. quaestor*, with a geographic distribution in northern Rio Grande do Sul, Santa Catarina and eastern Paraná. Lineage B, mainly occurred in a small area (Localities 5–7, Fig. 1) in the high altitudes in Rio de Janeiro State (Brazil) recorded in Teresópolis County area. Lineage C, included samples from two major physiognomies; (i) the Alto Paraná Atlantic Forests (Seasonal Dry forest, Fig. 1), covering the ranges of eastern Paraguay and northeast Argentina, (ii) Serra do Mar Coastal Forests (Dense Ombrophilous forest), which range the coast of the South and Southeast of Brazil, in at least São Paulo and Santa Catarina States. Lineage D, the sister group of the other three lineages, consist of specimens from the northern Rio Grande do Sul State (Brazil), occurring in a restrict area (Localities 25 and 32, Fig. 1). The species *O. rufus* and *O. josei* were recovered as sister to a strongly supported clade (PP = 0.98) formed by *O. quaestor* and lineages associated.

Results of the concatenated analysis showed a similar topology to that of the *Cyt-b* tree (Fig. 4). However, all lineages leading to *O. quaestor* and related recovered as monophyletic, but weakly supported (PP = 0.35). Similarly, lineages A to D found in *Cyt-b* tree (Fig. 3) showed low support posterior values (PP ≤ 0.49). *O. rufus* and *O. josei* was recovered as clostest clade, but with a weak support (PP = 0.56). Results of the *Fgb*-I7 matrix analyzed using BI analyses, no relationship was

resolved inter- and within the clades. The support were close to zero (PP = 0) in almost all nodes of *Fgb*-I7 tree (data not shown).

The average interspecific genetic distance (pairwise *p*-distance) among lineages were 1.97% (± 0.02%) for the *Cyt-b* dataset. Lineage A (assigned to *O. quaestor* sensu stricto) differed on average by 3.22% (± 0.52), 2.82% (± 0.49) and 5.23% (± 0.54) to lineages B, C and D, respectively; other mtDNA comparisons are depicted in Table 1. The overall intraspecific variation was 0.03% up to 0.07% in all lineages, considering the limits of standard deviation. The interspecific genetic distances based on *Fgb*-I7 were 0.7% (± 0.1) to *O. quaestor*. For this locus, relevant distances were only found between Lineage B (Teresópolis/RJ) and *O. quaestor* (Lineage A) with 1.6% (±0.2), Lineage C with 1.6% (±0.2), and Lineage D (Bom Jesus/RS) with 1.6% (±0.3). Intraspecific variation was close to 0 for *Fgb*-I7 for almost all clades, except Lineage B ranging 2.6% (± 0.4).

Divergence dating — We estimated the divergence date for the monophyletic *Cyt-b* lineages identified in the phylogenetic analyses (lineages A, B, C and D as labeled in Fig. 3 & 4) using a relaxed molecular clock. The dating analyses (Fig. 5) suggested that the most recent common ancestor of lineages leading to *O. quaestor* diverged at 0.794 Ma (95% highest posterior density (HPD) = 0.552–1.062 Ma), jointly with Lineage D divergence estimated in the Early/Middle Pleistocene. The lineages A and B+C split at 0.420 Ma (95% HPD, 0.259–0.616 Ma) in the Middle Pleistocene, further B and C Lineages split at 0.315 Ma (95% HPD, 0.173–0.482 Ma). In addition, the lineages B and C diverged in the Middle Pleistocene with probability to Late (Upper). The monophyly of the genus *Oxymycterus* was recovered, although not highly supported (PP = 0.77). The genus emerged around 1.689 Ma (95% HPD, 1.324–2.119 Ma), in the Early Pleistocene. The clade composed by *O. rufus* and *O. josei* is recovered as sister lineage with the lineages leading to

O. quaestor diverging about 1.033 Ma (95% HPD, 0.781–1.338 Ma), yet in Calabrian Stage (Middle Pleistocene).

Skull shape variation — Our reduced dataset includes 75 samples for Lineage A (*O. quaestor*), 3 for lineage B (*Oxymycterus* sp. 1), 16 for lineage C and 5 for lineage D (*Oxymycterus* sp. 2). Only for lateral view the Lineage A was 73 samples, due damage conditions insufficiently clear for landmarks (CZFURB 18723 and MCNU 2341). Highly significant differences were observed in skull shape among the four lineages whether dorsal, ventral and lateral views (Dorsal: MANOVA Wilks'λ = 0.081833, F = 5.3164, P < 0.001; Ventral: MANOVA Wilks'λ = 0.026228, F =3.3334, P < 0.001; Lateral: MANOVA Wilks'λ = 0.14073, F = 2.1865, P < 0.001). The genetic groups indicated 21.85% of the variation in the dorsal view, 15.97% in the ventral view, and 12.43% in the lateral view the *Oxymycterus quaestor* skull. The pairwise MANOVA showed significant differences in 6 of 6 for three views comparisons between the propose lineages. The R^2 and F values and significance levels are showed in Supplementary Data 5. The percentage of correct classification among the lineages were: 86.67% for the dorsal view, 82.82% for the ventral view, and 70.10% for the lateral view, the latter view with lower accuracy (Supplementary Data 5).

To visualize the shape of the skull, the principal component analysis (PCA) shows a large overlap of the dispersion clouds between the A and C lineages for all views (both total or reduced data set). Although PC2, at least for the dorsal view (Fig. 6a), indicate some separation between these lineages. However, PC1 separates the lineages D and B with distinction in all views, regardless of the data set (Fig. 6). The lateral view was the one that showed the smallest distinction between the groups. However, considering only the total data set, the samples from Joinville (type locality of *O. judex*) and Corupá (Colônia Hansa), in all the views, the dispersion clouds are inconclusive and it is not possible to determine which lineage could belong.

Skull size variation — The results of the ANOVA, show there is significant difference in size among lineages ($F = 10.78$; $P < 0.001$). Individuals from lineage D in the southernmost distribution (Fig. 1; localities 25 and 32) present the largest skulls, following the lineage C and A, whereas northernmost specimens (lineage B) have smaller skulls (Fig**.** 7). The Tukey HSD test for pairwise comparisons indicated significant differences for almost all clades ($P < 0.05$), except between lineages C and D.

DISCUSSION

Since the original description by Michael R. Oldfield Thomas in 1903, the contents and species limits of *O. quaestor* remained controversial. Few years later, Thomas (1909) described a large reddish hocicudo geographically close to Piraquara, Roça Nova, Paraná, Brazil: the *O. judex* collected in Joinville, Santa Catarina, Brazil, distinguished by its larger size and much larger brain-case when compare to *O. quaestor*. Later, Colin Campbell Sanborn in 1931 described a new species from Rio Paranay (near Caraguatay), Misiones Province, and when compared with *O. judex* topotypes, concluded that these specimens from Misiones Province belong to a distinct species, mainly by being larger than *O. judex* (on average body length), a longer, narrower, and flatter skull. Another remarks that must be considered is that together with the description of *O. quaestor* (1903), it is Oldfield Thomas indicated the presence of similar specimens from *Theresopolis*, *Rio Janeiro* (i.e. Teresópolis, Rio de Janeiro) and Santa Catarina (limited information in original description).

Due to the overall external similarity among large reddish hocicudos forms from Argentina, Paraguay and especially from South/Southeastern Brazil, an uncertain taxonomic history is associated to this group. Some authors as Cabrera (1961) and Reig (1987) includes it as junior

synonyms of *O. hispidus*. Except Oliveira (1998) and Hoffmann et al. (2002), several publications have referenced species designed to reddish rodents (i.e. *O. quaestor*, *O. judex* and *O. msionalis*), however without dataset treatment refined or criteria (Hershkovitz 1994; Fonseca et al., 1996; Galliari et al. 1996; Heinonen-Fortabat and Chebez, 1997; Graipel et al. 2006; Oliveira and Bonvicino 2006; Pardiñas et al. 2007; D'Elía et al. 2008; Bonvicino et al. 2008; Jayat et al. 2008; Paglia et al. 2012).

The most robust morphological review of the genus Oxymycterus was performed by Oliveira (1998), including comparisons with holotypes of three large reddish forms (*O. quaestor*, *judex* and *misionalis*). Based on linear measurements of skulls, these vouchers indicated performing a unique morphometric group called "*judex* group" (probably mistakenly, since *O. quaestor* is the oldest available name). Posteriorly, Hoffmann et al. (2002) in genetic and morphological analyses largely supported the existence of the "*judex group*" proposed by Oliveira (1998), but fail due misidentification between of these samples three species for this group (obviously due to being one of the reasons that drive this study). In addition, Cyt-*b* sequences of two specimens (annotated to *judex* and *quaestor*) is congruent for interspecific distances divergence (~ 2.8 %) (Hoffmann et al. 2002, Jayat et al. 2008). However, the sequences referred to *judex* by Hoffmann et al. (2002), according in our phylogenetic results belong the Lineage C (Fig. 3, 4 & 5). In this sense, the samples named to *quaestor* by Hoffmann et al. (2002) are present in Lineage B (*Oxymycterus* sp. 1), composed by samples from Teresópolis/RJ. The genetic distance found by Hoffmann et al. (2002) and Jayat et al. (2008) reflect similar results when compare the genetic distance between lineage B and C in Table 1. Notably, as mentioned above, this inaccuracy for the area of Teresópolis/RJ, may be correlated with the original description of *O. quaestor*, which further indicating specimens present in Santa Catarina, also points out vouchers from Teresópolis/RJ. In addition, D'Elía et al. (2008) mentioned that Cyt *b* haplotype recovered from Paraguay are

divergent around 0.5% when compare from Argentina and São Paulo State samples (São Paulo sequence deposited in Genbank by Hoffmann et al. under the tag *O. judex*), and also presents ~2.8% divergent from sequences from Teresópolis/RJ (wrongly deposited in Genbank by Hoffmann et al. under the tag *O. quaestor*, for reasons explained further). Gonçalves and Oliveira (2004) also deposited two sequences from Teresópolis/RJ, identified for lineage C and attributed to *O. quaestor* in Genbank. D'Elía et al. (2008) also raise an inaccuracy about *O. misionalis* limits. In brief, the genetic distances taken by D'Elía et al. (2008) against samples from Argentina and the State of São Paulo, presented a similar value for intraspecific genetic distance (Table 1), because they form a unique clade, named in our analyses as lineage C (Fig. 3 & 4). Furthermore, the distance 2.8% against *O. quaestor* (which is in fact identified into lineage B in our analyses) presents an inaccuracy, due a previously misconception above cited.

Although Musser and Carleton (2005), and more recently Oliveira and Gonçalves (2015) revision treat *O. judex* and *O. misionalis* as junior synonyms of *O. quaestor*, we understand that the relationship among large reddish hocicudos from the Atlantic Forest is yet unresolved taxonomic issue within the genus *Oxymycterus*. Thus, based on geometric morphometrics and phylogenetic analyses (as already mentioned above), in an effort to provide greater resolution of the relationships within *quaestor* group (also called here as large reddish hocicudos), detecting 4 lineages divergent at specific level, clarifying the patterns of this confusing taxonomic group than those obtained in previous studies.

Oxymycterus quaestor 'sensu stricto' — One of the most unexpected results of this study was that none of Cytochrome *b* sequences deposited in Genbank annotated to *Oxymycterus quaestor*, *O. judex* or *O. misionalis* (Supplementary Data 2), correspond in fact to the lineage evidenced in this study belonging to *Oxymycterus quaestor*. Based on the sequence of the *Cyt-b* gene (mtDNA),

differences were found between *O. quaestor* and the other lineages presents (ca. ≥ 2.82%, Table 1), with a highlight the lineage D with more than 5%. Although there a proposal about the degree of interspecific difference on genus *Oxymycterus* around 3.6% (Baker and Bradley 2006), sequence level that would evidence of distinction between species (considering the lineages B e C), does not support the formally evidence of different species. However, others valid species in this genus have a lowest divergence with *cyt-b* sequences, for example, the genetic distance between *O. rufus* and *O. josei* that presents a distance less than 2% or the case of *O. amazonicus* and *O. delator* that varied 2.71% (Hoffmann et al. 2002). Previous studies with sigmodontines rodents indicated low degree of resolution within the *Fgb*-I7 sequences relative to the *cyt-b* sequences (Carrol and Bradley 2005; Henson and Bradley 2009; Peçanha et al. 2017). In *O. nasutus* for example, showed low intraspecific divergence (close to 0) with de same nuclear locus (Peçanha et al. 2017). In this sense, comparisons with *Sigmodon* species for intra- and interspecific genetic distance values ranging 0.28 up to 1.6% to intraspecific and, 0.43 up to 6.38% to interspecific divergence (Carrol and Bradley 2005; Henson and Bradley 2009). Such this way, values presented in Table 1 for *Fgb*-I7, ranging 0.5% up to 1.6%, corroborate in distinguishing this lineage with the others. It is of interest to note the low genetic variation of *O. quaestor Cyt-b* haplotypes (average within clade genetic divergence is 0.5%) and the lack of phylogenetic relationships. Treated as lineage A in phylogenetic analysis (Fig. 3 & 4), this clade have sequences from 4 samples of Piraquara County (Paraná State, Brazil), included 3 from Mananciais da Serra/PR locality. The type locality of *O. quaestor* (described by Thomas in 1903 to Piraquara, Roça Nova/PR) it is located less than 3 kilometers from the sequences obtained from this study. Such results reinforces that populations from this locality belong and represent *O. quaestor*, as well as the other members of clade (Fig. 3, 4 & 5).

Regarding the geographic distribution, considering the data collected in this study, *Oxymycterus quaestor* is present in the domains of Southernmost Atlantic Forest range, across the

northern Rio Grande do Sul, Santa Catarina and central-eastern Paraná State in Brazil. Thus, distributed by the Brazilian Southern Plateau, limited by coastal mountains range (Serra do Mar, PR; Serra Geral, SC/RS, +1000 m) and lowlands until now in Santa Catarina coast almost in sea level (Fig. 5). Occupying mainly Mixed Ombrophilous Forest (Araucaria moist Forest) and Atlantic Forest grasslands (*campos de altitude*), but to a lesser extent in Dense Ombrophilous Forest (Serra do Mar Coastal Forest) in Santa Catarina State and Paraná State. We do not rule out the occurrence in areas of Seasonal Dry forests (Alto Paraná Forests) in Rio Grande do Sul State (Fig. 1).

Despite the PCA's display does not show a clear distinction, especially with the lineage C, the set of results obtained corroborate to which lineage A belongs to *O. quaestor*. The PCA's showed a difference between *O. quaestor* (lineage A) and lineages D and B, mainly considering PC1 in all views and datasets. Regarding the size observed in the skulls, statistically significant differences were observed through ANOVA and Tukey multiple comparisons, where it is plotted in an intermediate position, larger than the lineage B, but smaller than lineages D and C. In addition, the pairwise MANOVA for comparisons of skull shape indicates morphological high support differences between all the proposed groups, independent of the analyzed view. Lastly, the cross-validated classification results showed a classification accuracy more than 83% for this group. Except the Lineage B (*Oxymycterus* sp.1), *O. quaestor* have the smallest skulls in the group (Fig. 7). Furthermore, the BI with mtDNA and concatenated dataset (Fig. 3 & 4) are compatible with a scenario in which current populations are relatively young and would have colonized their current distribution recently. The lack of support on the internal nodes in phylogenies proposed further supports this idea. The time calibrated-tree show that probably occupied their contemporary occurrence area in the Middle Pleistocene with probability to expansion in Late Pleistocene (Fig. 5). A detailed phylogeographic study including time calibrated-tree, ancestral area reconstruction, neutrality tests and demographic analyses is needed to test this hypothesis.

Oxymycterus judex and O. misionalis – Given the topology of the *Cyt-b* gene tree (Fig. 3), the lineage C presents two subclades with low support. One including sequences from eastern Paraguay (Canindeyú Department) and northeastern Argentina (Misiones Province), associated to Seasonal Dry Forests (Alto Paraná Forest) and another in western Paraná State (in Seasonal Dry Forests), São Paulo and Santa Catarina State mainly in Dense Ombrophilous Forest (Serra do Mar Coastal Forest). Although we do not included sequences from locality type of *O. misionalis*, we incorporated *Cyt-b* sequence from Genbank (voucher CNP 851; Supplementary Data 1 and 2) from the locality Reserva Valle del Arroyo Cuña Pirú (Misiones, Argentina) as a represent more closely to type locality Libertador General San Martín, Misiones Province, Argentina (Pardiñas et al. 2007). Interestingly, the unique voucher sequenced for *Cyt-b* from Joinville locality (CZFURB 0942) appears included in this lineage in phylogenetic analyses (Fig. 3 & 4). Also, some samples from the Joinville (Estação Ecológica Bracinho do Piraí/SC), Corupá (Colonia Hansa/SC) localities and *O. judex* holotype (BM 9.11.19.19; Joinville/SC) did not present a pattern through scatterplots with other Lineage C samples (from Argentina, Paraguay and São Paulo State, Brazil) and can be verified between the dispersion of samples of *O. quaestor* (Fig. 6).

In this way, suggesting that areas around Joinville locality may harbor an area of sympatry (or syntopy), or even suggesting a role of local selection pressures as drivers of skull evolution. At first, our data suggest occurrence of secondary contacts among previously isolated lineages, although further studies are required to clarify this issue (Fig. 5). The geometric morphometric approach using data from coordinates of landmarks unrevealed clear differences in skull shape when compared with *O. quaestor* in the PCA's, even using the reduced dataset. As a reflection of this similarity in scatterplots the lineage C obtained less precision in cross-validated classification (37.5% for lateral, 62.5% for dorsal and 75% for ventral view), with most of the specimens being

classified as *O. quaestor*. Grids warped showed narrower skulls (mainly by PC1 in dorsal and ventral views) when compare with *O. quaestor*. However, only Tukey multiple comparisons for size, do not show differences statically with lineage D (with *Oxymycterus* sp. 2). Both probably are the largest lineages in *quaestor* group (Supplementary Data 5). Exploring the full dataset results in geometric morphometrics, the PCA's (Fig. 6) did not clearly show which lineage belongs to the samples from the Joinville and Corupá regions. Thus, we do not rule out the hypothesis that the holotype of *O. judex* (BM 9.11.19.19) is in fact a sample of *O. quaestor*, although the only sequence obtained for Joinville (Santa Catarina) remained in the same sequence lineage credited to *O. misionalis*. As mentioned previously, the description of *O. quaestor* presents a remark including similar specimens from Santa Catarina State, which does not rule out the hypothesis that can be included as a morphological variation of *O. quaestor*. Future sampling of molecular-based studies should include topotypical material as a way to tie names to clades with a good certainty for both. As explain above, reinforce designation of *O. judex* (Thomas, 1909) under *O. misionalis* (Sanborn, 1931) may in a way to be consistent with taxonomic traditional usage, but acknowledge that until topotypical material is assessed, nomenclatorial uncertainty will remain. Pardiñas et al. (2007) restricted the type locality to *O. misionalis* (to confluence of the río Paranay-Guazú with the río Paraná, Libertador General San Martín, Misiones) increasing accuracy for future approaches and records in the region. A similar approach, it could be applied to *O. judex* in precise attempt to distinguish them. The description of *O. judex* by Thomas in 1909 is only reported from "*Joinville, Santa Catherina*" (i.e. Santa Catarina) and additional information is not presented. It is worth emphasizing that at the beginning of the twentieth century, the municipality of Joinville had several districts, nowadays already emancipated in several cities in the South of Brazil (Santa Catarina state), which represented an extensive territory at that time, greater than it is today. In addition, the Atlantic Forests present in Southern Brazil suffered several economic cycles of deforestation,

logging and multiple uses, subjected to a variety of disturbances (Souza et al. 2012), mainly the *Araucaria angustifolia* deforestation since in early century 20th (Behling et al. 2009). Although not conclusive, such actions of environment modification during these hundred years after the original description, can affect future records, since no taxonomic approach was explored.

Future sampling efforts should include more representatives of the lineage C (or another samples record under tag *O. misionalis*/*judex* in scientific collections) to elucidate with more precision the geographical distribution of this lineage, as well as the distinction of *O. misionalis* and *judex*.

Two additional species-level lineages — In addition to providing further support for the distinction of *O. quaestor* and *O. judex*/*misionalis*, our study provides evidence for the existence of 2 additional species-level lineages within the *O. quaestor* species group, which are herein referred as *Oxymycterus* sp. 1 (lineage B) and *Oxymycterus* sp. 2 (lineage D) (Fig. 3, 4 & 6; Supporting Information S2). These two lineages were identified on the basis of the phylogenetic and geometric morphometrics analysis, respectively. The specimens sequences of *Oxymycterus* sp. 1 call attention to the restricted geographic ranges, restricted in high elevation (871m or more) in Serra dos Órgãos (northernmost domains of Serra do Mar mountain range) in Teresópolis county area, Rio de Janeiro State, Brazil (Fig. 1 — 5-7 localities; Fig. 5; Lineage B). This lineage appears as sister clade position for lineage C (*O. misionalis*/*judex*; Fig. 3, 4 & 5) with an average genetic distance of 2.62% for *Cyt-b* and 1.6% for *Fgb*-I7 (Table 1). Although the distance of the mitochondrial locus is lower than expected, considering the limits of sister lineages propose by Baker and Bradley (2006), the nuclear distance is highly divergent in relation to the lineage C, when compared to other studies with hocicudos (Peçanha et al. 2017). Few individuals was used for the proposed morphometric analysis; however, they presents distinct shape from the other lineages mainly by PC1 in all views

propose (Fig. 6), in addition to the smaller size (Fig. **7**). These facts of moderate to high genetic distance divergence, geometric morphometric results, MRCA and isolate geographic ranges, support the idea of one recent divergent lineage.

Oxymycterus sp. 2 was detected from 2 localities in the northern Rio Grande do Sul State: Bom Jesus and Bom Jesus/Paiquerê, both above 1000m (Fig. 1**;** Localities 25 and 32). These two localities are present in a transitional zone between Mixed Ombrophilous forests (Araucaria moist forest) and Atlantic Forest grasslands (*campos de altitude*) in high altitudes. The region are inserted near from Serra Geral mountain range, it is a mountain and deep valleys cutting the edge of the plateau, forming canyons. This lineage has diverged at the *Cyt-b* gene on average by 5.23% from *O. quaestor* (lineage A), 5.89% from *Oxymycterus* sp. 1, and 6.09% from *O. misionalis/judex* (lineage C) and 0.5 up to 1.6% with *Fgb*-I7 locus (Table 1). These results corroborate clearly that it is a new taxon, if considered the boundaries of Baker and Bradley (2006) and others studies exploring interspecific limits of nuclear locus (Carrol and Bradley 2005; Henson and Bradley 2009). This lineage presents distinct shape from the other lineages mainly by PC1 in all views propose (Fig. 6) and probably are the representatives of genus *Oxymycterus* with the largest and narrowest skulls (Fig. 7). According the dating estimates, *Oxymycterus* sp. 2 emerged as the most basal taxon of *quaestor* group, split at ca. 0.794 Ma (in the Early/Middle Pleistocene) from other lineages promoted in this study. In addition, the geometrics morphometrics approach showed differences in all views propose for others lineages and *Oxymycterus* sp 2. However, the locality Bom Jesus (Fig. 1; Localities 25) are record the presence of *O. quaestor* as well. Additional assessment about the sympatry with *O. quaestor* will be necessary to explore this issue.

Timescale of diversification — Our study estimated that the *Oxymycterus* diverged from *Juscelinomy*s in the Early Pleistocene (Calabrian Stage), around 1.977 Mya (95% HPD, 1.451–

2.627 Ma), based on mitochondrial *Cyt-b* gene. This estimate is incongruent and newer than the previous estimate obtained by Parada et al. (2013, 2015) and Steppan and Schenk (2017), which detected a divergence date of ~2.6 Mya (Late Pliocene/ Early Pleistocene). However, they did not include an exhaustive sample set and fossils of *Oxmycterus* species available, which may have biased their dating results using a multilocus approach. It is worth emphasizing that estimated theses dating on focus to Subfamily Sigmodontinae (Parada et al. 2013, 2015) and Superfamily Muroidea (Steppan and Schenk 2017) divergence, respectively. Herein, we estimating the first calibrate time-tree for genus *Oxymycterus*, using mtDNA *Cyt-b* gene and fossils calibrations, revealing the MRCA emerged around 1.689 Ma (95% HPD, 1.324–2.119 Ma), in Early Pleistocene. As with the divergence with *Juscelinomys*, our estimate for *Oxymycterus* also emerges more recent than the other previous studies suggest. The molecular phylogeny obtained in this study supports a monophyletic *Oxymycterus* genus, although with weakly supported (PP < 0.90). The '*quaestor* species group' formed a sister-clade with *O. rufus* and *O. josei*, in all phylogenetic approaches using mtDNA promoted in this study (Fig. 3 & 5, PP = 1 and PP = 0.90), recovering the same topology from other rodents previous phylogenies (Fabre et al. 2012; Parada et al. 2015; Steppan and Schenk 2017), and according our estimative, the divergence about 1.033 Ma (95% HPD, 0.781–1.338 Ma) in the Middle Pleistocene. Leite et al. (2014) reveal during the late Pleistocene, the akodontine genera *Akodon* and *Oxymycterus* have increase rates of diversification, three times higher than others Akodontini rodents. The Bayesian relaxed molecular clock analysis (Fig. 5), although not all species of *Oxymycterus* are present (11 of 16 current valid species) reveal part of this high diversification rate suggest by Leite et al. (2014), due to the presence of 2 cryptic lineages related to *O. quaestor*, 3 lineages for *rufus* group (*O. rufus* "Argentina", *O. rufus* "Brazil" and *O. josei*) and 3 lineages for *paramensis* group (lineages herein treated as Peru, Bolivia and Argentina). Through these inferences, we can presume that the alpha taxonomy is still poorly known and target

of challenges. In our calibrations, demonstrating that the *quaestor* group emerged at 0.794 Ma (95% HPD = 0.552–1.062 Ma) in the Early/Middle Pleistocene. Thus, the diversification timing raised in this study, suggests that Quaternary climatic cycles (highlighting Middle Pleistocene) might have played a role in the diversification of this lineages, as observed in previously sigmodontines studies with similar distribution such as *Akodon paranaensis* (Gonçalves et al. 2007), *Delomys* (Gonçalves and Oliveira 2014), further the congeners *Oxymycterus nasutus* (Peçanha et al. 2017) and *Oxymycterus itapeby* (Peçanha et al. 2019). Comparing the diversification times found in the calibrated phylogeny, the timing of lineages split corroborates with the transition of glacial-interglacial periods during the mid-Pleistocene, according to chronostratigraphy for geological time scale based on marine isotopes stages (Cohen and Gibbard 2011).

Our results lead us to understand that the large reddish hocidudos lineages (previously also treat here as *quaestor* group) have a great endemism in the southern Atlantic Forest, with moderate to high genetic diversity among lineages and probably stable population sizes along the geographic distribution.

Biogeography Inferences: ongoing diversification process in Atlantic Forest — Studies have identified areas of palaeoclimatic stability in South America (Werneck et al. 2011; Costa et al. 2017), and may to indicate potential refugia areas for quaestor group during interglacial/glacial periods and how the lineages were shaped. Concerning for Seasonal Dry Forests, the north-eastern Argentina, south-eastern Paraguay and a minor fragment in the Brazilian State of Mato Grosso do Sul seems to have experienced long-term stability (occurred since the Last Glacial Maximum [LGM] ~ 21 kyr BP) as a refugium for the glaciations to Dry Forests; nonetheless, there appear to be retraction in dry periods of the Pleistocene followed by expansion from refugia during interglacial periods (Werneck et al. 2011; Carnaval and Moritz 2008). However, Dry Forests from

São Paulo State appear as mosaic with unstable/stable regions according the authors predictions. Costa et al. (2017) identified stable areas from LGM until current from Southern Atlantic Forest, notably for high altitudes as Cambará do Sul/RS locality (Serra Geral mountain range and areas on Paraná, Santa Catarina States on meridional plateau) and São Paulo State at least Serra do Mar range. However, no there detail data about habits concerning *quaestor* group, although some authors describe presence in wetlands and altered vegetation in Mixed Ombrophilous Forest (Graipel et al. 2006) or even associated with abandoned crop fields or low secondary forests (Grazzini et al. 2015, D'Elía et al. 2008). Due the considerations suggested by these authors, it is possible for these lineages to occupy either open areas (grasslands) or forest, and probably one of the reasons for the wide dispersion along almost the entire South Atlantic Forest. The descritption of these studies corroborated with a persistence and distributions of lineages along the Southern Atlantic Forest, both in the *campos de altitude* (high-altitude zones) or in the forests formations in meridional plateau. The temporally stable areas plausibly may persistence and harbor moderate population stocks during climatic fluctuations, and also expected to maintain high genetic diversity than unstable recently colonized areas, and a (strong) phylogenetic structure marked between refugia (Hewitt 2004; Carnaval et al. 2009). Thus, the preliminary biogeographic and phylogeographic patterns of large reddish hocicudos coincide with the new models of dynamic forest refuges for southern Atlantic Forest which has a strong montane and subtropical component, and may be associated with taxa adapted to cold (Carnaval et al. 2014). A remarkable issue is the relationship between grasslands (*campos de altitude*) and forests during the late Quaternary (Upper Pleistocene and Holocene shifts) documented through of pollen records in the South and Southeast of Brazil (Behling 2002; Behling et al. 2004; Behling et al. 2005). These studies show general patterns of open areas (grasslands) up to the last glacial period (42,000-10,000 years BP) in the Pleistocene (encompassing the LGM), with the rise of forest formations into late Holocene and

climate drier and cooler than interglacial periods (Overbeck et al. 2007; Behling et al. 2009). However, combining palynological data and climate stability prediction models, Costa et al. (2017) suggests that the South and Southeast of Brazil may not have been a homogeneous area during Pleistocene and likely multiple small forest refugia may have existed during the grassland stage, allowing for a rapid forest expansion when the climate shifted to conditions favourable to a tropical forest, such as continental shelf that during the LGM, which could have allowed forests and forest-adapted species (small mammals in Atlantic Forest) to expand (Leite et al. 2016). Thus, the microrefugia, it seems to have a role in keep the diversity across the time in highlands and higher latitudes of Southern Atlantic Forest (Rull 2009). Here, although being speculative, our findings may suggest that quaternary climatic changes promoted diversification in these lineages, sometimes by isolation through high altitudes (vs plateau) or even by conditions of environmental stability, mainly during the glaciations. Nevertheless, according Gonçalves et al. (2007) patterns of phylogenies of Sigmodontinae in *campos de altitude* may be more complex than suggested by the palynological and paleoclimate data suggest and, which could represent mosaics of lineages shaped by different historical events.

Therefore, despite the *quaestor* group have a distribution across the meridional and Atlantic plateau, with similar distribution shape to *Akodon paranaensis* (Gonçalves et al. 2007), we do not identified lack of reciprocal monophyly between Atlantic plateau lineage (lineage B, *Oxymycterus* sp. 1) or and the others 3 lineages more related to meridional plateau (on the contrary, all clades well-resolved and highly supported for mtDNA analyses). In this way, such patterns suggest the connection among the highlands (Serra dos Órgãos) and meridional plateau lineages was ceased. However, we cannot disagree totally from Gonçalves et al. (2007), due the Bom Jesus locality (inserted in *campos de altitude* near from Serra Geral) presents both *O. quaestor* lineage (lineage A) or *Oxymycterus* sp. 2 (lineage D), evidencing that these lineages still maintains contact. For the

latter case, past events may have brought into contact two previously isolated lineages, or even limited to sympatry (or syntopy) during the climatic oscillations of the Pleistocene, and that for some reason still to be explored is taxonomically recognizable as a distinct evolutionary unit.

Apparently, none of the large volume or extension rivers, such as Pelotas (Uruguay), Iguaçu (Iguazu), Paraná, Paranapanema and Tietê seemed to have an influence on the isolation or vicariance in the lineages presented, although recent studies inferred that rivers might acted as semipermeable barriers along the time (Hurtado and D'Elía 2018). Thus, the time of divergence and/or the reconstruction of the ancestral distribution would be useful to describe the patterns of speciation and biogeographical pathways.

However, the *quaestor* group is not the only lineage/species of the genus with diversification process influenced by climatic oscillations of the Pleistocene. In addition to the lineages evidenced, in the end of the Pleistocene other groups, such as sister-clade (Fig. 5) *O. rufus*, distributed from Argentina and southeastern Brazil, seems to be similar diversification process between Pampas biome (Pampas Humedos) towards to south and in secondary forest areas in Atlantic Forest to north of geographic distribution.

CONCLUSION

This study shows that our knowledge on the alpha-taxonomy of *Oxymycterus* is still partial. For instance, the *cyt-b* and concatenated tree revealed at least two potential candidate species related with *O. quaestor* (Figure 3 & 4). For example, the *Oxymycterus* sp.2 (lineage D, Bom Jesus/RS) that perform a sister group with other *Oxymycterus quaestor* and lineages associated, and the *Oxymycterus* sp.1 (lineage B, Teresópolis/RJ) and represent a distinct species given its moderated divergence from its sister group (see genetic distances among clades in Table 1). In addition,

despite that Bayesian Inference presents results more consistent than geometric morphometric analyses, we have demonstrated in this study strong evidence (mainly based on *p*-distance and phylogenetic analyses) that *Oxymycterus quaestor* is indeed a valid and distinct species of specimens with similar appearance, which were along of the years attributed to *O. judex* and *O. misionalis*. However, due to the lack of additional data (both molecular and morphological) infer that lineage C belong to *O. judex* or *O. misionalis*, we suggest to consider it as a candidate revalidation species that needs to be further studied as well as phylogeographic aspects.

ACKNOWLEDGEMENTS

We thank B. Patterson (Field Museum of Natural History, Chicago, Illinois), F. Passos (Universidade Federal do Paraná, Brazil), J. Gualda (Museu de Zoologia da USP, Brazil) A. Franco (Museu de Zoologia da PUC-PR, Brazil), I. Sbalqueiro (Universidade Federal do Paraná, Brazil) and A. Silva Junior (Museu de História Natural Capão da Imbuia, Brazil) for allowing us to access and photograph specimens from their collections. We are also grateful to C. Conroy and J. Patton (Museum of Vertebrate Zoology, University of California/Berkeley, California) and R. Owen (Texas Tech University, Lubbock, Texas) for the loan of the tissue samples and access to photograph. We thank P. Cordeiro Estrela (Universidade Federal da Paraíba) by the images of the type series and E. Rachenberg (Universidade Regional de Blumenau) for helping with the laboratory work. This research was supported by the Coordenação de Aperfeiçoamento de Pessoal de Nível Superior (CAPES), Fundação de Amparo à Pesquisa do Estado do Rio Grande do Sul (FAPERGS-PRONEX/CNPq2015) and Conselho Nacional de Desenvolvimento Cientifico e Tecnológico (CNPq).

SUPPLEMENTARY DATA

Supplementary Data SD1. — Description of all sample of *Oxymycterus quaestor* used included in this study.

Supplementary Data SD2. — Genbank accession codes and target locus used in phylogenies reconstructions for mtDNA and concatenated approaches.

Supplementary Data SD3. — All sequences retrieve and deposited in Genbank used for reconstructed the time calibrated-tree.

Supplementary Data SD4. — Description and definition of landmarks positioned for each skull views.

Supplementary Data SD5. — General Supplementary tables results. Jackknife Cross-validation (A), Tukey HSD, honest significant difference (B) and pairwise MANOVA (C).

LITERATURE CITED

Adams, D. C. and E. Otárola-Castillo. 2013. geomorph: and R package for the collection and analysis of geometric morphometric shape data. Methods Ecol. Evol 4: 393-399.

Baker, R. J., and R. D. Bradley. 2006. Speciation in mammals and the genetic species concept. Journal of Mammalogy 87:643–662.

Behling, H. 2002. South and southeast Brazilian grassland during Late Quaternary times: a synthesis. Palaeogeography, Palaeoclimatology, Palaeoecology 177:19–27.

Behling, H., V. D. Pillar, L. Orloc, and S. G. Bauermann. 2004. Late Quatemary Araucaria forest, grassland (*Campos*), fire and climate dynamics, studied by high-resolution pollen, charcoal and multivariate analysis of the Cambara do Sul core in southern Brazil. Palaeogeography, Palaeoclimatology and Palaeoecology 203:277–297.

Behling, H., V. Jeske-Pieruschka, L. Schüler, and V. Pillar. 2009. Dinâmica dos campos no sul do Brasil durante o Quaternário Tardio. *In*: Campos Sulinos – Conservação e Uso Sustentável da Biodiversidade (V. Pillar, S. C. Müller, Z. M. Souza Castilhos, and A. V. A. Jacques, eds.). Ministério do Meio Ambiente, Brasília 13–25.

Behling, H.; Pillar, V.D. and Bauermann, S.G. 2005. Late Quaternary grassland (Campos), gallery forest, fire and climate dynamics, studied by pollen, charcoal and multivariate analysis of the São Francisco de Assis core in western Rio Grande do Sul (southern Brazil). Review of Palaeobotany and Palynology 133 (3-4): 235-248.

Bonvicino, C. R., J. A. Oliveira, and P. S. D'Andrea. 2008. Guia dos Roedores do Brasil, com chaves para gêneros baseadas em caracteres externos. OPAS/OMS, Rio de Janeiro, Centro Pan-Americano de Febre Aftosa. 120p.

Bookstein, F.L. (1991) Morphometric Tools for Landmark Data. Geometry and Biology. Cambridge University Press. 435 p.

Bradley, R. D. and R. J. Baker. 2001. A test of the genetic species concept: cytochrome-*b* sequences and mammals. Journal of Mammalogy 82:960–973.

Bradley, R.D., and D.D. Henson. 2009. Molecular systematics of the genus *Sigmodon*: results from mitochondrial and nuclear gene sequences. Can J Zool 87(3): 211–220.

Cabrera, A. 1961. Catalogo de los mamiferos de America del Sur. II (Sirenia, Perissodactyla, Artiodactyla, Lagomorpha, Rodentia). Revista del Museo Argentino de Ciencias Naturales "Bernardino Rivadavia" (Zoologia) 4: 309-732.

Carnaval, A.C. and Moritz, C. 2008. Historical climate modelling predicts patterns of current biodiversity in the Brazilian Atlantic forest. Journal of Biogeography 35, 1187– 1201.

Carnaval, A.C., Hickerson, M.J., Haddad, C.F.B., Rodrigues, M.T. & Moritz, C. 2009. Stability predicts genetic diversity in the Brazilian Atlantic Forest hotspot. Science 323, 785–789.

Carnaval, A.C., Waltari, E., Rodrigues, M.T., Rosauer, D., VanDerWal, J., Damasceno, R., Prates, I., Strangas, M., Spanos, Z., Rivera, D., Pie, M.R., Firkowski, C.R., Bornschein, M.R., Ribeiro, L.F., and Moritz, C. 2014. Prediction of phylogeographic endemism in an environmentally complex biome. Proc. R. Soc. B. 281(1792).

Carroll, D.S., and Bradley, R, D. 2005. Systematics of the genus *Sigmodon*: DNA sequences from beta-fibrinogen and cytochrome *b*. Southwest. Nat. 50(3):342–349.

Cohen, K. M., and Gibbard, P. L. 2011. Global chronostratigraphical correlation table for the last 2.7 million years: Subcommission on Quaternary Stratigraphy (International Commission on Stratigraphy), Cambridge, England. http://www.stratigraphy.org/index.php/ics-chart-timescale (accessed July 7, 2017).

Costa, G. C., et al. 2017. Biome stability in South America over the last 30 kyr: inferences from long-term vegetation dynamics and habitat modeling. Global Ecology and Biogeography 1–13.

D'Elía, G., Mora, I., Myers, P. and Owen, R.D. 2008. New and noteworthy records of Rodentia (Erethizontidae, Sciuridae,and Cricetidae) from Paraguay. Zootaxa 1784, 39-57.

Darriba, D., G. L. Taboada, R. Doallo, and D. Posada. 2012. Jmodeltest 2: more models, new heuristics and parallel computing. Nature Methods 9:772.

Di-Nizo, C.B., K.R.S. Banci, Y. Sato-Kuwabara, M.J.J.Silva. 2017. Advances in cytogenetics of Brazilian rodents: cytotaxonomy, chromosome evolution and new karyotypic data. CompCytogen, 11(4): 833–892.

Drummond, A. J. and A. Rambaut. 2007. BEAST: Bayesian evolutionary analysis by sampling trees. BMC Evol. Biol. 7: 214. http://beast.bio.ed.ac.uk/. Accessed 10 May 2016.

Fabre, P. H., A. H. Reeve, Y. S. Fitriana, K. P. Aplin, and K. M. Helgen. 2018. A new species of *Halmaheramys* (Rodentia: Muridae) from Bisa and Obi Islands (North Maluku Province, Indonesia). Journal of Mammalogy 99:187–208.

Fabre, P-H., L. Hautier., D. Dimitrov, E.J.P. Douzery. 2012. A glimpse on the pattern of rodent diversification: a phylogenetic approach. BMC Evolutionary Biology 12:88.

Fonseca, G.A.B., Herrmann, G., Leite, Y.L.R., Mittermeier, R.A., Rylands, A.B. and Patton, J.L. 1996. Lista anotada dos mamíferos do brasil. Occasional papers on conservation biology 4:1-38.

Galliari, C.A., Pardiñas, U.F.J. and Goin, F.J. 1996. Lista comentada de los mamíferos argentinos. Mastozoología Neotropical 3(1): 39–61.

Gonçalves, P. R., and J. A. Oliveira. 2004. Morphological and genetic variation between two sympatric forms of *Oxymycterus* (Rodentia: Sigmodontinae): an evaluation of hypotheses of differentiation within the genus. Journal of Mammalogy 85:148–161.

Gonçalves, P. R., and J. A. Oliveira. 2014. An integrative appraisal of the diversification in the Atlantic forest genus *Delomys* (Rodentia: Cricetidae: Sigmodontinae) with the description of a new species. Zootaxa 3760:001–038.

Gonçalves, P. R., P. Myers, J. F. Vilela, and J. A. Oliveira. 2007. Systematics of species of the genus *Akodon* (Rodentia: Sigmodontinae) in southeastern Brazil and implication for the biogeography of the Campos De Altitude. Miscellaneous Publications. Museum of Zoology, University of Michigan 197:1–24.

Graipel, M.E., J.J. Cherem, E.L. Monteiro-filho, and L. Glock. 2006. Dinâmica populacional de marsupiais e roedores no Parque Municipal da Lagoa do Peri, Ilha de Santa Catarina, sul do Brasil. Mastozoología Neotropical 13(1): 31-49.

Grazzini, G., C.M. Mochi-Junior, H. Oliveira, J.S. Pontes, F. Gatto-Almeida, and L.M. Tiepolo. 2015. Identidade, riqueza e abundãncia de pequenos mamíferos (Rodentia e Didelphimorphia) de área de Floresta com Araucária no estado do Paraná, Brasil. Papéis Avulsos de Zoologia (São Paulo) 55(15):217-230.

Hall, T. A. 1999. BioEdit: a user-friendly biological sequence alignment editor and analysis program for windows 95/98/NT. Nucleic Acids Symposium Series 41:95–98.

Heinonen Fortabat, S. and J. C. Chebez. 1997. Los mamíferos de los Parques Nacionales de la Argentina. Literature of Latin America, Monografía. N. 14. 70 p.

Hershkovitz, P. 1994. The description of a new species of South American hocicudo, or long-nose mouse, genus *Oxymycterus* (Sigmodontinae, Muroidea), with a critical review of the generic content. Fieldiana: Zoology (New Series) 79:1–43.

Hewitt G. 2004. Genetic consequences of climatic oscillations in the Quaternary. Philos. Trans. R. Soc. Lond. B: Biol. Sci. 359: 183-195.

Ho, S.Y.W., and M.J. Phillips. 2009. Accounting for calibration uncertainty in phylogenetic estimation of evolutionary divergence times. Syst Biol 58:367–380.

Hoffmann, F. G., E. P. Lessa, and M. F. Smith. 2002. Systematics of *Oxymycterus* with description of a new species from Uruguay. Journal of Mammalogy 83:408–420.

Hurtado, N., and G. D'Elía. 2018. A new species of long-tailed mouse, genus *Oligoryzomys* bangs, 1900 (rodentia: cricetidae), from the bolivian yungas. Zootaxa 4500:341–362.

Jayat, J. P., G. D'Elía, U. F. J. Pardiñas, M. D. Miotti, and P. E. Ortiz. 2008. A new species of the genus *Oxymycterus* (Mammalia: Rodentia: Cricetidae) from the vanishing Yungas of Argentina. Zootaxa 1911:31–51.

Katoh, K., and D.M. Standley. 2013. MAFFT Multiple Sequence Alignment Software Version 7: Improvements in Performance and Usability. Mol Biol Evol. 30: 772-780.

Klingenberg, C.P. 2011. MorphoJ: an integrated software package for geometric morphometrics. Mol Ecol Res.11: 353-357.
Kumar, S., G. Stecher, and K. Tamura. 2016. MEGA7: molecular evolutionary genetics analysis version 7.0 for bigger datasets. Molecular Biology and Evolution 33:1870–1874.

Leite, R. N., Kolokotronis, S., Almeida, F. C., Werneck, F. P., Rogers, D., & Weksler, M. 2014. In the wake of invasion: Tracing the historical biogeography of the South American cricetid radiation (Rodentia, Sigmodontinae). PLOS ONE 9(10): e100687.

Leite, Y. L. R., Costa, L. P., Loss, A. C., Rocha, R. G., Batalha-Filho, H., Bastos, A. C., … Pardini, R. (2016). Neotropical forest expansion during the last glacial period challenges refuge hypothesis. Proceedings of the National Academy of Sciences, 113(4), 1008–1013.

Librado, P. and Rozas, J. 2009. DnaSP v5: A software for comprehensive analysis of DNA polymorphism data. Bioinformatics 25: 1451-1452.

Luo, A. R., C. H. Ling, S. Y. W. Ho and C.-D. Zhu. 2018. Comparison of Methods for Molecular Species Delimitation Across a Range of Speciation Scenarios. Systematic biology 67:830–846.

Maestri, R., R. Fornel, D. Galiano, and T.R.O. Freitas. 2015. Niche Suitability Affects Development: Skull Asymmetry Increases in Less Suitable Areas. PLOS ONE 10 (4): e0122412.

Matocq, M.D., Q. R. Shurtliff, and C. R. Feldman. 2007. Phylogenetics of the woodrat genus *Neotoma* (Rodentia: Muridae): implications for the evolution of phenotypic variation in male external genitalia. Mol Phylogenet Evol. 42:637-652.

Musser, G. G., and M. D. Carleton. 2005. Superfamily Muroidea. Pp. 894-1531 in Mammal Species of the World: A Taxonomic and Geographic Reference (Wilson, D. E., and D. M. Reeder, eds.). Third ed. Johns Hopkins University Press, Baltimore, Maryland, USA.

Oliveira, J. 1998. Morphometric assesment of species groups in the South American rodent genus *Oxymycterus* Sigmodontinae, with taxonomic notes based on the analysis of type material. Ph.D. dissertation, Texas Tech University, Lubbock.

Oliveira, J. A., and P. R. Gonçalves. 2015. Suborder myomorpha: family cricetidae: subfamily sigmodontinae. Genus *Oxymycterus*. Pp. 247–268 *In:* Mammals of South America, volume 2—rodents (J. M. Patton, G. D'Elía, and U. F. J. Pardiñas, eds.). University of Chicago Press, Chicago, Illinois and London, United Kingdom.

Oliveira, J.A., and C.R. Bonvicino, 2006. Ordem rodentia. *In:* Mamíferos do Brasil (N.R. dos Reis, A.L. Peracchi, W.A. Pedro, I.P. de Lima, eds.). EDIFURB, Londrina, p. 347-406.

Overbeck, G. E., et al. 2007. Brazil's neglected biome: the South Brazilian *Campos*. Perspectives in Plant Ecology, Evolution and Systematics 9:101–116.

Paglia, A.P., Fonseca, G.A.B., Rylands, A.B., Herrmann, G., Aguiar, L.M.S., Chiarello, A.G., Leite, Y.L.R., Costa, L.P., Siciliano, S., Kierulff, M.C.M., Mendes, S.L., Tavares, V.C., Mittermeier, R.A. and Patton, J.L. 2012. Lista anotada dos mamíferos do Brasil/Annotated checklist of Brazilian mammals. 2. ed. Arlington, Conservation International.

Parada, A., G. D'Elía, and R. E. Palma. 2015. The influence of ecological and geographical context in the radiation of neotropical sigmodontine rodents. BMC Evolutionary Biology 15:172.

Parada, A., U. F. Pardiñas, J. Salazar-Bravo, G. D'Elía, and R. E. Palma. 2013. Dating an impressive neotropical radiation: molecular time estimates for the sigmodontinae (rodentia) provide insights into its historical biogeography. Molecular Phylogenetics and Evolution 66:960–968.

Pardiñas, U.F.J., D'Elía, G., and Ortiz, P.E. 2002. Sigmodontinos fósiles (Rodentia, Muroidea, Sigmodontinae) de América del Sur: Estado actual de su conocimiento y prospectiva. Mastozoología Neotrop. 9, 209–252.

Pardiñas, UFJ., P. Teta, G. D'Elía, S. Cirignoli, and P.E. Ortiz. 2007. Resolution of Some Problematic Type Localities for Sigmodontine Rodents (Cricetidae, Sigmodontinae), pp. 391-416 *In:* Kelt, D. A., E. P. Lessa, J. Salazar-Bravo, and J. L. Patton (eds.). 2007. The Quintessential Naturalist: Honoring the Life and Legacy of Oliver P. Pearson. University of California Publications in Zoology 134:1-981.

Peçanha, W. T., et al. 2017. Pleistocene climatic oscillations in Neotropical open areas: refuge isolation in the rodent *Oxymycterus nasutus* endemic to grasslands. PLOS ONE 12(11):e0187329.

Peçanha, W. T., et al. 2019. A new species of *Oxymycterus* (Rodentia: Cricetidae: Sigmodontinae) from a transitional area of Cerrado – Atlantic Forest in southeastern Brazil. *Journal of Mammalogy*, 100(2):578–598.

Quintana, C.A. 2002. Roedores cricétidos del Sanandresense (Plioceno tardío) de la provincia de Buenos Aires. Mastozoología Neotrop. 9, 263–275.

R Core Team. 2017. R: a Language and Environment for Statistical Computing. https://www.R-project.org/.

Rabassa J., and Coronato, A. 2009. Glaciations in Patagonia and Tierra del Fuego during the Ensenadan Stage/Age (Early Pleistocene–earliest Middle Pleistocene). Quaternary International 210 (1): 18–36.

Rambaut, A., Suchard, M.A., Xie, D., and Drummond, A.J. 2014. Tracer v1.6, Available from http://beast.bio.ed.ac.uk/Tracer

Reig, O. A. 1987. An assesment of the systematics and evolution of the Akodontini, with the description of new fossil species of *Akodon* (Cricetidae: Sigmodontinae). In Studies in Neotropical mammalogy, essays in honor of Philip Hershkovitz (B. D. Patterson and R. M. Timm, eds.). Fieldiana: Zoology 39:347–399.

Rohlf, F. J. 2015. The tps series of software. Hystrix 26:9–12.

Rohlf, F. J. and D. Slice. 1990. Extensions of the Procrustes method for the optimal superimposition of landmarks. Systematic Zoology 39:40–59.

Rull, V. 2009. Microrefugia. Journal of Biogeography 36:481–484.

Salazar-Bravo, J., U. F. J. Pardiñas, H. Zeballos, and P. Teta. 2016. Description of a new tribe of Sigmodontine rodents (Cricetidae: Sigmodontinae) with an updated summary of valid tribes and their generic contents. Occasional Papers of the Museum of Texas Tech University 338:1–24.

Sanborn, C. C. 1931. A new *Oxymycterus* from Misiones, Argentina. Proceedings of the Biological Society of Washington 44:1-2.

Schlager, S. 2017. “Morpho and Rvcg – Shape Analysis in R.” In Zheng G, Li S and Szekely G (eds.). *Statistical Shape and Deformation Analysis*, pp. 217–256.

Simmons, M.P. and Ochoterena, H. 2000. Gaps as Characters in Sequence-Based Phylogenetic Analysis. Systematic Biology 49, 369-381.

Smith, M. F., and J. L. Patton. 1993. The diversification of South American murid rodents: evidence from mitochondrial DNA sequence data for the akodontine tribe. Biological Journal of the Linnean Society 50:149–177.

Souza, A.F., L.S.R. Cortez, S. J. Longhi. 2012. Native forest management in subtropical South America: long-term effects of logging and multiple-use on forest structure and diversity. Biodivers Conserv. 21:1953–1969.

Steppan, S. J., and J. J. Schenk. 2017. Muroid rodent phylogenetics: 900-species tree reveals increasing diversification rates. PLOS ONE 12(8):e0183070.

Thomas, O. 1903. New species of *Oxymycterus*, *Thrichomys*, and *Ctenomys* from S. America. Annals and Magazine of Natural History XXVI, 226-229.

Thomas, O. 1909. Notes on some South- American Mammals, with Descriptions of new Species. Annals and Magazine of Natural History XXVIII, 230-242.

Viscozi, V., and A. Cardini. 2011. Leaf morphology, taxonomy and geometric morphometrics: a simplified protocol for beginners. PLOS ONE 6:e25630.

Werneck, F. P., G. C. Costa, G. R. Colli, D. E. Prado, and J. W. SitesJr. 2011. Revisiting the seasonally dry tropical forests historical distribution: new insights based on palaeodistribution modeling and palynological evidence. Global Ecology and Biogeography 20:272–288.

FIGURES

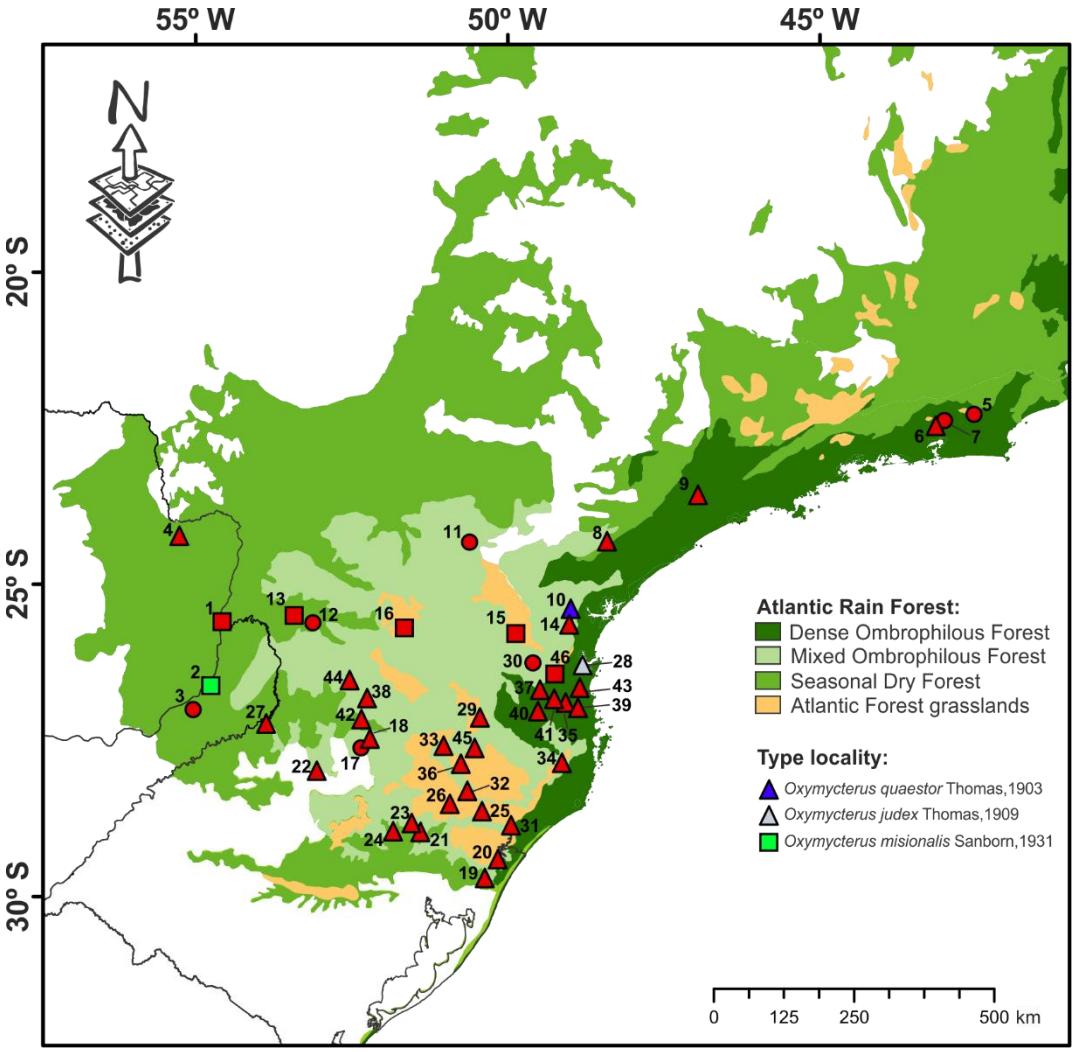

Figure 1. Map showing the collection approximate type localities of the specimens of *Oxymycterus quaestor* Thomas, 1903 (blue), *Oxymycterus judex* Thomas, 1909 (gray) and *Oxymycterus misionalis* Sanborn, 1931 (green) revised according this study. Locality numbers correspond to those in Supplementary Data 1. Circles indicate localities with specimens only included in the phylogenetic analysis; squares indicate localities with specimens that were only morphologically assessed; triangles indicate that specimens from those localities were included in both the phylogenetic and morphological analyses. The map were obtained from Ecoregions 2017© Resolve (available at: http://ecoregions2017.appspot.com/). Any rights in individual contents of the database are licensed under the Database Contents License: https:// creativecommons.org/licenses/by/4.0/), and edited with ArcMap 10.3 software.

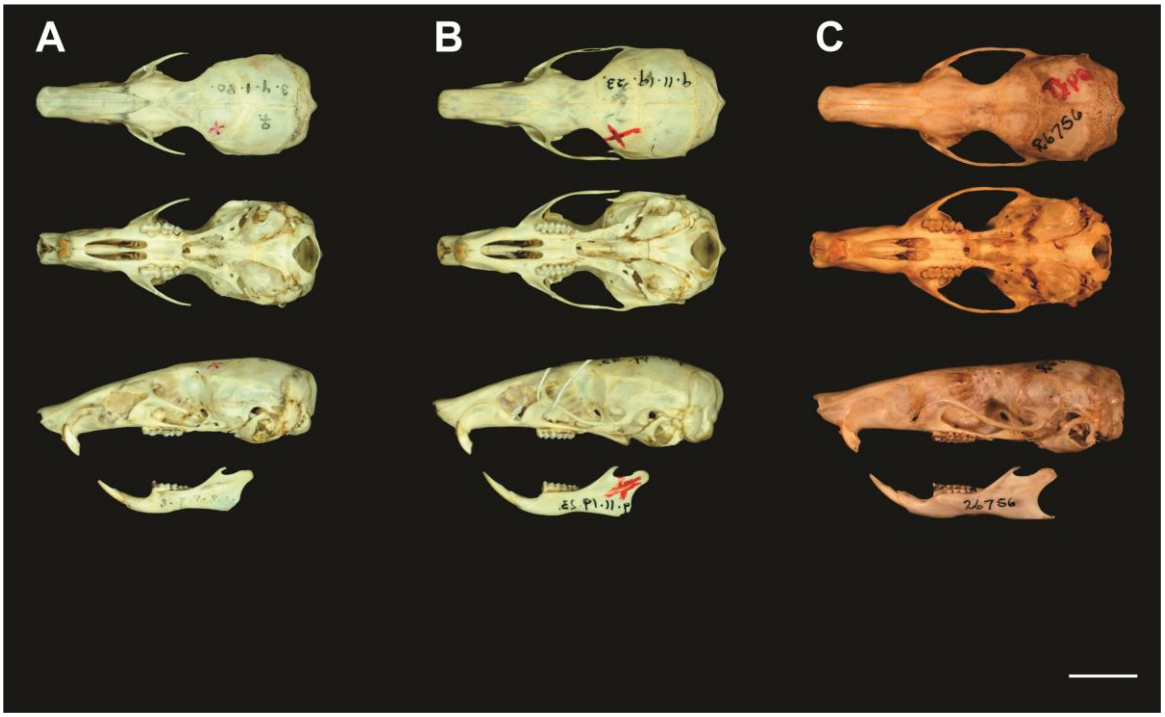

Figure 2. Dorsal, ventral, and lateral views of the skull and mandible (upper to bottom) to holotypes from *Oxymycterus quaestor* (**A**, BM 3.7.1.80), *Oxymycterus judex* (**B**, BM 9.11.19.19) and *Oxymycterus misionalis* (**C**, FMNH 26756). Scale bar = 10 mm.

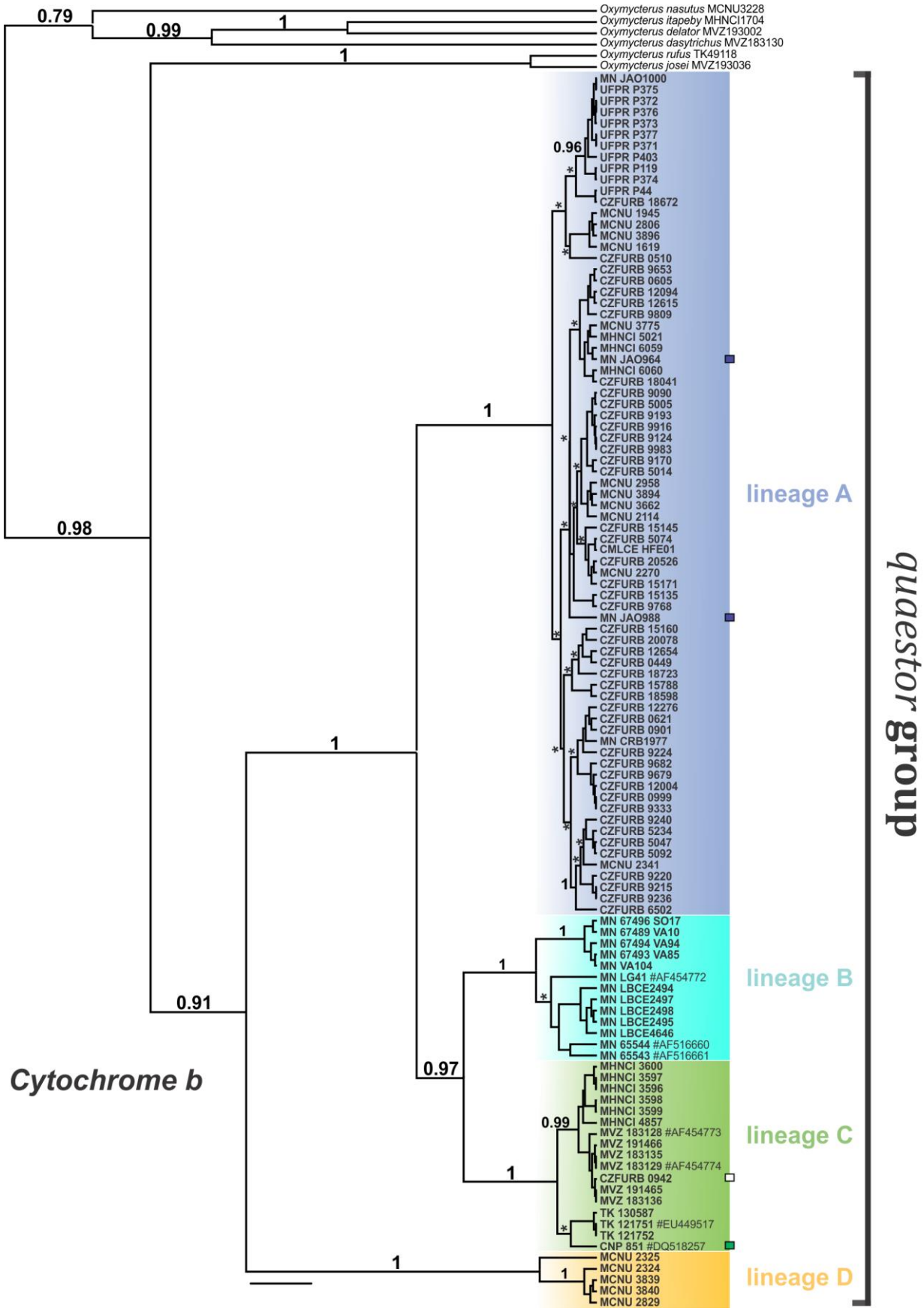
Oxymycterus nasutus MCNU3228
Oxymycterus itapeby MHNCI1704
Oxymycterus delator MVZ193002
Oxymycterus dasytrichus MVZ183130
Oxymycterus rufus TK49118
Oxymycterus josei MVZ193036
MN JAO1000
UFPR P375
UFPR P372
UFPR P376
UFPR P373
UFPR P377
UFPR P371
UFPR P403
UFPR P119
UFPR P374
UFPR P44
CZFURB 18672
MCNU 1945
MCNU 2806
MCNU 3896
MCNU 1619
CZFURB 0510
CZFURB 9653
CZFURB 0605
CZFURB 12094
CZFURB 12615
CZFURB 9809
MCNU 3775
MHNCI 5021
MHNCI 6059
MN JAO964
MHNCI 6060
CZFURB 18041
CZFURB 9090
CZFURB 5005
CZFURB 9193
CZFURB 9916
CZFURB 9124
CZFURB 9983
CZFURB 9170
CZFURB 5014
MCNU 2958
MCNU 3894
MCNU 3662
MCNU 2114
CZFURB 15145
CZFURB 5074
CMLCE HFE01
CZFURB 20526
MCNU 2270
CZFURB 15171
CZFURB 15135
CZFURB 9768
MN JAO988
CZFURB 15160
CZFURB 20078
CZFURB 12654
CZFURB 0449
CZFURB 18723
CZFURB 15788
CZFURB 18598
CZFURB 12276
CZFURB 0621
CZFURB 0901
MN CRB1977
CZFURB 9224
CZFURB 9682
CZFURB 9679
CZFURB 12004
CZFURB 0999
CZFURB 9333
CZFURB 9240
CZFURB 5234
CZFURB 5047
CZFURB 5092
MCNU 2341
CZFURB 9220
CZFURB 9215
CZFURB 9236
CZFURB 6502
MN 67496 SO17
MN 67489 VA10
MN 67494 VA94
MN 67493 VA85
MN VA104
MN LG41 #AF454772
MN LBCE2494
MN LBCE2497
MN LBCE2498
MN LBCE2495
MN LBCE4646
MN 65544 #AF516660
MN 65543 #AF516661
MHNCI 3600
MHNCI 3597
MHNCI 3596
MHNCI 3598
MHNCI 3599
MHNCI 4857
MVZ 183128 #AF454773
MVZ 191466
MVZ 183135
MVZ 183129 #AF454774
CZFURB 0942
MVZ 191465
MVZ 183136
TK 130587
TK 121751 #EU449517
TK 121752
CNP 851 #DQ518257
MCNU 2325
MCNU 2324
MCNU 3839
MCNU 3840
MCNU 2829
lineage A
lineage B
lineage C
lineage D
quaestor group
Cytochrome b

Figure 3. Phylogenetic trees based on Bayesian inference showing the relationships among 110 individuals of *quaestor* group for mitochondrial Cytochrome *b* gene (1137 bp). Numbers at nodes are Bayesian posterior probabilities; numbers in bold indicate high support (≥ 0.90). Nodes marked with asterisks are unsupported. Colors correspond to the lineages (Blue, lineage A; Ciano, lineage B; green, lineage C; Yellow, lineage D). Scale bar = 0.007 nucleotide substitutions. Genbank accession numbers of analyzed sequences are included at terminal labels with hashtag. The squares flagged on the tips indicate sequences derived from closely of types localities. Square Blue, Piraquara - Mananciais da Serra, Paraná State, Brazil; White, Joinville - Estação Ecológica Bracinho Piraí, Santa Catarina State, Brazil; Green, Reserva Valle del Arroyo Cuña Pirú, Misiones Province, Argentina.

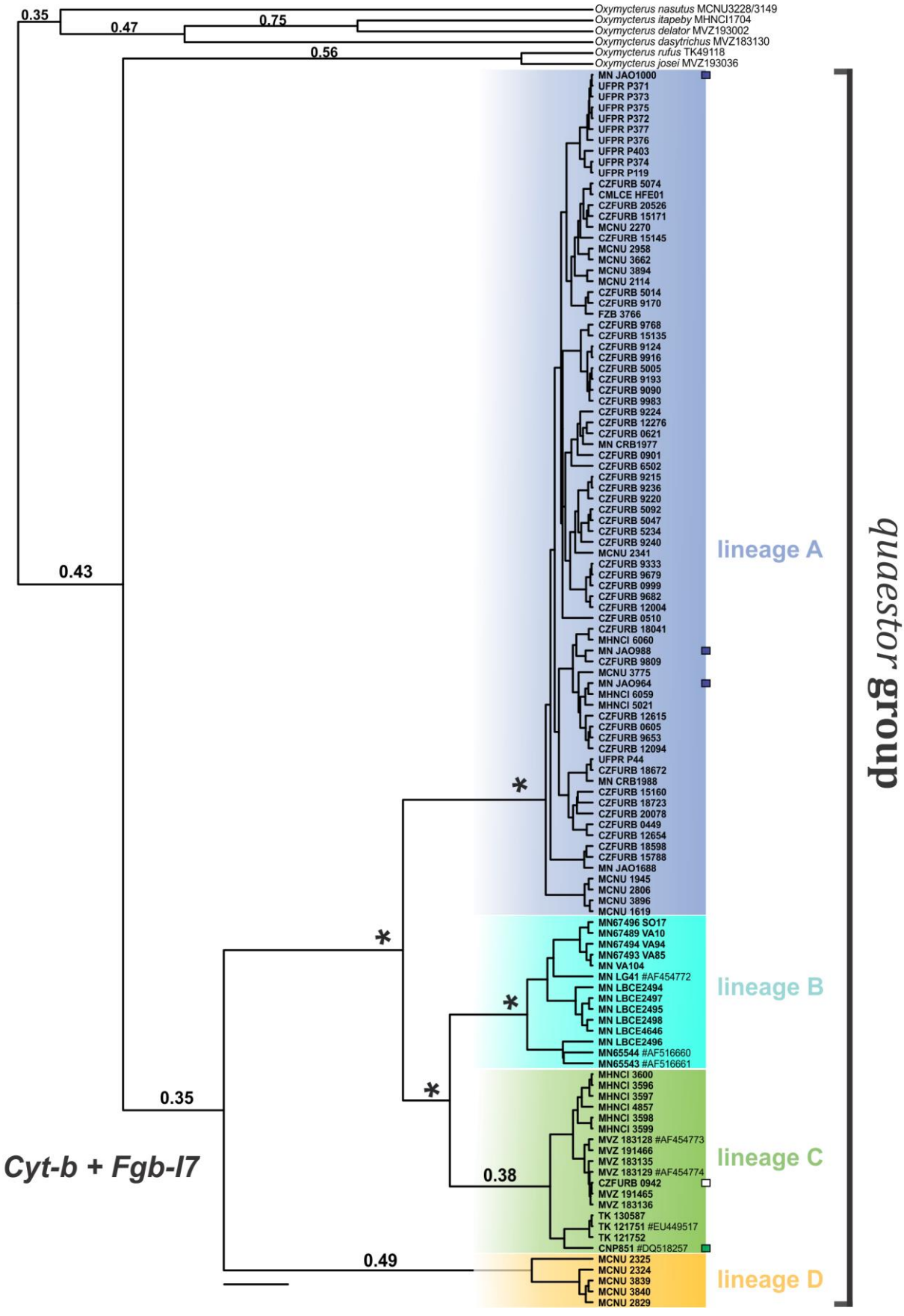
Oxymycterus nasutus MCNU3228/3149
Oxymycterus itapeby MHNCI1704
Oxymycterus delator MVZ193002
Oxymycterus dasytrichus MVZ183130
Oxymycterus rufus TK49118
Oxymycterus josei MVZ193036
0.35
0.47
0.75
0.56
0.43
0.35
0.38
0.49
*
*
*
*
MN JAO1000
UFPR P371
UFPR P373
UFPR P375
UFPR P372
UFPR P377
UFPR P376
UFPR P403
UFPR P374
UFPR P119
CZFURB 5074
CMLCE HFE01
CZFURB 20526
CZFURB 15171
MCNU 2270
CZFURB 15145
MCNU 2958
MCNU 3662
MCNU 3894
MCNU 2114
CZFURB 5014
CZFURB 9170
FZB 3766
CZFURB 9768
CZFURB 15135
CZFURB 9124
CZFURB 9916
CZFURB 5005
CZFURB 9193
CZFURB 9090
CZFURB 9983
CZFURB 9224
CZFURB 12276
CZFURB 0621
MN CRB1977
CZFURB 0901
CZFURB 6502
CZFURB 9215
CZFURB 9236
CZFURB 9220
CZFURB 5092
CZFURB 5047
CZFURB 5234
CZFURB 9240
MCNU 2341
CZFURB 9333
CZFURB 9679
CZFURB 0999
CZFURB 9682
CZFURB 12004
CZFURB 0510
CZFURB 18041
MHNCI 6060
MN JAO988
CZFURB 9809
MCNU 3775
MN JAO964
MHNCI 6059
MHNCI 5021
CZFURB 12615
CZFURB 0605
CZFURB 9653
CZFURB 12094
UFPR P44
CZFURB 18672
MN CRB1988
CZFURB 15160
CZFURB 18723
CZFURB 20078
CZFURB 0449
CZFURB 12654
CZFURB 18598
CZFURB 15788
MN JAO1688
MCNU 1945
MCNU 2806
MCNU 3896
MCNU 1619
MN67496 SO17
MN67489 VA10
MN67494 VA94
MN67493 VA85
MN VA104
MN LG41 #AF454772
MN LBCE2494
MN LBCE2497
MN LBCE2495
MN LBCE2498
MN LBCE4646
MN LBCE2496
MN65544 #AF516660
MN65543 #AF516661
MHNCI 3600
MHNCI 3596
MHNCI 3597
MHNCI 4857
MHNCI 3598
MHNCI 3599
MVZ 183128 #AF454773
MVZ 191466
MVZ 183135
MVZ 183129 #AF454774
CZFURB 0942
MVZ 191465
MVZ 183136
TK 130587
TK 121751 #EU449517
TK 121752
CNP851 #DQ518257
MCNU 2325
MCNU 2324
MCNU 3839
MCNU 3840
MCNU 2829
lineage A
lineage B
lineage C
lineage D
quaestor group
Cyt-b + Fgb-I7

Figure 4. Phylogenetic tree of *quaestor* group obtained by Bayesian inference of a concatenated-gene (*Cyt-b* + *Fgb*-I7) data set (1788 bp). Values above nodes correspond to posterior probabilities > 0.35. Colors correspond to the lineages (Blue, lineage A; Ciano, lineage B; green, lineage C; Yellow, lineage D). Scale bar = 0.007 nucleotide substitutions. GenBank accession numbers of analyzed sequences are included at terminal labels with hashtag. The squares flagged on the tips indicate sequences derived from closely of types localities. Square Blue, Piraquara - Mananciais da Serra, Paraná State, Brazil; White, Joinville - Estação Ecológica Bracinho Piraí, Santa Catarina State, Brazil; Green, Reserva Valle del Arroyo Cuña Pirú, Misiones Province, Argentina.

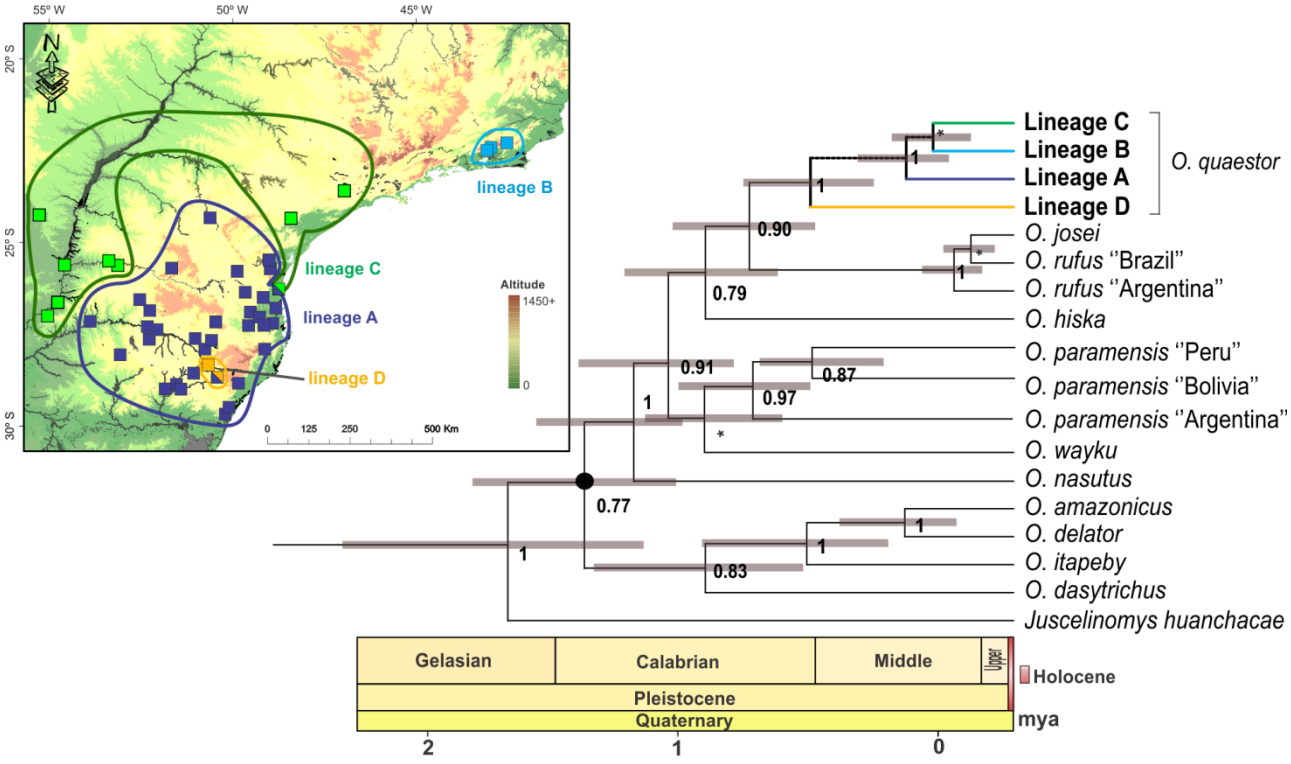

Figure 5. Phylogenetic and molecular dating results for the genus *Oxymycterus*. The tree is a chronogram (uncorrelated log-normal molecular clock) based on a BEAST MCMC analysis of the mitochondrial data set (cytochrome *b* gene). Black circles on the nodes correspond to the fossil calibration points. The 95% credibility intervals of molecular estimates (median height) are given for each node. Numbers at nodes are Bayesian Posterior Probabilities; numbers in bold indicate high support (≥ 0.75). Nodes marked with asterisks are unsupported. Colors correspond to the *quaestor* group lineages (Blue, lineage A; Ciano, lineage B; Green, lineage C; Yellow, lineage D). Scale bars were plotted with a geological time scale using the strap package in R. The map depicted clades into a geographic context.

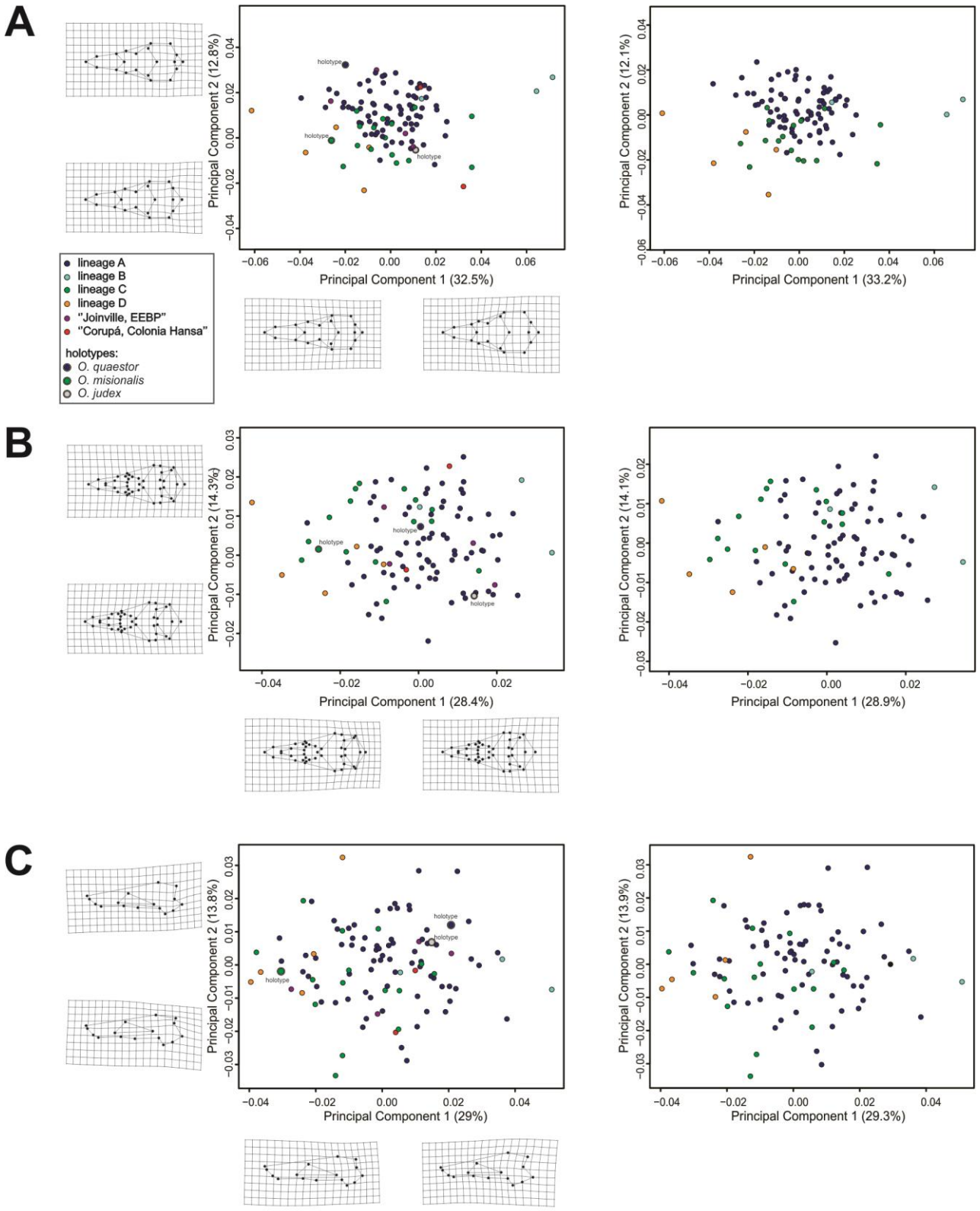

Figure 6. Scatterplot of principal component analysis (PCA) show the two first PCs for 4 lineages of *large reddish hocicudos. Upper* dorsal (A), middle ventral (B), and bottom lateral (C) views of the skull. On left, the full dataset and right, the reduced. Warped grids represent the extreme values of the first and second PC-axis. Grids are warped against the mean skull shape of *quaestor* group. Joinville, EEBP = Joinville, Estação Ecológica Bracinho Piraí.

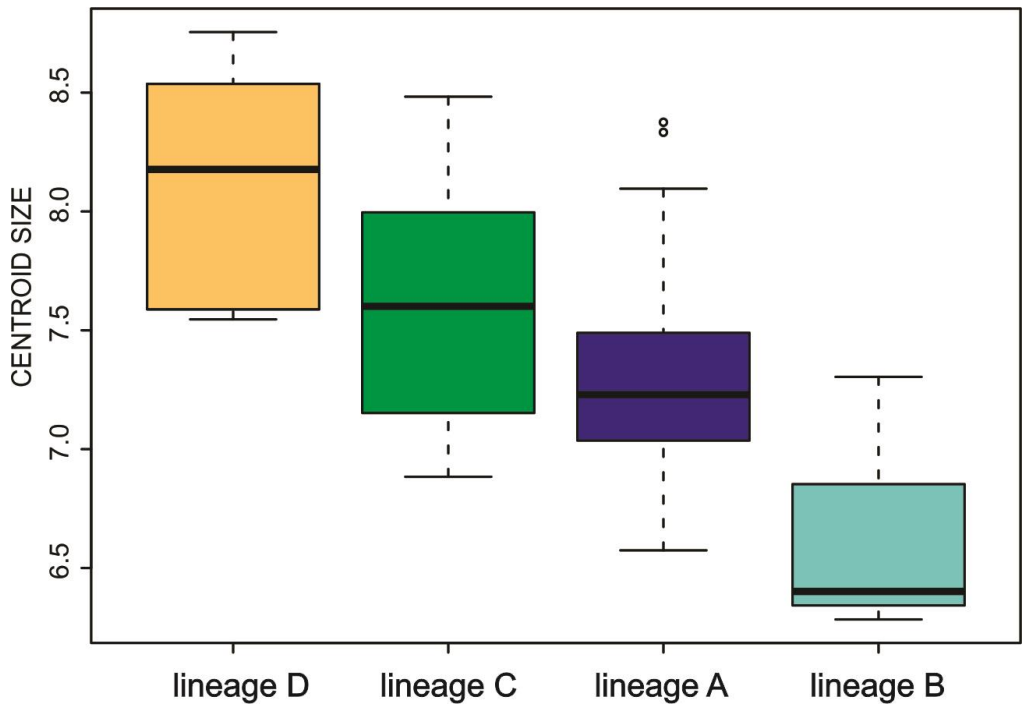

Figure 7. Boxplots of variability in centroid size among 4 lineages, ordered from smallest to largest. Different lineages denominated placed under the plots. The horizontal line represents the mean, box margins are at the 25th and 75th percentiles, bars extend to the 5th and 95th percentiles, and circles are outliers.

TABLES

Table 1. Genetic divergence (using *p*-distance) within and among between pairs of mitochondrial *Cytochrome b* and nuclear *Fibrinogen Beta Chain* (intron 7) genes recovered from different clades of *quaestor* group determined by the Bayesian phylogeny based on mtDNA and concatenated dataset. Highlighted, the values in bold are presented the overall distance; in brackets, intraspecific distance values.

Clade/Lineage					
Cytochrome b:	**N**	**Clade A**	**Clade B**	**Clade C**	**Clade D**
Clade A	75	[0.004 ± 0.001]	-	-	-
Clade B	13	0.0282 ± 0.0049	[0.006 ± 0.002]	-	-
Clade C	17	0.0322 ± 0.0052	0.0262 ± 0.0049	[0.005 ± 0.002]	-
Clade D	5	0.0523 ± 0.0054	0.0589 ± 0.0064	0.0609 ± 0.0068	[0.006 ± 0.002]
Overall	**110**	**0.0197 ± 0.002**			
Fibrinogen Beta Chain (Intron 7):					
Clade A	66	[0.005 ± 0.001]	-	-	-
Clade B	10	0.016 ± 0.002	[0.026 ± 0.004]	-	-
Clade C	10	0.004 ± 0.001	0.016 ± 0.002	[0.001]	-
Clade D	3	0.005 ± 0.002	0.016 ± 0.003	0.005 ± 0.002	[0]
Overall	**89**	**0.007 ± 0.001**			

N: number of individuals included in analyses.

SUPPLEMENTARY DATA

Supplementary Data 1. Description of all sample of *Oxymycterus* used included the Locality numbers correspond (code), Museum or Scientific collection voucher, Skull analyzed, Haplotype *Cyt-b*, Haplotype *Fgb*-I7, Country, State/Department or Province, Municipality/Locality, geographic Coordinates, Sex and Genbank accessions (Sequences generated in this study indicated in bold). Abreviations of Brazilian States: PR, Paraná; SC, Santa Catarina; RS, Rio Grande do Sul. Acronyms of the collections accessed: BM, British Museum, London (United Kingdom);CMLCE-UFRGS, Mastozoological Collection of the Cytogenetic Laboratory and Evolution at the Universidade Federal do Rio Grande do Sul, Porto Alegre (Brazil); CNP, Colección de Mamíferos del Centro Nacional Patagónico, Puerto Madryn (Argentina); CZFURB, Coleção Zoológica da Universidade Regional de Blumenau, Blumenau (Brazil); DZUP/CCMZ, Departamento de Zoologia da Universidade Federal do Paraná, Curitiba (Brazil); FMNH, Field Museum of Natural History, Chicago (USA); FZB-MCN, Fundação Zoobotânica do Rio Grande do Sul, Museu de Ciências Naturais, Porto Alegre (Brazil); MCNU, Museu de Ciências Naturais da Universidade Luterana do Brasil, Canoas (Brazil); MHNCI, Museu de História Natural "Capão da Imbuía", Curitiba (Brazil); MN [LG, LBCE VA, SO, JAO, CRB], Museu Nacional, Universidade federal do Rio de Janeiro, Rio de Janeiro (Brazil); MVZ, Museum of Vertebrate Zoology, University of California at Berkeley, Berkeley (USA); MZUSP, Museu de Zoologia da Universidade de São Paulo, São Paulo (Brazil); MZPUCPR, Museu de Zoologia da Pontifícia Universidade católica do Paraná, Curitiba (Brazil); TK [MNHNP], Museo Nacional de Historia Natural del Paraguay, San Lorenzo (Paraguay); UFPR-P, Departmento de Genética da Universidade Federal do Paraná, Curitiba (Brazil).

code	ID	skull	*Cyt-b*	*Fgb-I7*	Country	Area	locality	coordinates	Sex	Genbank
1	FMNH 23843	+	-	-	AR	Misiones	Puerto Aguirre	-25.599698, -54.58323	M	
2	FMNH 26754	+	-	-	AR	Misiones	Lib. Gen San Martín	-26.616667, -54.766667	M	
2	FMNH 26756	+	-	-	AR	Misiones	Lib. Gen San Martín	-26.616667, -54.766667	F	
2	FMNH 26757	+	-	-	AR	Misiones	Lib. Gen San Martín	-26.616667, -54.766667	M	
3	CNP 851	-	801 bp	-	AR	Misiones	Reserva Valle del Arroyo Cuña Pirú	-27.00145, -55.044038	-	DQ518257
4	TK 121751	+	1137 bp	660 bp	PY	Canindeyu	Colonia Britez Cue	-24.23916667, -55.26777778	F	EU449517
4	TK 121752	+	1137 bp	660 bp	PY	Canindeyu	Colonia Britez Cue	-24.23916667, -55.26777778	M	
4	TK 130587	+	801 bp	-	PY	Canindeyu	Colonia Britez Cue	-24.23916667, -55.26777778	F	
4	TK 141169	+	-	-	PY	Canindeyu	Colonia Britez Cue	-24.23916667, -55.26777778	F	
5	MN LG41	-	1113 bp	-	BR	RJ	Nova Friburgo, Sítio Xitaca	-22.281944, -42.530833	-	AF454772
6	MN 65544	-	801 bp	-	BR	RJ	Teresópolis	-22.411944, -42.965833	-	AF516661
6	MN 65543	-	801 bp	-	BR	RJ	Teresópolis	-22.411944, -42.965833	-	AF516660
6	FMNH 26592	+	-	-	BR	RJ	Teresópolis	-22.411944, -42.965833	F	
6	FMNH 26595	+	-	-	BR	RJ	Teresópolis	-22.411944, -42.965833	M	
6	FMNH 26587	+	-	-	BR	RJ	Teresópolis	-22.411944, -42.965833	F	
6	MN LBCE 2494	-	1137 bp	660 bp	BR	RJ	Teresópolis, Semidouro	-22.411944, -42.965833	-	
6	MN LBCE 2495	-	1137 bp	675 bp	BR	RJ	Teresópolis, Semidouro	-22.411944, -42.965833	-	

6	MN LBCE 2497	-	1137 bp	660 bp	BR	RJ	Teresópolis, Semidouro	-22.411944, -42.965833	-	
6	MN LBCE 2498	-	1137 bp	660 bp	BR	RJ	Teresópolis, Semidouro	-22.411944, -42.965833	-	
6	MN LBCE 2496	-	-	675 bp	BR	RJ	Teresópolis, Semidouro	-22.411944, -42.965833	-	
6	MN LBCE 4646	-	1137 bp	660 bp	BR	RJ	Teresópolis, Semidouro	-22.411944, -42.965833	-	
7	MN67496 SO17	-	1137 bp	660 bp	BR	RJ	Teresópolis, Pq Nac. da Serra dos Órgãos, Vale das Antas	-22.493056, -43.073333	-	
7	MN67489 VA10	-	1137 bp	660 bp	BR	RJ	Teresópolis, Pq Nac. da Serra dos Órgãos, Vale das Antas	-22.493056, -43.073333	-	
7	MN VA104	-	801 bp	-	BR	RJ	Teresópolis, Pq Nac. da Serra dos Órgãos, Vale das Antas	-22.493056, -43.073333	-	
7	MN67493 VA85	-	1137 bp	660 bp	BR	RJ	Teresópolis, Pq Nac. da Serra dos Órgãos, Vale das Antas	-22.493056, -43.073333	-	
7	MN67494 VA94	-	1137 bp	660 bp	BR	RJ	Teresópolis, Pq Nac. da Serra dos Órgãos, Vale das Antas	-22.493056, -43.073333	-	
8	MVZ 183128	+	1137 bp	-	BR	SP	Capão Bonito, Fazenda Intervales	-24.3333333, -48.4166667	F	AF454773
8	MVZ 183129	-	1041 bp	-	BR	SP	Capão Bonito, Fazenda Intervales	-24.3333333, -48.4166667	M	AF454774
8	MVZ 183135	-	1137 pb	660 bp	BR	SP	Capão Bonito, Fazenda Intervales	-24.3333333, -48.4166667	F	
8	MVZ 183136	-	1137 pb	660 bp	BR	SP	Capão Bonito, Fazenda Intervales	-24.3333333, -48.4166667	F	
8	MVZ 191465	+	1137 pb	660 bp	BR	SP	Capão Bonito, Fazenda Intervales	-24.3333333, -48.4166667	M	
8	MVZ 191466	-	1137 pb	660 bp	BR	SP	Capão Bonito, Fazenda Intervales	-24.3333333, -48.4166667	F	
9	MHNCI 3596	+	1137 pb	660 bp	BR	SP	Itapevi, Vila Verde	-23.587492, -46.959781	M	
9	MHNCI 3597	+	1137 pb	-	BR	SP	Itapevi, Vila Verde	-23.587492, -46.959781	F	
9	MHNCI 3598	+	1137 pb	660 bp	BR	SP	Itapevi, Vila Verde	-23.587492, -46.959781	F	
9	MHNCI 3599	+	1137 pb	660 bp	BR	SP	Itapevi, Vila Verde	-23.587492, -46.959781	M	
9	MHNCI 3600	+	1137 bp	660 bp	BR	SP	Itapevi, Vila Verde	-23.587492, -46.959781	F	
10	BM 3.7.1.80	+	-	-	BR	PR	Piraquara, Roça Nova	-25.472480, -49.014220	F	
10	MHNCI 3136	+	-	-	BR	PR	Piraquara, Sanepar	-25.491772, -48.994268	-	
10	UFPR-P44	-	801 bp	-	BR	PR	Piraquara	-25.441944, -49.062778	M	
10	MN JAO 1000	-	1137 pb	660 bp	BR	PR	Piraquara, Mananciais da Serra	-25.441944, -49.062778	-	
10	MN JAO 964	-	1137 pb	660 bp	BR	PR	Piraquara, Mananciais da Serra	-25.441944, -49.062778	-	

10	MN JAO 988	-	1137 pb	660 bp	BR	PR	Piraquara, Mananciais da Serra	-25.441944, -49.062778	-	
11	MN JAO 1688	-	-	660 bp	BR	PR	Telêmaco Borba	-24.323889, -50.615833	-	
12	MHNCI 4857	-	642 bp	-	BR	PR	Cruzeiro do Iguaçu, UHE Salto Caxias	-25.615833, -53.127778	M	
13	MHNCI 4471	+	-	-	BR	PR	Boa Vista da Aparecida, Flor da Serra	-25.491636, -53.376497	M	
13	MHNCI 4510	-	-	-	BR	PR	Boa Vista da Aparecida, Flor da Serra	-25.491636, -53.376497	F	
14	UFPR-P119	-	1137 bp	-	BR	PR	São José dos Pinhais, Guaricana	-25.708234, -48.975598	F	
14	UFPR-P371	-	1137 bp	658 bp	BR	PR	São José dos Pinhais, Guaricana	-25.708234, -48.975598	M	
14	UFPR-P372	-	1137 bp	-	BR	PR	São José dos Pinhais, Guaricana	-25.708234, -48.975598	F	
14	UFPR-P373	-	1137 bp	-	BR	PR	São José dos Pinhais, Guaricana	-25.708234, -48.975598	M	
14	UFPR-P374	-	1137 bp	660 bp	BR	PR	São José dos Pinhais, Guaricana	-25.708234, -48.975598	M	
14	UFPR-P375	-	1137 bp	658 bp	BR	PR	São José dos Pinhais, Guaricana	-25.708234, -48.975598	M	
14	UFPR-P376	-	1137 bp	-	BR	PR	São José dos Pinhais, Guaricana	-25.708234, -48.975598	M	
14	UFPR-P377	-	1137 bp	658 bp	BR	PR	São José dos Pinhais, Guaricana	-25.708234, -48.975598	M	
14	UFPR-P403	-	1137 bp	-	BR	PR	São José dos Pinhais, Guaricana	-25.708234, -48.975598	F	
14	MHNCI 1472	+	-	-	BR	PR	São José dos Pinhais, Guaricana	-25.708234, -48.975598	F	
14	MHNCI 1479	+	-	-	BR	PR	São José dos Pinhais, Guaricana	-25.708234, -48.975598	M	
14	MHNCI 1530	+	-	-	BR	PR	São José dos Pinhais, Guaricana	-25.708234, -48.975598	F	
14	MHNCI 1537	+	-	-	BR	PR	São José dos Pinhais, Guaricana	-25.708234, -48.975598	M	
14	MHNCI 1613	+	-	-	BR	PR	São José dos Pinhais, Guaricana	-25.708234, -48.975598	F	
14	MHNCI 1666	+	-	-	BR	PR	São José dos Pinhais, Guaricana	-25.708234, -48.975598	M	
15	MZPUCPR 1199	+	-	-	BR	PR	Lapa, Rodovia do Xisto Km82	-25.784685, -49.877846	-	
16	MHNCI 2146	+	-	-	BR	PR	Pinhão, Foz do Rio da Divisa	-25.695833, -51.66	M	
17	CMLCE HFE 01	-	1137 bp	660 bp	BR	RS	Erechim	-27.633889, -52.273889	M	
18	MN CRB 1977	-	1137 bp	675 bp	BR	RS	Aratiba	-27.393889, -52.3	-	
18	MN CRB 1988	-	-	675 bp	BR	RS	Aratiba	-27.393889, -52.3	-	

18	MCNU 280	+	-	-	BR	RS	Aratiba, Três barras	-27.320001, -52.247135	M	
18	MCNU 281	+	-	-	BR	RS	Aratiba, Três barras	-27.320001, -52.247135	M	
18	MCNU 282	+	-	-	BR	RS	Aratiba, Três barras	-27.320001, -52.247135	F	
18	MCNU 283	+	-	-	BR	RS	Aratiba, Três barras	-27.320001, -52.247135	M	
18	MCNU 285	+	-	-	BR	RS	Aratiba, Três barras	-27.320001, -52.247135	M	
18	MCNU 286	+	-	-	BR	RS	Aratiba, Três barras	-27.320001, -52.247135	F	
19	MCNU 1619	+	1137 bp	660 bp	BR	RS	Maquiné	-29.675000, -50.206944	M	
20	MCNU 1945	+	1137 bp	660 bp	BR	RS	Itati	-29.488889, -50.105000	F	
20	MCNU 2806	+	1137 bp	660 bp	BR	RS	Itati	-29.488889, -50.105000	F	
21	MCNU 2114	+	1137 bp	660 bp	BR	RS	Vila Flores	-28.862778, -51.532778	M	
22	MCNU 2341	+	1137 bp	660 bp	BR	RS	Chapada	-28.055000, -53.067778	M	
23	MCNU 2958	+	1137 bp	660 bp	BR	RS	Nova Roma do Sul	-28.990000, -51.407778	M	
23	MCNU 3662	+	1137 bp	660 bp	BR	RS	Nova Roma do Sul	-28.990000, -51.407778	F	
24	MCNU 3894	+	1137 bp	660 bp	BR	RS	Dois lajeados	-28.983889, -51.835833	M	
25	MCNU 2324	+	1137 bp	660 bp	BR	RS	Bom Jesus	-28.667778, -50.416944	M	
25	MCNU 2325	+	1137 bp	-	BR	RS	Bom Jesus	-28.667778, -50.416944	F	
25	MCNU 3775	+	1137 bp	660 bp	BR	RS	Bom Jesus	-28.667778, -50.416944	M	
25	MCNU 3839	+	1137 bp	-	BR	RS	Bom Jesus	-28.667778, -50.416944	M	
25	MCNU 3840	+	1137 bp	660 bp	BR	RS	Bom Jesus	-28.667778, -50.416944	F	
26	MCNU 2270	+	1137 bp	660 bp	BR	RS	Vacaria	-28.511944, -50.933889	M	
27	DZUP/CCMZ 187	+	-	-	BR	RS	Derrubadas, Pq. Est. Do Turvo	-27.145556, -53.886111	M	
27	FZB-MCN 3766	-	-	660 bp	BR	RS	Derrubadas, Pq. Est. Do Turvo	-27.145556, -53.886111	M	
28	BM 9.11.19.19	+	-	-	BR	SC	Joinville	-26.303889, -48.845833	M	
28	FMNH 34383	+	-	-	BR	SC	Joinville	-26.303889, -48.845833	M	
28	CZFURB 146	+	-	-	BR	SC	Joinville, Est. Eco. Bracinho Piraí	-26.296228, -49.018612	M	
28	CZFURB 909	+	-	-	BR	SC	Joinville, Est. Eco. Bracinho Piraí	-26.296228, -49.018612	M	
28	CZFURB 910	+	-	-	BR	SC	Joinville, Est. Eco. Bracinho Piraí	-26.296228, -49.018612	M	
28	CZFURB 942	-	1137 bp	-	BR	SC	Joinville, Est. Eco. Bracinho Piraí	-26.296228, -49.018612	F	
29	MHNCI 5021	+	1137 bp	-	BR	SC	Ponte Alta do Norte, Fazenda Rio das Pedras	-27.157778,-50.463889	F	

29	MHNCI 5023	+	-	-	BR	SC	Ponte Alta do Norte, Fazenda Rio das Pedras	-27.157778,-50.463889	M	
30	MHNCI 6059	+	1137 bp	-	BR	SC	Rio Negrinho, Fazenda Santa Alice	-26.253889, -49.517778	F	
30	MHNCI 6060	+	1137 bp	369 bp	BR	SC	Rio Negrinho, Fazenda Santa Alice	-26.253889, -49.517778	M	
31	MCNU 3896	+	1137 bp	-	BR	SC	Timbé do Sul	-28.83, -49.846944	M	
32	MCNU 2829	+	1137 bp	660 bp	BR	RS	Bom Jesus, Paiquere	-28.335829, -50.662092	F	
33	CZFURB 20526	+	1137 bp	660 bp	BR	SC	Abdon Batista, UHE Garibaldi	-27.610833, -51.022778	M	
34	CZFURB 449	+	1137 bp	660 bp	BR	SC	Anitápolis, Vale do IFC	-27.901944, -49.128889	M	
34	CZFURB 510	+	1137 bp	660 bp	BR	SC	Anitápolis, Vale do IFC	-27.901944, -49.128889	-	
35	CZFURB 621	+	1137 bp	660 bp	BR	SC	Blumenau, Parque Nacional da Serra do Itajaí, Parque das Nascentes	-26.908889, -49.072222	M	
35	CZFURB 9679	+	1137 bp	660 bp	BR	SC	Blumenau, Parque Nacional da Serra do Itajaí, Parque das Nascentes	-26.908889, -49.072222	M	
36	CZFURB 15135	+	1137 bp	660 bp	BR	SC	Campo Belo do Sul, Potreiro das Éguas, Fazenda Gateados	-27.898889, -50.760833	F	
36	CZFURB 15145	+	1137 bp	660 bp	BR	SC	Campo Belo do Sul, Potreiro das Éguas, Fazenda Gateados	-27.898889, -50.760833	M	
36	CZFURB 15160	+	1137 bp	660 bp	BR	SC	Campo Belo do Sul, Potreiro das Éguas, Fazenda Gateados	-27.898889, -50.760833	M	
36	CZFURB 15171	+	1137 bp	660 bp	BR	SC	Campo Belo do Sul, Potreiro das Éguas, Fazenda Gateados	-27.898889, -50.760833	M	
37	CZFURB 15788	+	1137 bp	660 bp	BR	SC	Dr. Pedrinho, Rebio Estadual Sassafrás	-26.713889, -49.482778	M	
37	CZFURB 18041	-	1137 bp	660 bp	BR	SC	Dr. Pedrinho, Rebio Estadual Sassafrás	-26.713889, -49.482778	M	
37	CZFURB 18598	+	1137 bp	660 bp	BR	SC	Dr. Pedrinho, Rebio Estadual Sassafrás	-26.713889, -49.482778	F	
37	CZFURB 18672	+	1137 bp	660 bp	BR	SC	Dr. Pedrinho, Rebio Estadual Sassafrás	-26.713889, -49.482778	M	
37	CZFURB 18723	+	1137 bp	660 bp	BR	SC	Dr. Pedrinho, Rebio Estadual Sassafrás	-26.713889, -49.482778	F	
38	CZFURB 12276	+	1137 bp	660 bp	BR	SC	Faxinal dos Guedes, BR282 Km484	-26.852778, -52.261001	-	
39	CZFURB 9768	+	1137 bp	660 bp	BR	SC	Gaspar, RPPN Figueira Branca	-26.930833, -48.958889	F	
39	CZFURB 9809	+	960 bp	660 bp	BR	SC	Gaspar, Bunge	-26.930833, -48.958889	M	
40	CZFURB 12615	+	1137 bp	-	BR	SC	Ibirama, PCH Salto Pilão	-27.056944, -49.517778	M	

40	CZFURB 12654	+	1137 bp	660 bp	BR	SC	Ibirama, PCH Salto Pilão	-27.056944, -49.517778	M	
41	CZFURB 605	+	1137 bp	-	BR	SC	Indaial, Parque Nacional da Serra do Itajaí, Parque das Nascentes, Vale do Espingarda	-26.897778, -49.231944	-	
41	CZFURB 991	+	-	-	BR	SC	Indaial, Parque Nacional da Serra do Itajaí, Parque das Nascentes, Vale do Espingarda	-26.897778, -49.231944	M	
41	CZFURB 999	+	1137 bp	660 bp	BR	SC	Indaial, Parque Nacional da Serra do Itajaí, Parque das Nascentes, Vale do Espingarda	-26.897778, -49.231944	M	
41	CZFURB 1000	+	-	-	BR	SC	Indaial, Parque Nacional da Serra do Itajaí, Parque das Nascentes, Vale do Espingarda	-26.897778, -49.231944	F	
41	CZFURB 5005	-	1137 bp	660 bp	BR	SC	Indaial, Parque Nacional da Serra do Itajaí, Parque das Nascentes, Vale do Espingarda	-26.897778, -49.231944	F	
41	CZFURB 5014	+	1137 bp	660 bp	BR	SC	Indaial, Parque Nacional da Serra do Itajaí, Parque das Nascentes, Vale do Espingarda	-26.897778, -49.231944	M	
41	CZFURB 9090	+	1137 bp	660 bp	BR	SC	Indaial, Parque Nacional da Serra do Itajaí, Parque das Nascentes, Vale do Espingarda	-26.897778, -49.231944	F	
41	CZFURB 9124	+	1137 bp	660 bp	BR	SC	Indaial, Parque Nacional da Serra do Itajaí, Parque das Nascentes, Vale do Espingarda	-26.897778, -49.231944	M	
41	CZFURB 9170	+	1137 bp	660 bp	BR	SC	Indaial, Parque Nacional da Serra do Itajaí, Parque das Nascentes, Vale do Espingarda	-26.897778, -49.231944	M	
41	CZFURB 9193	+	1137 bp	660 bp	BR	SC	Indaial, Parque Nacional da Serra do Itajaí, Parque das Nascentes, Vale do Espingarda	-26.897778, -49.231944	-	
41	CZFURB 9333	+	1137 bp	660 bp	BR	SC	Indaial, Parque Nacional da Serra do Itajaí, Parque das Nascentes, Vale do Espingarda	-26.897778, -49.231944	M	
41	CZFURB 9490	+	-	-	BR	SC	Indaial, Parque Nacional da Serra do Itajaí, Parque das Nascentes, Vale do Espingarda	-26.897778, -49.231944	M	

41	CZFURB 9653	+	1137 bp	660 bp	BR	SC	Indaial, Parque Nacional da Serra do Itajaí, Parque das Nascentes, Vale do Espingarda	-26.897778, -49.231944	-	
41	CZFURB 9682	-	1137 bp	660 bp	BR	SC	Indaial, Parque Nacional da Serra do Itajaí, Parque das Nascentes, Vale do Espingarda	-26.897778, - 49.231944	-	
41	CZFURB 9916	+	1137 bp	660 bp	BR	SC	Indaial, Parque Nacional da Serra do Itajaí, Parque das Nascentes, Vale do Espingarda	-26.897778, -49.231944	M	
41	CZFURB 9983	+	1137 bp	660 bp	BR	SC	Indaial, Parque Nacional da Serra do Itajaí, Parque das Nascentes, Vale do Espingarda	-26.897778, -49.231944	M	
41	CZFURB 12004	-	1137 bp	660 bp	BR	SC	Indaial, Parque Nacional da Serra do Itajaí, Parque das Nascentes, Vale do Espingarda	-26.897778, -49.231944	F	
42	CZFURB 901	+	1137 bp	660 bp	BR	SC	Itá, UHE Itá	-27.290833, -52.322778	M	
42	CZFURB 5047	+	1137 bp	660 bp	BR	SC	Itá, UHE Itá	-27.290833, -52.322778	F	
42	CZFURB 5074	-	1137 bp	660 bp	BR	SC	Itá, UHE Itá	-27.290833, -52.322778	M	
42	CZFURB 5092	+	1137 bp	660 bp	BR	SC	Itá, UHE Itá	-27.290833, -52.322778	-	
42	CZFURB 5234	-	1137 bp	660 bp	BR	SC	Itá, UHE Itá	-27.290833, -52.322778	M	
42	CZFURB 6502	+	1137 bp	660 bp	BR	SC	Itá, UHE Itá	-27.290833, -52.322778	F	
43	CZFURB 12094	+	1137 bp	660 bp	BR	SC	Luiz Alves, Braço Central	-26.720833, -48.932778	M	
44	CZFURB 9215	+	1137 bp	-	BR	SC	São Domingos, Aheqq	-26.557778, -52.531944	F	
44	CZFURB 9220	+	1137 bp	660 bp	BR	SC	São Domingos, Aheqq	-26.557778, -52.531944	M	
44	CZFURB 9224	+	1137 bp	660 bp	BR	SC	São Domingos, Aheqq	-26.557778, -52.531944	M	
44	CZFURB 9236	+	1137 bp	660 bp	BR	SC	São Domingos, Aheqq	-26.557778, -52.531944	-	
44	CZFURB 9240	+	1137 bp	660 bp	BR	SC	São Domingos, Aheqq	-26.557778, -52.531944	-	
45	CZFURB 20078	+	1137 bp	660 bp	BR	SC	São José do Cerrito, UHE Garibaldi	-27.662778, -50.581001	M	
46	FMNH 35354	+	-	-	BR	SC	Corupá, colônia Hansa	-26.425, -49.242778	M	
46	MZUSP 845	+	-	-	BR	SC	Corupá, colônia Hansa	-26.425, -49.242778	F	

Supplementary Data 2. Species, scientific collections voucher identification, Genbank accession codes and target locus used in phylogenies reconstructions for mtDNA and concatenated approaches. Sequences generated in this study indicated in bold on Table.

Species	Voucher ID	Genbank ID	Locus
*O. quaestor**	LG41	AF454772	Cytochrome *b* (mtDNA)
*O. quaestor**	MN 65544	AF516661	Cytochrome *b* (mtDNA)
*O. quaestor**	MN 65543	AF516660	Cytochrome *b* (mtDNA)
*O. judex**	AF454773	AF454773	Cytochrome *b* (mtDNA)
*O. judex**	AF454774	AF454774	Cytochrome *b* (mtDNA)
*O. misionalis**	CNP 851	DQ518257	Cytochrome *b* (mtDNA)
*O. misionalis**	TK 121751	EU449517	Cytochrome *b* (mtDNA)
O. delator	MVZ193002	MK331139	Cytochrome *b* (mtDNA)
O. delator	MVZ193002	**TBD**	Fibrinogen beta chain - 7 intron (nDNA)
O. nasutus	MCNU3228	MK331144	Cytochrome *b* (mtDNA)
O. nasutus	MCNU3149	**TBD**	Fibrinogen beta chain - 7 intron (nDNA)
O. itapeby	MHNCI1704	MK331135	Cytochrome *b* (mtDNA)
O. itapeby	MHNCI1704	**TBD**	Fibrinogen beta chain - 7 intron (nDNA)
O. dasytrichus	MVZ183130	**TBD**	Cytochrome *b* (mtDNA)
O. dasytrichus	MVZ183130	**TBD**	Fibrinogen beta chain - 7 intron (nDNA)
O. josei	MVZ193036	MK331138	Cytochrome *b* (mtDNA)
O. josei	MVZ193036	**TBD**	Fibrinogen beta chain - 7 intron (nDNA)
O. rufus	TK49118	AF454775	Cytochrome *b* (mtDNA)

* Nomenclature of species given by Genbank.

Supplementary Data 3. All sequences retrieve and deposited in Genbank used for reconstructed the time calibrated-tree. Listed are species, museum/scientific collections voucher ID and Genbank accession codes. The sequences generated in this study indicated in bold on Table.

Species (outgroups)	Voucher ID	Genbank ID
Juscelinomys huanchacae	LHE1644	JQ898084
O. quaestor "**Lineage A**"	MN JAO964	**TBD**
O. misionalis/judex "**Lineage C**"	CNP851	DQ518257
Oxymycterus sp. 1 "**Lineage B**"	MN67496 (SO17)	**TBD**
Oxymycterus sp. 2 "**Lineage D**"	MCNU2324	**TBD**
O. amazonicus	MZUSP21317	AF454765
O. delator	MVZ193002	MK331139
O. dasytrichus	MVZ183130	**TBD**
O. itapeby	MHNCI1704	MK331135
O. nasutus	MCNU3228	MK331144
O. wayku	CML7247	DQ518262
O. hiska	MVZ171518	U03542
O. josei	MVZ193036	MK331138
O. rufus "Argentina"	TK49118	AF454775
O. rufus "Brazil"	MZUFV713	AF516653
O. paramensis "Peru"	UMMZ160535	U03536
O. paramensis "Peru"	MVZ193021	**TBD**
O. paramensis "Bolivia"	MSB67277 (NK22836)	AY041197
O. paramensis "Bolivia"	MSB67278	**TBD**
O. paramensis "Argentina"	CML725	DQ518259
O. paramensis "Argentina"	MSB239810	**TBD**

Supplementary Data 4. Position of the landmarks (circles) digitized on the (A) dorsal, (B) ventral, and (C) lateral views of skull. Below, the definition of landmarks positioned for each skull views.

(A) Description of landmarks of skull dorsal view:

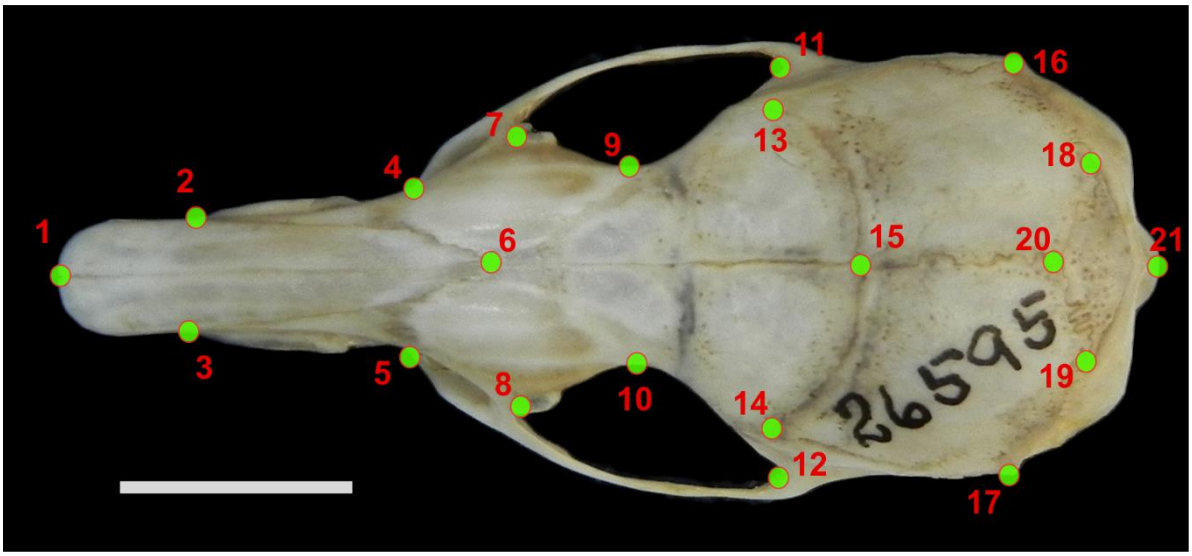

1: anteriormost point of suture between nasals; 2-3: anteriormost point of suture between nasal and premaxilla; 4-5: anteriormost point of zygomatic plate; 6: suture between nasals and frontals; 7-8: posteriormost margin of maximum constriction of antorbital bridge; 9-10: length margin of maximum constriction of interorbital region (frontal); 11-12: anteriormost margin of the maximum constriction of squamosal root of zygomatic arch; 13-14: suture between frontal, squamosal and parietal; 15: suture between frontals and parietals; 16-17: superiormost point of suture between parietal and occipital; 18-19: suture between parietal, interparietal and occipital; 20: suture between parietals and interparietal; 21: posteriormost point of occipital margin. Scale bar = 10 mm.

(B) Description of landmarks of skull ventral view:

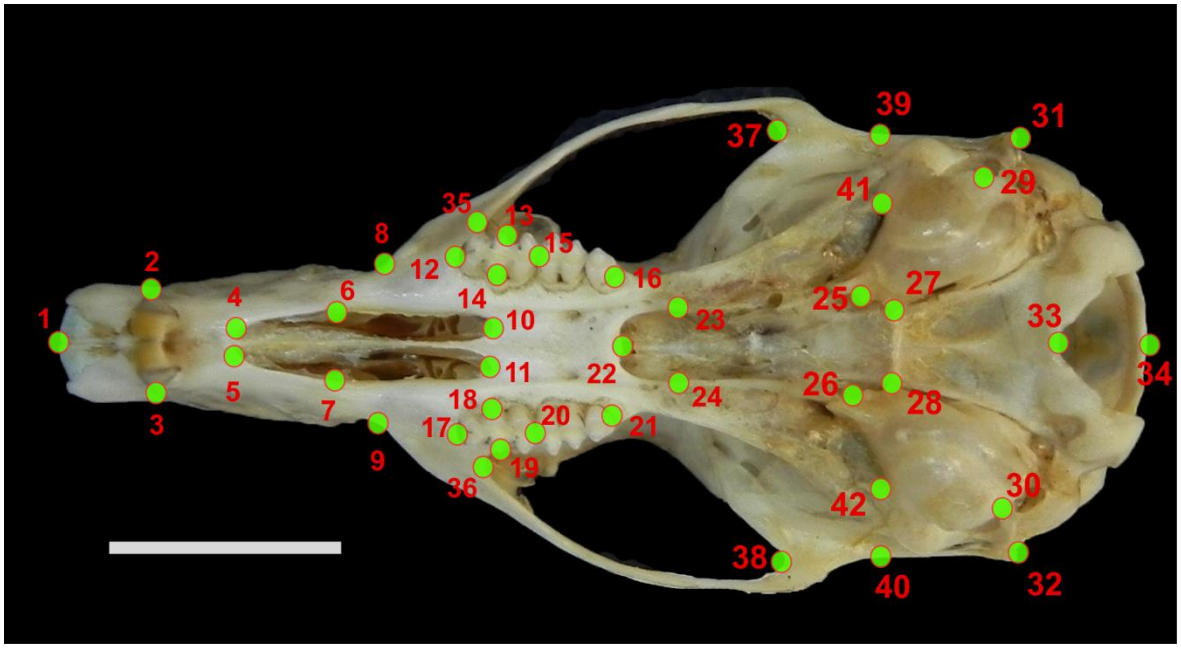

1: anteriormost point of suture between nasals; 2-3: lateralmost point of the alveolus of the incisor; 4-5: anteriormost margin of incisive foramen; 6-7: posteriormost point of suture between premaxilla and maxilla; 8-9: anteriormost margin of zygomatic plate; 10-11: posteriormost margin of incisive foramen; 12-17: anteriormost margin of first molar alveolus; 13-19: Labial margin of M1 at the level of the second lamina; 14-18: lingual margin of M1 at the level of the second lamina; 15-20: posterior margin of M1; 16-21: posteriormost margin of third molar; 22: posteriormost point of suture between palatines; 23-24: long length of mesopterygoid fossa after suture between palatines; 25-26: anterior extremity of tympanic bulla; 27-28: basis length of suture between basisphenoid and basiocciptal; 29-30: end of auditory bulla line; 31-32: superiormost margin of tympanic bulla (ectotympanic); 33: anteriormost point of inferior margin of foramen Magnum; 34: posteriormost point of superior margin of foramen magnum; 35-36: anteriormost margin of the maximum zygomatic plate posterior constriction; 37-38: posteriormost margin of the maximum anterior constriction of squamosal root of zygomatic; 39-40: posterior end of squamosal root of zygomatic bar; 41-42: anteriormost border of the paramastoid process. Scale bar = 10 mm.

(C) Description of landmarks of skull lateral view:

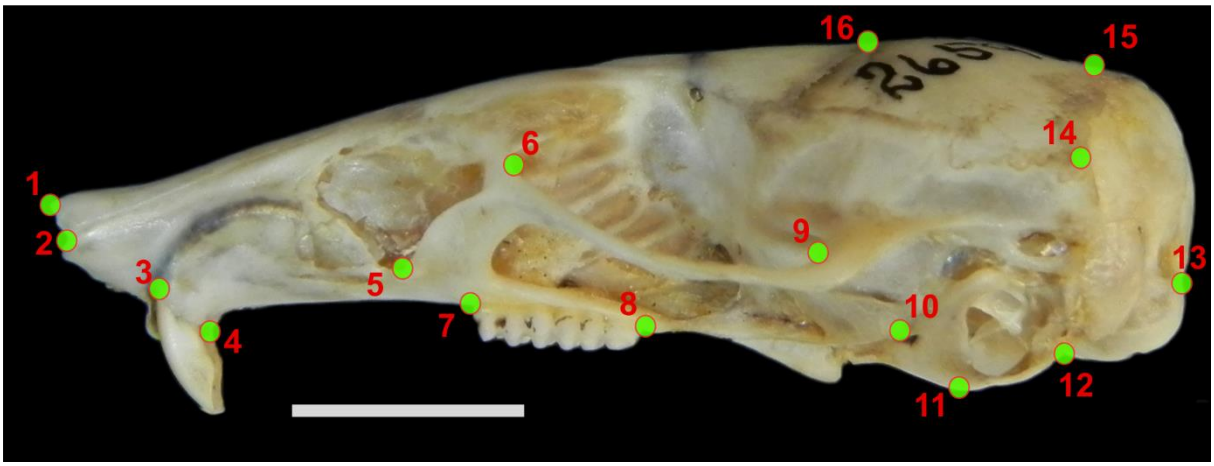

1: anteriormost point of nasal; 2: anteriormost point of the suture between the nasal and the premaxilla; 3: posteriormost point of incisor alveolus; 4: inferiormost point of incisor alveolus; 5: ventral extent of infraorbital foramen; 6: point of maximum posterior constriction of antorbital bridge; 7: anteriormost point of the molar row; 8: posteriormost point of the molar row; 9: point of maximum anterior constriction of squamosal root of zygomatic arch; 10: foramen ovale accessorius (closely tympanic bulla); 11: ventralmost point at the middle of the tympanic bulla; 12: inferior extremity on the boundary between the occipital condyle and the tympanic bulla; 13: curvature at the limit between the occipital condyle and the occipital bone; 14: suture between parietal, squamosal and occipital; 15: inferiormost point of suture between pariental and interparietal 16: superiormost point of suture between frontal and parietal. Scale bar = 10 mm.

Supplementary Data SD5. — General Supplementary tables results. Jackknife Cross-validation (A), Tukey HSD, honest significant difference (B) and pairwise MANOVA (C).

A. Percentage of correct classification from discriminant analysis, using Jackknife Cross-validation, for dorsal, ventral, and lateral view of skull for four lineages in *Oxymycterus* aff. *quaestor*.

Dorsal				
Group	D	C	A	B
Lineage D (N=5)	80	20	0	0
Lineage C (N=16)	0	62.50	37.50	0
Lineage A (N=75)	0	6.66	93.33	0
Lineage B (N=3)	0	33.33	0	66.67
Overall accuracy		86.86		
Ventral				
Group	D	C	A	B
Lineage D (N=5)	60	20	20	0
Lineage C (N=16)	6.25	75	18.75	0
Lineage A (N=75)	2.66	12	85.33	0
Lineage B (N=3)	0	0	0	100
Overall accuracy		82.82		
Lateral				
Group	D	C	A	B
Lineage D (N=5)	20	20	60	0
Lineage C (N=16)	6.25	37.50	50	6.25
Lineage A (N=73)	2.75	13.70	83.56	0
Lineage B (N=3)	0	33.33	66.67	0
Overall accuracy		70.10		

B. Tukey multiple comparisons of means 95% family-wise confidence level in *Oxymycterus* aff. *quaestor* lineages.

Lineages	diff	lower	upper	*P*
C x D	-0.5121831	-1.0702983	0.045932130	0.0839931
A x D	-0.8223568	-1.3254965	-0.319217161	0.0002632
B x D	-14.574.931	-2.2530267	-0.661959435	0.0000358
A x C	-0.3101738	-0.6101517	-0.010195854	0.0398594
B x C	-0.9453100	-1.6306647	-0.259955360	0.0027508
B x A	-0.6351363	-1.2765160	0.006243467	0.0532833

C. Pairwise MANOVA comparisons of skull shape for dorsal, ventral and lateral views between four lineages (A, B, C and D) of *Oxymycterus* aff. *quaestor*. The number of iterations for significance testing was 10,000.

Dorsal	R^2	*d.f.*	*F*	*P*
C x D	0.24956	1	6.3184	< 0.001
A x D	0.12183	1	10.821	< 0.001
B x D	0.67278	1	12.336	< 0.01
A x C	0.053984	1	5.0787	< 0.001
B x C	0.34342	1	8.8916	< 0.01
B x A	0.13122	1	11.479	< 0.001

Ventral	R^2	*d.f.*	*F*	*P*
C x D	0.14204	1	3.1456	< 0.01
A x D	0.092417	1	7.9426	< 0.001
B x D	0.57225	1	8.0268	< 0.05
A x C	0.068175	1	6.5115	< 0.001
B x C	0.24311	1	5.4602	< 0.01
B x A	0.052376	1	4.2006	< 0.001

Lateral	R^2	*d.f.*	*F*	*P*
C x D	0.13036	1	2.8481	< 0.01
A x D	0.06977	1	5.7002	< 0.001
B x D	0.55243	1	7.4058	< 0.05
A x C	0.046879	1	4.2791	< 0.001
B x C	0.20328	1	4.3376	< 0.01
B x A	0.043694	1	3.3811	< 0.01

CAPÍTULO 6.

CONSIDERAÇÕES FINAIS

Durante esta tese foi explorado, pela primeira vez, os limites genéticos intraespecíficos (utilizando sequências de mtDNA e nDNA) em espécies do gênero *Oxymycterus*, em especial aquelas distribuídas na Mata Atlântica Sul e dos Pampas brasileiros e uruguaios. Além disso, foi o primeiro trabalho a utilizar morfometria geométrica aplicada as espécies do gênero, de forma intra- e interespecífica.

Segundo a literatura, quatro espécies de *Oxymycterus* ocorrem no sul do Brasil: *O. dasythrichus*, *O. delator*, *O. nasutus* e *O. quaestor*. Com base nos dados obtidos, utilizando ampla revisão de material depositado em coleções insitutiocionais, confirmou-se a ocorrência de *dasythrichus*, *O. quaestor* e *O. nasutus*, bem como uma nova espécie nominal (*Oxymycterus itapeby*) e se sugeriu a existência de linhagens filogeográficas que potencialmente venham a ser reconhecidas como novas espécies (*Oxymycterus* sp.1 e sp.2). Em relação as linhagens com ampla distribuição pelo sul do Brasil: (i) *O. nasutus*, apresentou uma distribuição geográfica maior do que aquela reconhecida nas últimas revisões do gênero (Oliveira & Gonçalves 2015), estando presente tanto nos Pampas do Brasil e Uruguai (ecorregião das Savanas Uruguais), como nos campos de altitude ocorrente em elevações (~700 m) da Mata Atlântica no sul do Brasil; e (ii) *O. quaestor* (apresentado no capítulo 5 como grupo '*quaestor'*), ocorrendo na Mata Atlântica presente no sul e sudeste do Brasil, contemplou extensões geográfica em territórios da Argentina (província de Misiones) e Paraguai (departamentos de Canindeyú e Alto Paraná). *O. dasytrichus* se observou presente, não só limitado em sua distribuição ao estado do Paraná na região sul do Brasil, mas também com dois espécimes registrados no litoral do estado de Santa Catarina, além de novos

registros ao estado do Paraná (Anexo 1). Durante toda a extensa amostragem presente neste estudo, nenhuma amostra referente a *O. delator* foi identificada, pelos menos nos domínios da pequena porção do Cerrado no norte do estado do Paraná ou região sul do estado de São Paulo no Brasil, conforme indicado por Bonvicino et al. (2008) e Oliveira & Gonçalves (2015).

A primeira abordagem desta tese (Capítulos 2 e 3) foi explorar o padrão filogeografico e morfológico em *Oxymycterus nasutus*, espécie que ocupa áreas abertas nos Pampas e Campos de Altitude dentro da Floresta de Araucária (domínio da Floresta Atlântica). Embora *O. nasutus* tenha apresentado dois grupos que divergiram principalmente durante o Pleistoceno Médio (a partir de ~ 0,571 Ma), período compatível como o observado em diversas espécies de mamíferos (Turchetto-Zolet et al. 2013), os resultados indicaram que *O. nasutus* experimentou uma expansão populacional ao longo do tempo, com uma possível retração demográfica durante o período pós-glacial, um potencial microrefugio em áreas de campos. Apesar de estudos anteriores, com outros roedores sigmodontíneos, já tenham observado padrões de diferenciação em clina ao longo do eixo norte-sul nos Pampas (Quintela et al. 2016), e na Mata Atlântica (Maestri et al. 2016), esta é a primeira vez que o tal padrão foi encontrado na distribuição total de uma espécie do gênero *Oxymycterus*. Embora Gonçalves & Oliveira (2004) já tenham observado este padrão em clina para a forma do crânio em *O. dasytrichus*, estes autores utilizaram uma amostragem reduzida baseados em morfometria clássica (linear), contemplando parcialmente a distribuição desta espécie. Contudo, vale ressaltar que *O. nasutus* é uma espécie com distribuição em dois biomas, com espécimes maiores verificados ao norte (domínios da Mata Atlântica), e menores em direção ao sul (nos pampas) da sua distribuição. Paralelamente, a forma do crânio segue padrão similar de diferenciação em clina, resultado previamente indicado pelo Capítulo 2.

Os preditores utilizados na abordagem do Capítulo 3 (ou seja, distância genética, altitude, precipitação e produção primária líquida, principalmente) atuaram de maneira equilibrada para

explicar a variação da forma nas análises de redundância, mas diferem ligeiramente para as vistas dorsal e ventral. No entanto, diferentemente da forma, os atributos ambientais (com relevância apenas para altitude, precipitação e produtividade primária) possuem influência significativa no tamanho do crânio, do que os genéticos (62% vs. 4%), embora apresentem uma fração considerável de explicação conjunta (21%). Dessa forma, ao menos a esta espécie, a influência das características ambientais de cada ecorregião parece superar a regra de Bergmann para explicar o padrão de tamanho, visto que as condições de temperatura preditoras analisadas, não foram estatisticamente significantes.

Ainda, uma nova espécie de *Oxymycterus* presente em áreas de transição entre a Mata Atlântica e Cerrado, nos estados do Paraná e São Paulo (Brasil), foi descrito no Capítulo 4, aumentando para 16 o número de espécies válidas para o gênero. Comparativamente aos demais congêneres, está espécie forma um grupo filogenético com outras espécies com distribuições em ambientes savânicos, juntamente com *O. delator* e *O. amazonicus*.

Por último, no Capítulo 5, através de uma ampla abordagem amostral (a mais robusta em termos quantitativos até o momento), compreendendo quase toda a faixa de distribuição prevista para o grupo, e analises filogenéticas e morfometria geométrica, verificou-se que *O. quaestor* compreende quatro linhagens filogeográficas distintas, sendo uma relacionada a *O. quaestor*, outra com possível sinonímia com *O. judex*, e outras duas como potenciais novas espécies a serem descritas. Embora os resultados via morfometria geométrica foram menos consistentes para a distinção entre *O. quaestor* e *O. judex*, suportam a hipótese de duas linhagens divergentes dentro deste grupo (*Oxymycterus* sp.1 e sp.2). Os resultados gerados nesta tese sugerem que outras espécies do gênero *Oxymycterus* podem conter linhagens crípticas, e que a história evolutiva do grupo ainda está sujeita a novas informações sobre limites de distâncias genéticas, padrões morfológicos, biogeográficos e linhagens crípticas.

Contribuições à sistemática e história evolutiva de *Oxymycterus*

Uma das principais dificuldades em relação a *Oxymycterus* é que a sistemática do gênero tem sido muito instável, experimentando muitas mudanças de acordo com diferentes arranjos taxonômicos (Cabrera 1961; Hershkovitz 1994; Oliveira 1998; Musser & Carleton 2005; Bonvicino et al. 2008; Oliveira & Gonçalves 2015), principalmente devido a descontinuidade na detecção de caracteres morfológicos e citogenéticos (Gonçalves 2006; Di-Hizo et al. 2017), imprecisão sobre localidade-tipo (e.g. *O. rufus* Fischer, 1814 e *O. dasytrichus* Schinz, 1821), ausência de material físico de holótipo (e.g. *O. rufus* Fischer, 1814) ou mesmo espécies conhecidas apenas para poucas localidades ou mesmo localidade tipo (e.g. *O. nigrifrons* Osgood, 1944, *O. hucucha* Hinojosa et al. 1987, *O. hiska* Hinojosa et al. 1987, *O. caparaoe* Hershkovitz, 1998). Deste modo, qualquer abordagem está passível de interpretações errôneas, embora alguns pesquisadores tenham lançado luz sobre a sistemática do gênero, utilizando revisões de séries-tipo e coleções (Hershkovitz 1994; Oliveira 1998) ou utilizando abordagens filogenéticas (e.g. Hoffmann et al. 2002).

Desde as descrições da maioria das espécies precedida por Joel A. Allen e Michael R. Oldfield Thomas, no início do século XX e sucedida por demais naturalistas/pesquisadores, a primeira compilação taxonômica do gênero foi proposta por Hershkovitz (1994), onde descreve incialmente 23 formas nominais atribuídas ao gênero. Hershkovitz (1994), a partir de mensurações craniodentárias (do condilobasal e da série molar superior) e comprimento das garras traseiras, dos holótipos e/ou obtidos nas descrições originais, divide as formas nominais em 2 grupos: Divisão Andina e Atlântica, sendo que cada divisão possuindo 3 classes de tamanho (pequeno, médio e grande). O autor ainda especula que possivelmente as divisões possuíam um ancestral comum, e que divergiram em direção a ‘‘rota Atlântica’’ (onde é apontado possuindo as maiores formas), e outra em direção aos Andes, ‘‘evoluindo’’ (i.e., se diversificando) de forma independente.

Posteriormente, mais uma forma nominal foi adicionada, *O. caparaoe* (Hershkovitz 1998) incluído no grupo Atlântico, totalizando até então 24 formas.

Corroborando de forma parcial, o boxplot (Figura 12, Capítulo 4) apoia a hipótese de classes de tamanho, em pelo menos aos membros da divisão Atlântico proposto por Hershkovitz (1994), verificando *O. quaestor* e *O. dasytrichus* as maiores formas, e *O. amazonicus*, *O. nasutus*, além da espécie nova, as menores. Durante o desenvolvimento dessa tese, também foi gerada a mais refinada filogenia (incluindo linhagens crípiticas) em relação a diversidade do gênero, utilizando um marcador (cit-b), calibrada com registro fóssil (Anexo.2). Filogenias calibradas multilócus já foram incluindo *Oxymycterus* (Fabre et al. 2012; Parada et al. 2015; Steppan & Schenk 2017), no entanto, tais abordagens não contemplam todas linhagens. A filogenia grosseiramente aponta para formação de um clado Andino, formado por *O. wayku* e 3 linhagens atribuídas a *O. paramensis* (denominadas como linhagem Argentina, Peru e Bolívia). Apesar desta associação, a topologia apresenta *O. hiska* como uma linhagem irmã dos clados *O. rufus* + *O. josei* e *"*grupo *quaestor"*, embora com baixo suporte de probabilidade posterior (PP = 0.79). Porém, nesta filogenia gerada (Anexo.2), não foi verificada uma relação direta da topologia com a formação de um grupo Atlântico (Divisão Atlântica). Assim, possivelmente, a falta de resolução para formação de um grupo exclusivo a divisão Atlântica proposta por Hershkovitz (1994), poderia ser atribuída ao fato deste gênero tenha uma história evolutiva mais complexa do que simplesmente uma divisão ao longo do eixo leste-oeste na América do Sul.

Neste contexto, Reig (1984, 1987) propõe que a radiação da tribo Akodontini (principalmente entre os gêneros *Akodon*, *Oxymycterus* e *Necromys*) ocorreu em três principais direções ao longo da América do Sul: a partir de uma região central da Cordilheira dos Andes, conhecida/atribuída como Puna, a partir e durante o Plioceno inferior. Reig (1984) ainda menciona que durante o Mioceno Superior-Plioceno Inferior, os Akodontinos teriam se diversificado antes da

expansão/radiação, hipótese suportada por Smith & Patton (1993). Tal datação proposta de diversificação durante o Plioceno inferior é concordante com fósseis registrados a estes gêneros datados para os estágios das glaciações patagônicas, tais como: *Necromys bonapartei* no estágio Chapadmalalense Inferior (4 - 3.5 Ma), *Akodon lorenzinii* no estágio Vorohuense (2.85 - 2.55 Ma), e *Oxymycterus* cf. *rufus* e cf. *paramensis* no estágio Ensenadense (2.1 - 0.5 Ma), sendo todos estes registros atríbudos ao Plioceno inferior-Pleistoceno Superior (Pardiñas et al. 2002). No entanto, *O.* cf. *paramensis* ainda necessita confirmação se é referido a um fóssil do gênero. A partir deste ponto de diversificação, primeiramente uma linhagem teria ido em direção ao norte de puna, onde teria iniciado sua diversificação pelas encostas andinas úmidas; a segunda em direção aos vales do sul Andinos, onde possivelmente encontrou ambientes semelhantes ao de Puna (semelhantes a atual área de Tucumán na Argentina, região majoritariamente estépica, mas ligada ao sul da floresta de Yungas); e por último, a partir do sul de Puna em direção as planícies mais a leste, podendo ser comprendido em direção ao Atlântico (Reig 1984, 1987; Smith & Patton 1993). Estudos posteriores reforçam esta hipótese de diversificação a partir de uma região central da Cordilheira dos Andes (Smith & Patton 1993; Maestri et al. 2018), e apontam evidências do importante papel das planícies (*lowlands*) e do leste da América do Sul (Smith & Patton 1999; Gonçalves et al. 2018), particularmente para a diversificação da tribo Akodontini (Parada et al. 2015).

A grande diversificação observada em *Oxymycterus*, principalmente nas formas ‘‘Atlânticas’’ de Hershkovitz (1994)¸ plausívamente tenham relação com as glaciações patagônicas (tais como a Grande Glaciação Patagônica [GPG]) que se estenderam desde o final do Mioceno ao longo de todo o Plioceno e Pleistoceno, e que se tornaram mais frequentes após o Plioceno Superior (Rabassa & Coronato 2009). No início do Pleistoceno, várias glaciações pré-GPG foram identificadas, sendo a GPG aparecendo no final deste período entre 1.168-1.016 Ma (Rabassa & Coronato 2009). Dessa forma, as glaciações pré-GPG parecem ter impulsionado a diversificação do

gênero, inciada por volta de 1.689 Ma (95% HPD, 1.324–2.119 Ma), no ainda no Pleistoceno superior de acordo com a filogenia datada do capítulo 5, embora outras filogenias multilócus, que incluam o gênero em questão, apontem tempo de surgimento anteriores (Parada et al. 2015).

Maestri et al. (2018), em ampla abordagem sobre os processos biogeográficos históricos com roedores sigmodontíneos, apontam que alguma conexão entre os Andes e a Mata Atlântica persistiu em todo o Plioceno, e que possivelmente através de arcos de climas sazonalmente secos. Tais arcos, se estenderam dos Andes tropicais, passando pelo norte da Argentina até a Mata Atlântica no nordeste do Brasil, e foram vegetados no passado por florestas sazonalmente secas durante o Pleistoceno (Prado & Gibbs, 1993; Pennington et al. 2000). Embora Werneck et al. (2011), através de modelagem de paleodistribuição, encontre indícios de severas fragmentações e áreas instáveis em florestas sazonais secas ao longo do Pleistoceno na América do Sul. Assim, a conexão entre formas Andinas e Atlânticas, parece ter sido impulsionada por tal arco/corredor (como por exemplo a diversificação/distribuição das espécies mais basais do gênero, tais como: *O. delator*, *O. amazonicus* e *Oxymycterus*. sp. nova, ver discussão do Capítulo 4), e que apoia um importante papel das terras baixas e leste da América do Sul na diversificação sigmodontineos, em especial para *Oxymycterus*, mas que por si só, não explicaria a diversidade do gênero, principalmente para as formas Atlânticas de Hershkovitz (1994) e suas relações filogenéticas apresentadas nesta tese.

Com ênfsase em agrupamentos informais das espécies e formas nominais, Oliveira (1998) difere em relação a delimitação morfológica e geográfica da proposta de Hershkovitz (1994) para o gênero *Oxymycterus.* Através de uma abrangente revisão morfológica e livre de uma delimitação de tamanho (i.e classes de tamanho de Hershkovitz), sintetizando as informações contidas nas séries-tipo e nas descrições originais, Oliveira (1998) propos 10 grupos de espécies morfologicamente e geograficamente alopátricas, associando 22 das 23 formas nominais do gênero, sugerindo 5

potenciais novos táxons para representar populações da costa atlântica com morfótipos diferenciados. Embora nenhuma proposição taxonômica tenha sido oficializada, os resultados encontrados nesta tese vão parcialmente de encontro com a proposta de Oliveira (1998). A proposta de Oliveira, com ênfase as espécies/ou formas nominais em *Oxymycterus*, foi também posteriormente rediscutidos/remodelados por Gonçalves (2006).

Em suma, Oliveira (1998) aponta seis grupos de espécies aos domínios da costa Atlântica, sendo que alguns destes agrupamentos, como o grupo '*judex*' (no qual Oliveira incluíu mensurações morfométricas das séries tipo de *O. quaestor, O. judex, O. misionalis*, além de espécimes do estado do Rio de Janeiro atribuídas a *O. quaestor*), corroboram com os resultados encontrados nas relações filogenéticas via mtDNA deste trabalho (Fig. 3, Capítulo 4; Fig. 5, Capítulo 5), ainda que denominado nesta tese como grupo '*quaestor*' (devido ser a primeira espécie descrita deste grupo por Thomas em 1903). Embora Gonçalves (2006) já tenha mencionado uma variação de distância genética com base em sequências de cit-b (1% à 3.3%) para este grupo, este autor não incluiu sequências referentes a formas consideradas como '*O. misionalis*'. Nesta tese, além da inclusão de análises via morfometria geométrica, a análise molecular revelou ainda uma distinta linhagem ainda não descrita para este grupo de estudo, referenciada nesta tese como *Oxymycterus* sp.2 (apresentando uma distância genética acima de 5% em relação as linhagens A, B e C referentes ao grupo '*quaestor*') e a distinção da população do estado do Rio de Janeiro em uma nova linhagem.

Apesar de Oliveira (1998) considerar *O. delator* e *O. amazonicus* presentes em grupos distintos (grupo *delator* e grupo *amazonicus*), Gonçalves (2006) através de uma nova abordagem em relação a variabilidade morfológica, genética e panorama amostral, amplia a abragência do grupo *delator*, incluindo *O. amazonicus* e uma forma ainda descrita (referenciada como *Oxymycterus* sp.), além do próprio *O. delator*. Neste sentido, a abordagem filogenética com base em inferência bayesiana vai ao encontro deste agrupamento morfológico de Gonçalves (2006), onde

O. delator, *O. amazonicus*, juntamente com a espécie descrita no capítulo 4, perfazem um único clado, tanto na filogenia calibrada do capítulo 4 e 5 (e Anexo.2). Ainda que de forma especulativa, a forma alto-montana apontada por Gonçalves (2006), poderia ser uma extensão geográfica da espécie descrita no capítulo 4, presente em áreas de transição Cerrado-Mata Atlântica do sul/sudeste brasileiro (acima de 800 m), visto que a forma alto-montana ocorre em campos de altitude do Itatiaia, a mais de 2000 m no sudeste do Brasil.

Gonçalves (2006), ainda associa *O. nasutus* (que pertence a um grupo exlusivo a sua espécie de acordo com Oliveira 1998) a *O. caparaoe* (espécie até então restrita às zonas alto-montanas da Serra do Caparaó, no sudeste do Brasil, e não incluída por Oliveira a nenhum grupo, sendo designado como *Oxymycterus* sp. 5). Assim, devido a similaridade morfométrica e sobreposição de caracteres em análises discriminantes de variáveis canônicas entre estas duas espécies, além de serem reciprocamente monofiléticos (via reconstrução em parcimônia), novamente uma associação de caracteres morfológicos se perfaz correlacionada a reconstruções filogenéticas. Uma nova abordagem mais ampla, via inferência bayesiana poderia por a prova a consistência deste grupo. Porém, a filogeografia publicada do capítulo 2, e o padrão morfológico em clina ao longo do eixo norte-sul do capítulo 3 (dos Pampas uruguaios aos campos de altitude da Mata Atlântica no estado do Paraná, no Brasil), podem ser um primeiro indicío, ainda que indireto, que estas duas espécies sejam realmente relacionadas. *O. caparaoe* é uma espécie endêmica, e encontrada também em zonas campestres (também chamado de campos de altitude ou campos rupestres par ao sudeste brasileiro) acima de 2.500m, na Serra do Caparaó (Hershkovitz, 1998), e que devido aos efeitos das oscilações climáticas do Pleistoceno, promovidas pelas glaciações, estas linhagens que hoje são alopátricas, poderiam estar em contato, visto que o padrão de áreas abertas (dominados por gramíneas) poderia se estender até o sudeste brasileiro durante o último máximo glacial (Behling 2002).

Por fim os grupos *rufus*, *angularis* e *dasytrichus* ainda caracem de abordagens taxnômicas mais robustas, principalmente filogenéticas. Contudo, estudos posteriores Oliveira (1998) tenham contribuído em desvendar os padrões destes grupos. Gonçalves & Oliveira (2004), por exemplo, revela formas 'avermelhadas' e 'escuras' simpátricas de *Oxymycterus* encontradas em floresta secundária no sudeste do Brasil (município de Viçosa, no estado de Minas Gerais), demonstrando com base em mensurações lineares (= clássica) de crânio e abordagem filogenética via máxima parcimônia, que consistem em representantes das espécies *O. rufus* (forma avermelhada) e *O. dasytrichus* (forma escura). Curiosamente, *O. rufus* é uma espécie com distribuição predominante nos Pampas argentinos (da província de Buenos Aires à Corrientes), e que sua população isolada ao sudeste brasileiro, é de certa forma apoiada nas análises com base em inferência bayesiana nesta tese (Fig. 3, Capítulo 4; Fig. 5, Capítulo 5). Porém, *O. josei* emerge com uma linhagem irmã, em relação ao clado de *O. rufus* 'argentino', sendo *O. rufus* 'brasileiro' uma linhagem irmã (externa) a estes. Tal grupo, certamente será alvo de novas abordagens taxonômicas, principalmente para a sustenção destas linhagens. Ainda, devido a Oliveira (1998) considerar que o grupo *angularis* (presente ao norte da Mata Atlântica) e *dasytrichus* (predominante ao sul da Mata Atlântica), performam um continuo morfológico que engloba toda a gama de distribuição destes grupos, Oliveira & Gonçalves (2015) colocam *O. angularis* como sinônimo júnior em relação a *O. dasytrichus*, em uma ultima revisão. Entretanto, apesar da releitura da distribuição da espécie *O. dasytrichus* no Anexo I considerar a última revisão do gênero *Oxymycterus* (Oliveira & Gonçalves 2015), será necessário uma abordagem mais robusta em espectro amostral, tanto em aspectos morfológicos e genéticos para testar tal esquema taxonômico em sinonímia.

Vale a pena mencionar que após a revisão de Oliveira (1998), algumas espécies foram descritas como *O. josei* (Hoffmann et al. 2002), *O. wayku* (Jayat et al. 2008), além da descrita no Capítulo 4, que elevaria, até o presente, a 27 formas nominais para o gênero *Oxymycterus*. Deste

modo, os resultados da tese jogam luz sobre questões como limites genéticos intraespecíficos, história evolutiva das espécies com ocorrência na região sul do Brasil (com extensão a territórios argentinos, paraguaios e uruguaios), padrões de variação fenotípica e diversidade das espécies válidas do gênero.

Tais resultados apresentados nesta tese, corroboram parcialmente com as abordagens de classes de tamanho de Hershkovitz (1998), e as relações filogenéticas através de inferência bayesiana, seguem um padrão semelhante a proposta de grupos de espécies Oliveira (1998), ao menos para as espécies presente ao leste (Atlântico) da América do Sul. A perpectiva a partir desses resultados é a continuidade de abordagens com o grupo *Oxymycterus*, a fim de decifrar a história evolutiva de espécies também ocorrentes no Cerrado e da Mata Atlântica, como *O. delator* e *O. dasytrichus*, assim como as linhagens andinas, que inclusive possuem trabalhos em andamento (Ruelas & Pacheco 2018), que permitam comparar padrões filogeográficos, e que possivelmente venha a ter novos desdobramentos taxonômicos.

REFERÊNCIAS BIBLIOGRÁFICAS

Behling H. (2002) South and southeast Brazilian grassland during Late Quaternary times: a synthesis. Palaegeography, Palaeclimatology, Palaeoecology. 177:19-27.

Bonvicino CR, Oliveira JA, D'Andrea OS. (2008) Guia dos roedores do Brasil, com chaves para gêneros baseadas em caracteres externos. Centro Pan-Americano de Febre Aftosa - OPAS/OMS.

Cabrera, A. (1961) Catalogo de los mamiferos de America del Sur. II (Sirenia, Perissodactyla, Artiodactyla, Lagomorpha, Rodentia). Revista del Museo Argentino de Ciencias Naturales "Bernardino Rivadavia" (Zoologia) 4: 309-732.

Di-Nizo CB, Banci KRS, Sato-Kuwabara Y, Silva MJJ. (2017) Advances in cytogenetics of Brazilian rodents: cytotaxonomy, chromosome evolution and new karyotypic data. Comparative Cytogenetics 11(4): 833–892.

Fabre P-H, Hautier L, Dimitrov D, Douzery EJP. (2012) A glimpse on the pattern of rodent diversification: a phylogenetic approach. BMC Evolutionary Biology, 12:88.

Gonçalves PR, Christoff AU, Machado LF, Bonvicino CR, Peters FB. (2018) Unraveling Deep Branches of the Sigmodontinae Tree (Rodentia: Cricetidae) in Eastern South America. Journal of Mammalian Evolution, 1–22.

Gonçalves PR, Oliveira JA. (2004) Morphological and Genetic Variation between Two Sympatric Forms of *Oxymycterus* (Rodentia: Sigmodontinae): An Evaluation of Hypotheses of Differentiation within the Genus. Journal of Mammalogy, 85(1):148-161.

Gonçalves PR. (2006) Diversificação dos Roedores Sigmodontíneos em Formações Alto-Montanas da Mata Atlântica. Rio de Janeiro, Tese de Doutorado, Universidade Federal do Rio de Janeiro. 296p.

Hershkovitz P. (1994) The description of a new species of South American hocicudo, or long-nose mouse genus *Oxymycterus* (Sigmodontinae, Muroidea), with a critical review of the generic content. Fieldiana: Zoology (New Series), 1460 (79):1–43.

Hershkovitz P. (1998) Report on some sigmodontinae rodents collected in southeastern Brazil with descriptions of a new genus and six new species. Bonner zoologische Beiträge**,** 47: 193-256.

Hoffmann FG, Lessa EP, Smith MF. (2002) Systematics of *Oxymycterus* with description of a new species from Uruguay. Journal of Mammalogy**,** 83(2): 408-420.

Jayat JP, D'Elía G, Pardiñas UFJ, Miotti MD, Ortiz PE. (2008) A new species of the genus *Oxymycterus* (Mammalia: Rodentia: Cricetidae) from the vanishing Yungas of Argentina. Zootaxa, 1911: 31–51.

Maestri R, Upham NS, Patterson BD (2019) Tracing the diversification history of a Neogene rodent invasion into South America. Ecography, 42: 683-695.

Maestri R, Fornel R, Gonçalves GL, Geise L, Freitas TRO, Carnaval AC. (2016) Predictors of intraspecific morphological variability in a tropical hotspot: comparing the influence of random and non-random factors. Journal of Biogeography, 43: 2160–2172.

Musser GG, Carleton MD (2005) Superfamily Muroidea, pp 894–1531. *In:* Wilson DE, Reeder DM (eds.) Mammal Species of the World: a taxonomic and geographic reference 3. ed. Baltimore: The Johns Hopkins University Press, 2142 pp.

Oliveira JA. (1998) Morphometric assessment of species groups in the South American rodent genus *Oxymycterus* (Sigmodontinae), with taxonomic notes base on the analysis of type material. Tese de doutorado, Texas Tech University, 320 p.

Oliveira JA, Gonçalves PR. (2015) Suborder Myomorpha: Family Cricetidae: Subfamily Sigmodontinae. Genus *Oxymycterus In:* Patton JL, Pardiñas UFJ, D'Elía G. (eds.). Mammals of South America 2: Rodents. Chicago: University of Chicago Press, pp. 247-268.

Parada A, D'Elía G, Palma ED. (2015) The influence of ecological and geographical context in the radiation of Neotropical sigmodontine rodents. BMC Evolutionary Biology, 15:172.

Pardiñas UFJ, D'Elia G, Ortiz PE. (2002) Sigmodontinos fósiles (rodentia, muroidea, sigmodontinae) de América del sur: estado actual de su conocimiento y prospectiva. Mastozoología Neotropical / J. Neotrop. Mammal, 9(2):209-252.

Pennington RT, et al. (2000) Neotropical seasonally dry forests and Quaternary vegetation changes. Journal of Biogeography. 27: 261– 273.

Prado DE, Gibbs PE. (1993) Patterns of species distributions in the dry seasonal forests of South America. Annals of the Missouri Botanical Garden. 80: 902– 927.

Quintela FM, Fornel R, Freitas TRO. (2016) Geographic variation in skull shape of the water rat Scapteromys tumidus (Cricetidae, Sigmodontinae): isolation-by-distance plus environmental and geographic barrier effects? Anais da Academia Brasileira de Ciências, 88 (Suppl. 1), 451-466.

Rabassa J, Coronato A. (2009) Glaciations in Patagonia and Tierra del Fuego during the Ensenadan Stage/Age (Early Pleistocene–earliest Middle Pleistocene). Quaternary International, 210 (1-2): 18–36.

Reig OA. (1984) Distribuição geográfica e história evolutiva dos roedores muroideos sul-americanos (Cricetidae: Sigmodontinae). Revta Bras. Genet. 7(2):333-365.

Reig, O. A. (1987) An assesment of the systematics and evolution of the Akodontini, with the description of new fossil species of *Akodon* (Cricetidae: Sigmodontinae). In Studies in Neotropical mammalogy, essays in honor of Philip Hershkovitz (B. D. Patterson and R. M. Timm, eds.). Fieldiana: Zoology, 39:347–399.

Ruelas D, Pacheco V. (2018) Situación taxonómica y posición filogenética de *Oxymycterus juliacae* Allen 1900 (Rodentia: Cricetidae). Apresentado em: IV Congreso Latinoamericano y VIII Congreso Boliviano de Mastozoologia.

Smith MF, Patton JL. (1993) The diversification of South American murid rodents: Evidence from mitochondrial DNA sequence data for the akodontine tribe. Biological Journal of the Linnean Society. 50: 149-177.

Smith MF, Patton JL. (1999) Phylogenetic relationships and the radiation of sigmodontine rodents in South America: evidence from cytochrome b. Journal of Mammalian Evolution, 6 (2):89–128.

Steppan SJ, Schenk JJ. (2017) Muroid rodent phylogenetics: 900-species tree reveals increasing diversification rates. PLoS One. 12(8): e0183070.

Turchetto-Zolet AC, Pinheiro F, Salgueiro F, Palma-Silva C. (2013) Phylogeographical patterns shed light on evolutionary process in South America. Molecular Ecology, 22:1193–1213.

Werneck FP, Costa GC, Colli GR, Prado DE, Sites Jr, JW (2011) Revisiting the seasonally dry tropical forests historical distribution: new insights based on palaeodistribution modeling and palynological evidence. Global Ecology and Biogeography, 20:272–288.

ANEXOS

Anexo .1

Range extension of the Atlantic Forest Hocicudo, *Oxymycterus dasytrichus* (Schinz, 1821), to the state of Santa Catarina, southern Brazil.

Willian Thomaz Peçanha, Gislene Lopes Gonçalves, Sérgio Luiz Althoff, Thales Renato Ochotorena de Freitas & Iris Hass.

Recebido: 22 de Junho, 2015

Aceito: 15 Fevereiro, 2016

Publicado: 24 de fevereiro, 2016

Check List 12(1): 1847

doi: http://dx.doi.org/10.15560/12.1.1847

Check List the journal of biodiversity data

NOTES ON GEOGRAPHIC DISTRIBUTION

Check List 12(1): 1847, 24 February 2016 doi: http://dx.doi.org/10.15560/12.1.1847
ISSN 1809-127X

Range extension of the Atlantic Forest Hocicudo, *Oxymycterus dasytrichus* (Schinz, 1821), to the state of Santa Catarina, southern Brazil

Willian Thomaz Peçanha[1], **Gislene Lopes Gonçalves**[2*], **Sérgio Luiz Althoff**[3], **Thales Renato Ochotorena de Freitas**[2] and **Iris Hass**[1]

1 Universidade Federal do Paraná, Departamento de Genética, Laboratório de Citogenética e Genética da Conservação Animal, Rua Alcides Vieira Arcoverde, s/n°, CEP 81531-990, Curitiba, PR, Brazil
2 Universidade Federal do Rio Grande do Sul, Departamento de Genética, Laboratório de Citogenética e Evolução, Av. Bento Gonçalves, 9500 - Prédio 43323 CEP 91501-970, Porto Alegre, RS, Brazil
3 Universidade Regional de Blumenau, CCEN, Departamento de Ciências Naturais, Laboratório de Biologia Animal, Rua Antônio da Veiga, 140, Bairro Victor Konder, CEP 89012-900, Blumenau, SC, Brazil
* Corresponding author. E-mail: lopes.goncalves@ufrgs.br

Abstract: Six individuals of *Oxymycterus dasytrichus* (Schinz, 1821) were found on the coast of Paraná and Santa Catarina (in the Atlantic Forest), expanding the known geographical distribution of the species ca. 280 km southward. The specimens represent the first record of the species for the state of Santa Catarina, and new localities to the region of southern Paraná. The identification of the species relied mainly on interspecies comparative assessment of genetic distance based on DNA sequences data from the mitochondrial cytochrome-*b* gene and geographic distribution of taxa across biomes, particularly in the Atlantic Forest. Our findings highlight the role of protected areas, particularly the Guaraqueçaba Environmental Protection Area, to preserve small mammals.

Key words: Rodentia; Akodontini; Dense Ombrophilous Forest

The Neotropical sigmodontine rodent genus *Oxymycterus* Waterhouse, 1837 is diverse, with 15 recognized species (Oliveira and Gonçalves 2015), and geographically widespread, from central Argentina and southern Uruguay to the Amazon basin (Hershkovitz 1994). The species boundaries, phylogenetic relationships, and distribution remain poorly understood (Jayat et al. 2008). Several recent studies have significantly advanced the understanding of the taxonomy and phylogeny of *Oxymycterus* (e.g., Hoffmann et al. 2002; Gonçalves and Oliveira 2004; D'Elía et al. 2008; Jayat et al. 2008; Oliveira and Gonçalves 2015). However, distinct aspects of the geographic distribution of the species are still in question, particularly in highly diverse biomes such as the Atlantic Forest.

Oxymycterus dasytrichus (Schinz 1821), commonly named the Atlantic Forest Hocicudo (Bonvicino et al. 2008), is widely distributed in Dense Ombrophilous Forest along the Brazilian coast, in the states of Pernambuco, Sergipe, Alagoas, Bahia, Espírito Santo, Minas Gerais, Goiás, Rio de Janeiro, and São Paulo, from the coastal lowlands to altitudes of around 2,000 m in Itatiaia, Rio de Janeiro (Oliveira 1998; Hoffmann et al. 2002; Gonçalves and Oliveira 2004; Oliveira and Gonçalves 2015). Oliveira and Gonçalves (2015) also recorded this species to the state of Paraná, although they do not list specific localities. The type locality was restricted to the Rio Mucuri in Bahia (Avila-Pires 1965). Gonçalves and Oliveira (2004) used integrative molecular and morphological techniques to study this species over most of its distribution in the Atlantic Forest, and their results suggested the existence of a morphological differentiation along a north–south axis.

The species is currently classified as of Least Concern (LC) according to the IUCN Red List of Threatened Species, due to its wide distribution and high population densities (Bonvicino et al. 2008).

The present study expanded the distributional range of *O. dasytrichus* (Figure 1) along the Atlantic Forest, to ca. 280 km south of the nearest previously recorded locality, at Cananéia, São Paulo. The four new localities are on the coast of Paraná (PR) and Santa Catarina (SC) (Figure 2; Table 1). The climate is humid subtropical (Köppen Cfa) (Kottek et al. 2006); the mean annual

Figure 1. *Oxymycterus dasytrichus*. Photograph by Pablo R. Gonçalves.

rainfall on the coast of Paraná is 2,435 mm, and on the north coast of Santa Catarina is 1,690 mm, with mean annual temperatures of 21 and 20.2°C, respectively (Vanhoni and Mendonça 2008; Araujo et al. 2006). The new recording localities are:

I) Guaraqueçaba-Índios, PR (25°21′ S, 048°26′ W, 10 m above sea level [a.s.l.]), on the northern coast of Paraná, flanked by Paranaguá and Laranjeiras bays and the Serra do Mar coastal mountain range. The Guaraqueçaba Environmental Protection Area (APA) includes the largest continuous remnant of the Atlantic Forest on the Brazilian coast. Together with Vale do Ribeira and

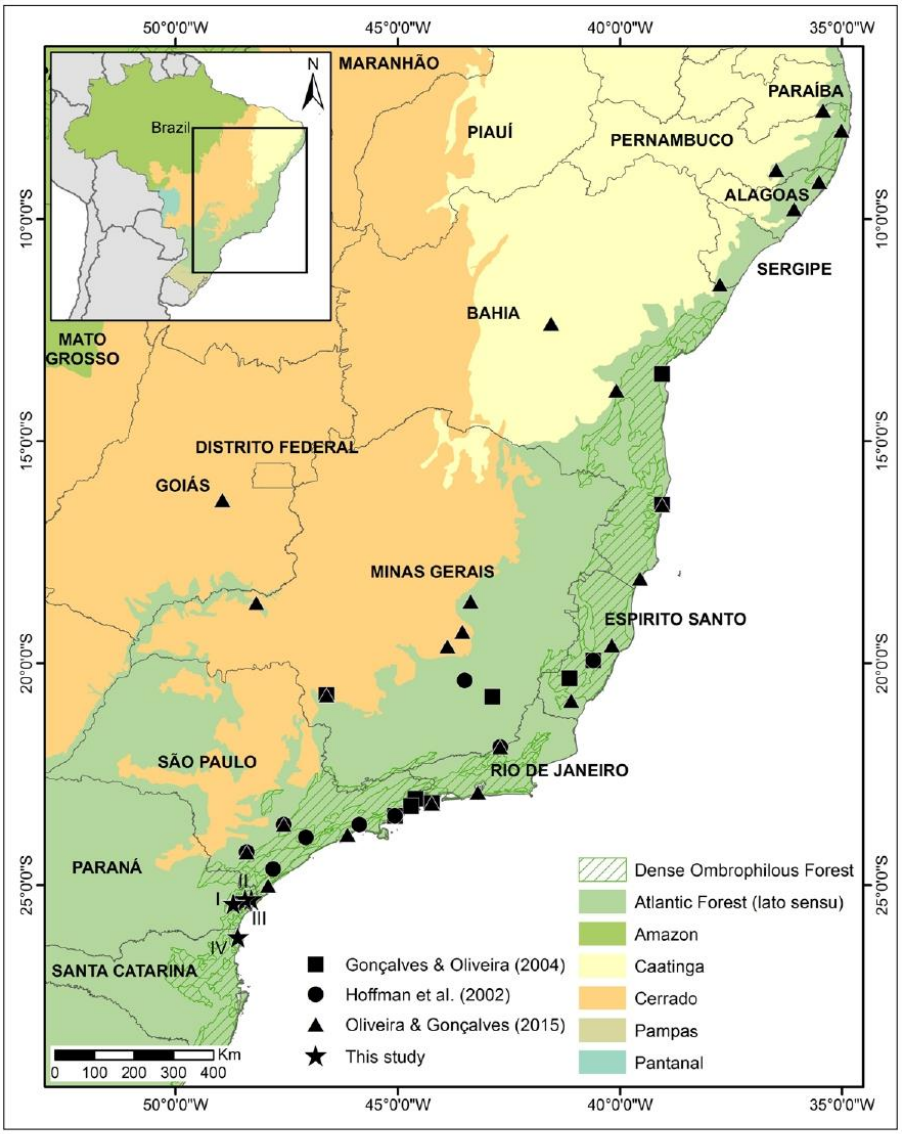

Figure 2. *Oxymycterus dasytrichus* distribution, primarily along the Atlantic Forest biome in Brazil. Stars indicate the locations of four new records from the Paraná and Santa Catarina coast. Numbers from I to IV are indicated in Materials and Methods.

Table 1. Locality records for *Oxymycterus dasytrichus,* including four new sites presented in this study.

State	Municipality	Locality	Latitude (S)	Longitude (W)	Reference*
Santa Catarina	Itapoá	—	26°10′	048°36′	This study
Paraná	Guaraqueçaba	Índios	25°21′	048°26′	This study
Paraná	Guaraqueçaba	Massarapuã	25°19′′	048°26′	This study
Paraná	Antonina	Bacia do Rio do Nunes	25°25′	048°42′	This study
São Paulo	Juquitiba	Barra do Rio Juquía	23°55′	047°04′	1
São Paulo	Salesópolis	Estação Biológica de Boracéia	23°38′	045°52′	1
São Paulo	—	—	24°37′	047°48′	1
São Paulo	Salto de Pirapora	Salto de Pirapora	23°38′	047°34′	1
São Paulo	Ubatuba	Ubatuba	23°26′	045°04′	1
São Paulo	Cananéia	Barra do Guarú	25°00′	047°55′	3
São Paulo	Capão Bonito	Fazenda Intervales	24°15′	048°24′	3
São Paulo	Salto de Pirapora	Salto de Pirapora	23°38′	047°34′	3
São Paulo	Bertioga	Varjão	23°51′	046°08′	3
São Paulo	Capão Bonito	Fazenda Intervales	24°15′	048°24′	1
São Paulo	Ubatuba	Ubatuba	23°26′	045°04′	2
Rio de Janeiro	Angra dos Reis	Ilha Grande	23°09′	044°14′	2
Rio de Janeiro	Paraty	Tarituba	23°03′	044°36′	2
Rio de Janeiro	Paraty	Paraty	23°13′	044°42′	2
Rio de Janeiro	Angra dos Reis	Ilha Grande	23°09′	044°14′	3
Rio de Janeiro	Rio de Janeiro	Tijuca, Fazenda Velha	22°54′	043°12′	3
Espírito Santo	Santa Teresa	Santa Teresa	19°56′	040°36′	2
Espírito Santo	Venda Nova do Imigrante	Venda Nova	20°20′	041°08′	2
Espírito Santo	Santa Teresa	Santa Teresa	19°56′	040°36′	1
Espírito Santo	Cachoeiro de Itapemirim	Castelinho	20°50′	041°06′	3
Espírito Santo	Santa Teresa	Reserva Florestal Nova Lombardia (Augusto Ruschi)	19°35′	040°11′	3
Minas Gerais	Além Paraíba	Além Paraíba	21°53′	042°42′	1
Minas Gerais	Ouro Preto	Ouro Preto	20°23′	043°30′	1
Minas Gerais	Passos	Passos	20°43′	046°36′	2
Minas Gerais	Viçosa	Viçosa	20°45′	042°52′	2
Minas Gerais	Além Paraíba	Além Paraíba	21°53′	042°42′	3
Minas Gerais	Araguari	Rio Jordão	18°38′	048°11′	3
Minas Gerais	Lagoa Santa/Conceição do Mato Dentro	Boca da Mata, km 104–105	19°02′	043° 25′	3
Minas Gerais	Serro	Fazenda Esperança	18°36′	043°22′	3
Minas Gerais	Lagoa Santa	Lagoa Santa	19°37′	043°53′	3
Minas Gerais	Passos	Passos	20°43′	046°36′	3
Goiás	Anápolis	Anápolis	16°19′	048°57′	3
Bahia	Cairu	Fazenda Subauma	13°29′	039°03′	2
Bahia	Palmeiras (Chapada Diamantina)	Gerais da Cachoeira da Fumaça	12° 31′	041° 33′	3
Bahia	Porto Seguro	Reserva Biológica Pau Brasil	16°26′	039°03′	3
Bahia	Mucuri	Rio Mucuri	18° 05′	039° 33′	3
Bahia	Jequié	Três Braços	13°51′	040° 05′	3
Sergipe	Cristinápolis	Fazendo Cruzeiro	11°28′	037°45′	3
Alagoas	Matriz de Camaragibe	Fazenda Santa Justina	09°09′	035°31′	3
Alagoas	São Miguel dos Campos	Mangabeiras	09°46′	036°05′	3
Pernambuco	Macaparana	Fazenda Água Fria	07°33′	035°26′	3
Pernambuco	São Lourenço da Mata	São Lourenço da Mata	08°00′	035°01′	3
Pernambuco	Garanhuns	Garanhuns	08°53′	036°29′	3

*1, Hoffmann et al. (2002); 2, Gonçalves and Oliveira (2004); 3, Oliveira and Gonçalves (2015). Geographical coordinates from 2 and 3 were estimated based on the municipality and/or location available.

Serra da Graciosa, the Guaraqueçaba APA is part of the Biosphere Reserve. The area adjacent to this sample locality also covers the Guaraqueçaba Ecological Station, including Superagüi National Park, and the Salto Morato and Sebuí Private Natural Heritage Reserves. Two males (UFPR-P752, UFPR-P754) and one female (UFPR-P760) were collected.

II) Guaraqueçaba-Massarapuã, PR (25°19′ S, 048°26′ W, 10 m a.s.l.), on a peninsula in the Guaraqueçaba APA. One male (UFPR-P757).

III) Antonina, basin of the Rio Nunes, PR (25°25′ S, 048°42′ W, 5 m a.s.l.) situated at sea level adjacent to the Serra do Mar on the coast of Paraná. One female (UFPR-P177).

IV) Itapoá, SC (26°10′ S, 048°36′ W, 18 m a.s.l.), on the northern coast of Santa Catarina, also in Dense Ombrophilous Forest (Atlantic Forest). One male (FURB 18669).

Specimens collected on the PR coast were caught in a Tomahawk trap, baited with corn and pineapple, in two field trips, one in June 1986 (UFPR-P177) and the other in April 1993 (UFPR-P752, UFPR-P754, UFPR-P757 and UFPR-P760). The single specimen captured on the northern coast of SC (FURB 18669; Figure 3) was caught in a Sherman trap baited with corn, in September 2011. These specimens are deposited in scientific collections at the Universidade Federal do Paraná (UFPR) and the Universidade Regional de Blumenau (FURB). Individuals were measured, tissues (muscle, kidney, liver and heart) were preserved in 96% ethanol at –20°C, and the skull and skin were prepared.

Total genomic DNA was purified from tissue samples of the six *O. dasytrichus* specimens using a PureLink DNA Extraction Kit (Invitrogen) following the manufacturer's instructions. A partial sequence (801 base pairs, bp) of the cytochrome-*b* (cyt-*b*) gene was amplified by polymerase chain reaction (PCR) using ca. 50 ng of DNA per sample, with primers and conditions described by Smith and Patton (1993). The PCR products were purified using the enzymatic method (Exonuclease I and Thermosensitive Alkaline Phosphatase, Thermo Scientific) and sequenced on an ABI 3700 sequencer (Applied Biosystems). Sequence data obtained were deposited in GenBank under accession numbers KU161271–KU161276 (Table 2).

In order to identify the genealogical position of the newly sequenced haplotypes of *O. dasytrichus*, we incorporated 11 sequences from southern Brazil (considered here as a reference for the species) provided by Hoffmann et al. (2002) and Gonçalves and Oliveira (2004) (Table 2). Ten other representative species of the genus were incorporated in the analysis (obtained from GenBank; Table 2) to discuss relationships of the species within the genus, using taxa with occurrence in Brazilian biomes, particularly the Atlantic forms, based on Gonçalves and Oliveira (2004) phylogenetic hypothesis. All data were aligned in the program MUSCLE (http://www.ebi.ac.uk/tools/msa/muscle) and manually adjusted in the software MEGA 6 (Tamura et al. 2013). The best-fit model of nucleotide substitution was determined based on the Akaike Information Criterion. Bayesian inference was used to reconstruct the phylogenetic relationships using BEAST 2.02 (Drummond et al. 2012) under the HKY model with a proportion of invariant sites and a gamma distribution. All parameters were estimated from the data. The Markov chains were run for 10 million generations and repeated four times to test for Markov chain–Monte Carlo chain convergence, and priors exceeded 200 to ensure effective sample sizes (ESS). Burn-in was determined in Tracer v1.5 (Drummond and Rambaut, 2007) based on parameter trajectories, and 10% of the first trees were then removed in TreeAnnotator. The consensus tree was visualized and edited in FigTree 1.3.1 (Rambaut 2009). Nodes with posterior probability

Figure 3. Dorsal, ventral and lateral views of the skull of *Oxymycterus dasytrichus* (CZFURB 18669) collected at Itapoá, Santa Catarina, Brazil. Photograph by Willian T. Peçanha. Scale bar = 10 mm.

Table 2. Sequences of the mitochondrial cytochrome b gene of *Oxymycterus* species used in the phylogenetic analysis and genetic distance comparisons, obtained from GenBank (accession number), with reference.

Species	GenBank Accession No.	Museum/ Institution ID*	Reference
O. hiska			
	U03542	MVZ 171518	Smith and Patton (1993)
O. nasutus			
	DQ518258	GD 577	Jayat et al. (2008)
	EF661854	—	Montes et al. (2008)
	AF175286	MVZ 182701	Hoffmann et al. (2002)
	AF175287	CA 695	Hoffmann et al. (2002)
O. josei			
	AF175288	MVZ 183264	Hoffmann et al. (2002)
	AF175289	MVZ 183265	Hoffmann et al. (2002)
O. amazonicus			
	AF454765	MZUSP 21317	Hoffmann et al. (2002)
O. delator			
	AF454766	UMMZ 137077	Hoffmann et al. (2002)
	AF454767	LPC 481	Hoffmann et al. (2002)
	U03525	UMMZ 133939	Smith and Patton (1993)
	DQ518256	MNHNP 2914	Jayat et al. (2008)
	AY275125	UMMZ 175101	D'Elía (2003)
O. dasytrichus			
	KU161273	UFPR-P752	This study
	KU161274	UFPR-P754	This study
	KU161276	UFPR-P760	This study
	KU161275	UFPR-P757	This study
	KU161272	UFPR-P177	This study
	KU161271	CZFURB 18669	This study
	AF454768	MVZ 183125	Hoffmann et al. (2002)
	AF454769	MVZ 183126	Hoffmann et al. (2002)
	AF454770	MVZ-JLP 16283	Hoffmann et al. (2002)
	AF454771	MNR-ML 125	Hoffmann et al. (2002)
	AF516662	MN 62254	Gonçalves and Oliveira (2004)
	AF516659	MN 65534	Gonçalves and Oliveira (2004)
	AF516658	MZUFV 659	Gonçalves and Oliveira (2004)
	AF516657	MN 65536	Gonçalves and Oliveira (2004)
	AF516663	MN 62258	Gonçalves and Oliveira (2004)
	AF516664	MN 62259	Gonçalves and Oliveira (2004)
	AF516665	MN 62260	Gonçalves and Oliveira (2004)
O. quaestor			
	AF454772	LG 41	Hoffmann et al. (2002)
	AF516660	MN 65544	Gonçalves and Oliveira (2004)
	AF516661	MN 65543	Gonçalves and Oliveira (2004)
O. judex			
	AF454773	MVZ 183128	Hoffmann et al. (2002)
	AF454774	MVZ 183129	Hoffmann et al. (2002)
O. rufus			
	AF454775	TK 49118	Hoffmann et al. (2002)
	AF454776	TK 49119	Hoffmann et al. (2002)
	AF454777	BAL 000511	Hoffmann et al. (2002)
	AF516652	PRG 903	Gonçalves and Oliveira (2004)
	AF516651	PRG 1013	Gonçalves and Oliveira (2004)
	AF516653	MZUFV 713	Gonçalves and Oliveira (2004)
	AF516654	MN 65522	Gonçalves and Oliveira (2004)
	AF516655	MN 65538	Gonçalves and Oliveira (2004)
	AF516666	AC 05	Gonçalves and Oliveira (2004)
	AF516667	AC 30	Gonçalves and Oliveira (2004)
	AF516668	PY 01	Gonçalves and Oliveira (2004)
	AF516669	PY 02	Gonçalves and Oliveira (2004)
	AY275126	UP AC004	D'Elía (2003)
	AY275127	UP 033	D'Elía (2003)
O. paramensis			
	DQ518259	CML 7251	Jayat et al. (2008)
	DQ518260	CNP 852	Jayat et al. (2008)
	DQ518261	CNP 850	Jayat et al. (2008)
O. wayku			
	DQ518262	CML 7247	Jayat et al. (2008)

* ***Brazil:*** *MZUSP, Museu de Zoologia da Universidade de São Paulo, São Paulo; MNR, ML, Museu Nacional de Rio de Janeiro, LG 41; MN, PRG, Museu Nacional, Universidade Federal do Rio de Janeiro, Rio de Janeiro, Museu de Zoologia "João Moojen de Oliveira"; MZUFV, Universidade Federal de Viçosa, Minas Gerais; LPC 458 at the Universidade Federal de Minas Gerais, Brazil.* ***Paraguay:*** *MNHNP, Museo Nacional de Historia Natural del Paraguay.* ***Uruguay:*** *GD, field number of Guillermo D'Elía (vouchers will be deposited at Museo Nacional de Historia Natural y Antropología, Montevideo); CA, Laboratorio de Evolución, Facultad de Ciencias, Montevideo.* ***Argentina.*** *CNP, UP, Colección de Mamíferos del Centro Nacional Patagónico Puerto Madryn; CML, Colección Mamiferos Lillo, Tucumán; MLP, AC, PY, Museo de La Plata, Buenos Aires; BAL 00-05-11 at the Museo de Historia Natural de la Plata, Berisso.* ***United States:*** *UMMZ, Museum of Zoology, University of Michigan, Ann Arbor; MVZ (JLP), Museum of Vertebrate Zoology, University of California, Berkeley (JLP, field numbers of The Museum); TK, Texas Tech University, Lubbock.*

(PP) ≥ 95% were considered to be supported (Alfaro et al. 2003). In order to characterize the genetic divergence between *O. dasytrichus* collected in PR and SC and those used as a reference (from southeast Brazil), pairwise genetic distances were calculated using the Kimura 2-parameters (K2P) model with 1000 replications bootstraps.

Taxonomy within *Oxymycterus* has been controversial because of difficulties in detecting discrete morphological and cytogenetic variation (Musser and Carleton 1993; Hershkovitz 1994; Oliveira 1998; Gonçalves and Oliveira 2004). Therefore, the identification of the six vouchers was based on some external morphology characters (such as coat color and skull) coupled with comparative assessment of DNA sequences (the mitochondrial gene cytochrome b) and distributional ranges.

Oxymycterus dasytrichus presents a dark-brown to paler brownish red without strong lining of back in the dorsum and dark-gray to paler, cinnamon or pinkish buff in the ventral (Oliveira and Gonçalves, 2015). Its skull is robust, proportionally larger in width dimensions of braincase, interorbital region and zygomatic plates, with longer molar tooth rows (mean 5.6 mm) comparably to other species of Atlantic Coast (Figure 4). Its variation in cranial measurements was reported by Gonçalves and Oliveira (2004). On the other hand, some species predominantly occurs in certain biomes; for example, the Atlantic Forest in the case of *O. dasytrichus*.

In the absence of discrete characters in *O. dasytrichus*, the identification of specimens relied mostly on lesser genetic distance associated to geographically distinct groups, using the nucleotide BLAST tool from the

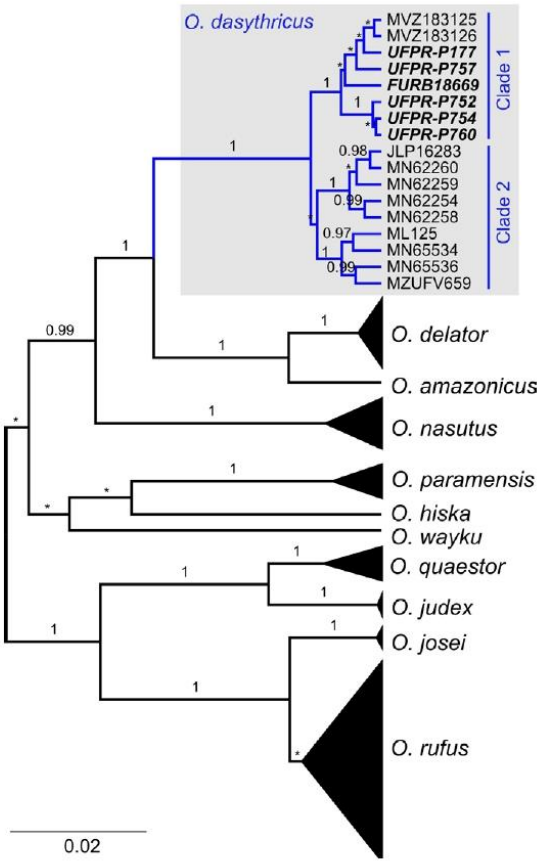

Figure 4. Bayesian consensus tree reconstructed based on 801 bp of the mitochondrial cytochrome b gene for *Oxymycterus dasytrichus* specimens collected in this study (UFPR-P752, UFPR-P754, UFPR-P760, UFPR-P757, UFPR-P177 and CZFURB 18669) and 11 sequences from the southeast, obtained from GenBank. Ten other lineages of *Oxymycterus* were incorporated (for specimen information see Table 2). Numbers above branches indicate posterior probability support. Asterisk represents values lower than 0.95.

NCBI database. Species presenting less than 5% of divergence collected in the same biome and assigned to *O. dasytrichus* by Gonçalves and Oliveira (2004), were used to attribute our samples to this taxon. Although some taxonomic mistakes are known to occur in the Genbank records, the consistency of close relationship to a large number of specimens collected along the Atlantic Forest previously identified as *O. dasytrichus* by experts in this group (using comparative morphology as well; Gonçalves and Oliveira 2004) led us to consider reliable such result.

The results from Bayesian inference analysis (Figure 4) indicated that the samples collected along the PR and SC coast belong to the *O. dasytrichus* group, because the haplotypes corresponding to the newly collected specimens from these sites are nested in the major clade formed by those previously referred as this species. Thus, our identification of the newly reported specimens relies on lesser divergence comparative to other species of the genus and diagnose made by Gonçalves and Oliveira (2004) of the specimens they reported from the Atlantic Forest, based on morphological and molecular data. Because no morphological diagnostic characters to identify species in this genus are known, in order to identify specimens we had to trust on comparisons based on genetic distances and morphology with previously identified specimens. Two internal haplogroups were recovered for *O. dasytrichus*: clade 1 formed by eight specimens/haplotypes (six from this study, and two from São Paulo and clade 2 formed by nine specimens/haplotypes from Rio de Janeiro, Espírito Santo, Minas Gerais and São Paulo. Whereas clade 1 received strong support, clade 2 was not supported. The K2P mean genetic distance between clades 1 and 2 was 2.1%, whereas that between species ranged from 6 to 12%.

Our data indicate that discoveries on general aspects of the biology (e.g., distributional range) of the genus *Oxymycterus* can still be made, even in a well-studied biome as the Atlantic Forest. Hoffmann et al. (2002) reported an intraspecific distance of 1.3% for the species across its northern and southern Atlantic Forest distribution. In our study we found similar divergence (1.4%), suggesting a shallow structure among haplotypes of clades 1 and 2. Such divergence does not seem to be determined strongly by a geographic cline since both clades include specimens from São Paulo. Thus, we did not find evidence to suggest that the populations represented by Clade 1 and Clade 2 are not conspecific. On the other hand, *O. dasytrichus* also occurs in the Caatinga and Cerrado (Costa and Leite 2012); therefore, such populations deserve particular effort in terms of comparative morphology and genetics since there is a greater distance to the Atlantic Forest populations and higher fixation of differences, and/or local adaptation to these distinct biomes, might exist.

The Atlantic Forest (lato sensu) coverage was reduced to 11–16% of the original area, in which 9% is protected areas, and 1% represents the original forest (Ribeiro et al. 2009). However, it is estimated that 1–8% of all the biodiversity in the planet is within this area (Silva and Casteleti 2003). According to Kauano et al (2012) the northern coast of Paraná is likely one of the least fragmented areas of the Atlantic, and is inserted in the "Serra do Mar", an important corridor of fauna and flora. Three of our four records were sampled in this region, which reinforces the significant role of protected areas, particularly the APA of Guaraqueçaba, not only to save small mammals, but as hotspot of endemic biodiversity refugee of the Atlantic Forest.

ACKNOWLEDGEMENTS

We are especially grateful to Ives José Sbalqueiro (UFPR), André Paulo Nascimento (FURB), Artur Stanke Sobrinho (FURB) and André Felipe Testoni (UFPR) for providing specimens used in molecular analysis. Also, we thank to Eliécer Gutiérrez and two anonymous referees whose suggestions significantly improved the last version of the manuscript. Thanks are also due Janet W. Reid for editing the text. We are grateful to CAPES for the award of a scholarship to the first author (WTP), and to CNPq for the financial support.

LITERATURE CITED

Alfaro, M.E., S. Zoller and F. Lutzoni. 2003. Bayes or bootstrap? A simulation study comparing the performance of Bayesian Markov chain Monte Carlo sampling and bootstrapping in assessing phylogenetic confidence. Molecular Biology and Evolution 20: 255–266. doi: 10.1093/molbev/msg028

Araújo, S.A, H. Haymussi, F.H. Reis and F.E. Silva. 2006. Caracterização climatológica do município de Penha, SC; pp. 11–28, in: J.O. Branco and A.W.C. Marenzi (orgs.). Bases ecológicas para um desenvolvimento sustentável: estudos de caso em Penha, SC. Itajaí: Editora Univali.

Avila-Pires, F.D. 1965. The type specimens of Brazilian mammals collected by Prince Maximilian zu Wied. American Museum Novitates 2209: 1–21. http://hdl.handle.net/2246/3320

Bradley, R.D. and R.J. Baker. 2001. A test of the genetic species concept: cytochrome-*b* sequences and mammals. Journal of Mammalogy, 82(4): 960–973. doi: 10.1644/1545-1542(2001)082<0960:ATOTGS>2.0.CO;2

Bonvicino, C., M. Weksler and A. Percequillo. 2008. *Oxymycterus dasytrichus*. The IUCN Red List of threatened species. Version 2014.3. Accessed at http://www.iucnredlist.org, 23 April 2015.

Cabrera, A. 1961. Catalogo de los mamíferos de América del Sur. Revista del Museo Argentino de Ciencias Naturales "Bernardino Rivadavia" Ciencias Zoológicas 4: 309–732.

D'Elía, G. 2003. Phylogenetics of Sigmodontinae (Rodentia, Muroidea, Cricetidae), with special reference to the akodont group, and with additional comments on historical biogeography. Cladistics 19(4): 307–323. doi: 10.1016/S0748-3007(03)00071-9

D'Elía, G., I. Mora, P. Myers and R.D. Owen. 2008. New and noteworthy records of Rodentia (Erethizontidae, Sciuridae, and Cricetidae) from Paraguay. Zootaxa 1784: 39–57.

Drummond, A.J., M.A. Suchard, D. Xie and A. Rambaut. 2012. Bayesian phylogenetics with BEAUti and the BEAST 1.7. Molecular Biology and Evolution 29: 1969–1973. doi: 10.1093/molbev/mss075

Drummond, A.J., Rambaut, A., 2007. Beast: Bayesian evolutionary analysis by sampling trees. BMC Evolutionary Biology 7: 214. doi: 10.1186/1471-2148-7-214

Gonçalves, P.R. and J.A. de Oliveira. 2004. Morphological and genetic variation between two sympatric forms of *Oxymycterus* (Rodentia: Sigmodontinae): an evaluation of hypotheses of differentiation within the genus. Journal of Mammalogy 85(1): 148–161. doi: 10.1644/BER-012

Hershkovitz, P. 1994. The description of a new species of South American hocicudo, or long-nose mouse genus *Oxymycterus* (Sigmodontinae, Muroidea), with a critical review of the generic content. Fieldiana: Zoology (New Series) 1460: 1–43. http://www.biodiversitylibrary.org/part/6663

Hoffmann, F.G., E.P. Lessa and M.F. Smith. 2002. Systematics of *Oxymycterus* with description of a new species from Uruguay. Journal of Mammalogy 83(2): 408–420. doi: 10.1644/1545-1542(2002)083%3C0408:SOOWDO%3E2.0.CO;2

Jayat, J.P., G. D'Elía, U.F.J. Pardiñas, M.D. Miotti and P.E. Ortiz. 2008. A new species of the genus *Oxymycterus* (Mammalia: Rodentia: Cricetidae) from the vanishing Yungas of Argentina. Zootaxa 1911: 31–51.

Kauano, E.E., J. M. D. Torezan, F.C.G. Cardoso and M.C.M. Marques. 2012. Landscape structure in the northern coast of Paraná state, a hotspot for the brazilian Atlantic Forest conservation. Revista Árvore 36: 961–970. doi: 10.1590/S0100-67622012000500018

Kottek, M., J. Grieser, C. Beck, B. Rudolf and F. Rubel. 2006. World map of the Köppen-Geiger climate classification updated. Meteorologische Zeitschrift 15(3): 259–263. doi: 10.1127/0941-2948/2006/0130

Montes, M.A., L.F.B. Oliveira and M.S. Mattevi. 2008. Phylogeny and evolution of the neotropical rodent genus *Akodon*: inferences from mitochondrial and nuclear DNA sequences data. Unpublished (Genbank data). http://www.ncbi.nlm.nih.gov/nuccore/EF661854

Musser, G.G., and M.D. Carleton. 1993. Family Muridae; pp. 501–755, in: D.E. Wilson and D.M. Reeder (eds.). Mammal species of the world: a taxonomic and geographic reference (Washington, D.C.: Smithsonian Institution Press.

Oliveira, J.A. 1998. Morphometric assessment of species groups in the South American rodent genus *Oxymycterus* (Sigmodontinae), with taxonomic notes based on the analysis of type material [PhD dissertation]. Lubbock: Texas Tech University. 320 pp.

Oliveira, J.A. and P.R. Gonçalves. 2015. Suborder Myomorpha: Family Cricetidae: Subfamily Sigmodontinae. Genus *Oxymycterus*; pp. 247–268 in: J.L. Patton, U.F.J. Pardiñas and G. D'Elía (eds.). Mammals of South America 2: Rodents. Chicago: University of Chicago Press. doi: 10.7208/chicago/9780226169606.001.0001

Costa, L.P and Y.L. Leite. 2012. Historical fragmentation shaping vertebrate diversification in the Atlantic forest biodiversity hotspot; pp. 283–306, in: B.D. Patterson and L.P. Costa (eds.). Bones, clones, and biomes: the history and geography of Recent Neotropical mammals. Chicago: University of Chicago Press. doi: 10.7208/chicago/9780226649214.001.0001

Rambaut, A. 2009. FigTree v1.3.1 2006–2009. Accessed at http://tree.bio.ed.ac.uk/software/figtree, 20 July 2015.

Ribeiro, M.C., J.P. Metzger, A.C. Martensen, F.J. Ponzoni and M.M. Hirota. 2009. The Brazilian Atlantic Forest: How much is left, and how is the remaining forest distributed? Implications for conservation. Biological Conservation 142(6): 1141–1153. doi: 10.1016/j.biocon.2009.02.021

Silva, J.M.C. da. and C.H.M. Casteleti. 2003. Status of the biodiversity of the Atlantic Forest of Brazil; pp. 43–59, in: C. Galindo-Leal and I.G. Câmara (eds.). The Atlantic Forest of South America: biodiversity status, threats, and outlook. Washington, D.C.: CABS and Island Press.

Smith, M.F. and J.L. Patton. 1993. The diversification of South American murid rodents: evidence from mitochondrial DNA sequence data for the akodontine tribe. Biological Journal of the Linnean Society 50: 149–177. doi: 10.1006/bijl.1993.1052

Tamura, K., G. Stecher, D. Peterson and S. Kumar. 2013. MEGA6: Molecular Evolutionary Genetics analysis version 6.0. Molecular Biology and Evolution 30: 2725–2729. doi: 10.1093/molbev/mst197

Vanhoni, F. and F. Mendonça. 2008. O clima do litoral do estado do Paraná. Revista Brasileira de Climatologia 3: 50–63. http://ojs.c3sl.ufpr.br/ojs2/index.php/revistaabclima/article/view/25423/17042

Received: 22 July 2015
Accepted: 15 February 2016
Academic editor: Eliécer E. Gutiérrez

Anexo.2

Phylogenetic and molecular dating for the genus *Oxymycterus* and close-relative Akodontini lineages.

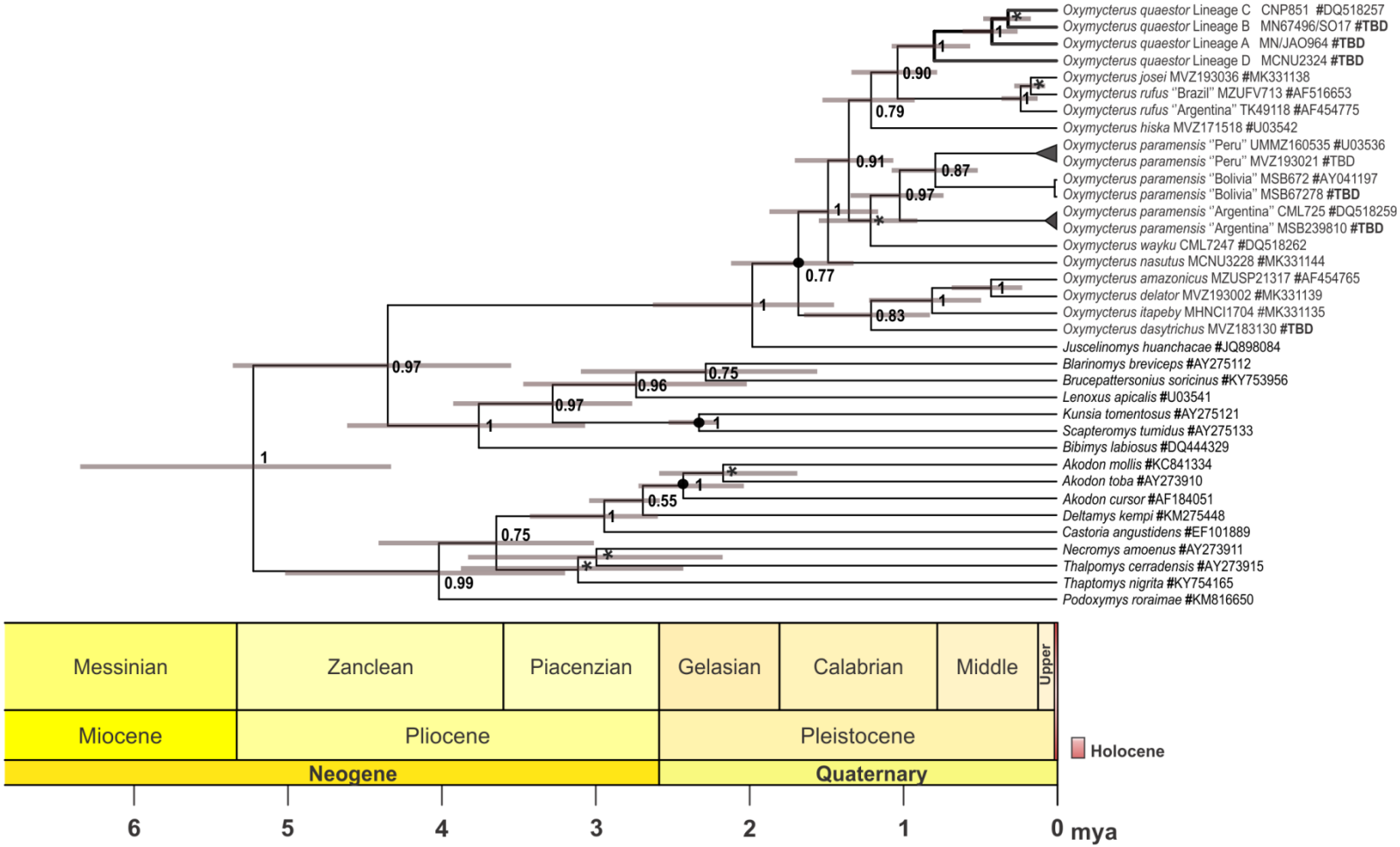

Figure. Phylogenetic tree is a chronogram (uncorrelated log-normal molecular clock) based on a BEAST MCMC analysis of the mitochondrial data set (cytochrome *b* gene). Black circles on the nodes correspond to the fossil calibration points. The 95% credibility intervals of molecular estimates (median height) are given for each node. Numbers at nodes are Bayesian Posterior Probabilities; numbers in bold indicate high support (≥ 0.75). Nodes marked with asterisks are unsupported. Scale bars were plotted with a geological time scale using the strap package in R.